THE SYNTHESIS AND CHARACTERIZATION OF PHOSPHONIUM INDENYLIDE COMPLEXES OF RUTHENIUM(II)

by

Kevin Fowler

A thesis submitted to the Department of Chemistry

In conformity with the requirements for

the degree of Doctor of Philosophy

Queen's University

Kingston, Ontario, Canada

(April, 2014)

Abstract

Phosphonium indenylides (PHIN) are a promising, yet relatively unexplored class of transition metal ligands. The ylidic resonance structure **b** of this compound is isoelectronic with the cyclopentadienyl ligand which is ubiquitous throughout organometallic chemistry. Phosphonium indenylides have been found to have electron donating properties between those of η^6-benzene and η^5-cyclopentadienyl ligands and are tuneable based on the nature of the phosphine used. In addition, upon coordination, phosphonium indenylides exhibit planar chirality. These properties may potentially lead to interesting coordination chemistry and applications in catalysis.

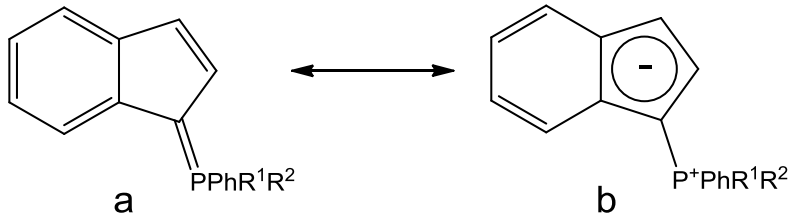

The phosphonium indenylides 1-$C_9H_6PPh_3$ (**I**), 1-$C_9H_6PMePh_2$ (**II**) and1-$C_9H_6PMe_2Ph$ (**III**) have been synthesized and reacted with $[CpRu(MeCN)_3]PF_6$ to form complexes of the type $[CpRu(\textbf{I-III})]PF_6$ (**V-VII**) which were characterized by NMR spectroscopy, ESI MS and X-ray crystallography. In an attempt to synthesize Ru-PHIN complexes with labile ligands attached to the metal centre, an arene exchange reaction between a PHIN ligand and $RuCl_2(\eta^6$-ethylbenzoate)(PPh_3) was employed to produce $RuCl_2(\textbf{II})(PPh_3)$ which was characterized by extensive NMR spectroscopy.

Acknowledgements

There are a number of people I would like to thank for making my time at Queen's an incredible experience. I will start off by thanking my supervisor Michael Baird for putting in a huge amount of time on me over the years. From the moment I entered the lab, Mike has been fair, encouraging, and insightful. Thanks for always trying to steer me in the right direction. Let's hope the Jays can finally pull it out this year.

The past and present members of the Baird lab have always made my time at Queen's enjoyable and stimulating. I'd like to especially thank AF for demonstrating a novel way to quench a sodium still. I would also like to thank all the students I taught in CHEM 397. I truly found teaching that lab rewarding and I think I learned as much as my students did.

There have been too many people whom I have crossed paths with to name that have made Queen's the center of many fond memories. The regulars at Jay's Bar and Grill, the Uehehe's, Andrew Fraser, Jason Hanthorn, and Ben Glasspoole, who made many a fall Sunday interesting, as well as Fern, Geoff, Graham, Kyle, Brando, Chad, and Ryan. I'd also like to thank Bronwyn Coombs as well as the Laurier guys, Kurt, Telly, and Brett, for dragging me out of Kingston every now and then. You have all given me so many great memories, like the lifting of the Stanley barrel; the Brinkhorst Memorial, and the many annual Fowlerships. Keep swinging for the fences guys.

Most importantly, I would like to thank my parents for providing never ending love and support. It goes without saying that I wouldn't be here today without you. I hope I have made you proud.

Lastly, I would like to thank the Toronto Maple Leafs for letting me down all these years.

Table of Contents

Abstract ii

Acknowledgements iii

List of Figures viii

List of Tables xiii

Chapter 1 : Introduction 1

1.1 The Ramirez Ylide 1

1.1.1 Ramirez Preparation of Phosphonium Cyclopentadienylides 2

1.1.2 Mathey Preparation of Phosphonium Cyclopentadienylides 3

1.1.3 Phosphoium Cyclopentadienylides from Pyrylium Salts 4

1.1.4 Synthesis of Diphosphine Ramirez Ylide Derivatives 7

1.1.5 Coordination of the Ramirez Ylide to Transition Metals 8

1.1.6 Difficulties with the Ramirez Ylide 14

1.2 Phosphonium Fluorenylides 15

1.2.1 Coordination of Phosphonium Fluorenylides 16

1.2.2 Electronic Structure of the Phosphonium Fluorenylides 17

1.3 Phosphonium Indenylides (PHINs) 19

1.3.1 PHIN Synthesis by Addition to $C_9H_7PPh_2$ 20

1.3.2 PHIN Synthesis from 1-Bromoindene 21

1.3.3 Interest in Phosphonium Indenylides 23

1.3.4 Phosphonium Indenylide Coordination to Cr 24

1.4 Ruthenium(II) Arene Compounds 26

1.4.1 Ruthenium(II) Arene Compounds from Cyclohexadienes 26

1.4.2 Arene Exchange Reactions of Ruthenium(II) – Arene Complexes 29

1.4.3 Intramolecular Ruthenium(II) – Arene Exchange Reactions 34

1.5 Research Aims 43

1.6 References 45

Chapter 2 : Experimental 48

2.1 General Considerations 48

2.2 X-ray Crystallography 49

2.3 DFT Calculations 49

2.4 General Synthesis of PHINs 50

2.4.1 Synthesis of 1-trimethylsilylindene 50

2.4.2 Synthesis of Dioxane Dibromide 50
2.4.3 Synthesis of 1-bromoindene with Dioxane Dibromide as Brominating Agent 51
2.4.4 Synthesis of 1-bromoindene with $Br_2Cl_4C_2$ as Brominating Agent 51
2.4.5 Synthesis of the Phosphonium Salts [1-$C_9H_7PR_3$]Br 52
2.4.6 Synthesis of [1-$C_9H_7PPh_2CH_2PPh_2$]Br 52
2.4.7 Synthesis of PHINs 1-$C_9H_6PR_3$ 53
2.4.8 Synthesis of 1-$C_9H_6PPh_2CH_2PPh_2$ (IV) 54
2.5 Synthesis of [RuCl(μ-Cl)(η^6-ethylbenzoate)]$_2$ 54
2.5.1 Birch Reduction of Benzoic Acid 55
2.5.2 Esterification of 1,4-Dihydrobenzoic Acid 55
2.5.3 Synthesis of [$RuCl_2$(η^6-ethylbenzoate)]$_2$ 56
2.6 Coordination of PHINs to Ruthenium using [CpRu(MeCN)$_3$]PF_6 56
2.6.1 Synthesis of [CpRu(1-$C_9H_6PPh_3$)]PF_6 (V) 56
2.6.2 Synthesis of [CpRu(1-$C_9H_6PMePh_2$)]PF_6 (VI) 57
2.6.3 Synthesis of [CpRu(1-$C_9H_6PMe_2Ph$)]PF_6 (VII) 57
2.6.4 NMR scale Synthesis of Isomers of [CpRu(1-$C_9H_6PPh_2CH_2PPh_2$)]PF_6 (VIII) 58
2.7 Attempted Coordination of PHINs to Ruthenium using $RuCl_3 \cdot nH_2O$ 58
2.7.1 Reaction of [$C_9H_7PMePh_2$]I with $RuCl_3 \cdot xH_2O$ 59
2.7.2 Reaction of III with $RuCl_3 \cdot xH_2O$ and Zn(s) 59
2.8 Coordination of PHINs to Ruthenium using [RuCl(μ-Cl)(η^6-arene)]$_2$ 60
2.8.1 Solvent-free Reaction of II with [RuCl(μ-Cl)(η^6-*p*-cymene)]$_2$ 60
2.8.2 Synthesis of $RuCl_2$(η^6-*p*-cymene)(η^1-1-$C_9H_6PPh_2CH_2PPh_2$) (IX) 61
2.8.3 Reaction of III with [RuCl(μ-Cl)(η^6-*p*-cymene)]$_2$ 61
2.8.4 Reaction of II with [RuCl(μ-Cl)(η^6-*p*-cymene)]$_2$ 62
2.8.5 Reaction of XII with PMe_2Ph 63
2.8.6 Reaction of II with [RuCl(μ-Cl)(η^6-ethylbenzoate)]$_2$ 64
2.9 Arene Exchange Reactions with $RuCl_2$(arene)(PR_3) 64
2.9.1 Reaction of II with $RuCl_2$(η^6-C_6H_6)(PPh_3) 64
2.9.2 Reaction of II with $RuCl_2$(η^6-ethylbenzoate)(PPh_3) (XIII) 65
2.10 References 66
Chapter 3 : Results and Discussion 67
3.1 New Approaches in the Synthesis of PHIN Ligands 67
3.1.1 Synthesis of 1-bromoindene using C_2Cl_4 Br_2 as Brominating Agent 67
3.1.2 Synthesis of [1-$C_9H_7PPh_2CH_2Ph_2$]Br 68

3.1.3 Synthesis of 1-$C_9H_6PPh_2CH_2PPh_2$ (IV) 73
3.2 Coordination of PHINs to Ruthenium using $[CpRu(MeCN)_3]PF_6$ 78
3.2.1 Spectral Analysis of $[CpRu(I)]PF_6$ (V) 79
3.2.2 Spectral Analysis of $[CpRu(1\text{-}C_9H_6PMePh_2)]PF_6$ (VI) 84
3.2.3 Spectral Analysis of $[CpRu(1\text{-}C_9H_6PMe_2Ph)]PF_6$ (VII) 89
3.2.4 X-ray Crystallographic Analysis of V, VI and VII 93
3.2.5 Computational Studies of for $[CpRu(I\text{-}III)]PF_6$ (V-VII) 98
3.3 Coordination of 1-$C_9H_6PPh_2CH_2PPh_2$ (IV) to $[CpRu(MeCN)_3)]PF_6$ 99
3.3.1 NMR Analysis of VIIIa 101
3.3.2 NMR Analysis of VIIIb 105
3.3.3 Computational Studies on the isomers of VIII 112
3.4 Attempted Coordination of PHINs to Ruthenium using $RuCl_3 \cdot xH_2O$ 115
3.4.1 Reaction of $[1\text{-}C_9H_7PMePh_2]I$ with $RuCl_3 \cdot xH_2O$ 115
3.4.2 Attempted Coordination of III to Ruthenium with $RuCl_3 \cdot xH_2O$ and Zn(s) 116
3.5 Coordination of PHINs to Ruthenium using $[RuCl(\mu\text{-}Cl)(\eta^6\text{-arene})]_2$ 117
3.5.1 Solvent-free Reaction of II with $[RuCl(\mu\text{-}Cl)(\eta^6\text{-}p\text{-cymene})]_2$ 117
3.5.2 Synthesis of $RuCl_2(\eta^6\text{-}p\text{-cymene})(\eta^1\text{-}1\text{-}C_9H_6PPh_2CH_2PPh_2)$ (IX) 120
3.5.3 Reaction of 1-$C_9H_6PPhMe_2$ (III) with $[RuCl(\mu\text{-}Cl)(\eta^6\text{-}p\text{-cymene})]_2$ 126
3.5.4 Reaction of 1-$C_9H_6PPh_2Me$ (II) with $[RuCl(\mu\text{-}Cl)(\eta^6\text{-}p\text{-cymene})]_2$ 133
3.5.5 Reaction of XII with PMe_2Ph 136
3.5.6 Reaction of 1-$C_9H_6PPh_2Me$ (II) with $[RuCl(\mu\text{-}Cl)(\eta^6\text{-ethylbenzoate})]_2$ 137
3.5.7 Conclusions from the Reaction of II and III with $[RuCl(\mu\text{-}Cl)(\eta^6\text{-}p\text{-cymene})]_2$ 139
3.6 Arene Exchange Reactions with $RuCl_2(arene)(PR_3)$ 140
3.6.1 Synthesis and Characterization of $RuCl_2(\eta^5\text{-II})(PPh_3)$ (XIII) 140
3.7 References 147
Chapter 4 : Conclusions and Future Work 148
4.1 Conclusions 148
4.2 Future Work 150
Appendix A : NMR Spectra 152
4.3 NMR Spectra of the isomers of $[1\text{-}C_9H_7PPh_2CH_2PPh_2]Br$ and IV 152
4.4 NMR spectra of V, VI, and VII 154
4.5 NMR spectra of VIIIa and VIIIb 157
Appendix B : X-ray Crystallographic Data 159
4.6 Crystal Data for isomer A of $[1\text{-}C_9H_6PPh2CH_2PPh_2]Br$ 159

4.7 Crystal Data for 1-$C_9H_6PPh_2CH_2PPh_2$ 160
4.8 Crystal Data for [CpRu(1-$C_9H_6PPh_3$)]PF_6 161
4.9 Crystal Data for [CpRu(1-$C_9H_6PPh_2Me$)]PF_6 162
4.10 Crystal Data for [CpRu(1-$C_9H_6PPhMe_2$)]PF_6 163
4.11 Crystal Data for $RuCl_2$(1-$C_9H_6PPh_2CH_2PPh_2$)(η^6-*p*-cymene) 164

List of Figures

Figure 1. Resonance structures of the Ramirez ylide 1
Figure 2. Synthesis of the Ramirez ylide 2
Figure 3. Preparation of $C_5H_4PMePh_2$ by Mathey and Lampin 3
Figure 4. Synthesis of 2,4,5-triphenylpyrylium perchlorate 4
Figure 5. Proposed mechanism for the formation of 2,4,5-triphenylpyrylium perchlorate 5
Figure 6. Synthesis of 2,4,5-triphenylphosphonium cyclopentadienylides from 2,4,5-triphenyl pyrylium salts 6
Figure 7. Synthesis of 2,4,5-triphenylphosphonium cyclopentadienyl cations. Deprotonation with NaOH gives the trisubstituted phosphonium cyclopentadienylides 6
Figure 8. Tautomerization of $C_5H_4PPh_2CH_2PPh_2$ 7
Figure 9. Reaction of bromofluorene with dppm and dppe showing formation of the bisphosphonium salt 8
Figure 10. Transition metal complexes of phosphonium cyclopentadienylides which have been characterized by X-ray crystallography (excludes complexes of group 8 metals) 9
Figure 11. Synthesis of $(C_5H_4PPh_3)M(CO)_3$ (M = Cr, Mo, W) 10
Figure 12. Molecular structure of $(C_5H_4PMePh_2)Cr(CO)_3$ 11
Figure 13. Synthesis of $Ru_6C(CO)_{14}(C_5H_4PPh_3)$ 12
Figure 14. Reaction of PPh_3 with a) $[Ru(C_5H_5)(C_5H_4O)]_2$ and b) $Ru(C_5H_5)(C_5H_4O)(MeCN)$ 13
Figure 15. Reaction of $[CpRu(Fv)RuCp]^{2+}$ with PPh_3 14
Figure 16. Synthesis of 9-dppm-fluorenylide 15
Figure 17. Synthesis of $(C_{13}H_8PPh_2CH_2PPh_2)M(CO)_4$ (M = Cr, W) 16
Figure 18. Synthesis of $(C_{13}H_8PPh_2CH_2PPh_2)PdCl_2$ 17
Figure 19. Reaction of triphenylphosphonium fluorenylide with dichlorocarbene and benzaldehyde 18
Figure 20. Resonance structures of $C_5H_4PPh_3$ and $C_{13}H_8PPh_3$ 19
Figure 21. Synthesis of phosphonium indenylides by alkylation of 1-$C_9H_6PPh_2$ 21
Figure 22. Synthesis of triphenylphosphonium indenylide reported by Crofts and Williamson 22
Figure 23. Synthesis of 1-$C_9H_6PPh_3$ using dioxane dibromide as brominating agent 23
Figure 24. Planar chirality of PHIN ligands 24
Figure 25. Synthesis of planar chiral PHIN complexes $(1\text{-}C_9H_6PMePh_2)Cr(CO)_3$ 25
Figure 26. Synthesis of $[RuCl(\mu\text{-}Cl)(\eta^6\text{-}p\text{-cymene})]_2$ from α-phellandrene 27

Figure 27. Breaking the chloride bridge of $[RuCl(\mu\text{-}Cl)(\eta^6\text{-}p\text{-}cymene)]_2$ with PPh_3 followed by removal of a chloride ligand to form a cationic ruthenium(II)-arene complex 28
Figure 28. Synthesis of the asymmetic transfer hydrogenation catalyst Ru(*S*,*S*-TsDPEN)(*p*-cymene) 29
Figure 29. Synthesis of $[RuCl(\mu\text{-}Cl)(trindane)]_2$ 31
Figure 30. Arene exchange reactions of $(\eta^6\text{-}C_6H_6)RuH(\eta^1\text{-}C_6H_5)(PMe_3)$ with deuterated benzene, toluene and mesitylene 32
Figure 31. Arene exchange of $Ru(CO)(Xantsil)(\eta^6\text{-}toluene)$ with benzene 33
Figure 32. Arene exchange of $[RuCl(\mu\text{-}Cl)(\eta^6\text{-}ethylbenzoate)]_2$ with benzo-15-crown-5 33
Figure 33. Immobilization of $RuCl_2(PR_3)$ fragment on polystyrene by arene exchange 34
Figure 34. General scheme for intramolecular arene exchange reaction to form η^6:η^1 tethered ruthenium(II) arene complexes with phosphine donors 35
Figure 35. Synthesis of $[RuCl(\eta^6\text{:}\eta^1\text{-}(PCy_2(CH_2)_3Ph))(=C=C=CPh_2)]OTf$ which was used as a catalyst for ring closing metathesis 36
Figure 36. Some η^6:η^1 tethered ruthenium(II) arene complexes synthesized by arene exchange . 36
Figure 37. Synthesis of P-chiral phosphetane η^6:η^1 ruthenium(II) arene complexes 37
Figure 38. Synthesis of a single diastereomer of $RuCl_2(\eta^6\text{:}\eta^1\text{-}PMe(t\text{-}Bu)(CH_2CH_2\text{-}naphthyl)$ 38
Figure 39. Synthesis of $RuCl(aniline)(\eta^6\text{:}\eta^1\text{-}(R)\text{-}PPh_2(CH_2)_2CHPh)$ which did not epimerize on heating 39
Figure 40. Synthesis of the η^6:η^1 coordination mode of a PArN ligand 40
Figure 41. Fast arene exchange with DavePhos 41
Figure 42. Tethered η^6:η^1 ruthenium arene complexes with N donor groups synthesized by arene exchange 42
Figure 43. Synthesis of η^6:η^1 tethered ruthenium(II) arene complexes with carbene donor groups 42
Figure 44. Bromination of indenyl lithium with $C_2Cl_4Br_2$ 68
Figure 45. Synthesis of the isomers of $[1\text{-}C_9H_7PPh_2CH_2PPh_2]Br$ 69
Figure 46. Numbering scheme for $[1\text{-}C_9H_7PPh_2CH_2PPh_2]Br$ and $1\text{-}C_9H_7PPh_2CH_2PPh_2$ (IV) 69
Figure 47. ^{31}P NMR spectrum of isomers A and B of $[1\text{-}C_9H_7PPh_2CH_2Ph_2]Br$ in CD_2Cl_2 70
Figure 48. ^1H NMR spectrum of $[1\text{-}C_9H_7PPh_2CH_2PPh_2]Br$ in CD_2Cl_2 71
Figure 49. Molecular structure of isomer A of $[1\text{-}C_9H_7PPh_2CH_2PPh_2]Br$ (Numbering different from that shown in Figure 46 72
Figure 50. Synthesis of $1\text{-}C_9H_7PPh_2CH_2PPh_2$ (IV) 73
Figure 51. ^1H NMR spectrum of $1\text{-}C_9H_7PPh_2CH_2PPh_2$ (IV) in CD_2Cl_2 74

Figure 52. COSY spectrum of 1-$C_9H_7PPh_2CH_2PPh_2$ (IV) 75
Figure 53. ^{31}P NMR spectrum of 1-$C_9H_6PPh_2CH_2PPh_2$ (IV) in CD_2Cl_2 76
Figure 54. Molecular structure of 1-$C_9H_7PPh_2CH_2PPh_2$ (IV) (Number different from that shown in Figure 46 77
Figure 55. Synthesis of PHIN-Ru(II) complexes [CpRu(I-III)]PF_6 (V-VII) 78
Figure 56. Numbering scheme for PHIN ligands I-III 79
Figure 57. ^1H NMR spectrum of [CpRu(1-$C_9H_6PPh_3$)]PF_6 (V) in CD_2Cl_2 80
Figure 58. COSY spectrum of [CpRu(1-$C_9H_6PPh_3$)]PF_6 (V) 80
Figure 59. ESI-MS of [CpRu(1-$C_9H_6PPh_3$)]PF_6 (V) (bottom) and the calculated isotope pattern (top) 83
Figure 60. ^1H NMR spectrum of [CpRu(1-$C_9H_6PMePh_2$)]PF_6 (VI) in CD_2Cl_2 84
Figure 61. COSY spectrum of [CpRu(1-$C_9H_6PMePh_2$)]PF_6 (VI) in CD_2Cl_2 85
Figure 62. NOESY spectrum of [CpRu(1-$C_9H_6PMePh_2$)]PF_6 (VI) in CD_2Cl_2 85
Figure 63. VI does not undergo interfacial exchange of the PHIN ligand on the NMR timescale 86
Figure 64. ^1H-^{13}C HSQC spectrum of [CpRu(1-$C_9H_6PMePh_2$)]PF_6 (VI) in CD_2Cl_2 86
Figure 65. ESI-MS of [CpRu(1-$C_9H_6PMePh_2$)]PF_6 (VI) (bottom) and the calculated isotope distribution (top) 88
Figure 66. ^1H NMR spectrum of [CpRu(1-$C_9H_6PMe_2Ph$)]PF_6 (VII) in CD_2Cl_2 89
Figure 67. COSY spectrum of[CpRu(1-$C_9H_6PMe_2Ph$)]PF_6 (VII) in CD_2Cl_2 90
Figure 68. ^1H-^{13}C HMBC spectrum of [CpRu(1-$C_9H_6PMe_2Ph$)]PF_6 (VII) in CD_2Cl_2 90
Figure 69. ESI-MS of [CpRu(1-$C_9H_6PMe_2Ph$)]PF_6 (VII) (bottom) and the calculated isotope distribution (top) 92
Figure 70. Resonance Structures of the PHINs 93
Figure 71. Molecular structure of V (Numbering different from that shown in Figure 56) 95
Figure 72. Molecular Structure of VI (Numbering different from that shown in Figure 56) 96
Figure 73. Molecular structure of VII (Numbering different from that shown in Figure 56) 97
Figure 74. ^{31}P NMR spectrum of a mixture of VIIIa and VIIIb in CD_2Cl_2 100
Figure 75. Proposed structure of VIIIa based on NMR data 101
Figure 76. ^1H NMR spectrum of a mixture of VIIIa and VIIIb in CD_2Cl_2 with peaks assigned to VIIIa highlighted 102
Figure 77. ^1H-^{31}P HMBC spectrum of VIIIa 103
Figure 78. COSY spectrum of a mixture of VIIIa and VIIIb (H(2)-H(3) correlation is circled). 103
Figure 79. Potential allylic isomers of VIIIb 105
Figure 80. ^1H NMR spectrum of an aged sample containing predominantly VIIIb in CD_2Cl_2 ... 106

Figure 81. NOESY spectrum of an aged sample containing predominantly VIIIb which shows exchange cross peaks from the unknown species VIIIc (in teal) 107
Figure 82. COSY spectrum of an aged sample containing predominantly VIIIb (H(2)-H(3) correlation is circled) 108
Figure 83. ^{1}H-^{31}P HMBC spectrum of an aged sample containing predominantly VIIIb (H(7)-P(2) correlation is circled). 108
Figure 84. ^{1}H-^{13}C HSQC spectrum of an aged sample containing predominantly VIIIb in CD_2Cl_2 110
Figure 85. Proposed structure of VIIIb based on NMR data 111
Figure 86. Calculated structure of the η^3-allylic isomer corresponding to VIIIb 114
Figure 87. ^{1}H NMR spectrum of the precipitate formed from the reaction of $RuCl_3 \cdot xH_2O$ with [1-$C_9H_7PMePh_2$]I in CD_2Cl_2 116
Figure 88. ^{1}H NMR spectrum of the toluene extract from the solvent-free reaction of [RuCl(μ-Cl)(η^6-*p*-cymene)]$_2$ with II in toluene D_8 119
Figure 89. Proposed scheme for the formation of $RuCl_2$(p-cymene)($PMePh_2$) from heating II and [RuCl(μ-Cl)(η^6-*p*-cymene)]$_2$ 119
Figure 90. ^{1}H-^{31}P HMBC spectrum of the toluene extract from the solvent-free reaction of [RuCl(μ-Cl)(η^6-*p*-cymene)]$_2$ with II in toluene D_8 120
Figure 91. Synthesis of $RuCl_2$(η^6-*p*-cymene)(η^1-IV) (IX) 121
Figure 92. Molecular structure of $RuCl_2$(η^6-*p*-cymene)(η^1-IV) (IX) (Numbering different from that shown in Figure 46) 122
Figure 93. ^{1}H NMR spectrum of $RuCl_2$(η^6-*p*-cymene)(η^1-IV) (IX) in CD_2Cl_2 123
Figure 94. NOESY spectrum of $RuCl_2$(η^6-*p*-cymene)(η^1-IV) (IX) in CD_2Cl_2 (H(3)-H(4) correlation is circled) 123
Figure 95. COSY spectrum of $RuCl_2$(η^6-*p*-cymene)(η^1-IV) (IX) in CD_2Cl_2 124
Figure 96. ^{1}H-^{31}P HMBC spectrum of $RuCl_2$(η^6-*p*-cymene)(η^1-IV) (IX) in CD_2Cl_2 125
Figure 97. ^{1}H NMR spectrum of X (along with [RuCl(μ-Cl)(η^6-*p*-cymene)]$_2$) in DMSO d_6 126
Figure 98. COSY spectrum of a sample containing X and [RuCl(μ-Cl)(η^6-*p*-cymene)]$_2$ (H(2)-H(3) correlation is circled) 127
Figure 99. NOESY spectrum of a sample containing X and [RuCl(μ-Cl)(η^6-*p*-cymene)]$_2$ 128
Figure 100. Proposed structure for X based on NMR data 129
Figure 101. ^{1}H NMR spectrum of XI (along with [RuCl(μ-Cl)(η^6-*p*-cymene)]$_2$) in DMSO d_6 .. 131
Figure 102. COSY spectrum of XI (along with [RuCl(μ-Cl)(η^6-*p*-cymene)]$_2$) in DMSO d_6 (H(2)-H(3) correlation is circled) 131

Figure 103. Aliphatic region of the ^{1}H spectrum of the kinetic product from the reaction of II with $[RuCl(\mu\text{-}Cl)(\eta^{6}\text{-}p\text{-cymene})]_2$ in CD_2Cl_2 133
Figure 104. ^{1}H NMR spectrum of XII (along with $[RuCl(\mu\text{-}Cl)(\eta^{6}\text{-}p\text{-cymene})]_2$) in DMSO d_6. 135
Figure 105. COSY spectrum of XII (along with $[RuCl(\mu\text{-}Cl)(\eta^{6}\text{-}p\text{-cymene})]_2$) in DMSO d_6 (H(2)-H(3) correlation is circled) 135
Figure 106. ^{1}H NMR spectrum of XII formed by the reaction of II with $[RuCl(\mu\text{-}Cl)(\eta^{6}\text{-}$ethylbenzoate$)]_2$ 137
Figure 107. ESI-MS of XII (bottom) synthesized from the reaction of II and $[RuCl(\mu\text{-}Cl)(\eta^{6}\text{-}$ethylbenzoate$)]_2$. The calculated isotope distribution is shown on top 138
Figure 108. Synthesis of XII from $[RuCl(\mu\text{-}Cl)(\eta^{6}\text{-ethylbenzoate})]_2$ 139
Figure 109. Synthesis of $RuCl_2(\eta^{5}\text{-II})(PPh_3)$ (XIII) 141
Figure 110. ^{1}H-^{31}P HMBC spectrum of $RuCl_2(\eta^{5}\text{-II})(PPh_3)$ (XIII) in CD_2Cl_2 141
Figure 111. ^{1}H NMR spectrum of $RuCl_2(\eta^{5}\text{-II})(PPh_3)$ (XIII) in CD_2Cl_2 142
Figure 112. COSY spectrum of $RuCl_2(\eta^{5}\text{-II})(PPh_3)$ (XIII)in CD_2Cl_2 (H(2)-H(3) correlation is circled) 143
Figure 113. NOESY spectrum of $RuCl_2(\eta^{5}\text{-II})(PPh_3)$ (XIII) in CD_2Cl_2 (H(3)-H(4) correlation is circled) 145
Figure 114. ^{1}H-^{13}C HMBC spectrum of $RuCl_2(\eta^{5}\text{-II})(PPh_3)$ (XIII) in CD_2Cl_2 145
Figure 115. ^{1}H-^{13}C HSQC spectrum of $RuCl_2(\eta^{5}\text{-II})(PPh_3)$ (XIII) in CD_2Cl_2 146

List of Tables

Table 1. Selected bond lengths for [1-$C_9H_7PPh_2CH_2PPh_2$] and IV 72
Table 2. ^1H and ^{13}C NMR data for 1-$C_9H_7PPh_2CH_2PPh_2$ (IV) 76
Table 3. ^1H and ^{13}C NMR data for $C_9H_6PPh_3$ (I) and [CpRu(I)]PF_6 (V) 82
Table 4. ^1H and ^{13}C NMR data for 1-$C_9H_6PMePh_2$ (II) [CpRu(II)]PF_6 (VI) 87
Table 5. ^1H and ^{13}C NMR data for 1-$C_9H_6PMe_2Ph$ (III) and [CpRu(III)]PF_6 (VII) 91
Table 6. Selected bond lengths for [CpRu(1-$C_9H_6PPh_3$)]PF_6 (V) 95
Table 7. Selected bond lengths for [CpRu(1-$C_9H_6PMePh_2$)]PF_6 (VI) 96
Table 8. Selected bond lengths for [CpRu(1-$C_9H_6PMe_2Ph$)]PF_6 (VII) 97
Table 9. Calculated bond dissociation energies of the complexes [CpRu(Ligand)]$^+$ relative to C_6H_6 (kcal/mol) 98
Table 10. ^1H and ^{13}C NMR data for VIIIa 104
Table 11. ^1H and ^{13}C NMR data for chelating complexes VIIIb and VIIIc 109
Table 12. ^1H NMR data for the four inequivalent phenyl groups of VIIIb 110
Table 13. Calculated energies of isomers of [CpRu(IV)]PF_6 113
Table 14. Selected bond lengths for $RuCl_2(\eta^6$-*p*-cymene)(η^1-IV) (IX) 122
Table 15. ^1H and ^{13}C NMR data for $RuCl_2(\eta^6$-*p*-cymene)(η^1-IV) IX 125
Table 16. ^1H and ^{13}C NMR data for X (^{13}C data from HSQC and HMBC experiments) 130
Table 17. ^1H and ^{13}C NMR data for XI 132
Table 18. ^1H and ^{13}C NMR data for XII 134
Table 19. ^1H and ^{13}C NMR data for $RuCl_2(\eta^5$-II)(PPh_3) (XIII) 144

Chapter 1: Introduction

1.1 The Ramirez Ylide

In 1956, Ramirez and Levy reported the first of a new class of phosphonium ylides, triphenylphosphonium cyclopentadienylide which has subsequently been referred to as the "Ramirez ylide" (Figure **1**).[1-6] The Ramirez ylide was found to behave quite differently from previously characterized phosphonium ylides in that it had a relatively high dipole moment (7.0 D), was relatively stable, not decomposing in hot alkali solutions, and did not react with ketones to form olefins in the typical Wittig reaction.[1] The unusual properties of the Ramirez ylide were attributed to the electron delocalization over the five-membered ring in the zwitterionic resonance structure shown below.

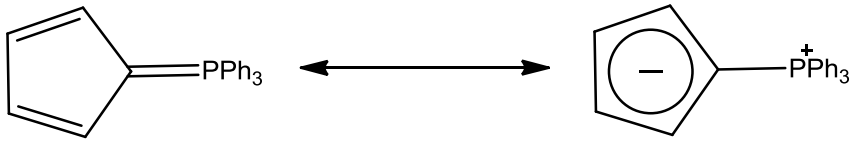

Figure 1. Resonance structures of the Ramirez ylide

Further corroboration for the increased contribution from the zwitterionic resonance structure came from X-ray crystallographic analysis which gave a C(1)-P bond length of 1.718 Å.[7] Typical P-Ph bond lengths are around 1.78 Å, while the $P=CH_2$ bond length of 1.66 Å in $PPh_3P=CH_2$ has significant double bond character and may be used to approximate a carbon-phosphorus double bond. Therefore, the P-C(1) bond in the Ramirez ylide is intermediate between a single and double bond. In addition, the ^{13}C NMR spectrum showed the carbon-phosphorus coupling constant was similar to that of a carbon-phosphorus single bond and that the ^{13}C chemical shift was similar to that of an aliphatic carbon.[8]

The zwitterionic resonance structure of the Ramirez ylide attracted the attention of coordination chemists due to its similarity to the cyclopentadienyl (Cp) anion. As the Cp anion is used throughout organometallic chemistry, and the Ramirez ylide has quite different electronic and steric properties, it was anticipated that the Ramirez ylide would have very interesting coordination chemistry itself. Thus, several research groups investigated the organometallic chemistry of the Ramirez ylide throughout the 1970's and into the 1980's. In the years since research has stagnated with few reports concerning the coordination of the Ramirez ylide or its derivatives to a transition metal until the Baird lab began investigating the field.

1.1.1 Ramirez Preparation of Phosphonium Cyclopentadienylides

The Ramirez ylide was prepared using the method outline in Figure **2**. The first step in this scheme is the reaction of two equivalents of triphenylphosphine with 1,3-dibromocyclopentene which was prepared by the reaction of cyclopentadiene with Br_2. This resulted in the formation of a diphosphonium salt which was then deprotonated twice with two equivalents of NaOH to yield the ylide in 41% yield. During the first deprotonation, one of the triphenylphosphine moieties was displaced, although this monophosphonium salt was not isolated.[1]

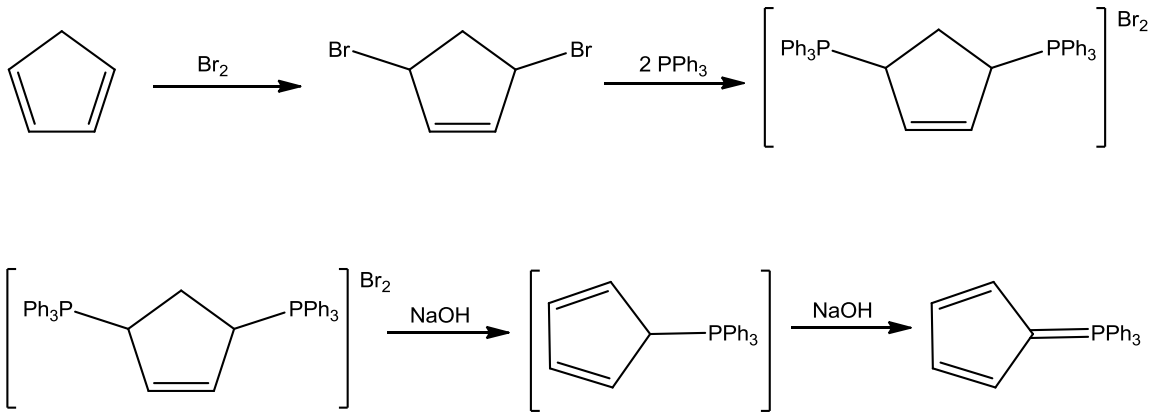

Figure 2. Synthesis of the Ramirez ylide

The use of phosphines other than PPh_3 has proven problematic using the method outlined in Figure **2** and Ramirez did not extend it to prepare other derivatives. The tri-n-propylphosphine derivative has been reported,[9] but it is the only known derivative prepared using the Ramirez methodology. Attempts to extend this method to prepare other phosphonium cyclopentadienylides in the Baird lab resulted in the formation of black tars, presumably from oligomerization or polymerization. Thus, while the Ramirez method works quite well for the PPh_3 analogue, it is not a general route to the synthesis of phosphonium cyclopentadienylides.

1.1.2 Mathey Preparation of Phosphonium Cyclopentadienylides

Mathey and Lampin[10] reported the synthesis of methyldiphenylphosphonium cyclopentadienylide using a method quite different method from that of Ramirez. First, cyclopentadienyl diphenyl phosphine was prepared from the reaction of TlCp and chlorodiphenylphosphine. This was then methylated with MeI and deprotonated by butyllithium to give the phosphonium cyclopentadienylide (Figure **3**).

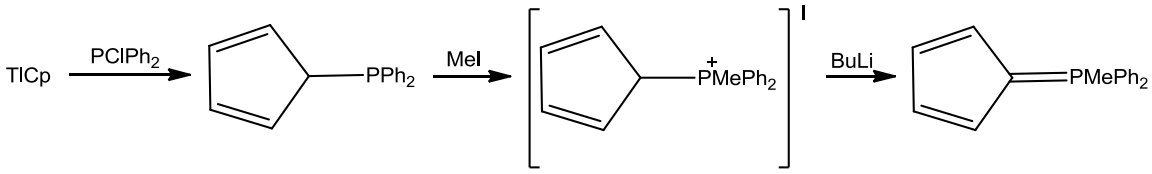

Figure 3. Preparation of $C_5H_4PMePh_2$ by Mathey and Lampin

Unfortunately, this method suffers from some major drawbacks of its own. While chlorodiphenylphosphine is relatively cheap, few chloro disubstituted phosphines are available and those which are available are generally quite expensive. This presents challenges for the synthesis of Ramirez ylide derivatives, especially in bulk quantities. In addition, the product of

the first reaction, $CpPR_2$ is thermally unstable, presumably undergoing a Diels-Alder dimerization reaction. It must be immediately reacted with a suitable electrophile to form the phosphonium salt, which is thermally stable. In principle, many carbon nucleophiles other than methyl iodide may be used; however, only the methyl derivative has been reported.

1.1.3 Phosphoium Cyclopentadienylides from Pyrylium Salts

In 2010, a rather serendipitous synthesis of phosphonium cyclopentadienylides was reported from the reaction of a phosphine with a trisubstituted pyrylium salt.[12] 2,4,5-Triphenylpyrylium perchlorate could be synthesized by the reaction of 2,4,5-triphenylcyclopentadiene with perchloric acid and oxygen (Figure **4**).[11] The proposed reaction mechanism (Figure 5) involves oxidation of the allylic C-H bond of the substituted cyclopentadiene followed by protonation of the resultant hydroperoxide and reaggangement to form the pyrylium salt.

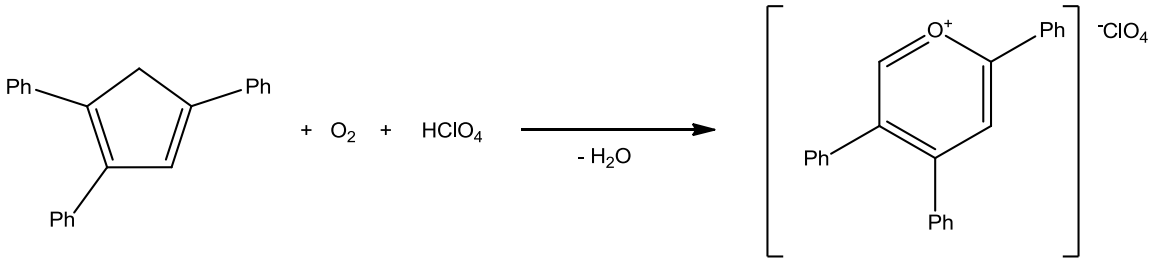

Figure 4. Synthesis of 2,4,5-triphenylpyrylium perchlorate

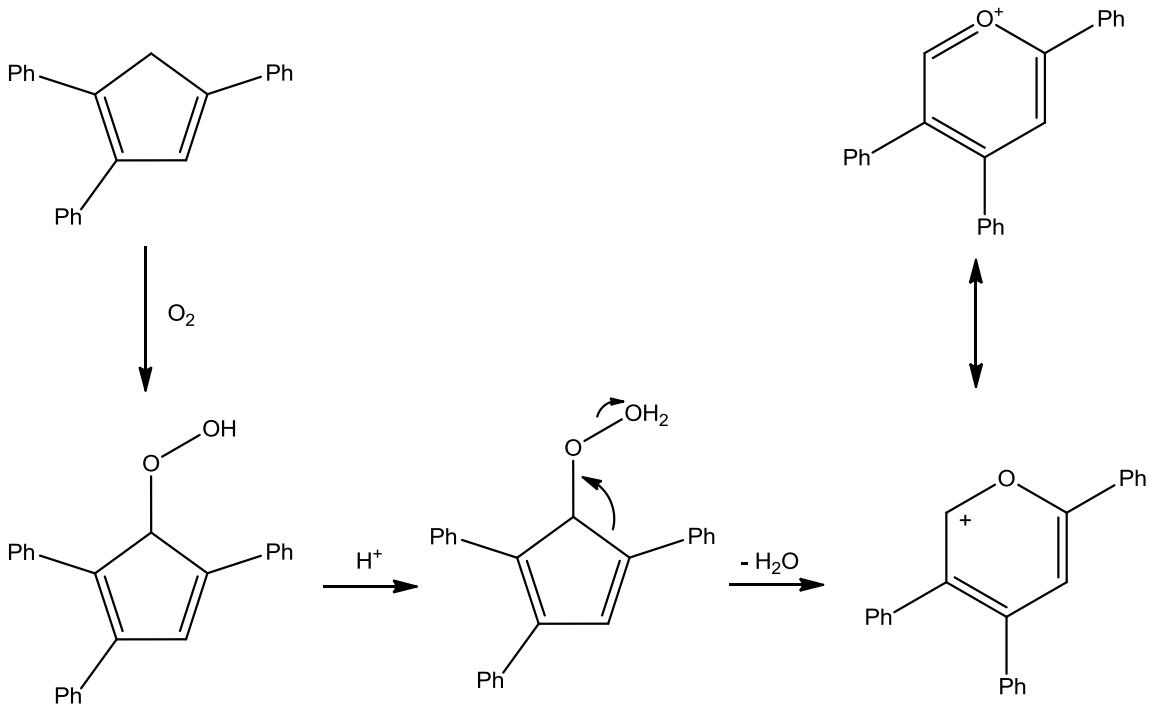

Figure 5. Proposed mechanism for the formation of 2,4,5-triphenylpyrylium perchlorate

The α-position of pyrylium salts bears a partial positive charge and should, therefore, be electrophilic. Various nucleophiles have been used to synthesize a wide range of cyclic and heterocyclic compounds which are often products of great interest to organic chemists. 2,4,5-triphenylpyrylium perchlorate reacts with a variety of phosphines at the unsubstituted α position to give 2,4,5-triphenylphosphonium cyclopentadienylides (Figure **6**).[12] The proposed mechanism (Figure 7) for this reaction involves attack of the phosphine at the unsubstituted α position of the pyrylium salt followed by tautomerization to the ring opened unsaturated ketone. This intermediate was isolated and characterized by X-ray crystallography and NMR spectroscopy. It was found to react with a second equivalent of phosphine to give the diphosphine complex. This complex can undergo an intramolecular Wittig reaction to give the triphenyl phosphonium 2,4,5-triphenylcyclopentadienyl cation with can be deprotonated with NaOH to give the phosphonium cyclopentadienylide.

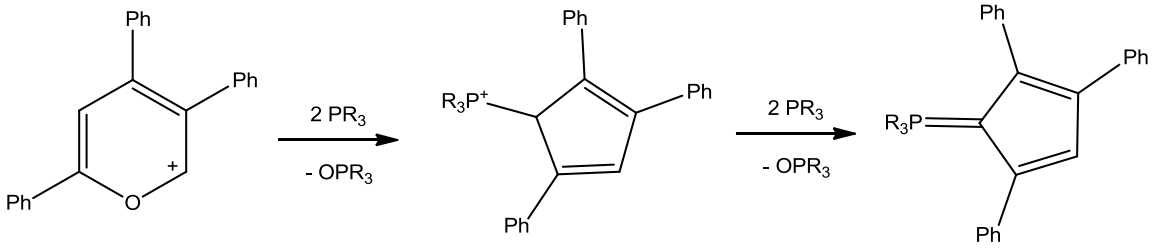

Figure 6. Synthesis of 2,4,5-triphenylphosphonium cyclopentadienylides from 2,4,5-triphenyl pyrylium salts

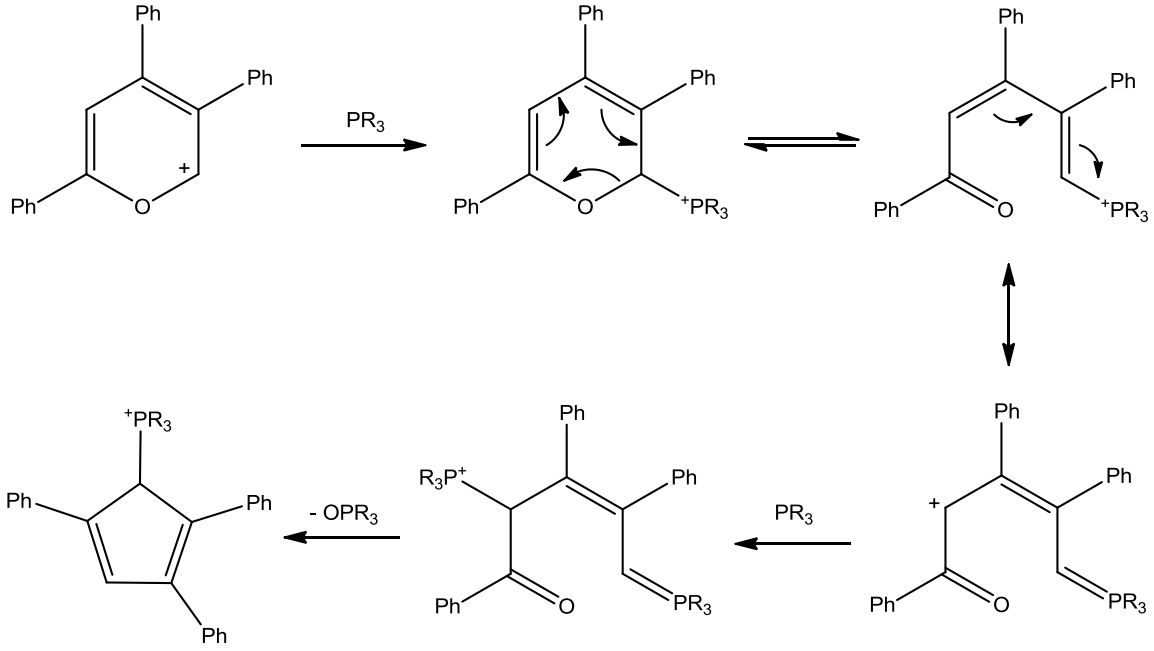

Figure 7. Synthesis of 2,4,5-triphenylphosphonium cyclopentadienyl cations. Deprotonation with NaOH gives the trisubstituted phosphonium cyclopentadienylides

The reaction is especially interesting in that, heretofore, no methodology had been developed to vary the phosphine substituent on the phosphonium cyclopentadienylides. Thus far, phosphonium 2,4,5-triphenylcyclopentadienylides have been prepared with four phosphines: PMe_3, PEt_3, PMe_2Ph and $PMePh_2$.[12] Unfortunately, there are no reports of less substituted pyrylium salts undergoing a similar reaction with a phosphine to yield phosphonium

cylcopentadienylides. This limits the utility of this reaction as phenyl groups attached to the C_5 ring may delocalize the negative charge of the zwitterionic resonance structure of the phosphonium cyclopentadienylides, resulting in a poorer electron donor and a weaker binding ligand.

1.1.4 Synthesis of Diphosphine Ramirez Ylide Derivatives

Derivatives of the Ramirez ylide with diphosphines have been reported using the same methodology as with monophosphines. Thus, 1,1-bis(diphenylphosphino)methane (dppm) was reacted with bromocyclopentadiene and deprotonated with KOH to form the ylide. $C_5H_4PPh_2CH_2PPh_2$ tautomerized and slowly polymerized at room temperature (Figure **8**).

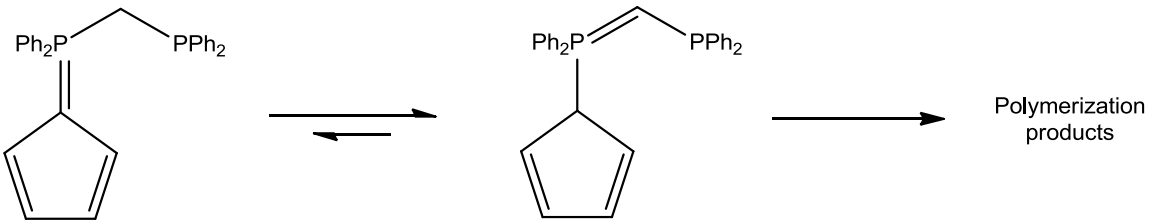

Figure 8. Tautomerization of $C_5H_4PPh_2CH_2PPh_2$

Problems also plagued the synthesis of the ethylene bridged derivative. Reacting 1,2-bis(diphenylphosphino)ethane (dppe) with bromocyclopentadiene resulted in the formation of the desired phosphonium salt along with formation the bisphosphonium salt (Figure **9**). The reaction of two equivalents of bromocyclopentadiene with dppm is unfavourable due to the decrease in nucleophilicity of the phosphine group upon formation of the phosphonium centre. This effect is diminished greatly on increasing the length of the carbon linker. The desired monophosphonium salt could be isolated and deprotonated with KOH giving the ylide in a 14% yield. The coordination chemistry of both of these phosphonium ylides has not been explored.

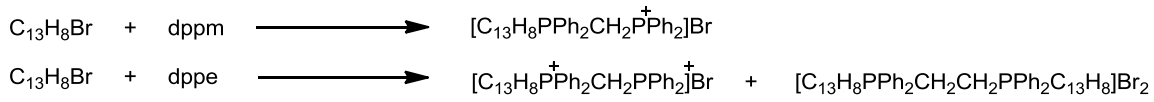

Figure 9. Reaction of bromofluorene with dppm and dppe showing formation of the bisphosphonium salt

1.1.5 Coordination of the Ramirez Ylide to Transition Metals

As mentioned earlier, due to the zwitterionic resonance structure of the Ramirez ylide being isoelectronic with both neutral arenes and the Cp anion, both of which are used extensively in coordination chemistry and catalysis, it was anticipated that the Ramirez ylide itself would form potentially interesting organometallic complexes. Since its discovery, there have been many reports of coordination of the Ramirez ylide to transition metals and this chemistry has been thoroughly reviewed.[13] The group 6 metal carbonyl species are among the most extensively studied and have allowed for comparison of the electronic properties of $C_5H_4PPh_3$ with both neutral arene and anionic Cp ligands. Ruthenium complexes with neutral arene and anionic Cp ligands have proven to be effective catalysts for a wide range of organic transformations (see Section 1.4). The usefulness of ruthenium-arene complexes as catalysts has not prompted investigation of similar ruthenium phosphonium cyclopentadienylide complexes. This may be due, in part, to the difficulty encountered in purifying coordination compounds of the Ramirez ylide. Often, unseparatable mixtures are obtained which are characterized by IR spectroscopy and elemental analysis. This has been a general problem in investigations of the coordination chemistry of the Ramirez ylide. The transition metal complexes (excluding those of group 8 metals which will be discussed in detail below) of the Ramirez ylide and $C_5H_4PMePh_2$ which have been characterized by X-ray crystallography are shown in Figure **10**.

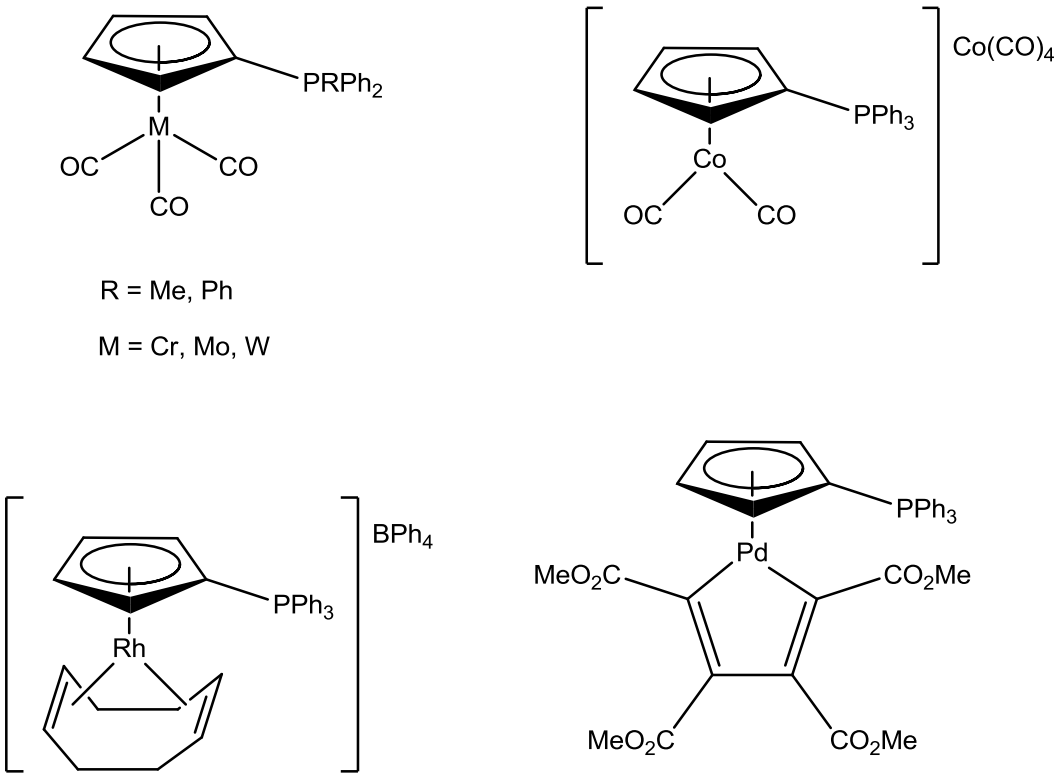

Figure 10. Transition metal complexes of phosphonium cyclopentadienylides which have been charactereized by X-ray crystallography (excludes complexes of group 8 metals)

It is well beyond the scope of this introduction to discuss the entirety of the known coordination chemistry of the Ramirez ylide; therefore, this section will include only a general discussion of the group 6 metal carbonyl species as these are among the most well characterized examples of Ramirez ylide coordination compounds, followed by a detailed discussion of the few ruthenium complexes that have been reported thus far. The coordination chemistry of the Ramirez ylide has been recently reviewed.[13]

The similarities between the zwitterionic resonance structure of the Ramirez ylide and benzene were noted by Wilkinson and it was hypothesized that complexes of the type $M(C_5H_4PPh_3)(CO)_3$ (M = Cr, Mo, W), analogous to previously characterized metal - arene complexes, $M(arene)(CO)_3$, could be easily prepared.[14] It was found that reaction of the Ramirez

ylide with the metal hexacarbonyls $Cr(CO)_6$ and $Mo(CO)_6$ in refuxing diglyme afforded the tricarbonyl species $Cr(C_5H_4PPh_3)(CO)_3$ and $Mo(C_5H_4PPh_3)(CO)_3$ in good yields (Figure **11**).[15] The corresponding tungsten complex could be prepared by reacting the Ramirez ylide with $W(MeCN)_3(CO)_3$ in diglyme at 110 °C (Figure **11**). These complexes were analyzed by IR and ^1H NMR spectroscopy and it was found that the C_5 ring protons shifted upfield considerably upon coordination. The tetraphenyl derivative of the Ramirez ylide, $C_5Ph_4PPh_3$ was reacted with $Mo(CO)_3(MeCN)_3$ in refluxing THF to form the molybdenum tricarbonyl species $Mo(C_5Ph_4PPh_3)(CO)_3$ in 60% yield.[16]

Group 6 metal complexes of $C_5H_4PMePh_2$, $(\eta^5\text{-}C_5H_4PMePh_2)M(CO)_3$ (M = Cr, Mo, W), have been prepared through a similar manner as those of the corresponding complexes of $C_5H_4PPh_3$ (Figure **11**). These complexes have been extensively characterized by NMR spectroscopy, IR spectroscopy an X-ray crystallography.

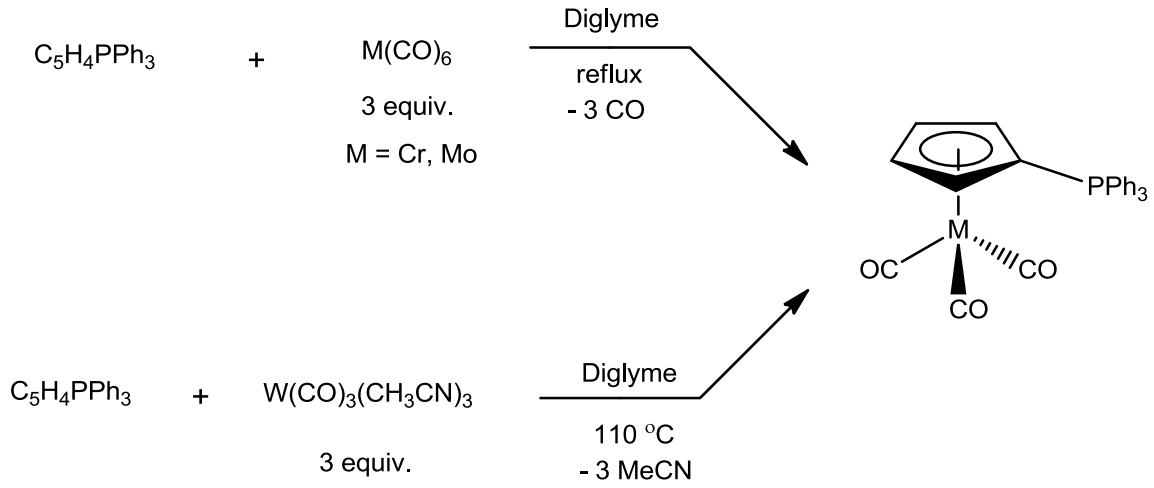

Figure 11. Synthesis of $(C_5H_4PPh_3)M(CO)_3$ (M = Cr, Mo, W)

Analyzing the complexes $M(C_5H_4PMePh_2)(CO)_3$ (M = Cr, Mo, W) by X-ray crystallography gives valuable insight into the electronic character of the ylide (Figure **12** for the Cr complex). In all cases, the P-C(1) bond length increased upon coordination to the metal center

from 1.727 Å to ~1.76 Å.[17] Thus, upon coordination there is an increase in the zwitterionic character of the phosphonium cyclopentadienylides which is to be expected, as it is this resonance structure that is primarily responsible for binding to the metal.

Upon coordination to a metal, the four ring protons of shifted upfield by at least 1 ppm while the P-Me group shifted downfield slightly. The upfield shift of the four ring protons is also observed in the related Ramirez ylide group 6 metal carbonyl complexes.[13] All five ring carbons also shift upfield considerably upon coordination by between 9 and 25 ppm.[17]

The complexes $M(C_5H_4PMePh_2)(CO)_3$ (M = Cr, Mo, W) were also characterized by IR spectroscopy in which two carbonyl stretching frequencies were observed. The peaks for the Cr complex were observed at 1915 and 1812 cm^{-1}, values which are intermediate between those of the isoelectronic species $(\eta^6\text{-}C_6H_6)Cr(CO)_3$ (1971 and 1892 cm^{-1}) and $[(\eta^5\text{-}C_5H_5)Cr(CO)_3]^-$ (1895 and 1778 cm^{-1}). Thus the electron donating properties of the ligand $C_5H_4PMePh_2$ lie between those of benzene and the Cp anion.

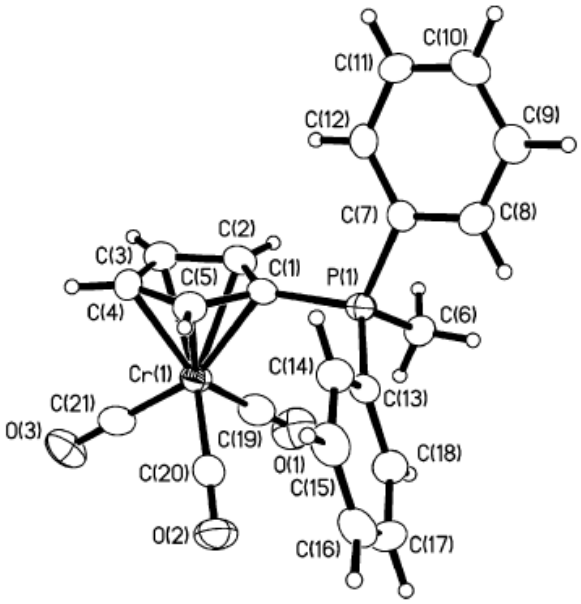

Figure 12. Molecular structure of $(C_5H_4PMePh_2)Cr(CO)_3$

DFT calculations on the complexes $(C_5H_4PMePh_2)M(CO)_3$ (M = Cr, Mo, W) suggest that donation from the HOMO and HOMO-1 orbitals of $C_5H_4PMePh_2$ into the d_{xy} and d_{yz} orbitals of chromium are the primary interactions involved in ligand binding. In addition, the computations suggest that the ylide-$Cr(CO)_3$ bond dissociation energy is some 30% higher than the analogous ring-metal dissociation energy of the arene complex $(\eta^6\text{-}C_6H_6)Cr(CO)_3$.[17]

There are three reports of coordination of the Ramirez ylide to ruthenium and a discussion of all three follows. In 1995, the Ramirez ylide was reacted with the cluster compound $Ru_6C(CO)_{17}$ and an excess of the decarbonylating agent trimethylamine N-oxide to afford $Ru_6C(CO)_{14}(C_5H_4PPh_3)$ (Figure **13**).[18] X-ray crystallography confirmed that the ylide was bound in an η^5 mode and the P-C(1) bond length was 1.793 Å; a value considerably longer than that of the uncoordinated ylide (1.718 Å). This finding can be attributed to an increase in contribution from the zwitterionic resonance structure of the Ramirez ylide upon coordination.[18]

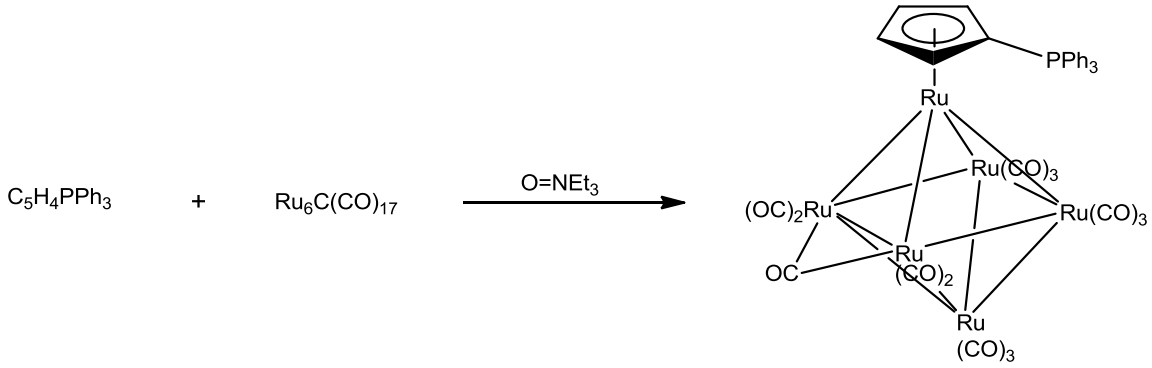

Figure 13. Synthesis of $Ru_6C(CO)_{14}(C_5H_4PPh_3)$

Interestingly, phosphines have been found to react with cationic ruthenium cyclopentadienyl complexes to form coordinated phosphonium cyclopentadienylides. In the first such report, $[CpRu(\eta^5\text{-}C_5H_4O)]_2[PF_6]_2$ reacted with nucleophiles including PMe_3, PPh_3 and PCy_3 to form disubstituted ruthenocenes (Figure **14**).[19] The tricyclohexylphosphine derivative was

analyzed by X-ray crystallography and the P-C(1) bond length was found to be 1.790 Å. Similar complexes were observed when PMe_3 and PCy_3 were reacted with the monomeric MeCN adduct of the previous starting material, $[CpRu(\eta^5\text{-}C_5H_4O)(MeCN)][PF_6]$; however, with PPh_3, substitution occurred at the cyclopentadienone ring affording the novel β-hydroxy derivative of the Ramierz ylide (Figure **14**).[19] The authors seem to be unaware of previous work involving the Ramirez ylide and no comparisons were made.

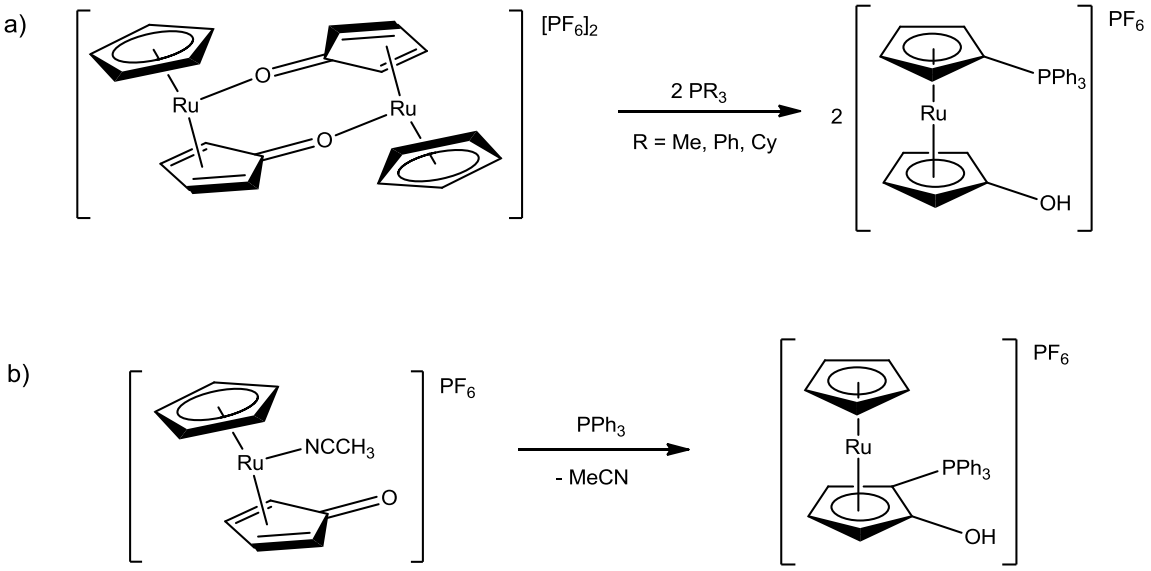

Figure 14. Reaction of PPh_3 with a) $[Ru(C_5H_5)(C_5H_4O)]_2$ and b) $Ru(C_5H_5)(C_5H_4O)(MeCN)$

In a similar manner, when PPh_3 was reacted with $[CpRu(Fv)RuCp][BF_4]_2$ (Fv = fulvalene) the 1'- bisubstituted ruthenocene shown in Figure **15** was formed as the major product.[20] The structure of this complex was confirmed by X-ray crystallography and the P-C(1) bond length was found to be 1.769 Å, a value somewhat shorter than that observed in previously characterized ruthenium phosphonium cyclopentadienylide complexes. Again, the authors did not mention the Ramirez ylide or any of its coordination compounds.

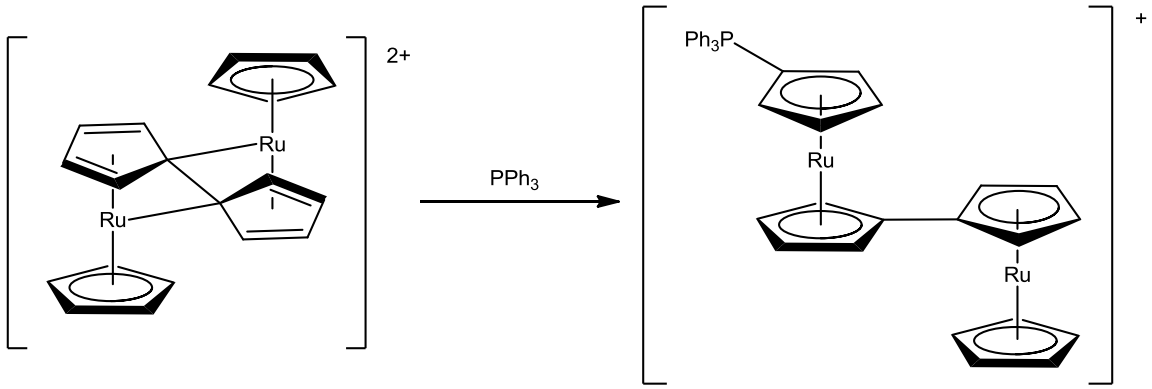

Figure 15. Reaction of $[CpRu(Fv)RuCp]^{2+}$ with PPh_3

1.1.6 Difficulties with the Ramirez Ylide

Many problems have plagued the use of phosphonium cyclopentadienylides and have resulted in stagnation in the field. Although there are three methods for the synthesis of these compounds, none allows for the synthesis of more than a few derivatives; hence the majority of the coordination chemistry of phosphonium cyclopentadienylides has focused on the Ramirez ylide. Many of these studies did not result in the formation of characterizable material. For example, in the only report of coordination of the Ramirez ylide to the group 4 metals zirconium and halfnium apparent 1:1 adducts of the metal tetrachlorides and the ylide were produced, but elemental analyses disagreed with the suggested composition and recrystallization proved impossible.[21] That there are no other reports of the synthesis of zirconium phosphonium cyclopentadienylide complexes is strange given the widespread use of zirconocene derivatives as catalysts for α-olefin polymerization.[22] While the synthesis of phosphonium cyclopentadienylide complexes with metals from nearly every group of the transition metal series have been attempted, there are few examples of complexes characterized by X-ray crystallography (Figure **10**). It has often proven difficult to purify the products resulting from the reaction of a metal precursor with phosphonium cyclopentadienylides. It is for these reasons that interest in the

chemistry of the Ramirez ylide and its derivatives stagnated for several decades until the field was reopened several years ago by the Baird lab.

1.2 Phosphonium Fluorenylides

The synthesis of 9-bromofluorene is straightforward and the product is stable. The reaction of 9-bromofluorene with triphenylphosphine followed by deprotonation with a suitable base affords triphenylphosphonium fluorenylide[23] and this was reported before Ramirez and Levy synthesized triphenylphosphonium cyclopentadienylide, although, little attention has been paid to it, and there are no reports of its coordination to a metal. Much later the dppm derivative was synthesized by the 1:1 reaction of dppm with 9-bromofluorene followed by deprotonation with $Ph_3P{=}CH_2$ in excellent yield (Figure **16**).[24] Unfortunately, single crystals were not analyzed by X-ray crystallography and the P-C(9) bond length remains unknown.

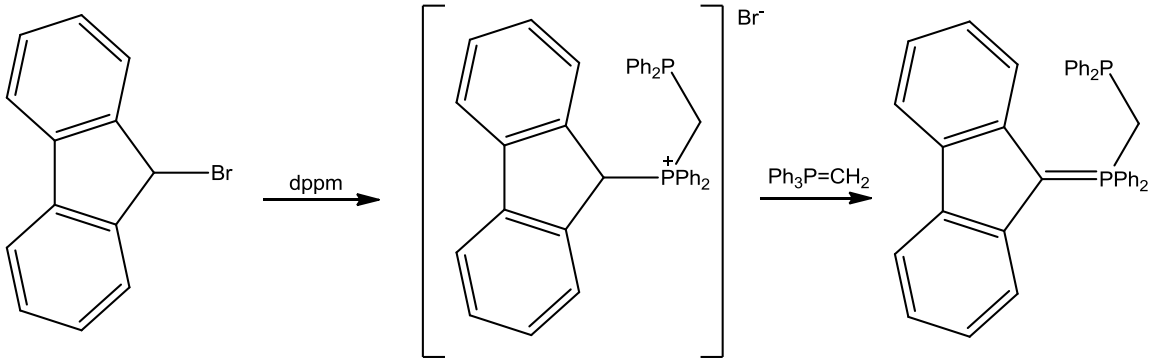

Figure 16. Synthesis of 9-dppm-fluorenylide

Complications arose upon going from the methylene to the ethylene and propylene bridged derivatives. As previously mentioned (see Section 1.1.4), the formation of a phosphonium centre decreases the nucleophilicity of a neighbouring phosphine. Thus, dppm only reacts with 9-bromofluorene in a 1:1 fashion and formation of the bisphosphonium salt is unfavourable. Increasing the length of the bridge between the phosphines decreases this effect

leading to both phosphine centres reacting with 9-bromofluorene. Thus, the reaction of dppe with 9-bromofluorene resulted in a 73% yield of the monosubstituted product and of a small amount of the bisphosphonium salt.[25] The monophosphonium salt could be deprotonated with $Ph_3P{=}CH_2$ to afford the monophosphonium fluorenylide with a pendant phosphine. The reaction with 1,3-bis(diphenylphosphino)propane (dppp) resulted only in formation of the bis-salt.[25] Again, these were not characterized by X-ray crystallography and, to date, these are the only reported phosphonium fluorenylides

1.2.1 Coordination of Phosphonium Fluorenylides

There is only one report detailing the synthesis of coordination complexes of phosphonium fluorenylides.[25] The reaction of dppm-fluorenylide with typical group 6 metal precursors $W(CO)_3(MeCN)_3$ and $Cr(CO)_6$ were reported resulting in the formation of M(dppm-fluorenylide)$(CO)_3$ (M = Cr, W) (Figure **17**). Although these complexes were only analyzed by IR and ^1H NMR spectroscopy, the phosphonium fluorenylide appeared to coordinate through both the pendant phosphine and in an η^1 mode through C(9); a coordination mode not observed with the Ramirez ylide.[25]

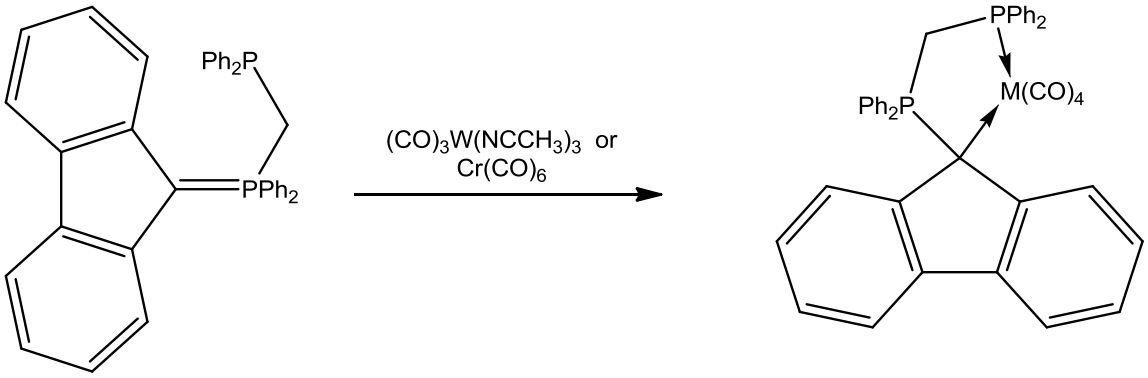

Figure 17. Synthesis of $(C_{13}H_8PPh_2CH_2PPh_2)M(CO)_4$ (M = Cr, W)

Similar coordination modes were observed when group 10 metal complexes were used. Thus, the reaction of $PdCl_2(PPh_2)_2$ with dppm-fluorenylide resulted in the formation of $PdCl_2(\eta^1{:}\eta^1$-dppm-fluorenylide) again, with coordination through both the pendant phosphine and C(9) (Figure **18**). The authors attributed this unprecedented coordination mode to the short linker between the five-membered ring and the pendant phosphine, which did not allow the metal to migrate to the five-membered ring of the fluorenylide.

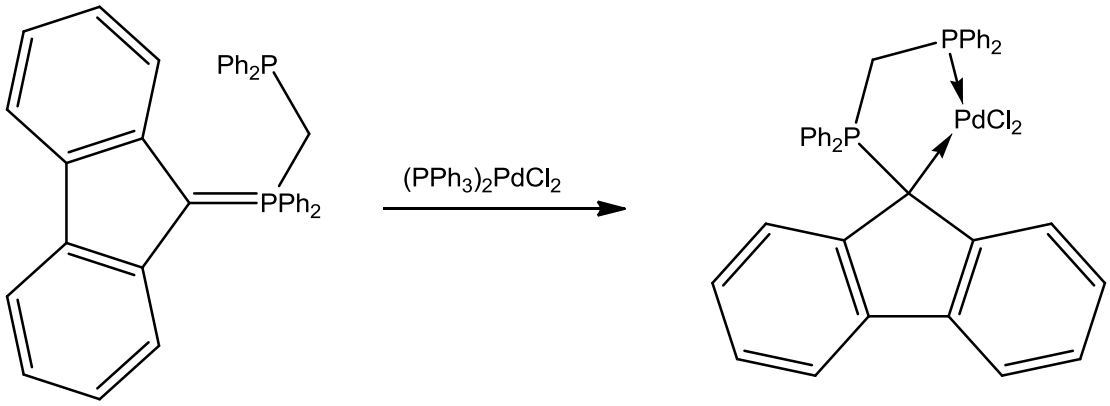

Figure 18. Synthesis of $(C_{13}H_8PPh_2CH_2PPh_2)PdCl_2$

1.2.2 Electronic Structure of the Phosphonium Fluorenylides

There is substantial evidence that the phosphonium fluorenylides have a very different electronic structure from the Ramirez ylide. Unlike the Ramirez ylide, the phosphonium fluorenylides do undergo Wittig reactions with aldehydes (Figure **19**) indicating that there is some localization of negative charge on C(9).[26] In addition, the reactivity of the phosphonium fluorenylides with dichlorocarbene is quite different from that of the phosphonium cyclopentadienylides. Treatment of triphenyl phosphonium fluorenylide with chloroform and KO^tBu affords the C(9) substituted product and the free phosphine (Figure **19**).[27] This product was not observed in a similar reaction with the Ramirez ylide.

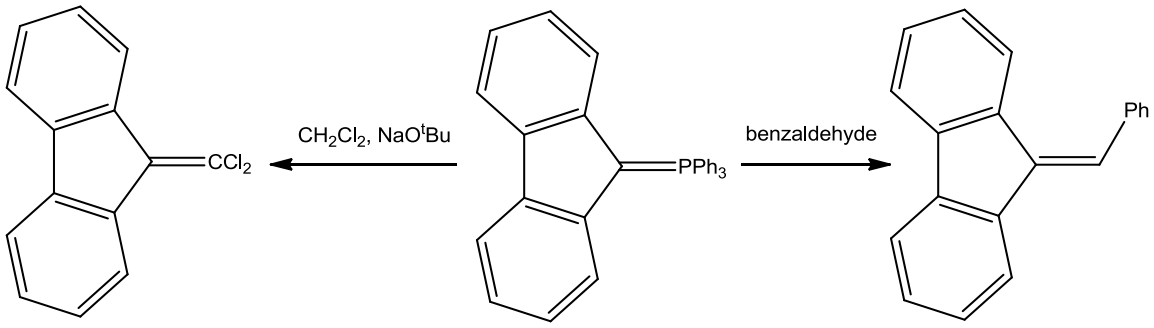

Figure 19. Reaction of triphenylphosphonium fluorenylide with dichlorocarbene and benzaldehyde

The depiction of the resonance structures of the Ramirez ylide in Figure **1** may be too simplistic; an additional zwitterionic resonance structure can be envisioned with a negative charge localized on the ylidic carbon. By analyzing reactivity patterns, this resonance structure makes little, if any, contribution in the Ramirez ylide; however, it appears to be very important for the phosphonium fluorenylides (Figure 20). Localization of charge on C(9) also explains the mode of coordination of the phosphonium fluorenylides to transition metals.

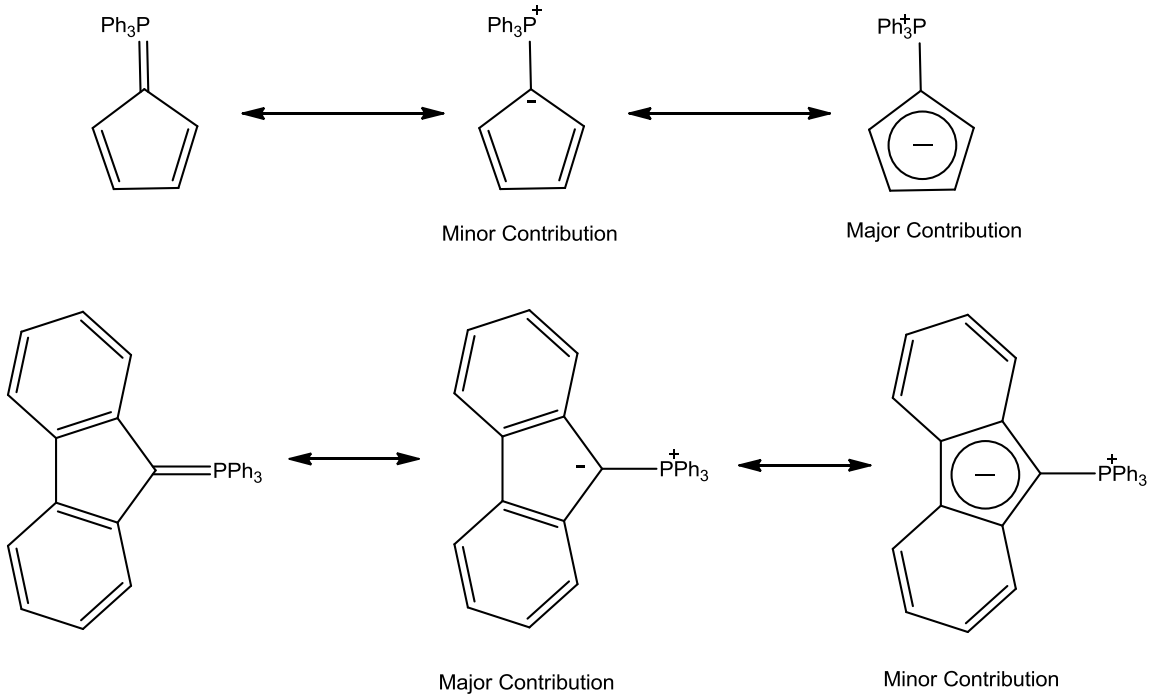

Figure 20. Resonance structures of $C_5H_4PPh_3$ and $C_{13}H_8PPh_3$

1.3 Phosphonium Indenylides (PHINs)

In 1967, Crofts and Williamson reported the synthesis of triphenylphosphonium indenylide[28] through a circuitous synthetic route which is described in Scetion 1.3.2 and it was expected that this compound would have similar properties to the related Ramirez ylide. Two resonance structures were proposed analogous to those of the Ramirez ylide; however, despite the aromatic nature of the zwitterionic structure, the coordination chemistry of this potential ligand was not investigated and no report involving phosphonium indenylides was published for several decades.

In 2004, Rufanov et al. reported the synthesis of two benzyldiphenylphosphonium indenylides, 1-$C_9H_6PPh_2(CH_2C_6H_5)$ and 1-$C_9H_6PPh_2(CH_2C_6F_5)$ by a method which will be detailed in Section 1.3.1.[29] Again, the coordination chemistry of these potential ligands with transition metals was not investigated. The Baird lab has since come up with a general method for the synthesis of phosphonium indenylides from 1-bromoindene.

Interestingly, one year before the report by Crofts and Williamson, 1-$C_9H_6PPh_3$ was apparently synthesized and its reactivity with dichlorocarbene was investigated.[30] The authors merely noted that they have produced a new phosphonium ylide and noted its melting point (213 – 214 °C) and elemental analysis. No other characterization method was mentioned, nor the synthetic procedure. Needless to say, given the difficulty in synthesizing 1-bromoindene (see Section 1.3.2), the veracity of this report is questionable.

1.3.1 PHIN Synthesis by Addition to $C_9H_7PPh_2$

A non-general method to synthesize phosphonium indenylides, analogous to that employed by Mathey *et al*. to prepare derivatives of the Ramirez ylide, involves the alkylation of 1-$C_9H_7PPh_2$ followed by deprotonation with a suitable base (Figure **21**).[29,31] 1-$C_9H_7PPh_2$ can be synthesized by lithiating indene and quenching with chlorodiphenylphosphine and, unlike $C_5H_4PPh_2$, does not undergo Diels-Alder dimerization; not needing to be used immediately as is required for $C_5H_4PPh_2$.[31] Reacting 1-$C_9H_7PPh_2$ with a carbon electrophile, usually an alkyl or benzyl iodide, followed by deprotonation with a base, such as NaH, affords the PHIN (Figure **21**). Although the stability of 1-$C_9H_7PPh_2$ towards dimerization makes this method to synthesize phosphonium indenylides more facile than phosphonium cyclopentadienylides, as with Mathey's preparation, this scheme is limited by the number of chlorodiaryl phosphines commercially available.

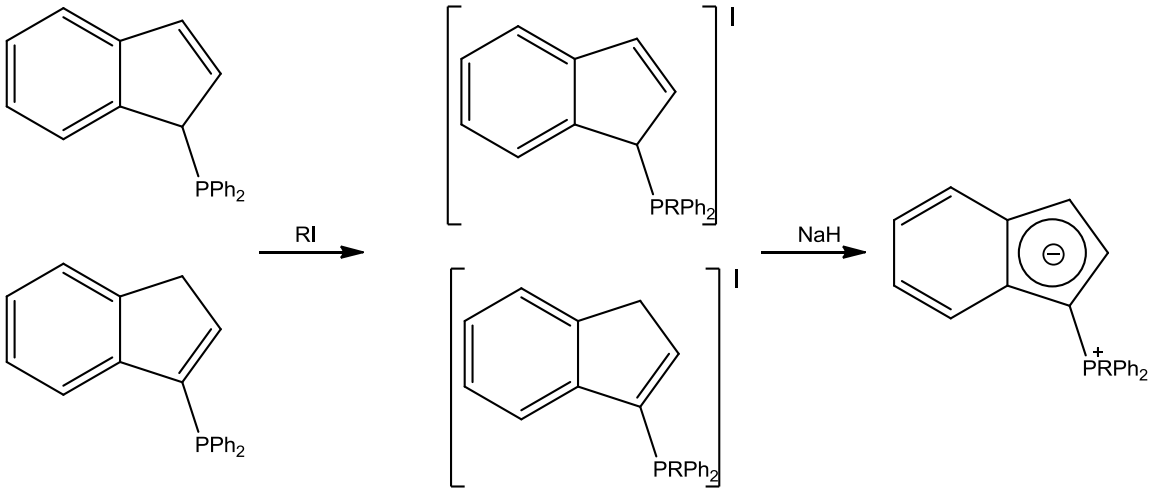

Figure 21. Synthesis of phosphonium indenylides by alkylation of 1-$C_9H_6PPh_2$

Utilizing this method, the PHINs 1-$C_9H_6PPh_2(CH_2C_6H_5)$ and 1-$C_9H_6PPh_2(CH_2C_6F_5)$ were reported in 2004.[29] Subsequently, the PHIN 1-$C_9H_6PMePh_2$ was synthesized in the Baird lab after which, it was compared to the related Ramirez ylide $C_5H_4PMePh_2$.[31]

1.3.2 PHIN Synthesis from 1-Bromoindene

Many phosphonium ylides are synthesized by the reaction of a phosphine with an alkylbromide or alkyliodide followed by deprotonation with a strong base. Therefore, a general route into PHIN ligands involves the synthesis of 1-bromoindene; a target that has proven difficult to synthesize. In 1944 it was reported that 1-bromoindene could be formed in low yield by the reaction of indene with N-bromosuccinimide.[32] Later, Crofts and Williamson found that this method gave extremely low yields (<5%) and was very inconsistent.[28] It is likely that 1,2-bromoindene is formed in this reaction.

An alternative route to 1-bromoindene involves purposely forming 1,2-dibromoindene and then eliminating HBr with 2,6-lutidine to form 1-bromoindene again in low yield (Figure **22**).[28] 1-bromoindene was then treated with triphenylphosphine for two weeks resulting in

formation of the phosphonium salt [1-$C_9H_7PPh_3$]Br which was subsequently deprotonated with ammonia yielding 1-$C_9H_6PPh_3$. This product was, unfortunately, not fully characterized, and there remains some ambiguity as to the efficacy of the reaction. Notably, it has been suggested that the elimination of HBr from 1,2-dibromoindane should favour the formation of 3-bromoindene.[33]

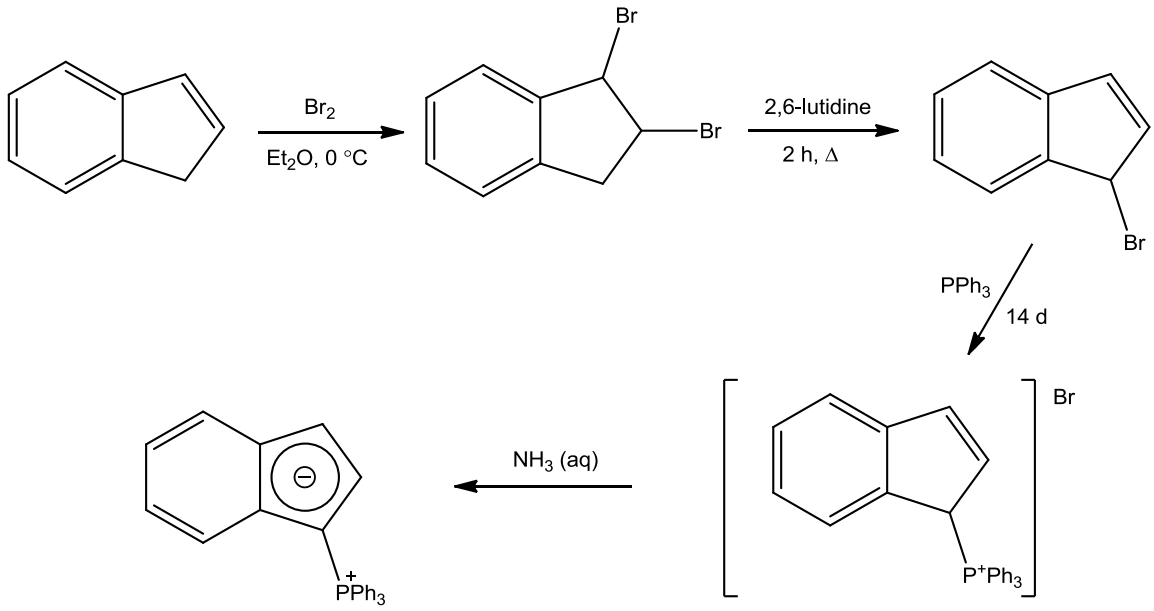

Figure 22. Synthesis of triphenylphosphonium indenylide reported by Crofts and Williamson

A more efficient synthesis of 1-bromoindene was developed in 1980 which takes advantage of the ease of C-Si bond cleavage by electrophiles (Figure **23**).[33,34] In this scheme, indene is lithiated and then quenched with chlorotrimethylsilane to afford 1-trimethylsilyl indene. This can then be reacted with dioxane dibromide to give, after column chromatography, 1-bromoindene in a moderate yield (< 50%). Unfortunately, even after a column, the product is often still impure and must be passed through multiple columns to get pure 1-bromindene. In addition, the reaction is light sensitive and dioxane dibromide, a highly thermally unstable complex, must be added dropwise to a reaction flask at -78 °C thus presenting a challenge simply to set the reaction up.[34]

Reacting 1-bromoindene with a phosphine, such as PPh_3, results in the slow formation of a phosphonium salt which exists as a mixture of regioisomers as shown in Figure **23**. The ratio of the two regioisomers seems to vary randomly from batch to batch. Deprotonation of both regioisomers of the phosphonium salt with NaH results in the slow formation of the green phosphonium indenylide in good yield (Figure **23**).

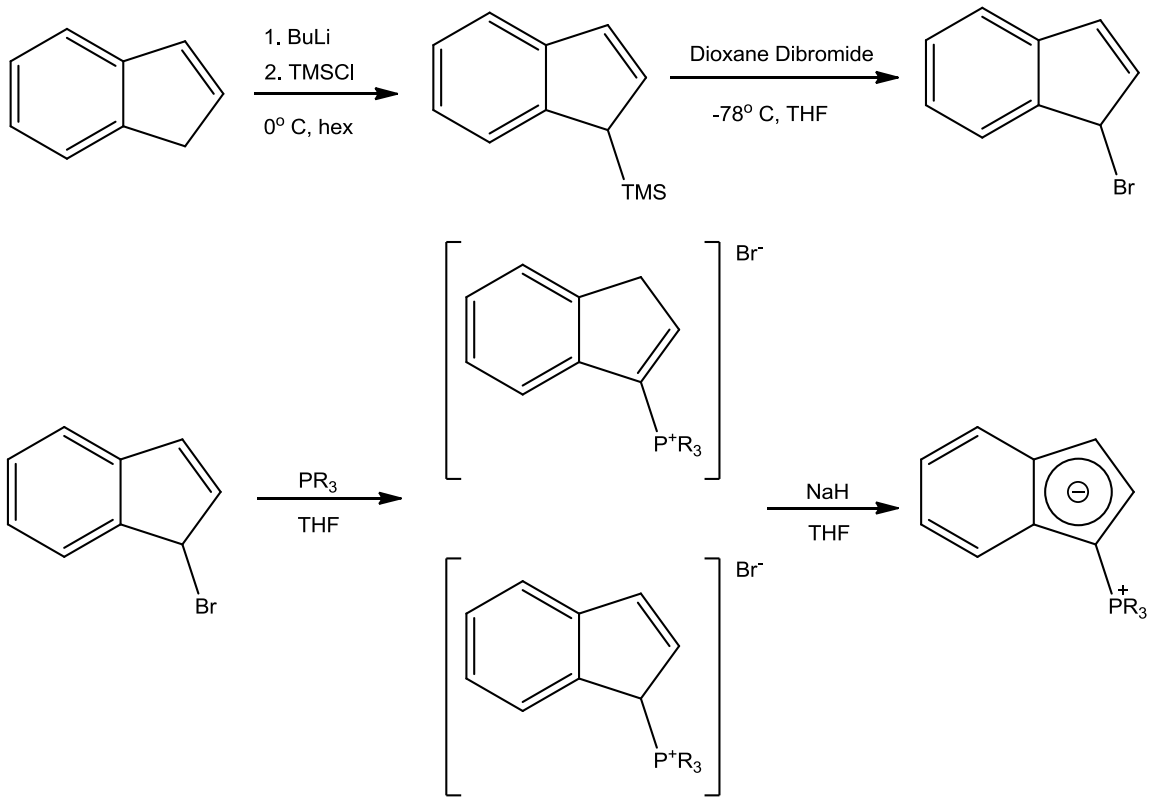

Figure 23. Synthesis of 1-$C_9H_6PPh_3$ using dioxane dibromide as brominating agent

1.3.3 Interest in Phosphonium Indenylides

There are several reasons why PHINs may be interesting ligands in transition metal chemistry. As PHINs have similar electronic structure to the phosphonium cyclopentadienylides, they also have electron donating abilities intermediate between those of the Cp anion and neutral arenes. The experimental confirmation of this will be discussed in Section 1.3.4. Transition metal

complexes of both types are extremely common and widely used in catalysis as we expect that the PHINs will also show promise as ligands in coordination chemistry.

One of the major drawbacks to widespread use of phosphonium cyclopentadienylides was the lack of a general synthetic method for their synthesis. The scheme outlined in Figure **23** is a general method for the synthesis of PHINs, thus allowing the effects of varying the phosphine on the electronic and steric environments of PHIN transition metal complexes to be explored. Fine tuning of these properties is of utmost importance in catalyst design.

Finally, PHINs are pro-planar chiral with the result that chiral compounds are formed upon complexation with a metal (Figure **24**). Section 1.3.4 details the synthesis and characterization of such a planar chiral chromium PHIN complex. The coordination of a planar chiral moiety directly to a catalytically active metal centre may yield effective catalysts for asymmetric organic transformations.

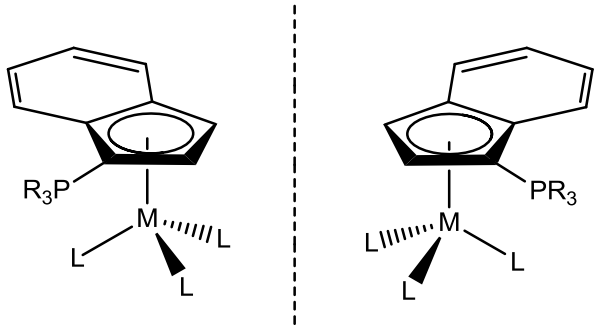

Figure 24. Planar chirality of PHIN ligands

1.3.4 Phosphonium Indenylide Coordination to Cr

Coordination of 1-$C_9H_6PMePh_2$ to Cr can be effected using a similar procedure to that employed for the Ramirez ylide and $C_5H_4PMePh_2$ (*vide supra*). Thus, $Cr(CO)_6$ was refluxed in diglyme with 1-$C_9H_6PMePh_2$ to generate $Cr(\eta^5\text{-}1\text{-}C_9H_6PMePh_2)(CO)_3$ (see Figure **25**) in moderate

yield and this product was analyzed by IR and NMR spectroscopy and X-ray crystallography.[31] The IR spectrum of this complex exhibited *v*(CO) at 1916 (s), 1816 (s) and 1802 (sh) cm^{-1} which are very similar to those of the related phosphonium cyclopentadienylide complex $Cr(\eta^5\text{-}C_5H_4PMePh_2)(CO)_3$ (1915 and 1812 cm^{-1}) (see Section 1.1.5). The electron donating properties of PHINs are therefore similar to those of the phosphonium cyclopentadienylides.

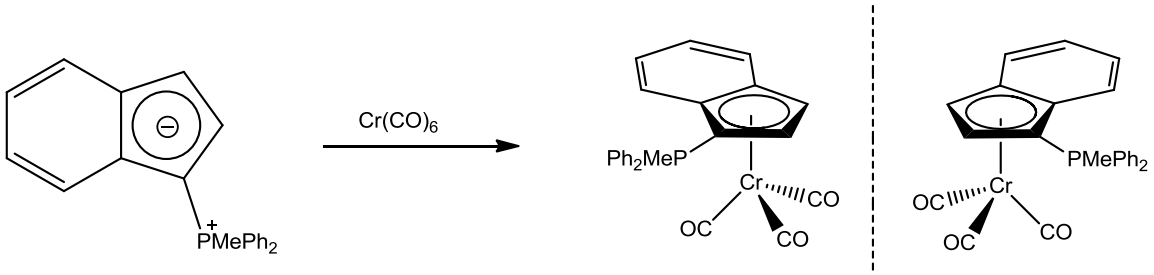

Figure 25. Synthesis of planar chiral PHIN complexes $(1\text{-}C_9H_6PMePh_2)Cr(CO)_3$

The NMR spectra of $Cr(\eta^5\text{-}1\text{-}C_9H_6PMePh_2)(CO)_3$ showed many differences from the uncoordinated ylide. In the ^1H NMR spectrum, the two C_5 ring protons shifted upfield by over 1 ppm. Similar shifts upon coordination have been observed for the related phosphonium cyclopentadienylides.[17] The P-Me moiety shifted downfield somewhat, while the phenyl region remained mostly unchanged.[31]

The ^{13}C spectrum showed upfield shifts for all C_5 ring carbons by as much as 30 ppm as compared to the uncoordinated ylide. Coordination of phosphonium cyclopentadienylides is accompanied by a somewhat smaller upfield shift.[17] The two phenyl groups in $Cr(\eta^5\text{-}1\text{-}C_9H_6PMePh_2)(CO)_3$ are expected to be diastereotopic as the PHIN ligand is pro-planar chiral (see Figure **24**) and it was thus revealing to observe that there were two sets of peaks in the phenyl region, each with identical coupling constants.[31]

Upon coordination, the P-C(1) bond length increased from 1.711 Å to 1.753 Å, indicating an increase in single bond character. However, this bond length is still intermediate between a P –

C single bond (P-Ph average is 1.788 Å) and a P-C double bond ($P=CH_2$ in $Ph_3P=CH_2$ is 1.66 Å and, as a non-stabilized ylide, has significant double bond character). Again, these values are similar to those observed for related phosphonium cyclopentadienylide complexes.[17]

Interestingly, two of the Cr-C bonds lengths in the C_5 ring are significantly longer than the remaining three. Thus, while the bonds C(1)-Cr, C(2)-Cr and C(3)-Cr are between 2.16 and 2.2 Å, the remaining two bonds, C(4)-Cr and C(5)-Cr are lengthened to over 2.55 Å. This is not similar to the analogous phosphonium cyclopentadienylide complexes in which all M-C_5 ring bond lengths are similar in length. The Cr-C bond lengths in $Cr(\eta^5\text{-}C_5H4PMePh_2)(CO)_3$ seem to vary randomly over the range 2.18 – 2.25 Å. Similar complexes with Mo and W also showed no general trend in bond lengths.[17]

1.4 Ruthenium(II) Arene Compounds

Ruthenium compounds have found extensive use as catalysts in organic synthesis and this field has been reviewed extensively.[35-37] The chemistry of π-arene ruthenium(II) complexes received considerable attention over the past several decades motivated in part by the applications of these complexes in organic synthesis.[38,39] Ruthenium arene complexes have been used extensively as catalysts for many classes of reactions, most notably: Diels-Alder reaction,[40-43] enyne cycloaddition,[44] asymmetric transfer hydrogenation,[45] alkene metathesis[46-50] and C-H bond activation.[51] This section will detail the typical methods to synthesize ruthenium arene complexes.

1.4.1 Ruthenium(II) Arene Compounds from Cyclohexadienes

By far the most common precursors used to prepare ruthenium arene complexes are the chloro-bridged dimers $[RuCl(\mu\text{-}Cl)(\eta^6\text{-arene})]_2$.[52,53] These are readily synthesized by the oxidation

of 1,3- or 1,4- cyclohexadiene derivatives with $RuCl_3 \cdot xH_2O$ in ethanol or methanol (Figure **26**). One of the most common complexes of this type is $[RuCl(\mu\text{-}Cl)(\eta^6\text{-}p\text{-cymene})]_2$ due in part to the fact that the dienes it can be made from, α-phellandrene or limonene, are inexpensive (Figure **26**). A wide variety of chloro-bridged ruthenium arene complexes have been synthesized, including many with functional groups attached to the arene ring and the scope of this chemistry is too large for inclusion here.[54]

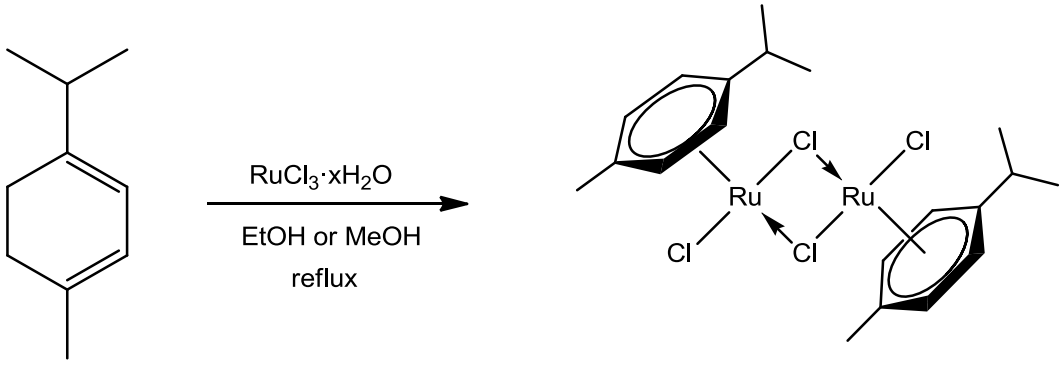

Figure 26. Synthesis of $[RuCl(\mu\text{-}Cl)(\eta^6\text{-}p\text{-cymene})]_2$ from α-phellandrene

Chloro-bridged ruthenium arene dimers, such as $[RuCl(\mu\text{-}Cl)(\eta^6\text{-}p\text{-cymene})]_2$, are attractive starting materials for ruthenium(II) arene chemistry for several reasons. The chloride bridge can be readily cleaved by nucleophiles (L) to form complexes of the type $RuCl_2(\eta^6\text{-arene})(L)$ (Figure **27**).[53,55] The scope of nucleophiles used is quite broad, with amine and phosphine donor ligands being among the most common. With phosphines, such as PPh_3, this reaction proceeds quantitatively at room temperature within 0.5 h to form $RuCl_2(\eta^6\text{-arene})(PPh_3)$.[56] Second, the chloride ligands can be replaced with neutral ligands to prepare the cationic and dicationic complexes $[RuClL_2(\eta^6\text{-arene})]^+$ and $[RuL_3(\eta^6\text{-arene})]^{2+}$ again with amine, alcohol, phosphine and arsine donors being the most common. Typically, the choride ligand is removed with the sodium or silver salt of a bulky anion (Figure **27**). One of the more interesting examples of breaking the chloride bridge followed by removal of a chloride ligand is in the

formation of ruthenium arene complexes which function as catalysts for the asymmetric transfer hydrogenation of ketones (see below). Third, the chloride ligands can be easily replaced with other anionic ligands through a metathesis reaction. Using these methods and combinations thereof, there is a rich chemistry involving chloro-bridged ruthenium arene complexes.

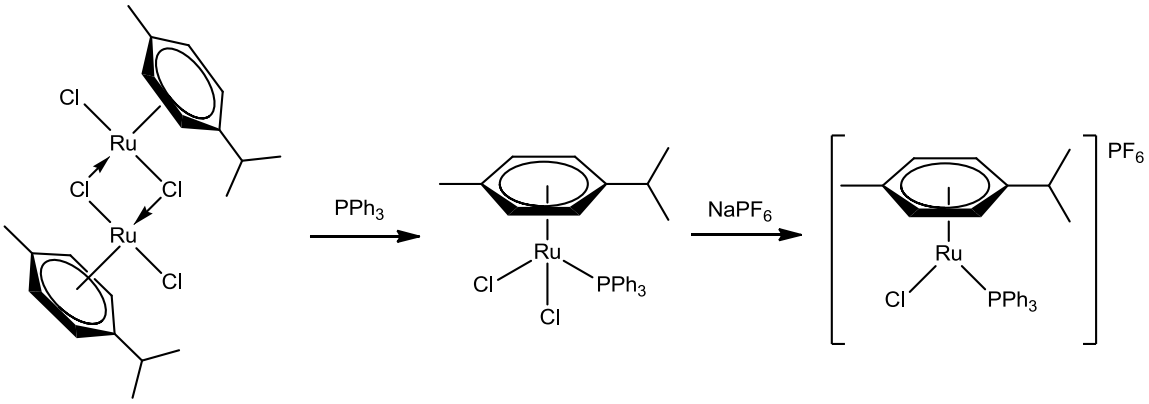

Figure 27. Breaking the chloride bridge of $[RuCl(\mu\text{-}Cl)(\eta^6\text{-p-cymene})]_2$ with PPh_3 followed by removal of a chloride ligand to form a cationic ruthenium(II)-arene complex

One of the major goals of ruthenium-arene chemistry is the synthesis of complexes which can catalyze asymmetric organic reactions. The product arising from breaking the chloride bridge of $[RuCl(\mu\text{-}Cl)(\eta^6\text{-arene})]_2$ with a ligand (L), $RuCl_2(\eta^6\text{-arene})(L)$, is pseudo-tetrahedral and chiral-at-metal complexes may therefore be formed by removing one of the chloride ligands. Computational studies suggest that unsaturated 16-electron species generated from loss of such a ligand rapidly racemize.[57] There are many examples of coordinatively saturated chiral-at-metal ruthenium-arene complexes in which isomerization is observed.[58] While chiral-at-metal piano stool complexes are well known, they have only been able to effect asymmetric organic reactions stoichiometrically.[57]

The majority of chiral ruthenium-arene catalysts have a chiral nucleophilic ligand. A prominent series of examples are the chiral ruthenium piano stool complexes first reported by Noyori which have been used to catalyze the asymmetric transfer hydrogenation of ketones.

Typically a chiral 1,2-diamine[59,60] or β-aminoalcohol[61] is reacted with $[RuCl(\mu\text{-}Cl)(\eta^6\text{-arene})]_2$ and a base such as KOH. To form the active catalyst, first the chloride bridge of $[RuCl(\mu\text{-}Cl)(\eta^6\text{-arene})]_2$ is broken with the amine acting as a nucleophile. Two equivalents of KOH are then required to remove two chloride ligands and deprotonate the 1,2-diamine or β-aminoalcohol twice to form the active catalyst (Figure **28**).[62] With (1*S*,2*S*)-*N*-p-toluenesulfonyl-1,2-diphenylethylenediamine (*S*,*S*-TsDPEN) as chiral diamine the complex Ru(*S*,*S*-TsDPEN)(arene) is formed (Figure **28**) which catalyzes the asymmetric transfer hydrogenation of acetophenone in 98% yield and 97% ee.[59]

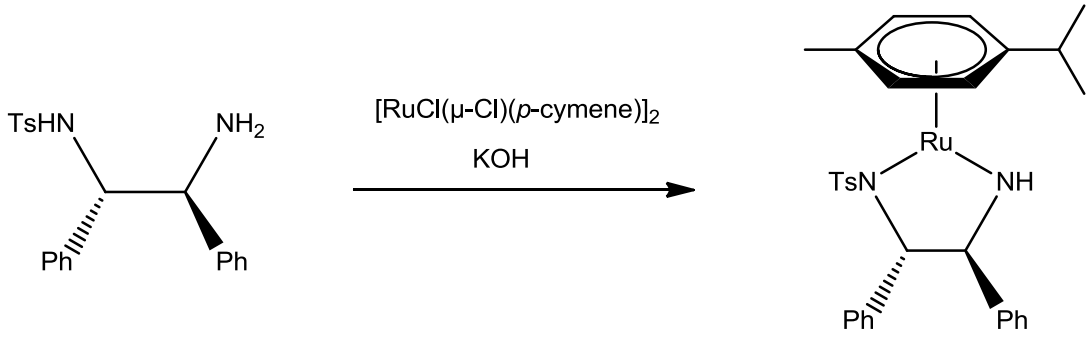

Figure 28. Synthesis of the asymmetic transfer hydrogenation catalyst Ru(*S*,*S*-TsDPEN)(*p*-cymene)

1.4.2 Arene Exchange Reactions of Ruthenium(II) – Arene Complexes

While the synthesis of complexes of the type $[RuCl(\mu\text{-}Cl)(\eta^6\text{-arene})]_2$ is quite facile from the corresponding 1,3- or 1,4-cyclohexadiene, in many cases, these dienes are not readily available. The most common synthetic route to 1,4-cyclohexadienes is the Birch reduction; however, the substrate scope of this reaction is limited. In order to overcome these problems, arene exchange reactions have been explored in which an easily formed ruthenium(II) arene dimer $[RuCl(\mu\text{-}Cl)(\eta^6\text{-arene}^1)]_2$ is reacted with a second arene at elevated temperature to form

$[RuCl(\mu\text{-}Cl)(\eta^6\text{-arene}^2)]_2$. Similarly, arenes with a donor atom attached through a short hydrocarbon chain may easily cleave the chloride bridge and then undergo intramolecular arene exchange at elevated temperature (see Section 1.4.3). In the past two decades, these strategies have been used to synthesize a range of ruthenium(II) arene complexes that can't be readily made from cyclohexadienes.

The generally accepted mechanism for arene exchange on any metal centre involves successive changes in hapticity of the arene ligand from η^6 to η^4 to η^2 before being released either before, or during attack of the incoming arene ligand. These reactions typically require temperatures greater than 100 °C, especially if the solvent is either aromatic or non-coordinating because the generation of highly unsaturated species is energetically unfavourable.[63] The stability of arene ligands across a given $M(arene)L_3$ series has been found to be directly correlated with electron donating ability.[63-65] Thus, arenes with electron donating substituents form stronger metal-arene bonds than benzene while those with electron accepting substituents form weaker metal-arene bonds.[54]

The first example of exchange of an arene ligand on ruthenium(II) was in the synthesis by Bennett of $[RuCl(\mu\text{-}Cl)(\eta^6\text{-}C_6(CH_3)_6)]_2$ which was prepared by adding $[RuCl(\mu\text{-}Cl)(\eta^6\text{-}p\text{-cymene})]_2$ to molten hexamethylbenzene.[66] Unreacted hexamethylbenzene was removed by washing with hexanes and decanting. Drying the resulting red-brown solid under reduced pressure gave $[RuCl(\mu\text{-}Cl)(\eta^6\text{-}C_6(CH_3)_6)]_2$ in 80% yield.

Similarly, the trindane complex $[RuCl(\mu\text{-}Cl)(\eta^6\text{-trindane}]_2$ was prepared in good yield by adding $[RuCl(\mu\text{-}Cl)(\eta^6\text{-}p\text{-cymene}]_2$ to an excess of molten trindane for four days (Figure **29**) and then washing the orange product with hexanes and Et_2O.[67] NMR studies concluded that the neutral complex is in equilibrium with an ionic isomer, $[((trindane)Ru)_2(\mu\text{-}Cl)_3]Cl$. In polar solvents, such as CD_3NO_2, the equilibrium was shifted almost completely to the ionic isomer. The formation of the ionic isomer was attributed to the increased steric bulk of the trindane ligand.[67]

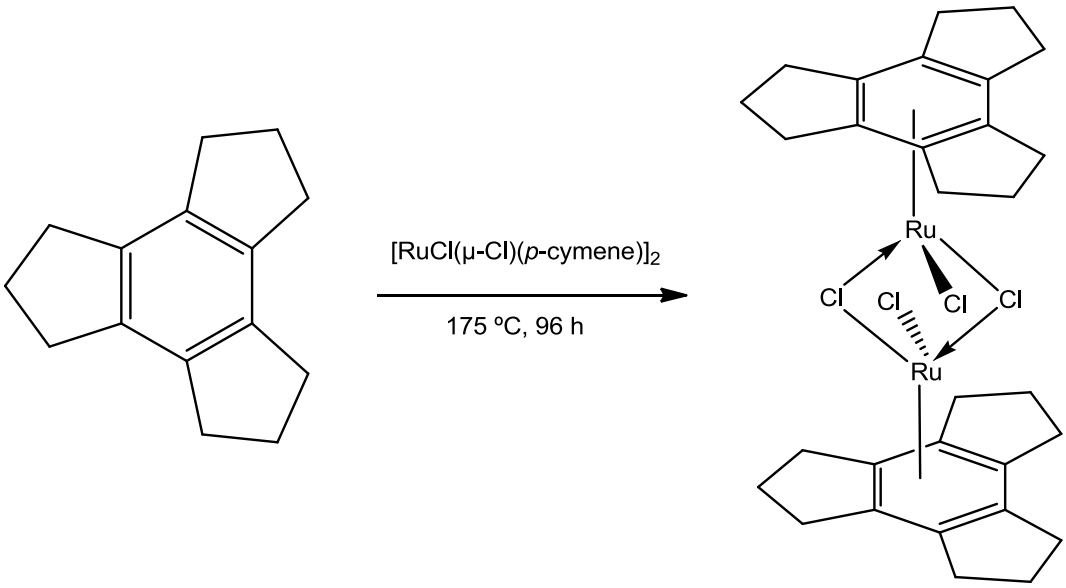

Figure 29. Synthesis of $[RuCl(\mu\text{-}Cl)(trindane)]_2$

Green and co-workers found that the ^1H NMR spectrum of $(\eta^6\text{-}C_6H_6)RuH(\eta^1\text{-}C_6H_5)(PMe_3)$ in deuterated benzene became very different upon heating to 80 °C overnight. Both arene ligands and the hydride had exchanged with deuterated benzene to give $(\eta^6\text{-}C_6D_6)RuD(\eta^1\text{-}C_6D_5)(PMe_3)$ in over 80% yield (Figure **30**).[68] Heating the benzene complex with toluene, *o*-xylene or *m*-xylene to 100 °C for several days resulted in similar exchange processes. Heating mesitylene or p-xylene with $(\eta^6\text{-}C_6H_6)RuH(\eta^1\text{-}C_6H_5)(PMe_3)$ to 100 °C for four days resulted in exchange of only the $\eta^6\text{-}C_6H_6$ moiety (Figure **30**). This was attributed to steric hindrance from the σ-methyl group.[68]

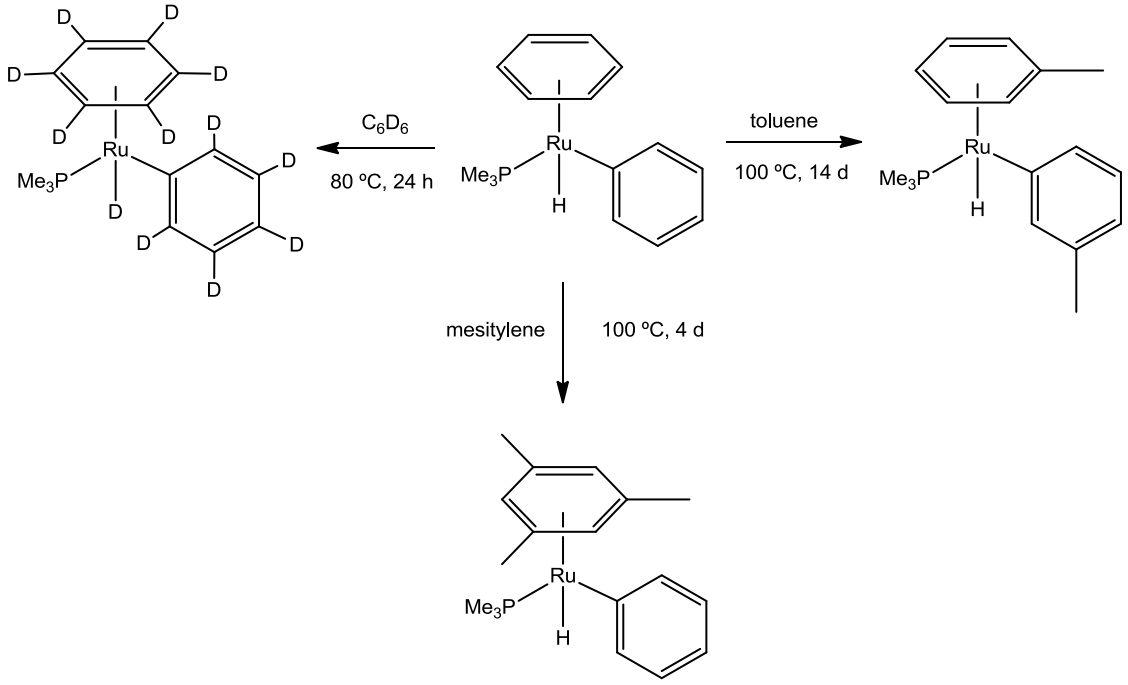

Figure 30. Arene exchange reactions of (η^6-C_6H_6)RuH(η^1-C_6H_5)(PMe_3) with deuterated benzene, toluene and mesitylene

There is one example of arene exchange on a ruthenium(II) complex occurring at room temperature. The ligand (9,9-dimethylxanthene-4,5-diyl)(bis-dimethylsilyl), or xantsil, is a strongly electron donating ligand with an ether linkage that may coordinate to a metal centre. The complex Ru(CO)(xantsil)(η^6-toluene) exchanged the toluene moiety with the solvent, benzene, in one hour at room temperature (Figure **31**).[69] Both the electron donating ability of the ligand, and its ether group may assist in stabilizing unsaturated intermediates in the arene exchange reaction allowing it to take place under ambient conditions.[69]

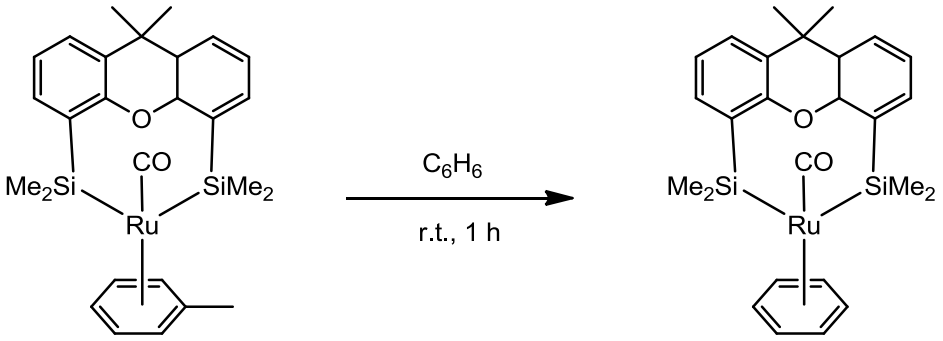

Figure 31. Arene exchange of Ru(CO)(Xantsil)(η^6-toluene) with benzene

Several benzocrownether ligands have also been coordinated to ruthenium(II) through an arene exchange reaction. Thus, benzo-15-crown-5, dibenzo-15-crown-5, dibenzo-18-crown-6 and dibenzo-24-crown-8 could be coordinated to ruthenium(II) by adding $[RuCl(\mu\text{-}Cl)(\eta^6\text{-ethylbenzoate}]_2$ to a melt of the benzocrownether (Figure **32**).[70] Extracting any unreacted benzocrown ether with Et_2O and drying under reduced pressure gave the pure products $[RuCl_2(\eta^6\text{-benzocrownether})]_2$. The melting points of the chosen benzocrownethers were between 135 and 180 °C; at which temperatures the ruthenium ethylbenzoate complex rapidly decomposed. Yields were around 50% with formation of black material from decomposition of the benzocrownether.[70]

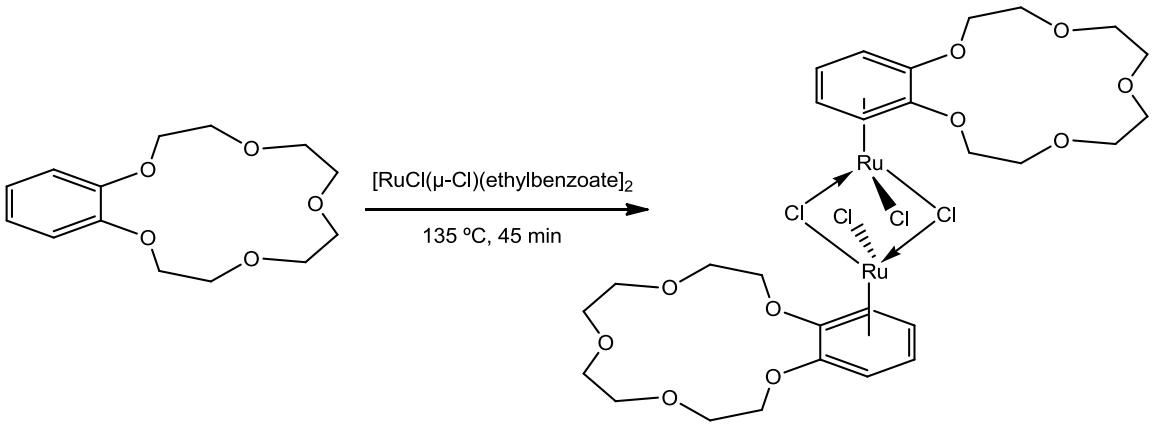

Figure 32. Arene exchange of $[RuCl(\mu\text{-}Cl)(\eta^6\text{-ethylbenzoate})]_2$ with benzo-15-crown-5

An interesting application of the arene exchange reaction is in the generation of immobilized catalysts. The piano-stool complex (η^6-$C_6H_5CO_2Et$)$RuCl_2(PPh_3)$ was reacted with polystyrene at 120 °C for 24 h in cyclohexane resulting in exchange of the ethylbenzoate moiety and generation of the polymer supported ruthenium-arene complex (Figure **33**),[71] which could then be used as a catalyst for hydrogenation of acetophenone or as a precatalyst for ring closing metathesis.[72] This polymer supported catalyst was an effective catalyst for the transfer hydrogenation of acetophenone; however, a catalyst loading of 20% was required.[72]

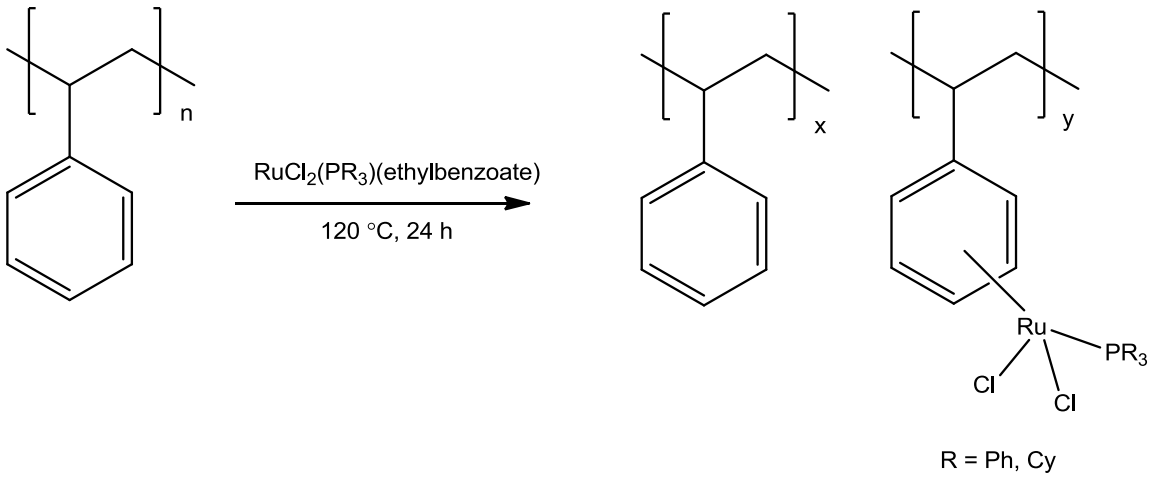

Figure 33. Immobilization of $RuCl_2(PR_3)$ fragment on polystyrene by arene exchange

1.4.3 Intramolecular Ruthenium(II) – Arene Exchange Reactions

Arene exchange reactions have been used to produce a number of tethered ruthenium – arene complexes. Typically, an arene is attached to a nucleophilic donor species via a two or three carbon linking unit. The nucleophile, typically a phosphine, is then used to break the chloride bridge of a $[RuCl(\mu\text{-}Cl)(\eta^6\text{-arene})]_2$ dimer (Figure **34**); a facile reaction that is typically quantitative in less than one hour at room temperature. High temperatures, and often high pressures, are then employed to displace the coordinated arene with the arene covalently attached to the donor ligand.

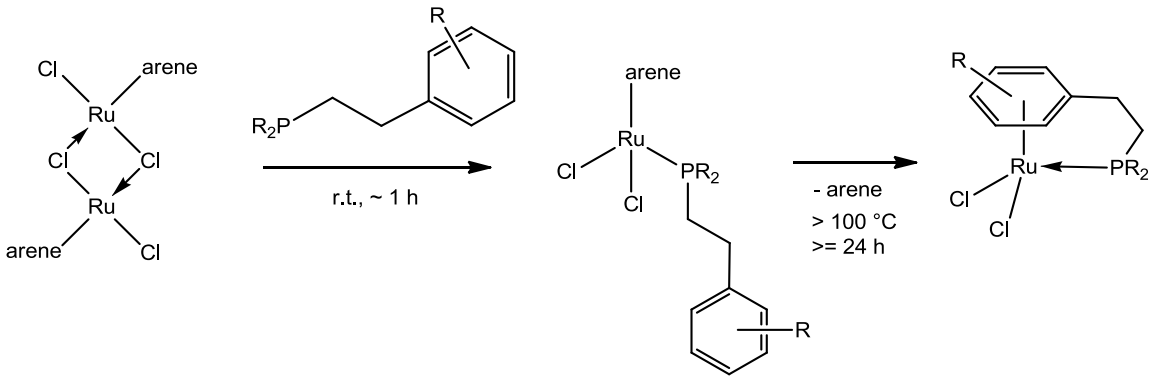

Figure 34. General scheme for intramolecular arene exchange reaction to form η^6:η^1 tethered ruthenium(II) arene complexes with phosphine donors

The simplest of the tethered ruthenium(II) arene complexes formed by arene exchange involved $PPh_2(CH_2)_3Ph$ as an η^6:η^1 ligand.[73] $[RuCl(\mu\text{-}Cl)(\eta^6\text{-}p\text{-cymene})]_2$ was reacted with $PPh_2(CH_2)_3Ph$ at room temperature in dichloromethane to form the mononuclear complex $RuCl_2(\eta^6\text{-}p\text{-cymene})(PPh_2(CH_2)_3Ph)$. This complex was then heated to 130 °C in chlorobenzene to effect an arene exchange reaction producing the tethered complex $RuCl_2(\eta^6{:}\eta^1\text{-}(PPh_2(CH_2)_3Ph))$ (Figure **36**a). The dicyclohexane derivative $RuCl_2(\eta^6{:}\eta^1\text{-}(PCy_2(CH_2)_3Ph))$ (Figure **36**b) was prepared in an identical manner from $PCy_2(CH_2)_3Ph$[74] as well as the di-*tert*-butyl derivative $RuCl_2(\eta^6{:}\eta^1\text{-}(P(t\text{-}Bu)_2(CH_2)_3Ph))$ (Figure **36**c) from $P(t\text{-}Bu)_2(CH_2)_3Ph$.[75]

Reacting the cyclohexane derivative, $RuCl_2(\eta^6{:}\eta^1\text{-}(PCy_2(CH_2)_3Ph))$, with AgOTf followed by a propargylic alcohol (1,1-diphenylpropynol) resulted in the formation of a ruthenium alleneylidene $[RuCl(\eta^6{:}\eta^1\text{-}(PCy_2(CH_2)_3Ph))(=C=C=CPh_2)]OTf$ (Figure **35**).[48] This complex was found to not be as active a catalyst for ring closing metathesis of several dienes as similar untethered ruthenium(II) arene complexes bearing phosphine and allenylidene ligands such as $[RuCl(\eta^6\text{-p-cymene})PPh_3(=C=C=CPh_2)]OTf$.[48]

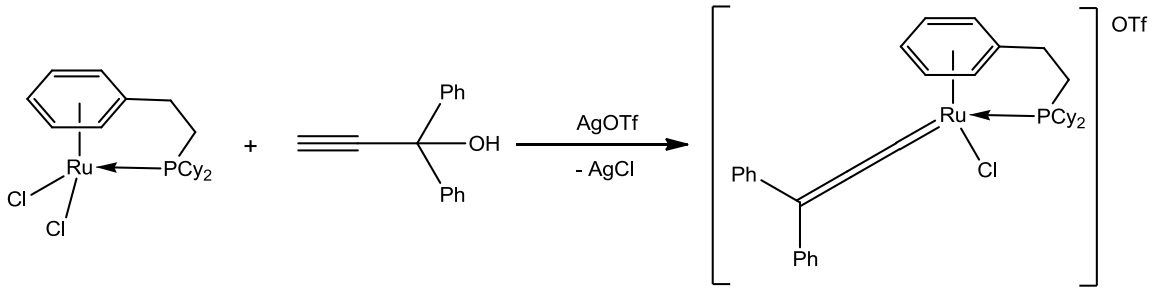

Figure 35. Synthesis of $[RuCl(\eta^6:\eta^1\text{-}(PCy_2(CH_2)_3Ph))(=C=C=CPh_2)]OTf$ which was used as a catalyst for ring closing metathesis

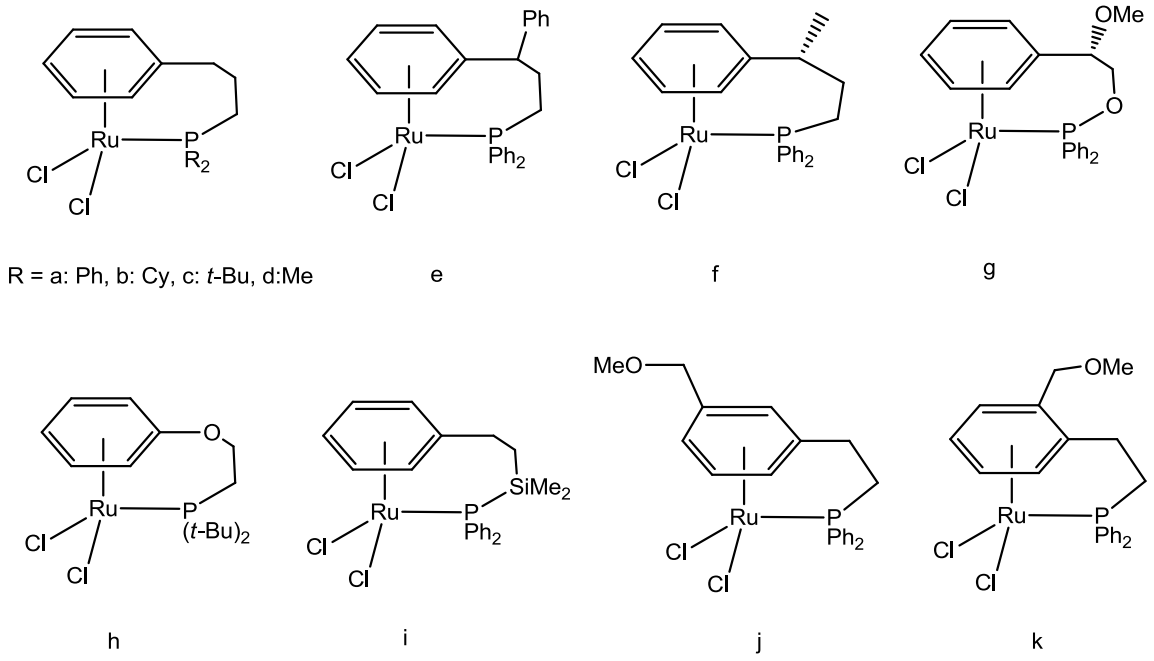

Figure 36. Some $\eta^6:\eta^1$ tethered ruthenium(II) arene complexes synthesized by arene exchange

The dimethyl derivative $RuCl_2(\eta^6:\eta^1\text{-}(PMe_2(CH_2)_3Ph))$ was prepared by first reacting the phosphine $PMe_2(CH_2)_3Ph$ with $[RuCl(\mu\text{-}Cl)(\eta^6\text{-}o\text{-}MeC_6H_4CO_2Me)]_2$ in CH_2Cl_2 for one hour to form the mononuclear complex $RuCl_2(\eta^6\text{-}o\text{-}MeC_6H_4CO_2Me)(PMe_2(CH_2)_3Ph)$ in 85% yield. This was then heated to 120 °C in dichloromethane in a sealed vessel for several days to produce

$RuCl_2(\eta^6{:}\eta^1\text{-}(PMe_2(CH_2)_3Ph))$ (Figure **36**d).[76] The authors found that attempting to effect the arene exchange reaction under photolytic conditions resulted in decomposition of the starting materials.

Chiral phosphetanes attached to an arene group have also been coordinated to ruthenium(II) to form tethered complexes. The phosphetanes were reacted with $[RuCl(\mu\text{-}Cl)(\eta^6\text{-}ethylbenzoate)]_2$ in dichloromethane at room temperature for 3 hours to give the mononuclear complex $RuCl_2(\eta^6\text{-}p\text{-}cymene)$(phosphetane). These were then heated in the same solvent to 120 °C in a sealed vessel for 24 h to give the arene exchange products $RuCl_2(\eta^6{:}\eta^1\text{-}phosphetane)$ in around 40% yield (Figure **37**) after purification by elution through a silica column with acetone/ethyl acetonate (1:1) as eluent.[77]

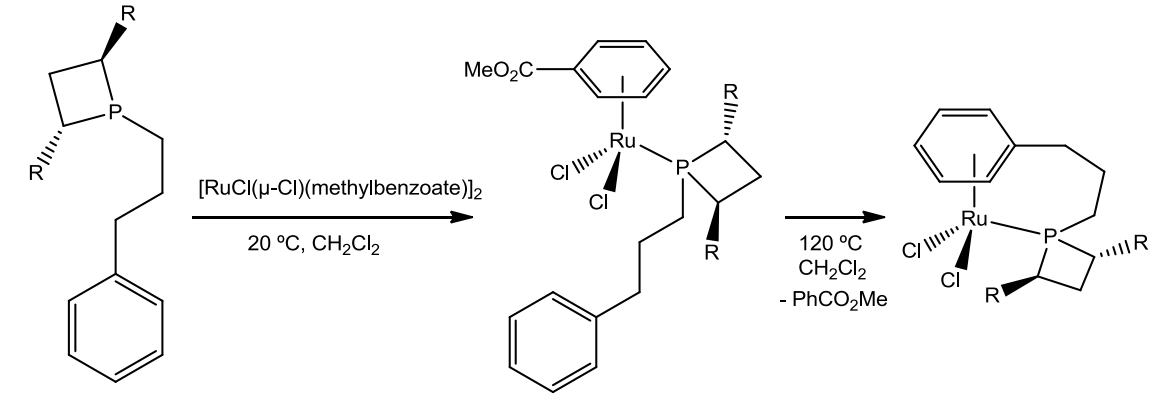

Figure 37. Synthesis of P-chiral phosphetane $\eta^6{:}\eta^1$ ruthenium(II) arene complexes

P-Chiral phosphines with three different organic groups have also been used to form tethered ruthenium(II) arene complexes. A phosphine, (*S*)-P(Me)(t-Bu)($(CH_2)_2$(arene)) (arene = C_6H_5, 3,5-$Me_2C_6H_4$, C_6Me_5, 2-naphthyl, 3-$MeOC_6H_5$), was reacted with $[RuCl(\mu\text{-}Cl)(\eta^6\text{-}p\text{-}cymene)]_2$ at room temperature in dichloromethane for one hour to form $RuCl_2(\eta^6\text{-}p\text{-}cymene)$[(*R*)-P(Me)(t-Bu)($(CH_2)_2$(arene))] (see Figure **38** for the synthesis of the 2-naphthyl derivative) in >90% yield.[78] These complexes were then heated to 120 °C in chlorobenzene to effect an arene

exchange reaction, forming $RuCl_2(\eta^6{:}\eta^1$-(*R*)-P(Me)(t-Bu)((CH_2)$_2$(arene))) with a yield typically around 60%. The 2-naphthyl derivative contains both a plane of chirality and a centre of chirality and was formed as a single diastereomer (Figure **38**).[78]

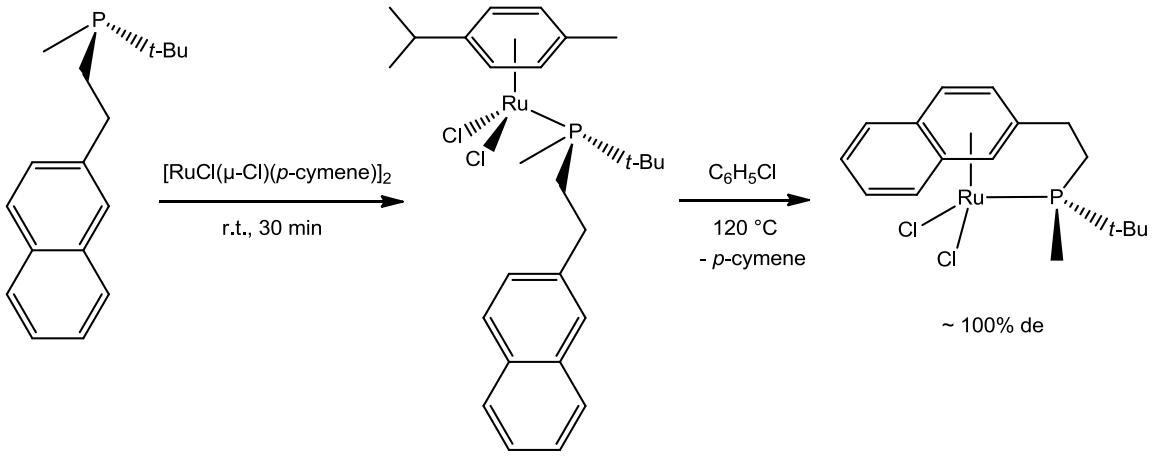

Figure 38. Synthesis of a single diastereomer of $RuCl_2(\eta^6{:}\eta^1$-PMe(t-Bu)(CH_2CH_2-naphthyl)

Functionalizing the tether chain has also been studied. The ligands $PR_2CH_2CHPh_2$ (R = Ph, Cy) were coordinated in a manner similar to those described above with [RuCl(μ-Cl)(η^6-ethylbenzoate)]$_2$ as ruthenium source. Thus a mixture of [RuCl(μ-Cl)(η^6-ethylbenzoate)]$_2$ and the ligand were stirred briefly in dichloromethane and then refluxed until the arene exchange reaction was complete (as monitored by ^{31}P NMR), forming $RuCl_2(\eta^6{:}\eta^1$-$PR_2CH_2CHPh_2$) (Figure **36**e).[79]

Chirality may be incorporated into the tether linking the phosphine and the arene units. The ligand diphenyl-((*R*)-3-phenylbutyl)phosphine was synthesized and heated with [RuCl(μ-Cl)(η^6-methylbenzoate)]$_2$ in dichloromethane at 120 °C in a sealed vessel giving $RuCl_2(\eta^6{:}\eta^1$-(*R*)-$PPh_2(CH_2)_2CHCH_3Ph$) in an 85% yield after 24 h (Figure **36**f).[80] One of the chloride ligands could be removed with $NaBF_4$ and replaced with an amine such as aniline. The resulting pseudo-tetrahedral metal complex contained centres of chirality at the metal and on the ligand and mixtures of diastereomers were formed. Over a range of temperatures, these did not epimerize (Figure **39**).[80]

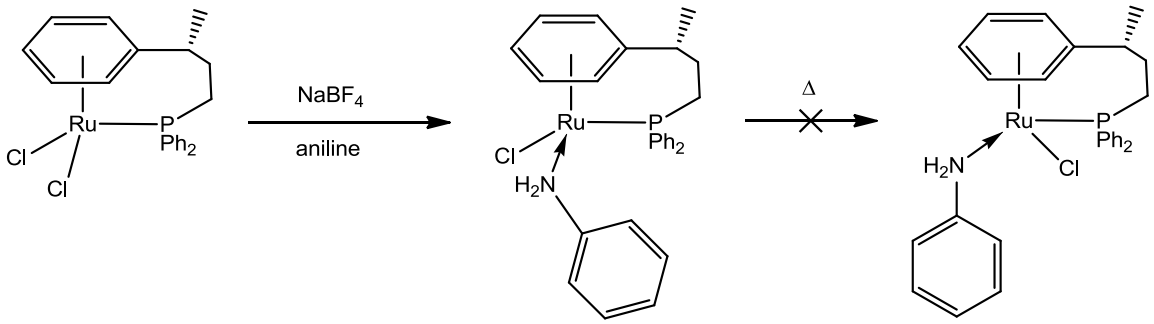

Figure 39. Synthesis of RuCl(aniline)(η^6:η^1-(R)-$PPh_2(CH_2)_2CHPh$) which did not epimerize on heating

In a similar manner, a tethered ligand was prepared with a chiral methoxy group. The ligand (S)-(2-methoxy-2-phenylethoxy)diphenylphosphine was prepared and reacted with $[RuCl(\mu\text{-}Cl)(\eta^6\text{-methylbenzoate})]_2$ in a dichloromethane in a sealed vessel at 120 °C to form $RuCl_2(\eta^6:\eta^1\text{-}(R)\text{-}PPh_2(CH_2)_2CH(OMe)Ph)$ (Figure **36**g).[81] Again, a chloride ligand could be removed with $NaPF_6$ and replaced with a primary amine yielding $[RuCl(amine)(\eta^6:\eta^1\text{-}(R)\text{-}PPh_2(CH_2)_2CH(OMe)Ph)]PF_6$ as a mixture of diastereomers. With aniline as primary amine, one of the diastereomers could be isolated. Unfortunately, this complex gave poor enantioselectivity when used as a precatalyst for the asymmetric transfer hydrogenation of acetophenone.[81]

This is not the sole example of a heteroatom incorporated into the tethering chain. The phosphine $P(t\text{-}Bu)_2(CH_2)_2OPh$ was reacted with $[RuCl(\mu\text{-}Cl)(\eta^6\text{-}p\text{-cymene})]_2$ in CH_2Cl_2 at room temperature for 3 hours to form RuCl2(η^6-*p*-cymene)($P(t\text{-}Bu)_2(CH_2)_2OPh$) in 87% yield. This complex was then heated to 130 °C for 18 hours to effect an arene exchange reaction producing $RuCl_2(\eta^6:\eta^1\text{-}P(t\text{-}Bu)_2(CH_2)_2OPh)$ (Figure **36**h) in 98% yield.[75] The phosphine $PPh_2SiMe_2(CH_2)_2Ph$) was reacted with $[RuCl(\mu\text{-}Cl)(\eta^6\text{-}o\text{-}MeC_6H_4CO_2Me)]_2$ in CH2Cl2 for 1 hour to form RuCl2(η^6-*p*-cymene)($PPh_2SiMe_2(CH_2)_2Ph$)) in 98% yield. An arene exchange reaction took place upon heating this complex in THF to 120 °C in a sealed vessel (Figure **36**i) for 3 days forming $RuCl_2(\eta^6:\eta^1\text{-}PPh_2SiMe_2(CH_2)_2Ph)$ in 71% yield.[76]

Tethered ruthenium(II) arene complexes with functionality incorporated into the arene moiety have also been reported. The ligands *o*-$C_6H_4(CH_2OH)CH_2CH_2PPh_2$ and *m*-$C_6H_4(CH_2OH)CH_2CH_2PPh_2$ were synthesized and reacted with $[RuCl(\mu\text{-}Cl)(\eta^6\text{-ethylbenzoate})]_2$ in dichloromethane to form the mononuclear complexes $RuCl_2(\eta^1\text{-}o\text{-}C_6H_4(CH_2OH)CH_2CH_2PPh_2)$ and $RuCl_2(\eta^1\text{-}m\text{-}C_6H_4(CH_2OH)CH_2CH_2PPh_2)$. These complexes could undergo arene exchange reactions by heating at 120 °C in a sealed vessel giving a quantitative yield of $RuCl_2(\eta^6\text{:}\eta^1\text{-}o\text{-}C_6H_4(CH_2OH)CH_2CH_2PPh_2)$ and $RuCl_2(\eta^6\text{:}\eta^1\text{-}m\text{-}C_6H_4(CH_2OH)CH_2CH_2PPh_2)$ (Figure **36**j and k).[82] The authors obtained very low yields for the arene exchange reaction when using $[RuCl(\mu\text{-}Cl)(\eta^6\text{-}p\text{-cymene})]_2$ as ruthenium source or using photolytic conditions.

A second functional group attached to the arene and capable of coordinating to a ruthenium centre to form an $\eta^6\text{:}\eta^1\text{:}\eta^1$- coordinated ruthenium(II) arene piano-stool complex with coordinated phosphine, arene and imine groups (PArN ligand) has also been reported. The PArN ligand was reacted with $[RuCl(\mu\text{-}Cl)(\eta^6\text{-ethylbenzoate})]_2$ in dichloromethane to give the mononuclear complex which was then heated at 120 °C in a sealed vessel giving a quantitative yield of the $\eta^6\text{:}\eta^1$-ruthenium(II) arene complex (Figure **40**).[83]

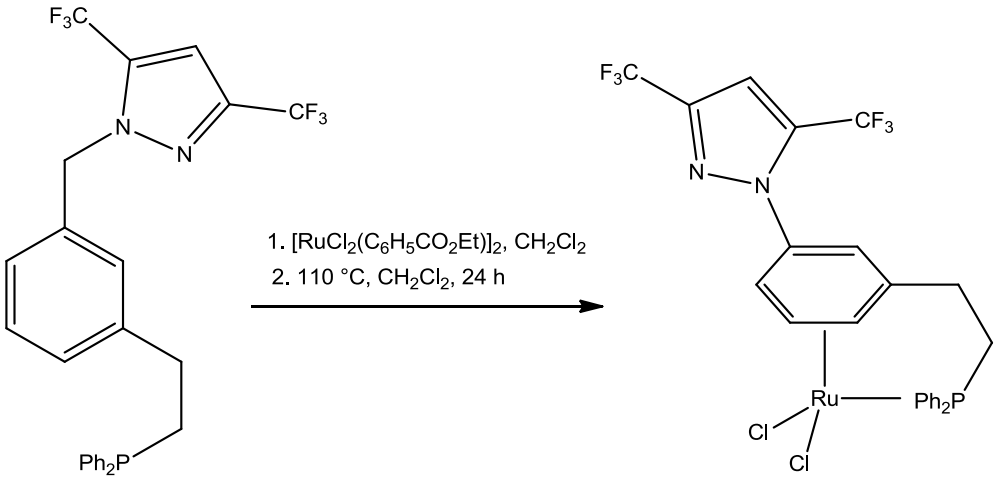

Figure 40. Synthesis of the $\eta^6\text{:}\eta^1$ coordination mode of a PArN ligand

Arene exchange takes place much more easily with electron rich arenes as the incoming ligand. Thus 2-dicylohexylphosphino-2'-(*N*,*N*-dimethylamino)biphenyl (DavePhos) was reacted with $[RuCl(\mu\text{-}Cl)(\eta^6\text{-benzene})]_2$ in DMF for 15 min at 100 °C to give the tethered complex shown in Figure **41** in 98% yield.[84] Both reaction time and temperature required for arene exchange were lower for this ligand than previously reported examples detailed above.

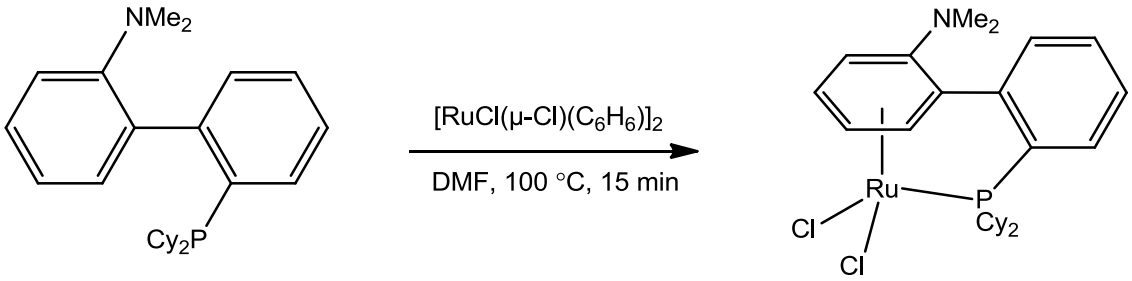

Figure 41. Fast arene exchange with DavePhos

Nitrogen donors can be used to break the chloride bridge of $[RuCl(\mu\text{-}Cl)(\eta^6\text{-arene})]_2$ complexes. If an arene moiety is attached to the amine then arene exchange may take place at elevated temperature. The complexes $RuCl_2(\eta^6{:}\eta^1\text{-}(NH_2(CH_2)_3Ph))$ and $RuCl_2(\eta^6{:}\eta^1\text{-}(NH_2(CH_2)_2Ph))$ were formed by reacting either 3-phenyl-1-propylamine or phenethylamine with $[RuCl(\mu\text{-}Cl)(\eta^6\text{-ethylbenzoate})]_2$ in refluxing dichloroethane with a few drops of THF added for at least 41 hours.[85] Complexes with the trimethylsilyl functional group in ortho-, meta-, or para-positions of the arene moiety were later prepared in a similar manner (Figure **42**).[86]

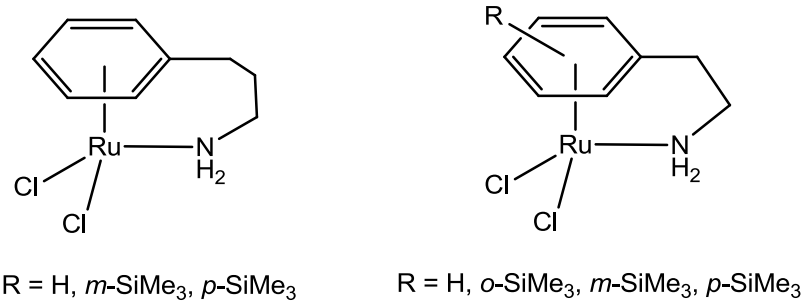

Figure 42. Tethered η^6:η^1 ruthenium arene complexes with N donor groups synthesized by arene exchange

Carbon donors can also be used in a similar manner to nitrogen and phosphorus to form (η^6-arene-η^1-carbene)-ruthenium(II) complexes. A series of bis(imidazolylidine) complexes with at least one arylmethyl-*N* chain were prepared and reacted with[RuCl(μ-Cl)(η^6-*p*-cymene)]$_2$ in toluene at 100 °C. This resulted in exchange of the arene ligand along with coordination of the carbene to form the complexes shown in Figure **43**. The complex with a ether group was found to be an effective ring opening metathesis polymerization catalyst for norbornadiene after reacting with silver triflate and the propargylic acid $CHCCPh_2(OH)$.[87]

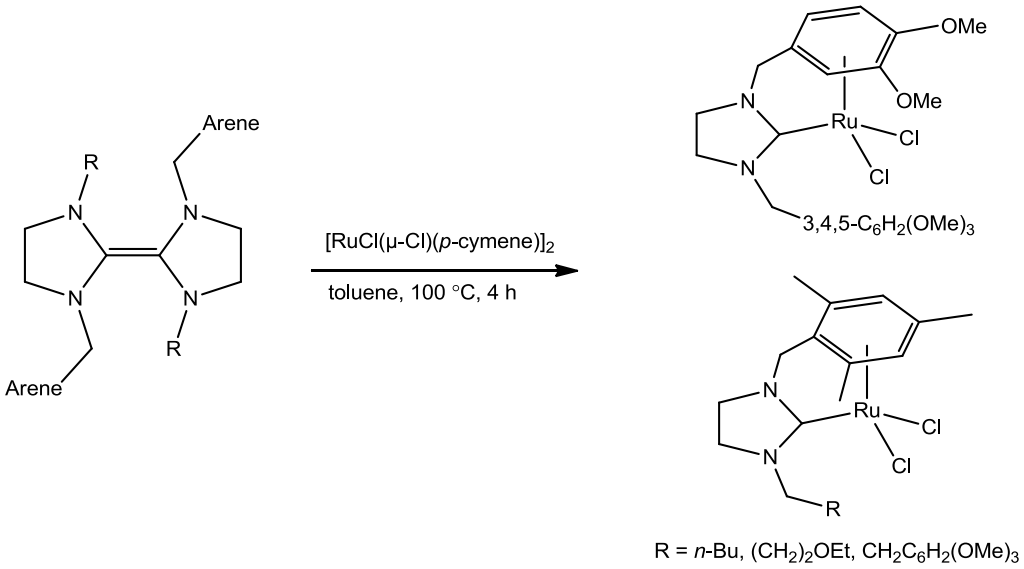

Figure 43. Synthesis of η^6:η^1 tethered ruthenium(II) arene complexes with carbene donor groups

The catalytic performance of several of these tethered arene-ruthenium complexes has been tested, most often in the catalysis of olefin metathesis reactions. Unfortunately, in virtually every case they performed poorly. Yields for various organic reactions were typically low and, interestingly, lower than analogous untethered complexes. Chirality has been imparted to tethered arene-ruthenium complexes; however, they have, thus far, not been shown to impart significant enantioselectivity as catalysts for organic reactions. For example, the chiral tethered arene complex seen in Figure **36**g, (1R)-dichloro[σ(P):η^6-[(2-(*P*,*P*-diphenylphosphinoxy)-1-methoxyethyl)benzene)]ruthenium(II), was reacted with $NaPF_6$ and aniline to afford the chiral cationic aniline complex. This complex was able to catalyze the transfer hydrogenation of acetophenone, but only with 9% ee, indicating virtually no transfer of chirality.

1.5 Research Aims

The phosphonium indenylides are a class of stable aromatic ligands whose coordination chemistry remains virtually unexplored nearly half a century after their discovery. They have electron donating properties intermediate between those of neutral arenes and the Cp anion and they form planar chiral complexes upon coordination to a transition metal. These intriguing properties beg the question as to why the coordination chemistry of the phosphonium indenylides has not been explored given how important arene and Cp ligands are in organometallic chemistry. The main goal of this present research is therefore to explore the coordination chemistry of phosphonium indenylides with ruthenium(II). As π-arene ruthenium complexes have seen such a vast array of applications, the preparation of potentially catalytically active π-PHIN ruthenium complexes is the end goal. In order to achieve this, PHIN-ruthenium(II) complexes with labile or easily removed ligands must be synthesized.

In order to gain a better understanding of the coordination chemistry of the PHINs, the complexes $[CpRu(1\text{-}C_9H_6PR_3)]PF_6$ (R = Me, Ph) have been synthesized from the commercially available complex $[CpRu(MeCN)_3]PF_6$. In an effort to form complexes with labile ligands attached arene exchange reactions of a PHIN with $[RuCl(\mu\text{-}Cl)(\eta^6\text{-}p\text{-cymene})]_2$, $[RuCl(\mu\text{-}Cl)(\eta^6\text{-ethylbenzoate})]_2$ and $RuCl_2(PPh_3)(\eta^6\text{-ethylbenzoate})$ have been explored. The results are reported herein.

1.6 References

(1) Ramirez, F.; Levy, S. *J. Org. Chem.* **1956**, *21*, 488.
(2) Ramirez, F.; Levy, S. *J. Org. Chem.* **1956**, *21*, 1333.
(3) Ramirez, F.; Levy, S. *J. Am. Chem. Soc.* **1957**, *79*, 67.
(4) Ramirez, F.; Dershowitz, S. *J. Org. Chem.* **1957**, *22*, 41.
(5) Ramirez, F.; Levy, S. *J. Am. Chem. Soc.* **1957**, *79*, 6167.
(6) Ramirez, F.; Levy, S. *J. Org. Chem.* **1958**, *23*, 2035.
(7) Ammon, H. L.; Wheeler, G. L.; Watts, P. H. *J. Am. Chem. Soc.* **1973**, *95*, 6158.
(8) Gray, G. A. *J. Am. Chem. Soc.* **1973**, *95*, 7736.
(9) Yoshida, Z.-i.; Iwata, K.; Yoneda, S. *Tetrahedron Lett.* **1971**, *12*, 1519.
(10) Mathey, F.; Lampin, J. P. *Tetrahedron* **1975**, *31*.
(11) Gong, W.-T.; Ning, G.-L.; Li, X.-C.; Wang, L.; Lin, Y. *J. Org. Chem*, **2005**, *70*, 5768.
(12) Xu, T.; Gong, W.-t.; Ye, J.-w.; Lin, Y.; Ning, G.-l. *Organometallics* **2010**, *29*, 6744.
(13) Brownie, J. H.; Baird, M. C. *Coord. Chem. Rev.* **2008**, *252*, 1734.
(14) Abel, E. W.; Singh, A.; Wilkinson, G. *Chem. Ind. (London)* **1959**, 1067.
(15) Kotz, J. C.; Pedrotty, D. G. *J. Organomet. Chem.* **1970**, *22*, 425.
(16) Cashman, D.; Lalor, F. J. *J. Organomet. Chem.* **1971**, *32*, 351.
(17) Brownie, J. H.; Baird, M. C.; Schmider, H. *Organometallics* **2007**, *26*, 1433.
(18) Blake, A. J.; Johnson, B. F. G.; Parsons, S.; Shephard, D. S. *J. Chem. Soc., Dalton Trans.* **1995**, *0*, 495.
(19) Kirchner, K.; Mereiter, K.; Schmid, R.; Taube, H. *Inorg. Chem.* **1993**, *32*, 5553.
(20) Watanabe, M.; Sato, M.; Takayama, T. *Organometallics* **1999**, *18*, 5201.
(21) Holy, N. L.; Nalesnik, T. E.; Warfield, L. T. *Inorg. Nucl. Chem. Lett.* **1977**, *13*.
(22) Kaminsky, W. *Catal. Today* **1994**, *20*, 257.
(23) Pinck, L.; Hilbert, G. *J. Am. Chem. Soc.* **1947**, *69*, 723.
(24) Schmidbaur, H.; Deschler, U. *Chem. Ber.* **1981**, *114*, 2491.
(25) Holy, N.; Deschler, U.; Schmidbaur, H. *Chem. Ber.* **1982**, *115*, 1379.
(26) Johnson, A. *J. Org. Chem.* **1959**, *24*, 282.
(27) Oda, R.; Ito, Y.; Okano, M. *Tetrahedron Lett.* **1964**, *5*, 7.
(28) Crofts, P. C.; Williamson, M. P. *J. Chem. Soc.* **1967**, 1094.
(29) Rufanov, K. A.; Ziemer, B.; Hummert, M.; Schutte, S. *Eur. J. Inorg. Chem.* **2004**, 4759.
(30) Ito, Y.; Okano, O.; Oda, R. *Tetrahedron* **1966**, *22*, 2615.
(31) Brownie, J. H.; Baird, M. C. *J. Organomet. Chem.* **2008**, *693*, 2812.
(32) Buu-Hoi. *Ann.* **1944**, *556*, 1.
(33) Woell, J. B.; Boudjouk, P. *J. Org. Chem.* **1980**, *45*, 5213.
(34) Murphy, J. A.; Patterson, C. W. *J. Chem. Soc., Perkin Trans. 1* **1993**, 405.
(35) Trost, B. M.; Toste, D.; Pinkerton, A. B. *Chem. Rev.* **2001**, *101*, 2067.
(36) Murahashi, S. I. *Ruthenium in Organic Synthesis*; Wiley - VCH: Weinheim, 2004.
(37) Trost, B. M.; Frederiksen, M. U.; Rudd, M. T. *Angew. Chem. Int. Ed.* **2005**, *44*, 6630.
(38) Faller, J.; Parr, J. *Curr. Org. Chem.* **2006**, *10*, 151.
(39) Rigby, J. H.; Kondratenko, M. A. In *Topics Organomet Chem*; Kundig, P. E., Ed.; Springer-Verlag: Berlin Heidelberg, 2004; Vol. 7, p 181.

(40) Davenport, A. J.; Davies, D. L.; Fawcett, J.; Russell, D. R. *J. Chem. Soc., Dalton Trans.* **2004**, 1481.
(41) Faller, J. W.; Fontaine, P. P. *Organometallics* **2005**, *24*, 4132.
(42) Carmona, D.; Lamata, M. P.; Viguri, F.; Rodriguez, R.; Lahoz, F. J.; Dobrinovitch, I. T.; Oro, L. A. *J. Chem. Soc., Dalton Trans.* **2008**, 3328.
(43) Schreiber, D. F.; Ortin, Y.; Müller-Bunz, H.; Phillips, A. D. *Organometallics* **2011**.
(44) Diver, S. T.; Giessert, A. J. *Chem. Rev.* **2004**, *104*, 1317.
(45) Noyori, R.; Hashiguchi, S. *Acc. Chem. Res.* **1997**, *30*, 97.
(46) Furstner, A.; Furstner, A.; Picquet, M.; Bruneau, C.; H. Dixneuf, P. *Chem. Commun.* **1998**, 1315.
(47) Jafarpour, L.; Huang, J.; Stevens, E. D.; Nolan, S. P. *Organometallics* **1999**, *18*, 3760.
(48) Fürstner, A.; Liebl, M.; Lehmann, C. W.; Picquet, M.; Kunz, R.; Bruneau, C.; Touchard, D.; Dixneuf, P. H. *Chem. Eur. J.* **2000**, *6*, 1847.
(49) Miyaki, Y.; Onishi, T.; Ogoshi, S.; Kurosawa, H. *J. Organomet. Chem.* **2000**, *616*, 135.
(50) Cetinkaya, B.; Demir, S.; Ozdemir, I.; Toupet, L.; Semeril, D.; Bruneau, C.; Dixneuf, P. H. *New J. Chem.* **2001**, *25*, 519.
(51) Arockiam, P. B.; Bruneau, C.; Dixneuf, P. H. *Chem. Rev.* **2012**, *112*, 5879.
(52) Gimeno, J.; Cadierno, V.; Crochet, P. *Comprehensive Organometallic Chemistry III*; Elsevier: Oxford, 2007; Vol. 6.
(53) Bennett, M. A.; Smith, A. K. *J. Chem. Soc., Dalton Trans.* **1974**, 233.
(54) Therrien, B. *Coord. Chem. Rev.* **2009**, *253*, 493.
(55) Zelonka, R. A.; Baird, M. C. *J. Organomet. Chem.* **1972**, *44*, 383.
(56) Serron, S. A.; Nolan, S. P. *Organometallics* **1995**, *14*, 4611.
(57) Ward, T. R.; Schafer, O.; Daul, C.; Hofmann, P. *Organometallics* **1997**, *16*, 3207.
(58) Brunner, H. *Eur. J. Inorg. Chem.* **2001**, *2001*, 905.
(59) Hashiguchi, S.; Fujii, A.; Takehara, J.; Ikariya, T.; Noyori, R. *J. Am. Chem. Soc.* **1995**, *117*, 7562.
(60) Hashiguchi, S.; Fujii, A.; Haack, K.-J.; Matsumura, K.; Ikariya, T.; Noyori, R. *Angew. Chem. Int. Ed.* **1997**, *36*, 288.
(61) Takehara, J.; Hashiguchi, S.; Fujii, A.; Inoue, S.-i.; Ikariya, T.; Noyori, R. *Chem. Commun.* **1996**, *0*, 233.
(62) Haack, K.-J.; Hashiguchi, S.; Fujii, A.; Ikariya, T.; Noyori, R. *Angew. Chem. Int. Ed.* **1997**, *36*, 285.
(63) Muetterties, E. L.; Bleeke, J. R.; Sievert, A. C. *J. Organomet. Chem.* **1979**, *178*, 197.
(64) Gastinger, R.; Klabunde, K. *Transition Met. Chem.* **1979**, *4*, 1.
(65) Silverthorn, W. E. In *Adv. Organomet. Chem.*; Stone, F. G. A., Robert, W., Eds.; Academic Press: 1975; Vol. Volume 13, p 47.
(66) Bennett, M. A.; Matheson, T. W.; Robertson, G. B.; Smith, A. K.; Tucker, P. A. *Inorg. Chem.* **1980**, *19*, 1014.
(67) Gupta, H. K.; Lock, P. E.; Hughes, D. W.; McGlinchey, M. J. *Organometallics* **1997**, *16*, 4355.
(68) Green, M. L. H.; Joyner, D. S.; Wallis, J. M. *J. Chem. Soc., Dalton Trans.* **1987**, 2823.
(69) Tobita, H.; Hasegawa, K.; Gabrillo Minglana, J. J.; Luh, L.-S.; Okazaki, M.; Ogino, H. *Organometallics* **1999**, *18*, 2058.

(70) Geldbach, T. J.; Brown, M. R. H.; Scopelliti, R.; Dyson, P. J. *J. Organomet. Chem.* **2005**, *690*, 5055.
(71) Akiyama, R.; Kobayashi, S. *Angew. Chem. Int. Ed.* **2002**, *41*, 2602.
(72) Kobayashi, S.; Akiyama, R. *Chem. Commun.* **2003**, *0*, 449.
(73) Smith, P. D.; Wright, A. H. *J. Organomet. Chem.* **1998**, *559*, 141.
(74) Simal, F.; Jan, D.; Demonceau, A.; Noels, A. F. *Tetrahedron Lett.* **1999**, *40*, 1653.
(75) Jung, S.; Ilg, K.; Brandt, C. D.; Wolf, J.; Werner, H. *J. Chem. Soc., Dalton Trans.* **2002**, *0*, 318.
(76) Bennett, M. A.; Edwards, A. J.; Harper, J. R.; Khimyak, T.; Willis, A. C. *J. Organomet. Chem.* **2001**, *629*, 7.
(77) Pinto, P.; Götz, A. W.; Marconi, G.; Hess, B. A.; Marinetti, A.; Heinemann, F. W.; Zenneck, U. *Organometallics* **2006**, *25*, 2607.
(78) Aznar, R.; Muller, G.; Sainz, D.; Font-Bardia, M.; Solans, X. *Organometallics* **2008**, *27*, 1967.
(79) Abele, A.; Wursche, R.; Klinga, M.; Rieger, B. *J. Mol. Catal. A: Chem.* **2000**, *160*, 23.
(80) Pinto, P.; Marconi, G.; Heinemann, F. W.; Zenneck, U. *Organometallics* **2004**, *23*, 374.
(81) Weber, I.; Heinemann, F. W.; Bauer, W.; Superchi, S.; Zahl, A.; Richter, D.; Zenneck, U. *Organometallics* **2008**, *27*, 4116.
(82) Therrien, B.; Ward, T. R.; Pilkington, M.; Hoffmann, C.; Gilardoni, F.; Weber, J. *Organometallics* **1998**, *17*, 330.
(83) Therrien, B.; Ward, T. R. *Angew. Chem. Int. Ed.* **1999**, *38*, 405.
(84) Faller, J. W.; D'Alliessi, D. G. *Organometallics* **2003**, *22*, 2749.
(85) Melchart, M.; Habtemariam, A.; Novakova, O.; Moggach, S. A.; Fabbiani, F. P. A.; Parsons, S.; Brabec, V.; Sadler, P. J. *Inorg. Chem.* **2007**, *46*, 8950.
(86) Ito, M.; Komatsu, H.; Endo, Y.; Ikariya, T. *Chem. Lett.* **2009**, *38*, 98.
(87) Özdemir, I.; Demir, S.; Çetinkaya, B.; Toupet, L.; Castarlenas, R.; Fischmeister, C.; Dixneuf, P. H. *Eur. J. Inorg. Chem.* **2007**, 2862.

Chapter 2: Experimental

2.1 General Considerations

Unless otherwise noted, all manipulations were performed under a dry, deoxygenated argon atmosphere using standard Schlenk line techniques. Argon was deoxygenated by passage through a heated column of BASF copper catalyst, and then dried by passage through a column of 4A molecular sieves. Glassware was allowed to cool under vacuum. Handling and storage of air-sensitive compounds was done using an MBraun Labmaster glove box. NMR spectra were recorded using Bruker AV400, AV500 and AV600 spectrometers. All ^{1}H and ^{13}C NMR were referenced to carbons or residual protons present in the deuterated solvents with respect to TMS at δ 0. ^{31}P NMR spectra were referenced to external 85% H_3PO_4. IR spectra were acquired on a Perkin Elmer Spectrum One FT-IR spectrometer at a spectral resolution of 4 cm^{-1}. Elemental analyses were conducted by Canadian Microanalytical Service Ltd. of Delta, BC. Mass spectra were obtained by the author on a Waters Micromass ZQ quadrupole mass spectrometer using 1:1 THF:MeCN or MeOH as solvent.

THF, CH_2Cl_2, hexanes, toluene and diethyl ether were purchased from Aldrich in 18 L kegs packed under nitrogen and dried by passage through a column of activated alumina. THF, CH_2Cl_2 and diethyl ether were further purified by storage over 3A molecular sieves which were activated by drying in a vacuum oven at 250 °C for at least 24 h. CH_3CN, DMSO, ethanol and $CHCl_3$ were degassed by bubbling argon and dried by storage over activated 3A molecular sieves. NMR solvents were purchased from Cambridge Isotope Laboratories or Aldrich and were degassed by bubbling argon and dried by storage over activated 3A molecular sieves. All other reagents were purchased from either Aldrich or Strem Chemicals and used as received.

The ruthenium(II) complexes $[RuCl(\mu\text{-}Cl)(\eta^6\text{-}C_6H_6)]_2$, $[RuCl(\mu\text{-}Cl)(\eta^6\text{-}p\text{-cymene})]_2$, $RuCl_2(\eta^6\text{-}p\text{-cymene})PMePh_2$ and $[RuCl_2(1,5\text{-cyclooctadiene})]_n$ were prepared by literature procedures.[1,2]

2.2 X-ray Crystallography

X-ray crystal structure determinations were performed by Ruiyao Wang at Queen's University. Crystals were mounted on glass fibers with epoxy glue and data collections were performed on a Bruker smart CCD 1000 Xd Mo K-ray diffractometer with graphite-monochromatic K_α radiation (λ = 0.71073 Å) controlled with Cryostream Controller 700. No significant decay was observed during data collections. Data were processed on a Pentium PC using the Bruker AXS Crystal Structure Analysis Package.[3] Neutral atom scattering factors were taken from Cromer and Waber.[4]

2.3 DFT Calculations

All molecular calculations were performed by Peter Budzelaar at the University of Manitoba. Calculations were performed to gain insights into the electronic structures of $[CpRu(1\text{-}C_9H_6PPh_3)]PF_6$, $[CpRu(1\text{-}C_9H_6PMePh_2)]PF_6$, $[CpRu(1\text{-}C_9H_6PMe_2Ph)]PF_6$ and the isomers of $[CpRu(1\text{-}C_9H_6PPh_2CH_2Ph_2)]PF_6$. A series of DFT calculations were performed using the TZVP basis[5] set and the functional b3-lyp[6,7] using the Turbomole program[8,9] coupled to an external optimizer (PQS OPTIMIZE[10]). Final geometries were checked by vibrational analysis (no imaginary frequencies), which was also used to calculate thermal corrections. Final energies were calculated using an expanded basis set, TZVPP.[11] To account for solvent effects, either the entropy contributions to the free energies were scaled by two-thirds of their gas-phase values,[12,13] or an electronic correction with COSMO (ε = 9.9, CH_2Cl_2)[14] was used.

2.4 General Synthesis of PHINs

The general synthesis of PHINs involves the reaction of 1-bromoindene with a phosphine followed by deprotonation with NaH. As mentioned in the introduction, 1-bromoindene is a challenging target and the only reported method which appears viable is from the cleavage of the C-Si bond of trimethylsilyl indene with dioxane dibromide.[15,16] Other brominating agents including *N*-bromosuccinamide, $CHBr_3$ and Br_2 did not yield 1-bromoindene.

2.4.1 Synthesis of 1-trimethylsilylindene[16]

In a Schlenk flask with a dropping funnel, 3.0 g indene (25 mmol) was added to 80 mL dry hexanes forming a colourless solution. The mixture was cooled to 0 °C and 20 mL of 1.4 M n-butyllithium (28 mmol) was added over a period of several minutes as a white precipitate formed. The mixture was stirred for 1 h and 3.4 mL chlorotrimethyl silane (27 mmol) was added dropwise over several minutes. After 24 hr, the mixture was poured into 100 mL cold water and the organic layer was separated. Salts were extracted with three more portions of cold water, the organic layer was dried with $MgSO_4$ and the solvent was removed using a rotary evaporator to yield a yellow oil. Yield 3.5 g (75%). ^{1}H NMR ($CDCl_3$): 0.013 (s, Si(C*H*$_3$)$_3$; 3.55 (s, C*H*Si(CH$_3$)$_3$; 6.67 (dd, ArCH=C*H*); 6.94 (dd, ArC*H*=CH); 7.2 – 7.5 (m, Ar).

2.4.2 Synthesis of Dioxane Dibromide[17]

An Erlenmeyer flask open to air was charged with 15 mL of dioxane. With vigourous stirring, 10 mL of bromine was added dropwise over a period of several minutes. The warm, deep red solution was poured into 50 mL of hexanes which had been cooled to -78 °C resulting in the precipitation of an orange solid. This solid was isolated by filtration immediately giving 39.0 g (92% yield) of dioxane dibromide as orange crystals which were stored at -20 °C.

2.4.3 Synthesis of 1-bromoindene with Dioxane Dibromide as Brominating Agent[16]

To a Schlenk flask fitted with a dropping funnel, 3.1 g 1-trimethylsilylindene (16 mmol) and 30 mL dry THF were added. This solution was covered with aluminum foil and cooled to -78 °C. 4.7 g dioxane dibromide (19 mmol) was added to the dropping funnel under a strong flow of Ar along with 25 mL THF and the resulting suspension was added dropwise over several minutes to the solution of 1-trimethylsilyl indene. After 24 h, the solvent was evaporated with a rotary evaporator and the resulting orange-brown oil was eluted through a silica column with hexanes. Fractions containing 1-bromoindene were collected and the solvent was removed to give a yellow oil. Yield 1.68 g (52%)

2.4.4 Synthesis of 1-bromoindene with $Br_2Cl_4C_2$ as Brominating Agent

1.0 mL indene (8.5 mmol) was dissolved in 30 mL Et_2O and the colourless solution was cooled to 0°C. To this solution, 3.5 mL of a 2.5 M solution of n-butyllithium (8.5 mmol) was added dropwise over several minutes and the solution was stirred for 3 h. This solution of indenyl lithium was then added via cannula to a solution of 2.78 g dibromotetrachloroethane (8.5 mmol) in 25 mL Et_2O after which the solution turned orange and a white precipitate formed. After stirring for 1 h, the precipitate was extracted with 3x 50 mL portions of water, the organic phase was dried with $MgSO_4$, filtered and the solvent was removed under reduced pressure. The resultant orange oil was eluted through a silica column with pentane as the eluent and the second yellow fraction was collected and the solvent removed. 0.88 g of yellow oil (54% yield). ^{1}H NMR (CD_2Cl_2): 5.48 (s, C*H*Br), 6.6 (dd, C=C*H*CHBr), 6.82 (d, CH_2=CHCHBr), 7.25-7.33 (aromatic). Reported ^{1}H NMR ($CDCl_3$): 5.48 (br s, C*H*Br), 6.6 (dd, C=C*H*CHBr), 6.82 (d, CH_2=CHCHBr), 7.13-7.67 (aromatic).[15]

2.4.5 Synthesis of the Phosphonium Salts [1-$C_9H_7PR_3$]Br

A solution of 3.5 g of 1-bromoindene (17.9 mmol) and 5.14 g of PPh_3 (19.6 mmol) in 50 mL of THF was stirred for 72 h at room temperature to give a white precipitate of the phosphonium salt. This was collected by filtration, washed with 2x 10 mL portions of Et_2O and dried under reduced pressure to give [1-$C_9H_7PPh_3$]Br as a white powder which contained a mixture of isomers, the ratio of which varied randomly from batch to batch. The yield was 4.0 g (49%). ^{1}H NMR ($CDCl_3$): δ 4.1 (m, C*H*$_2$CH=CPPh_3, isomer A), 6.7 (m, C*H*PPh_3, isomer B), 7.7-7.8 (aromatic). ^{31}P NMR (CD_2Cl_2): δ 12.5 (isomer A), 26.6 (isomer B).

The similar reaction of 1-bromoindene with $PMePh_2$ resulted in the formation of [1-$C_9H_7PMePh_2$]Br as a white powder which was filtered, washed with Et_2O and dried under vacuum to give [1-$C_9H_7PMePh_2$]Br in 89% yield. The product again contained a mixture of regioisomers which varied in relative amounts from batch to batch. ^{1}H NMR (CD_2Cl_2): δ 3.9 (br s, C*H*$_2$CCH=C of isomer A), 3.1 (d, P-C*H*$_3$ of isomer B) 2.8 (d, P-C*H*$_3$ of isomer A). ^{31}P NMR (CD_2Cl_2): δ 13.6 (isomer A), 25.9 (isomer B).

In a similar manner, the reaction of 1-bromoindene with PMe_2Ph resulted in the formation of was a white powder which was filtered, washed with Et_2O and dried under vacuum to give [1-$C_9H_7PMe_2Ph$]Br is 48% yield. The product contained a mixture of regioisomers. ^{1}H NMR (CD_2Cl_2): δ 3.9 (br s, C*H*$_2$CCH=C of isomer A), 2.9 (d, P-C*H*$_3$ of isomer B) 2.4 (d, P-C*H*$_3$ of isomer A). ^{31}P NMR (CD_2Cl_2): δ 13.4 (isomer A), 27.4 (isomer B).

2.4.6 Synthesis of [1-$C_9H_7PPh_2CH_2PPh_2$]Br

To a solution of 1.24 g of dppm (3.2 mmol) in 50 mL of toluene was added dropwise 0.88 g of 1-bromoindene (4.5 mmol). The resulting reaction mixture was stirred at room temperature for 24 h as an off-white precipitate formed. The precipitate was filtered off, washed with 3x 5 mL portions of toluene and 2x 5 mL portions of hexanes and was dried under reduced

pressure to give 1.2 g (74% yield) of the phosphonium salt [1-$C_9H_7PPh_2CH_2PPh_2$]Br as a mixture of regioisomers, the ratios of which varied randomly from batch to batch. The ^{1}H NMR of isomer A and B are complicated and the aromatic regions were not assigned. ^{1}H NMR of isomer **A** (CD_2Cl_2): δ 4.94 (t, J = 14.4 Hz, $^+$*P*Ph_2C*H*$_aH_bPPh_2$), δ 4.53 (t, J = 14.4 Hz, $^+$*P*Ph_2CH_a*H*$_bPPh_2$), δ 6.60 (m, C=CC*H*P^+Ph_2), δ 6.86 (m, C*H*=CHCHP^+Ph_2), δ 7.23 (overlap, C=CHC*H*P^+Ph_2), 7.05 – 8.11 (m, aromatic). ^{31}P NMR of isomer **A** (CD_2Cl_2): δ 30.4 ($^+$*P*$Ph_2CH_2PPh_2$, d, J_{PP} = 62.0 Hz), -25.6 ($^+PPh_2CH_2$*P*Ph_2, d). ^{1}H NMR of isomer **A** (CD_2Cl_2): δ3.80 (s, C*H*$_2$CH=CP^+Ph_2), δ 4.48 (d, J = 14.3 Hz, P^+Ph_2C*H*$_2PPh_2$), δ 8.05 (d, CH_2C*H*=CP^+Ph_2), δ 7.05 – 8.11 (m, aromatic). ^{31}P NMR of isomer **B** (CD_2Cl_2): 14.4 ($^+$*P*$Ph_2CH_2PPh_2$, d, J_{PP} = 63.6 Hz), -25.5 ($^+PPh_2CH_2$*P*Ph_2, d).

2.4.7 Synthesis of PHINs 1-$C_9H_6PR_3$

A Schlenk flask was charged with 0.63 g NaH (26.2 mmol) and 60 mL of THF. Under a strong flow of Ar, 4.0 g [1-$C_9H_7PPh_3$]Br (8.8 mmol) was added and the mixture was stirred for 96 h. The green solution was then filtered through a plug of Celite topped with neutral alumina. The solvent volume was reduced to 20 mL and the solution was layered with hexanes and stored at –30 °C. The resulting green solid was filtered, washed with 2x 10 mL portions of hexanes and dried under reduced pressure to yield 2.58 g (65% yield) of 1-$C_9H_6PPh_3$ (**I**). ^{1}H NMR (CD_2Cl_2): δ 6.56 ((t, $J_{HH} = J_{HP}$ = 4.2 Hz, Ph_3PCCH=C*H*)), 6.61 (t, $J_{HH} = J_{HP}$ = 4.5 Hz, Ph_3PCC*H*=CH), 6.7-7.0 (C_6 ring of **I**), 7.5-7.7 (aromatic). ^{31}P NMR (CD_2Cl_2): δ 10.39.

The syntheses of 1-$C_9H_6PMePh_2$ (**II**) was carried out in a similar manner from the reaction of a threefold excess of NaH with [1-$C_9H_6PMePh_2$]Br to form **II** as a green solid in a yield of 85%. ^{1}H NMR (CD_2Cl_2): δ 2.50 (d, J_{HP} = 12.6 Hz, PC*H*$_3$), 6.46 (t, $J_{HH} = J_{HP}$ = 4.2 Hz, PCCH=C*H*), 6.74 (t, $J_{HH} = J_{HP}$ = 4.5 Hz, PCC*H*=CH), 6.8-7.1 (C_6 ring of **II**), 7.5-7.7 (aromatic). ^{31}P NMR (CD_2Cl_2): δ 5.69.

The synthesis of 1-$C_9H_6PMe_2Ph$ (**III**) was carried out in a similar manner from the reaction of a threefold excess of NaH with [1-$C_9H_6PMe_2Ph$]Br to form **III** as a green solid in a yield of 94%. ^{1}H NMR (CD_2Cl_2): δ 2.21 (d, J_{HP} = 13.2 Hz, PC*H*$_3$), 6.64 (t, J_{HH} = J_{HP} = 4.5 Hz, PCCH=C*H*), 6.98 (t, J_{HH} = J_{HP} = 4.5 Hz, PCC*H*=CH), 6.8-7.2 (C_6 ring of **III**), 7.5-7.7 (aromatic). ^{31}P NMR (CD_2Cl_2): δ 1.78.

2.4.8 Synthesis of 1-$C_9H_6PPh_2CH_2PPh_2$ (IV)

A Schlenk flask was charged with 0.12 g of NaH (5 mmol) and 60 mL of THF. Under a strong flow of Ar, 2.23 g of [1-$C_9H_7PPhCH_2PPh_2$]Br (4.46 mmol) was added and the mixture was stirred for 12 h turning green and then brown. The resulting mixture was filtered through Celite and the solvent was removed under reduced pressure to give a brown solid which was redissolved in a minimum amount of CH_2Cl_2 and layered with hexanes. The resulting precipitate was filtered, washed with methanol and dried under reduced pressure to give 1.76 g (79% yield) of (**IV**) as a green solid. Analysis of the ^{1}H NMR spectrum is complex and assignments can be found in the Discussion. ^{31}P NMR (CD_2Cl_2): δ 7.52 (d, J_{PP} = 61 Hz, *P*$^+$$Ph_2CH_2PPh_2$), -28.3 (d, $P^+Ph_2CH_2$*P*Ph_2).

2.5 Synthesis of [RuCl(μ-Cl)(η^6-ethylbenzoate)]$_2$

Ruthenium-arene complexes of the type [$RuCl_2$(arene)]$_2$ are easily prepared by reaction of a 1,3- or 1,4- cyclohexadiene with $RuCl_3 \cdot xH_2O$ in an alcoholic solution. The cyclohexadienes can either be purchased or, if not commercially available, prepared by Birch reduction. The 1,4-cyclohexadiene derivative required to make [RuCl(μ-Cl)(η^6-ethylbenzoate)]$_2$, ethyl-1,4-cyclohexadiene-3-carboxylate, is not commercially available. Birch reduction of ethylbenzoate typically results in reduction of the ester group; however, Birch reduction of benzoic acid to give

1,4cyclohexadiene-3-carboxylic acid, followed by esterification with ethanol may be used to prepare ethyl-1,4-cyclohexadiene-3-carboxylate.[18]

2.5.1 Birch Reduction of Benzoic Acid

Approximately 300 mL of NH_3 was condensed into a 1 L three-neck flask fitted with a mechanical stirrer and a dry ice/ethanol condenser. 12.7 g of benzoic acid (0.104 mol) and 50 mL ethanol (dried over 4 Å molecular sieves) were added and the solution was cooled to -78 °C. 7.0 g Na(s) (0.306 mol) was added slowly in small pieces over 1 h with vigorous stirring. 16 g NH_4Br (0.163 mol) was added slowly and the mixture was stirred for 1 h after which the mixture was warmed to room temperature and the ammonia was allowed to evaporate overnight leaving a white solid.

250 mL H_2O was added to the white solid forming a colourless solution. Concentrated HCl was added slowly until a pH of 1 was reached and resulted in the precipitation of a white solid which was extracted with 3x 50 mL portions of Et_2O, dried with $MgSO_4$, filtered. The solvent was removed on a rotory evaporator to give a yellow oil containing a mixture of 1,4-dihydrobenzoic acid and benzoic acid which was used without distillation.

2.5.2 Esterification of 1,4-Dihydrobenzoic Acid

The yellow oil containing both 1,4-dihydrobenzoic acid and benzoic acid was dissolved in 75 mL of ethanol and 3 mL H_2SO_4 was added. The light yellow solution was refluxed for 24 h after which the solution was cooled and ethyl-1,4-cyclohexadiene-3-carboxylate along with benzoic acid were precipitated out as a white solid by addition of 200 mL H_2O. The white solid was extracted with 2x 50 mL portions of Et_2O which were then combined, washed with 70 mL H_2O, 75 mL 5% sodium bicarbonate solution and 70 mL of brine. The ether layer was then dried

with $MgSO_4$, filtered and the solvent was removed on a rotory evaporator giving a yellow oil which contained both ethyl-1,4-cyclohexadiene-3-carboxylate and ethylbenzoate and was used without distillation.

2.5.3 Synthesis of $[RuCl_2(\eta^6\text{-ethylbenzoate})]_2$

2.1 g $RuCl_3 \cdot xH_2O$ (~8 mmol) was dissolved in 80 mL of dry ethanol. To this, 7 mL of a yellow oil containing both ethyl-1,4-cyclohexadiene-3-carboxylate and ethylbenzoate was added and the resulting black solution was refluxed for 15 h. A brick red precipitate formed which was isolated by filtration and was washed with 10 mL ethanol and 10 mL Et_2O and then dried under air yielding 2.2 g of $[RuCl_2(\eta^6\text{-ethylbenzoate})]_2$ (85% yield). ^{1}H NMR ($CDCl_3$): δ 1.34 (t, J_{HH} = 7 Hz, $CO_2CH_2CH_3$), 4.39 (q, J_{HH} = 7 Hz, $CO_2CH_2CH_3$), 5.70 (t, J_{HH} = 6 Hz, *m*-Ar), 5.90 (t, J_{HH} = 6 Hz, *p*-Ar), 6.39 (d, J_{HH} = 6 Hz, *o*-Ar).

2.6 Coordination of PHINs to Ruthenium using $[CpRu(MeCN)_3]PF_6$

The cationic complex $[CpRu(MeCN)_3]PF_6$ readily undergoes exchange reactions in solution in which the three acetonitrile ligands are displaced by an arene.[19] It is therefore an ideal precursor to synthesize ruthenium(II)-PHIN complexes.

2.6.1 Synthesis of $[CpRu(1\text{-}C_9H_6PPh_3)]PF_6$ (V)

0.145 g of $[Cp(Ru(MeCN)_3)]PF_6$ (0.33 mmol) was dissolved in 40 mL of CH_2Cl_2 and a solution of 0.127 g of **I** (0.33 mmol) in 20 mL CH_2Cl_2 was added. The bright red solution was stirred for 15 min and the solvent was evaporated under vacuum. X-ray quality crystals were obtained by slow evaporation of a concentrated CH_2Cl_2 solution but bulk purification proved problematic. Layering a THF solution with hexanes or Et_2O resulted in obtaining only impure

product. Washing with benzene did remove some trace impurities; however, many were still left. Additionally, recrystallization from hot MeCN again resulted in the recovery of impure product (Anal. Found: C, 53.10; H, 4.04. Calculated: C, 55.90; H, 3.87). ^{1}H and ^{13}C NMR assignments are not trivial and a full analysis may be found in the Discussion. ^{31}P NMR (CD_2Cl_2): δ 24.3 (s). ESI MS: observed: 542.9 $[M]^+$, calculated: 543.0.

2.6.2 Synthesis of [CpRu(1-$C_9H_6PMePh_2$)]PF_6 (VI)

0.12 g of [Cp(Ru(MeCN)$_3$)]PF_6 (0.28 mmol) was dissolved in 40 mL of CH_2Cl_2 and a solution of 0.08 g **II** (0.25 mmol) in 20 mL CH_2Cl_2 was added. The bright red solution was stirred for 15 min and the solvent was evaporated under vacuum. X-ray quality crystals were obtained by slow evaporation of a concentrated CH_2Cl_2 solution, however, bulk purification proved problematic. Layering a THF solution with hexanes of an acetone solution with toluene resulted in obtaining only impure product. Washing with benzene did remove some trace impurities; however, ^{1}H NMR spectroscopy and elemental analysis indicated that this material was still impure (Anal. Found: C, 49.48; H, 3.63. Calculated: C, 51.85; H, 3.81). ^{1}H and ^{13}C NMR assignments are not trivial and a full analysis may be found in the Discussion. ^{31}P NMR (CD_2Cl_2): δ 23.3 (s). ESI MS: observed: 481.3 $[M]^+$, calculated: 481.0.

2.6.3 Synthesis of [CpRu(1-$C_9H_6PMe_2Ph$)]PF_6 (VII)

0.05 g of [Cp(Ru(MeCN)$_3$)]PF_6 (0.12 mmol) was dissolved in 20 mL CH_2Cl_2 and a solution of 0.03 g of **III** (0.12 mmol) in 20 mL CH_2Cl_2 was added. The bright red solution was stirred for 15 min and the solvent was evaporated under vacuum. Washing the resulting powder with benzene and drying under vacuum for several days gave analytically pure material. X-ray quality crystals were obtained by slow evaporation of a concentrated CH_2Cl_2 solution. ^{1}H and ^{13}C

NMR assignments are not trivial and a full analysis may be found in the Discussion. ^{31}P NMR (CD_2Cl_2): δ 22.4 (s). ESI MS: observed: 419.1 $[M]^+$, calculated: 419.0. Elemental analysis for $RuP_2F_6C_{22}H_{22}$: Found: C 46.76, H 3.86; Calculated: C 46.90, H 3.94.

2.6.4 NMR scale Synthesis of Isomers of $[CpRu(1\text{-}C_9H_6PPh_2CH_2PPh_2)]PF_6$ (VIII)

A solution containing 0.01 g of $[CpRu(MeCN)_3]PF_6$ (0.02 mmol) and 0.012 g of **IV** (0.02 mmol) in 0.6 mL CD_2Cl_2 quickly turned red upon mixing and the reaction was monitored by ^{1}H and ^{31}P NMR over a period of 10 days. Upon analyzing the ^{31}P NMR spectra, an apparent kinetic product (**VIIIa**), with ^{31}P chemical shifts of δ 23.0 and -29.1, and a thermodynamic product (**VIIIb**), with ^{31}P chemical shifts of δ 37.7 and 58.1, were formed. The ratio of these two isomers was initially ~1:1; however, after 10 days, **VIIIa** was no longer present and the amount of **VIIIb** had increased relative to the solvent peak. ^{1}H and ^{13}C NMR assignments are not trivial and a full analysis may be found in the Discussion. The ESI MS spectrum of a mixture of **VIIIa** and **VIIIb** exhibited one ruthenium(II) species centered at m/*z* 665 (calculated for [CpRu(**IV**)]$^+$: 655.1 m/*z*) with an isotopic distribution in agreement with a monoruthenium complex.

Additionally, an AB quartet gradually appeared with ^{31}P chemical shifts of δ 21.63 and 21.24, and was the dominant product after a sample was left for 6 months; after which time the atmosphere in the NMR tube was almost certainly compromised. The ESI MS spectrum of this sample exhibited a multiplet centered at m/*z* 681with an isotopic pattern in agreement with a monoruthenium complex.

2.7 Attempted Coordination of PHINs to Ruthenium using $RuCl_3 \cdot nH_2O$

Since the most common method for making arene ruthenium(II) complexes is through oxidation of 1,3- or 1,4-cyclohexadienes, a route to PHIN ruthenium complexes may be

envisaged by dehydrogenation of the phosphonium salts [1-$C_9H_7PR_3$]X (X = Br, I). Alternatively, $RuCl_3$ may be reduced in the presence of a PHIN ligand resulting in coordination.

2.7.1 Reaction of $[C_9H_7PMePh_2]I$ with $RuCl_3 \cdot xH_2O$

830 mg $[C_9H_7PMePh_2]I$ (1.80 mmol) was dissolved in 40 mL EtOH (dried over 3Å mol. sieves) and 300 mg $RuCl_3 \cdot xH_2O$ (~1.1 mmol) was added under a strong flow of argon. A red-brown precipitate began to form slowly. After stirring for 24 h, the mixture was filtered yielding a chocolate brown precipitate and an orange filtrate which were both dried under vacuum.

The ^1H NMR spectrum of both the filtrate and the precipitate showed no peaks in the olefinic region. A P-Me group was observed in the precipitate as a doublet at δ 2.62 (d, J_{HP} = 13.8 Hz). The ^{31}P NMR spectrum of the precipitate showed many peaks of varying intensity while the ^{31}P spectrum of the filtrate showed one main peak at δ 23.9. This peak was coupled to several peaks in the aliphatic region as well as the P-Me group at δ 2.62 and a full discussion of this spectrum can be found in the Discussion. The same major product in the filtrate was obtained by repeating the above reaction and either adding Zn powder or refluxing the reaction mixture overnight.

2.7.2 Reaction of III with $RuCl_3 \cdot xH_2O$ and Zn(s)

94 mg of $RuCl_3 \cdot xH_2O$ (~0.36 mmol) was dissolved in 40 mL of THF. To this, 78 mg Zn powder (1.2 mmol) was added under a strong flow of argon. A solution of 10 mg **III** (0.39 mmol) in 40 mL of THF was added and the very dark brown solution was heated to reflux for 4 h, cooled to room temperature, filtered through Celite and the filtrate was evaporated to dryness under vacuum yielding a dark green solid.

The ^{1}H NMR spectrum of this solid did not show any P-Me groups, while the ^{31}P spectrum showed five peaks of varying intensity between δ 20 and 30 as well as a small amount of unreacted **III**. Both the ^{1}H and ^{31}P spectra will be analyzed in the Discussion.

2.8 Coordination of PHINs to Ruthenium using [RuCl(μ-Cl)(η^{6}-arene)]$_2$

The chloro-bridged ruthenium arene dimers undergo several types of reactions, two of which are arene exchange and breakage of the chloride bridge by a nucleophile. With PHIN ligands derived from monophosphines, arene exchange reactions may occur at elevated temperatures, while with a PHIN ligand derived from a diphosphine such as **IV**, the pendant phosphine may act as a nucleophile to break the chloride brigde forming a monoruthenium species.

2.8.1 Solvent-free Reaction of II with [RuCl(μ-Cl)(η^{6}-*p*-cymene)]$_2$

65 mg [RuCl(μ-Cl)(η^{6}-*p*-cymene)]$_2$ (0.10 mmol) and 125 mg **II** (0.40 mmol) were added to a Schlenk flask and were heated to ~250 °C with a sand bath for 1 h. The mixture was cooled to ambient temperature and 15 mL of toluene was added. The brown-red solution was decanted and evaporated to dryness. The ^{31}P NMR of this red solid in C_7D_8 had a main peak at δ 20.4 and a less intense peak at δ 24.2 but no unreacted **II**. For analysis of the ^{1}H and ^{31}P NMR spectra see Discussion. ^{1}H NMR (C_7D_8): 1.49 (d, J_{HP} = 13.3 Hz), 1.95 (d, J_{HP} = 11.4 Hz), 4.75 (dd J_{HH} = 5.3 Hz), 6.9-7.1 (aromatic), 7.61 (dd, J_{HH} = 6.8 Hz, J_{HP} = 10.6 Hz).

2.8.2 Synthesis of $RuCl_2(\eta^6$-*p*-cymene)$(\eta^1$-1-$C_9H_6PPh_2CH_2PPh_2)$ (IX)

0.2 g of **IV** (0.4 mmol) and 0.155 g of $[RuCl(\mu\text{-}Cl)(\eta^6$-*p*-cymene)$]_2$ (0.25 mmol) were dissolved in 30 mL CH_2Cl_2 and the red-brown solution was stirred for 30 min. The solvent was reduced to 15 mL, 20 mL hexanes was added and the solvent volume was again reduced to 15 mL. The resulting orange precipitate was filtered, washed with hexanes and recrystallized several times from CH_2Cl_2 / hexanes. X-ray quality crystals were obtained from slow evaporation of a saturated THF solution. ^1H and ^{13}C NMR assignments are not trivial and a full analysis may be found in the Discussion. ^{31}P NMR (CD_2Cl_2): 24.3 (d, J_{PP} = 41.7 Hz, $^+PPh_2CH_2\mathit{P}Ph_2$); δ 2.9 (d, $^+\mathit{P}Ph_2CH_2PPh_2$).

2.8.3 Reaction of III with $[RuCl(\mu\text{-}Cl)(\eta^6$-*p*-cymene)$]_2$

214 mg **III** (0.85 mmol) and 237 mg $[RuCl(\mu\text{-}Cl)(\eta^6$-*p*-cymene)$]_2$ (0.39 mmol) were dissolved in 100 mL dry THF and the reddish-brown solution was stirred for 4 h. The solvent was reduced to 30 mL and the mixture was cooled to -30°C resulting in the precipitation of a brown solid which was filtered and dried overnight under reduced pressure. This solid was found to be only sparingly soluble in CH_2Cl_2; however, it was quite soluble in MeCN and DMSO. The ^{31}P NMR spectrum of this solid in DMSO d_6 had one peak at δ 23.6 (**X**). The ^1H NMR spectrum showed significant amounts of $[RuCl(\mu\text{-}Cl)(\eta^6$-*p*-cymene$)]_2$. Attempts to purify **X** by adding either toluene or Et_2O to a concentrated MeCN solution failed to give pure product as did washing the solid with THF. ^1H NMR (DMSO d_6): $[RuCl(\mu\text{-}Cl)(\eta^6$-*p*-cymene$)]_2$, δ 1.16 (d, J_{HH} = 6.8 Hz, $(C\mathit{H}_3)_2$CH-Ar), 2.06 (s, $C\mathit{H}_3$-Ar), 2.8 (hept, $(CH_3)_2C\mathit{H}$-Ar), 5.74-5.79 (Ar); **X**, δ 1.06 (dd, J_{HH} = 6.9 Hz, $(C\mathit{H}_3)_2$CH-Ar), 1.60 (s, $C\mathit{H}_3$-Ar), 2.85 (dd, J_{HP} = 14.5 Hz, P-Me_2), 6.06 (s, $C\mathit{H}CPPhMe_2$), 6.38-6.48 (*p*-cymene Ar), 6.74 (s, $C\mathit{H}CHCPPhMe_2$), 7.45-7.7 (C_6 ring of **III**), 7.7-8.1 (aromatic).

90 mg **III** (0.36 mmol) and 110 mg [RuCl(μ-Cl)(η^6-*p*-cymene)]$_2$ (0.18 mmol) were dissolved in 100 mL dry THF and the reddish-brown solution was heated to reflux overnight after which the solution was cooled, filtered and dried under vacuum to give a brown solid. The ^{31}P NMR spectrum of this solid in DMSO d_6 had a major product at δ 23.2 (**XI**) and **X** as a minor product. The ^{1}H NMR spectrum showed significant amounts of [RuCl(μ-Cl)(η^6-*p*-cymene)]$_2$. Performing the same reaction with toluene as solvent instead of THF also resulted in precipitation of a brown solid which contained a mixture of **X** and **XI**. Attempts to purify **XI** by adding THF to a concentrated MeCN solution failed to give pure product. ^{1}H NMR (DMSO d_6): **XI**, δ 2.66, 2.71 (dd, J_{HP} = 14.6 Hz, P-Me_2), 5.58 (s, C*H*CPPhMe_2), 6.20 (s, C*H*CHCPPhMe_2), 6.6-7.0 (C_6 ring of **III**), 7.6-7.9 (aromatic).

2.8.4 Reaction of II with [RuCl(μ-Cl)(η^6-*p*-cymene)]$_2$

206 mg of **II** (0.66 mmol) and 180 mg of [RuCl(μ-Cl)(η^6-*p*-cymene)]$_2$ (0.30 mmol) were dissolved in 100 mL of THF and the red-orange solution was stirred for 24 h. The solvent volume was reduced to 10 mL and 20 mL of Et_2O was added resulting in the precipitation of a yellow – brown solid. This was collected by filtration and dried under vacuum. This solid was found to be only sparingly soluble in CH_2Cl_2; however, it was quite soluble in MeCN and DMSO. The ^{31}P NMR spectrum of this solid in DMSO d_6 had a major product at δ 22.9 and a minor product at δ 23.6 (**XII**). The ^{1}H NMR spectrum showed significant amounts of the [RuCl(μ-Cl)(η^6-*p*-cymene)]$_2$. ^{1}H NMR (DMSO d_6): δ 0.91 (dd, J_{HH} = 4.5 Hz, Ar-CH(C*H*$_3$)$_2$), 1.5 (s, C*H*$_3$-Ph) 2.04 (hept, J_{HH} = 4.5 Hz, Ar-C*H*(CH_3)$_2$), 2.10 (s, Ar-CH_3), 3.45 (d, J_{HP} = 14.1 Hz, P-C*H*$_3$), 5.62 (s, C*H*CPMe_2Ph), 6.82 (s, C*H*CHCPMe_2Ph), 5.8-6.4 (C_6 ring of **II**), 7.4-8.0 (aromatic).

216 mg of **II** (0.69 mmol) and 210 mg of [RuCl(μ-Cl)(η^6-*p*-cymene)]$_2$ (0.34 mmol) were dissolved in 110 mL of THF and the resulting red-orange solution was heated to reflux for 48 h. The solvent volume was reduced to 20 mL under reduced pressure and 40 mL hexanes was added

resulting in the precipitation of an orange solid. The ^{31}P NMR spectrum of this solid showed that it contained **XII** as a major product. The ^{1}H NMR spectrum showed significant amounts of the [RuCl(μ-Cl)(η^6-*p*-cymene)]$_2$. Attempts to purify **XII** by slowly adding Et_2O to a concentrated MeCN solution or layering a concentrated CH_2Cl_2 solution with hexanes failed to give pure product. ^{1}H NMR (DMSO d_6): δ 3.17 (d, J_{HP} = 14.3 Hz, P-C*H*$_3$), 4.91 (s, C*H*CPMePh$_2$), 6.27 (s, C*H*CHCPMePh$_2$), 6.2-6.9 (C_6 ring), 7.6-7.9 (aromatic).

150 mg of **II** (0.48 mmol) and 145 mg of [RuCl(μ-Cl)(η^6-*p*-cymene)]$_2$ (0.24 mmol) were dissolved in 60 mL of toluene and the red solution was heated to reflux for 48 h during which time a brown precipitate formed. The precipitate was filtered, washed with 3x 10 mL portions of hexanes and dried under reduced pressure. The ^{31}P NMR spectrum of this solid in DMSO d_6 showed that it contained **XII** as the sole phosphorus containing product. The ^{1}H NMR spectrum showed significant amounts of the [RuCl(μ-Cl)(η^6-*p*-cymene)]$_2$.

2.8.5 Reaction of XII with PMe_2Ph

Stock solutions of **XII,** which contained some [RuCl(μ-Cl)(η^6-*p*-cymene)]$_2$, (25 mg in 2.0 mL MeCN d_3) and PMe_2Ph (15 μL in 0.5 mL MeCN d_3) were prepared in MeCN d_3. **XII** was then reacted with PMe_2Ph in ratios of roughly 2:1, 1:1 and 2.5:1 and these reactions were analyzed by ^{1}H and ^{31}P NMR. No reaction was observed between **XI** and PMe_2Ph at ratios of 2:1 and 1:1. At a ratio of 2.5:1, decomposition of **XII** with the concomitant generation of uncoordinated **II** was observed.

2.8.6 Reaction of II with [RuCl(μ-Cl)(η^6-ethylbenzoate)]$_2$

66 mg **II** (0.21 mmol) and 66 mg [RuCl(μ-Cl)(η^6-ethylbenzoate)]$_2$ (0.11 mmol) were dissolved in 15 mL THF and the resulting red-brown solution was refluxed for 24 h. The mixture was then cooled and filtered, yielding a brown solid which was washed with THF and Et_2O and then dried under vacuum. The ^{1}H NMR of this solid showed that it contained **XI**. The ^{31}P NMR spectrum of this solid in DMSO d_6 had one peak at δ 23.6 corresponding to **XI**. The ^{31}P NMR spectrum of the filtrate did not contain **II,** indicating that it had been consumed, but a significant amount of [RuCl(μ-Cl)(η^6-ethylbenzoate)]$_2$ remained.

2.9 Arene Exchange Reactions with $RuCl_2$(arene)(PR_3)

Arene exchange reactions can also take place with complexes of the type $RuCl_2$(η^6-arene)(PR_3) which can be easily be prepared from [RuCl(μ-Cl)(η^6-arene)]$_2$ and a phosphine.[1] These reactions are typically quantitative in less than 1 h and the product, $RuCl_2$(arene)(PR_3) does not require isolation.

2.9.1 Reaction of II with $RuCl_2$(η^6-C_6H_6)(PPh_3)

30 mg **II** (0.09 mmol) and 49 mg $RuCl_2$(η^6-C_6H_6)(PPh_3) (0.09 mmol) were dissolved in 25 mL THF and the resulting red-brown solution was heated to reflux for 1 h. The solvent was removed under vacuum, and the dark red solid was redissolved in a minimum of THF. Hexanes was added to precipitate out a dark black solid. ^{31}P NMR showed that this solid contained mostly unreacted $RuCl_2$(η^6-C_6H_6)(PPh_3) and **II**.

2.9.2 Reaction of II with $RuCl_2(\eta^6$-ethylbenzoate)(PPh_3) (XIII)

120 mg $[RuCl(\mu\text{-}Cl)(\eta^6\text{-ethylbenzoate})]_2$ (0.19 mmol) and 15 mL of THF were added to a round bottom flask creating a red heterogeneous mixture. To this, 99 mg of PPh_3 (0.38 mmol) was added and the mixture was stirred until a red homogeneous solution formed (~0.5 h). A solution of 122 mg of **II** (0.38 mmol) was dissolved in 10 mL of THF and was added to the solution of $RuCl_2(\eta^6$-ethylbenzoate)(PPh_3) forming a deep red solution which was heated to reflux for 24 h, over which time the solution turned very dark green-brown. The solution was cooled to room temperature, the solvent volume was reduced to ~8 mL under vacuum and the mixture was cooled to -30 °C resulting in the precipitation of **XIII** as a dark brown solid. This was filtered and washed with 3x 5 mL portions of Et_2O and the resulting grey solid was dried under vacuum overnight. Yield: 93 mg, 33%. ^1H and ^{13}C assignments of **XIII** are not trivial and can be found in the discussion section. ^1H NMR (CD_2Cl_2): δ 3.45 (d, J_{HP} = 14.1 Hz, P-Me), 3.56 (s, C*H*CPPh_2Me), 4.90 (s, C*H*CHCPPh_2Me), 6.50-7.22 (C_6 ring protons of **II**), 7.2-7.4 (Ar of PPh_3), 7.61-7.90 (Ar of **II**). ^{31}P NMR (CD_2Cl_2): δ 22.6 (d, J = 6 Hz, P^+PMePh_2), δ 43.1 (d, PPh_3).

2.10 References

(1) Bennett, M. A.; Smith, A. K. *J. Chem. Soc., Dalton Trans.* **1974**, 233.
(2) Müller, J.; Fischer, E. O. *J. Organomet. Chem.* **1966**, *5*, 275.
(3) Bruker AXS Crystal Structure Analysis Package, Version 5.10 (SMART NT) (Version 5.053), SAINT-Plus (Version 6.01), SHELXTL (Version 5.1)); Bruker AXS Inc.: Madison, WI, 1999.
(4) Cromer, D. T.; Waber, J. T. *INternational Tables for X-ray Crystallography*; Kynoch Press: Birmingham, UK, 1974; Vol. 4.
(5) Schafer, A.; Huber, C.; Ahlrichs, R. *J. Chem. Phys.* **1994**, *100*, 5829.
(6) Becke, A. D. *J. Chem. Phys.* **1993**, *98*, 1372.
(7) Becke, A. D. *J. Chem. Phys.* **1993**, *98*, 5648.
(8) Ahlrichs, R.; Bär, M.; Baron, H.-P.; Bauernschmitt, R.; Böcker, S.; Ehrig, M.; Eichkorn, K.; Elliott, S.; Furche, F.; Haase, F.; Häser, M.; Hättig, C.; Horn, H.; Huber, C.; Huniar, U.; Kattannek, M.; Köhn, A.; Kölmel, C.; Kollwitz, M.; May, K.; Ochsenfeld, C.; Ohm, H.; Schäfer, A.; Schneider, U.; Treutler, O.; Tsereteli, K.; Unterreiner, B.; Von Arnim, M.; Weigend, F.; Weis, P.; Weiss, H. Turbomole Version 5; Theoretical Chemistry Group, University of Karlsruhe, Karlsruhe, Germany, 2002.
(9) Treutler, O.; Ahlrichs, R. *J. Chem. Phys.* **1995**, *102*, 346.
(10) Baker, J. *J. Comput. Chem.* **1986**, *7*, 385.
(11) Weigend, F.; Furche, F.; Ahlrichs, R. *J. Chem. Phys.* **2003**, *119*, 12753.
(12) Tobisch, S.; Ziegler, T. *J. Am. Chem. Soc.* **2004**, *126*, 9059.
(13) Raucoules, R.; de Bruin, T.; Raybaud, P.; Adamo, C. *Organometallics* **2009**, *28*, 5358.
(14) Klamt, A.; Schuurmann, G. *J. Chem. Soc., Perkin Trans. 2* **1993**, 799.
(15) Woell, J. B.; Boudjouk, P. *J. Org. Chem.* **1980**, *45*, 5213.
(16) Murphy, J. A.; Patterson, C. W. *J. Chem. Soc., Perkin Trans. 1* **1993**, 405.
(17) Billimoria, J. D.; Maclagan, N. F. *J. Chem. Soc* **1954**, 3257.
(18) Habtemariam, A.; Betanzos-Lara, S.; Sadler, P. J. *Inorg. Synth.* **2010**, *35*, 160.
(19) Trost, B. M.; Older, C. M. *Organometallics* **2002**, *21*, 2544.

Chapter 3: Results and Discussion

3.1 New Approaches in the Synthesis of PHIN Ligands

One of the major barriers to the exploration of the coordination chemistry of the phosphonium cyclopentadienylides is the lack of a general synthesis. As the majority of phosphonium ylides are prepared by reacting a bromoalkane with a phosphine and then deprotonating with a strong base, it was thought a general route to synthesizing phosphonium indenylides may be possible by first making 1-bromoindene and following a similar procedure.

The synthesis of 1-bromoindene is fairly challenging and several methods have been published which appear now to fail. The first report of the synthesis of 1-bromoindene was in 1947 and involved using N-bromosuccinimide to brominate indene.[1,2] The final product was not characterized and this approach has subsequently been found to produce negligible quantities of 1-bromoindene.[3] Before the present work, the only reliable method to produce 1-bromoindene was by cleavage of the C-Si bond of 1-trimethylsilylindene with dioxane dibromide at -78 °C in an inert atmosphere and in the dark.[3,4] Adding further to the complications of this reaction is that dioxane dibromide is a highly thermally unstable solid that begins decomposing immediately at room temperature. Even samples stored at -30 °C decompose over a period of many months. In an effort to find an alternative brominating agent, *N*-bromosuccinimide, bromoform, Br_2 and 1,2-dibromoethane were tried as brominating agents. None of these produced quantities of 1-bromoindene detectable by ^{1}H NMR.

3.1.1 Synthesis of 1-bromoindene using $C_2Cl_4Br_2$ as Brominating Agent

Dibromotetrachloroethane was suggested as a brominating agent[5] as it effects bromination by a different mechanism from the aforementioned brominating agents and may therefore be effective in the synthesis of 1-bromoindene. Adding a THF solution of

dibromotetrachloroethane to a solution of indenyl lithium in THF gave 1-bromoindene in good yield and with greater purity than when synthesized from dioxane dibromide and trimethylsilyl indene (Figure **44**). TLC analysis of the crude product showed only two side-products which were easily removed by elution through a silica column with pentane as eluent. 1-Bromoindene produced in this way is identical by NMR to that produced using dioxane dibromide. While this reaction is moisture sensitive, it is not thermally or light sensitive. Dibromotetrachloroethane is a far more effective brominating agent for the synthesis of 1-bromoindene than any reported reagent and should be used in the future instead of dioxane dibromide.

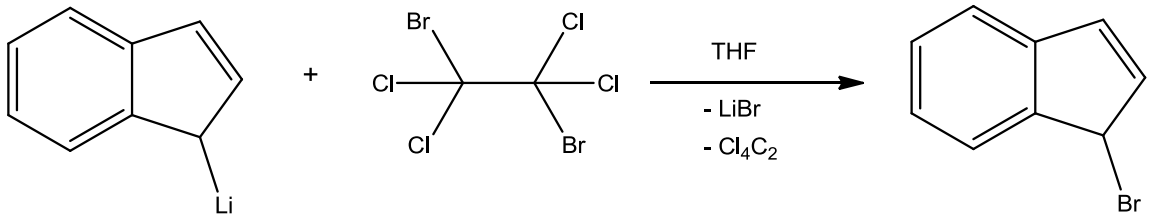

Figure 44. Bromination of indenyl lithium with $C_2Cl_4Br_2$

3.1.2 Synthesis of [1-$C_9H_7PPh_2CH_2Ph_2$]Br

The reaction of dppm with a slight excess of 1-bromoindene in THF resulted in the formation of the expected phosphonium salt [1-$C_9H_7PPh_2CH_2PPh_2$]Br as a mixture of regioisomers (Figure **45**, the number scheme is shown in Figure **46**). The ^{31}P NMR spectrum of [1-$C_9H_7PPh_2CH_2PPh_2$]Br contained two pairs of doublets (Figure **47**), with those at δ 30.4 and −25.6 (J_{PP} = 62.0 Hz) being assigned to isomer **A** and those at δ 14.4 and −25.5 (J_{PP} = 63.6 Hz) to isomer **B**. The resonance with a negative chemical shift is assigned to the dangling –PPh_2 unit because of the close similarity to the chemical shift of dppm (δ −23.6) while the ^{31}P HMBC (See Appendix) spectrum which showed only correlations with peaks in the aromatic region (the lack of correlations with the methylene protons will be discussed below).

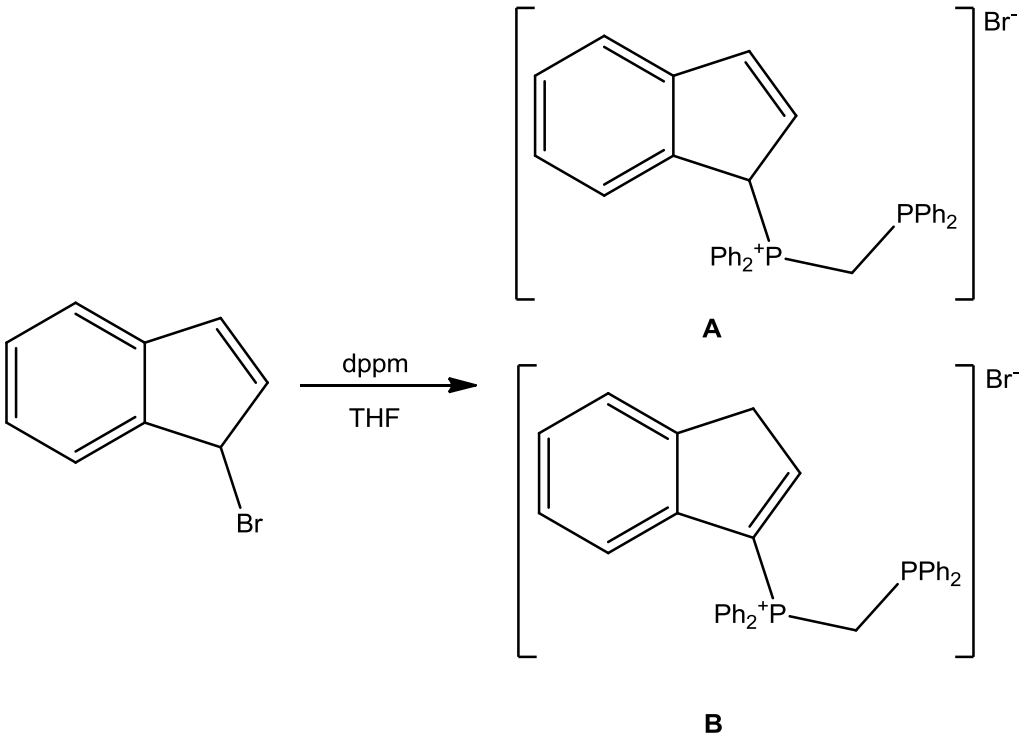

Figure 45. Synthesis of the isomers of [1-$C_9H_7PPh_2CH_2PPh_2$]Br

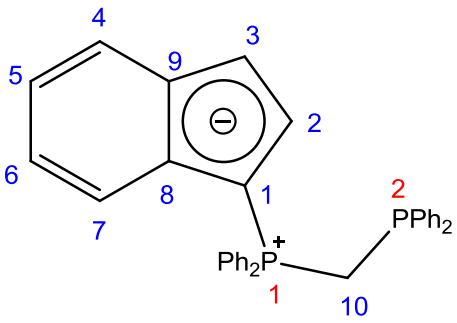

Figure 46. Numbering scheme for [1-$C_9H_7PPh_2CH_2PPh_2$]Br and 1-$C_9H_7PPh_2CH_2PPh_2$ (**IV**)

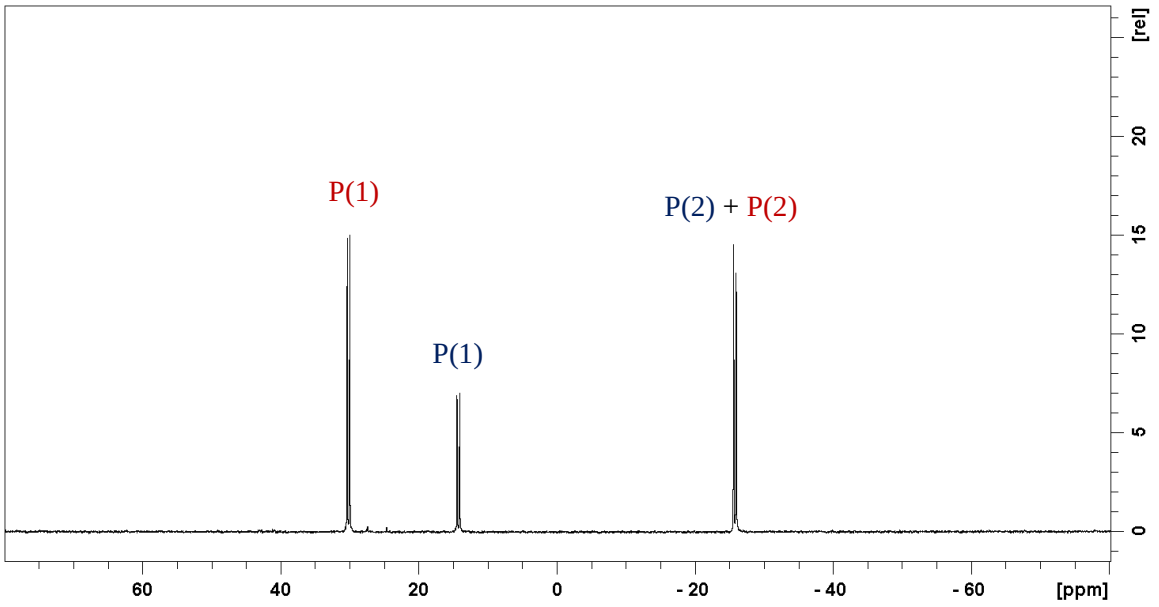

Figure 47. ^{31}P NMR spectrum of isomers **A** and **B** of [1-$C_9H_7PPh_2CH_2Ph_2$]Br in CD_2Cl_2

Differentiating isomers **A** and **B** is relatively straightforward as isomer **A** contains a stereogenic carbon at C(1) (refer to Figure **46** for numbering scheme). Thus, the methylene protons P-CH_2-P are diastereotopic and distinct one-hydrogen triplets are found at δ 4.53 and 4.94 ($^2J_{HP}$ = $^2J_{HP}$ = 14.6 Hz) (Figure **48**). A ^{31}P HMBC showed that these protons were coupled with the phosphonium resonance at δ 30.4 but not to the phosphine resonance at δ −25.6. The two-hydrogen doublet split by phosphorus at δ 4.49 was then assigned to the P-CH_2-P group of isomer **B** based on a ^{31}P HMBC spectrum which showed that these protons were coupled with the phosphonium resonance at δ 14.4 and weakly with the phosphine resonance at δ −25.5. The large difference in $^2J_{HP}$ between the methylene protons and the phosphonium and phosphine resonances is due to differences in the s character of the two types of P-CH_2 bonds. The values of J_{HP} of trigonal phosphines (p^3 bonding) are generally much lower than the corresponding values of J_{HP} of analogous tetrahedral phosphonium (sp^3 bonding) compounds.[6-8] The aromatic region of isomers **A** and **B**, shown in Figure **48**, is very complicated due to each isomer having several different phenyl environments and was therefore not assigned.

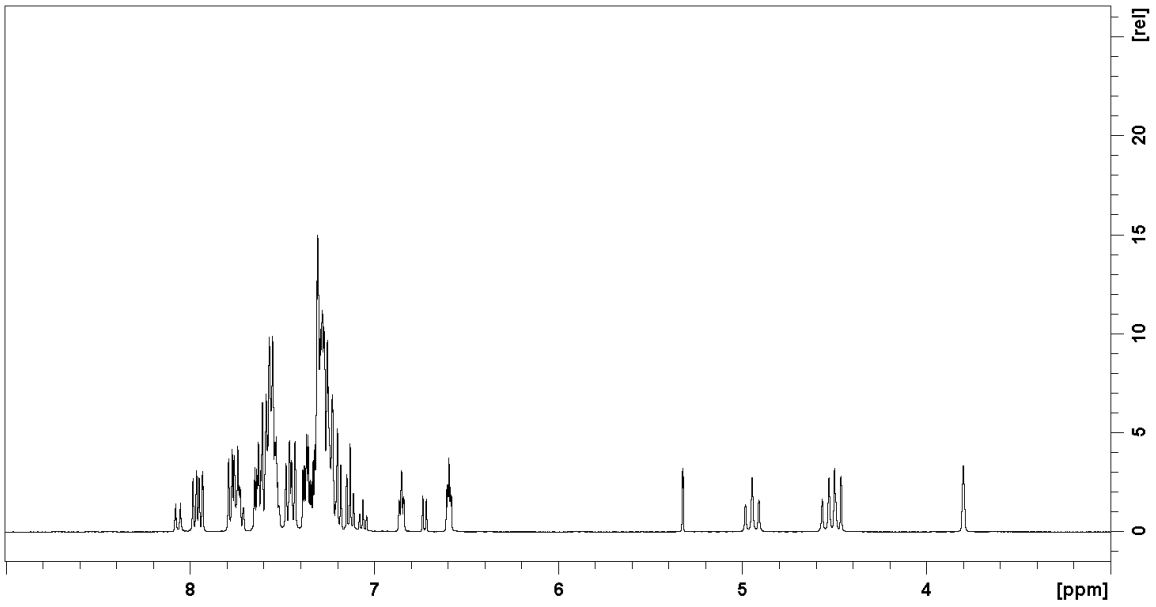

Figure 48. ^{1}H NMR spectrum of [1-$C_9H_7PPh_2CH_2PPh_2$]Br in CD_2Cl_2

X-ray quality crystals of isomer **A** were obtained by layering a dichloromethane solution with hexanes and the molecular structure can be seen in Figure 49. Important bond lengths can be found in Table 1 (refer to Figure 46 for numbering of the PHIN ligand).

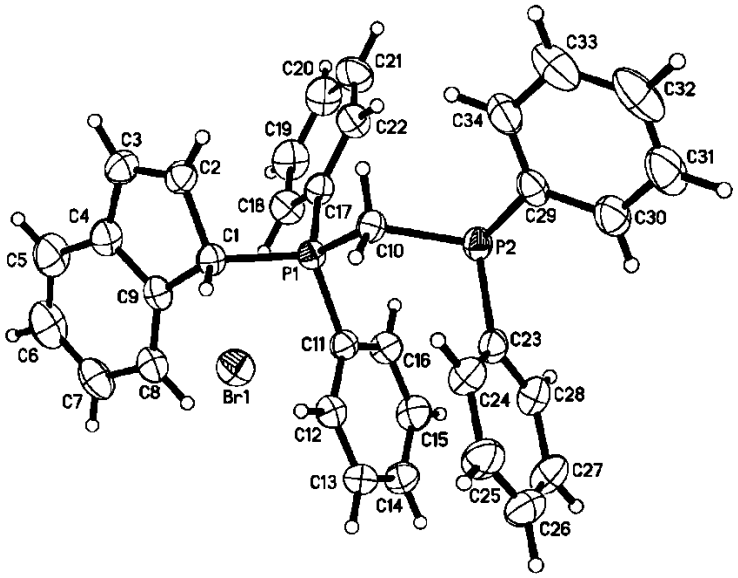

Figure 49. Molecular structure of isomer **A** of [1-$C_9H_7PPh_2CH_2PPh_2$]Br (Numbering different from that shown in Figure 46

Table 1. Selected bond lengths for [1-$C_9H_7PPh_2CH_2PPh_2$] and **IV**

Bond (Å)	[1-$C_9H_7PPh_2CH_2PPh_2$]Br	1-$C_9H_6PPh_2CH_2PPh_2$
P(1)-C(1)	1.8250(17)	1.715(3)
P(1)-C(10)	1.8014(16)	1.812(2)
P(2)-C(10)	1.8745(17)	1.859(3)
C(1)-C(2)	1.515(2)	1.441(3)
C(2)-C(3)	1.335(3)	1.365(4)
C(3)-C(9)	1.456(3)	1.429(3)
C(9)-C(4)	1.394(3)	1.404(4)
C(4)-C(5)	1.376(4)	1.378(4)
C(5)-C(6)	1.382(4)	1.401(4)
C(6)-C(7)	1.393(3)	1.371(3)
C(7)-C(8)	1.388(3)	1.410(3)
C(9)-C(8)	1.402(3)	1.427(3)
C(1)-C(8)	1.509(2)	1.441(3)
P(1)-Ph (avg)	1.794	1.814
P(2)-Ph (avg)	1.838	1.835

This is the first reported X-ray crystal structure of a phosphonium salt of a PHIN or phosphonium cyclopentadienylide. As expected, the P(1)-C(1) bond length of 1.8250(17) Å is typical of a P-C single bond and is longer than the P(1)-Ph bond lengths (~1.8 Å). The C-C bonds of [1-$C_9H_7PPh_2CH_2Ph_2$]Br show expected patterns of 'long' and 'short' bonds expected for the structure of isomer **A** (Figure **47**): the C(1)-C(2) bond, 1.515(2) Å, is considerably longer than the other C-C bonds of the C_5 ring and is clearly a single bond, while the C(2)-C(3) bond is relatively short, 1.335(3) Å, and is a double bond. The C-C bonds of the C_6 ring are all quite similar, varying between 1.376(4) and 1.402(3) Å. There is no evidence of conversion of isomer **A** to isomer **B**.

3.1.3 Synthesis of 1-$C_9H_6PPh_2CH_2PPh_2$ (IV)

Deprotonation of [1-$C_9H_7PPh_2CH_2PPh_2$]Br with NaH in THF gave the green, air-sensitive PHIN ligand **IV** (Figure **50**) in good yield which was fully characterized by NMR spectroscopy and X-ray crystallography.

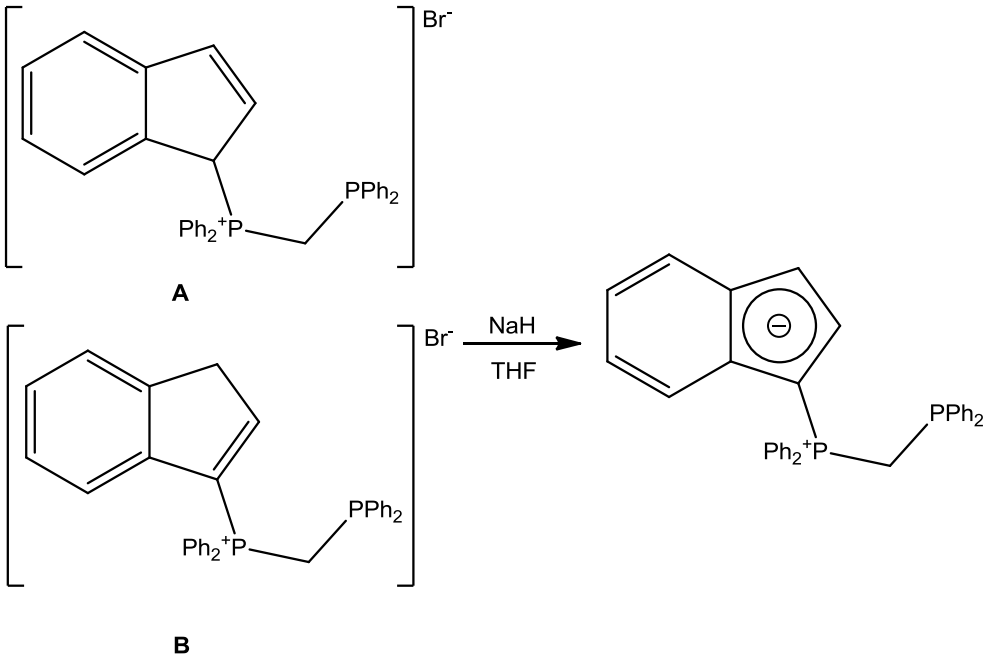

Figure 50. Synthesis of 1-$C_9H_7PPh_2CH_2PPh_2$ (**IV**)

The ^{1}H NMR spectrum of **IV** is shown in Figure **51** and ^{1}H and ^{13}C assignments may be found in Table **2**. The P-CH_2-P group is readily identified as a doublet at δ 3.73 coupled to phosphorus. From a COSY spectrum (Figure **52**) the triplets at δ 6.91 and 6.57 are coupled only to each other while a NOESY spectrum (Appendix) shows a through space interaction between the latter and a signal at δ 7.59. Thus the peaks at δ 6.91, 6.57 and 7.59 may be assigned to H(2), H(3) and H(4) respectively. Peaks at δ 6.87, 6.70 and 6.90 could be assigned to H(5), H(6) and H(7) on the basis of correlations in the COSY spectrum (Figure **52**). ^{13}C chemical shifts were determined by HSQC and HMBC spectra (Appendix).

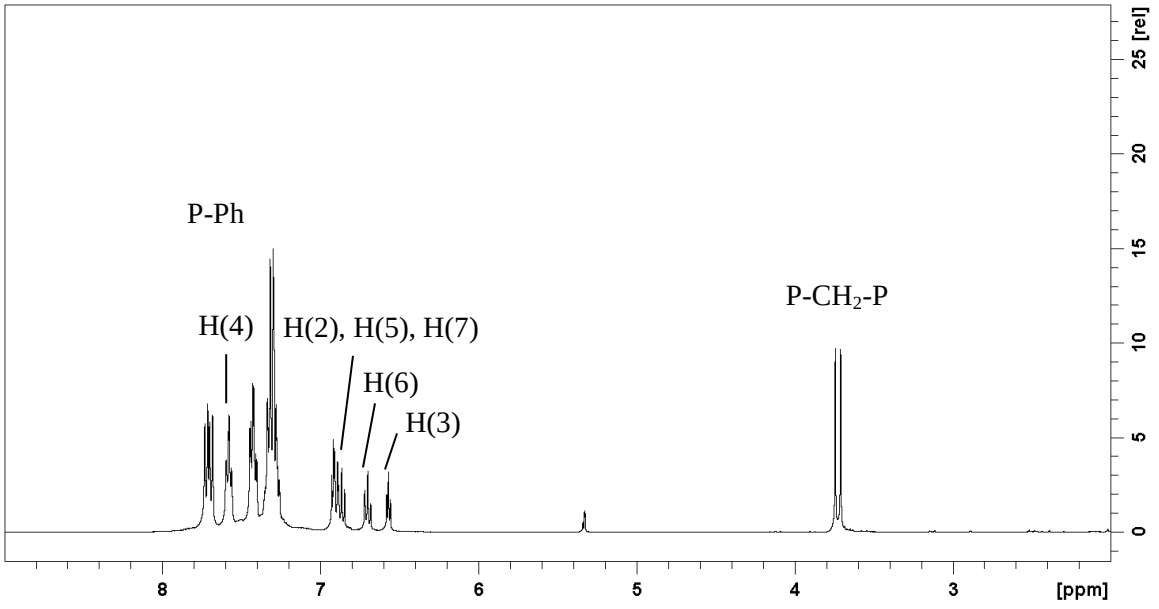

Figure 51. ^{1}H NMR spectrum of 1-$C_9H_7PPh_2CH_2PPh_2$ (**IV**) in CD_2Cl_2

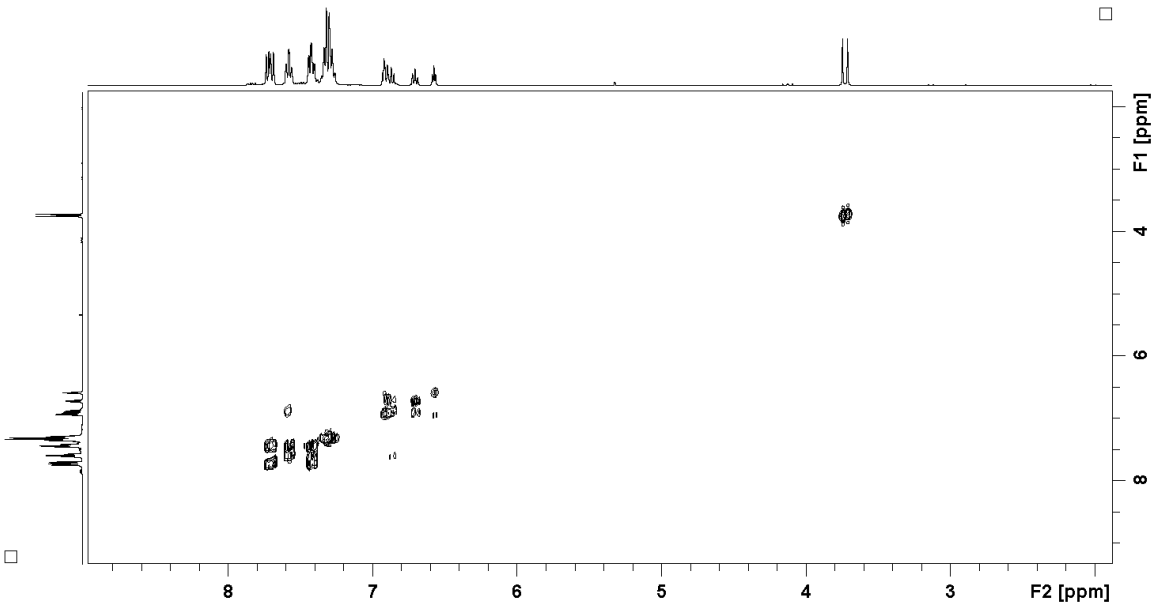

Figure 52. COSY spectrum of 1-$C_9H_7PPh_2CH_2PPh_2$ (**IV**)

The ^{31}P NMR spectrum of **IV** showed a pair of doublets at δ 7.5 and −28.3 (J_{PP} = 61.0 Hz) (Figure **53**). From the ^{31}P HMBC spectrum, the peak at δ 7.5 was coupled to protons H(2) and H(3) and is therefore the ylidic phosphorus P(1) and the peak at δ -28.3 may be assigned to the pendant phosphine P(2). The J_{HP} values for the methylene protons were again very different: 13.5 Hz for the ylidic phosphorus and ~0 Hz for the pendant phosphine. The ^{31}P HMBC spectrum indicates that P(2) is only coupled with a series of overlapping peaks in the aromatic region. As with the phosphonium salt [1-$C_9H_7PPh_2CH_2PPh$]Br, this is due to the differences in s character of the two P-CH_2 bonds.

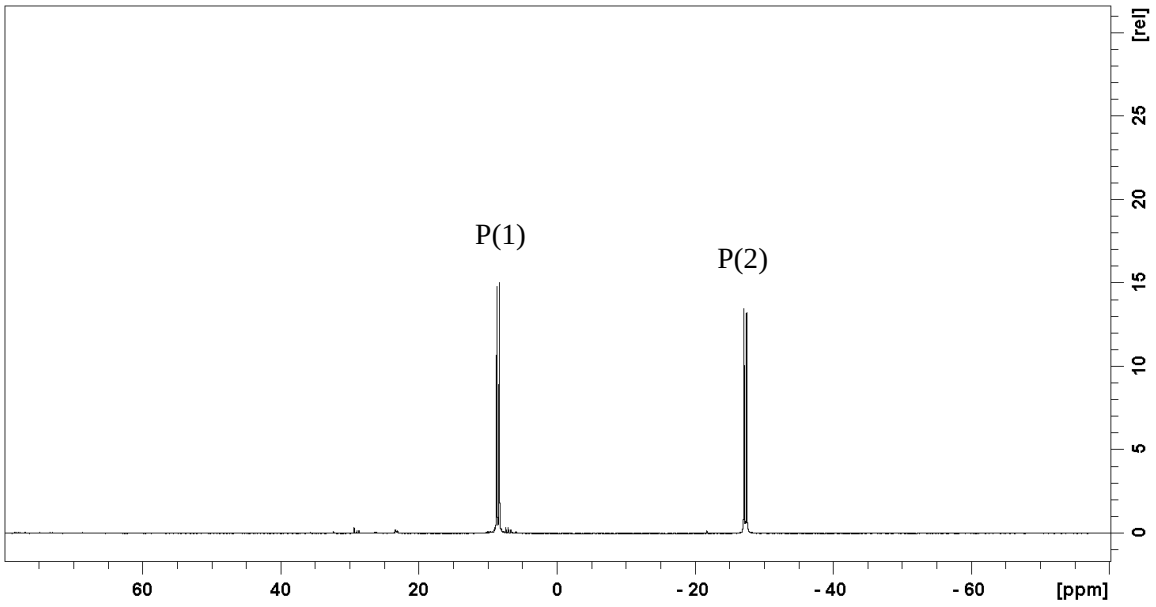

Figure 53. ^{31}P NMR spectrum of 1-$C_9H_6PPh_2CH_2PPh_2$ (**IV**) in CD_2Cl_2

Table 2. ^{1}H and ^{13}C NMR data for 1-$C_9H_7PPh_2CH_2PPh_2$ (**IV**)

H, C Position	δ (^{1}H)[a]	δ (^{13}C)
1	-	66.7 (dd, $^{1}J_{CP}$ 2.3, 120.1)
2	6.91 (t, $^{3}J_{H-H}$, $^{3}J_{H-P}$ 4.8)	126.8 (d, $^{2}J_{C-P}$ ~14)
3	6.57 (t, $^{3}J_{H-H}$, $^{4}J_{H-P}$ 4.8)	107.0 (d, $^{3}J_{C-P}$ 15.4)
4	7.59 (m)	120.6 (s)
5	6.87 (^{3}t, J_{H-H} 7.4)	117.3 (s)
6	6.70 (^{3}t, J_{H-H} 7.4)	117.9 (s)
7	6.90 (m)	117.8 (s)
8	-	135.9 (d, J_{C-P} 14.1)
9	-	138.3 (d, J_{C-P} 15.8)
P-CH_2-P	3.73 (d, $^{2}J_{H-P}$ 13.5)	27.2 (dd, $^{1}J_{C-P}$ 57.4, 35.4)
Ph	7.20-7.75 (m)	128-136

X-ray quality crystals of **IV** were grown by layering a dichloromethane solution with hexanes. The molecular structure can be seen in Figure 54 and selected bond lengths can be found in Table 1. The bond lengths of **IV** are typical of phosphonium cyclopentadienylides and indenylides (see Introduction) with the P(1)-C(1) bond length being 1.715(3) Å, a value similar to that observed in **I-III** (1.72 Å).[9] That this bond length is considerably shorter than the analogous bond of the phosphonium salt [1-$C_9H_7PPh_2CH_2PPh_2$]Br (1.8250(17) Å) indicates that the P-C bond in **IV** has substantial double bond character. The bond angles of the C_5 ring are all close to those expected for a regular pentagon (109°); however, the C(2)-C(3) bond is considerably shorter than the other bonds of this ring indicating a degree of electron localization. As in **I-III**, the bonds C(4)-C(5) and C(6)-C(7) are shorter relative to the other bonds of the C_6 ring.[9]

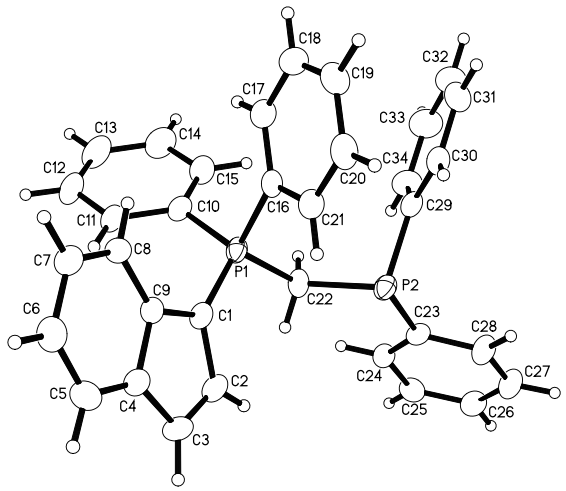

Figure 54. Molecular structure of 1-$C_9H_7PPh_2CH_2PPh_2$ (**IV**) (Number different from that shown in Figure 46

3.2 Coordination of PHINs to Ruthenium using $[CpRu(MeCN)_3]PF_6$

Before the present work, only one PHIN transition metal complex was known: $Cr(CO)_3(1\text{-}C_9H_6PMePh_2)$.[10] An easily synthesized ruthenium(II) PHIN complex was therefore sought both to demonstrate that PHIN ligands could form robust ruthenium complexes and to understand the spectroscopic characteristics of said complexes. The commercially available complex $[CpRu(MeCN)_3]PF_6$ allowed for such a proof of principle.

The acetonitrile ligands of $[CpRu(MeCN)_3)]PF_6$ are labile in solution[11] and may easily be replaced by substitution with a PHIN ligand. Reacting $[CpRu(MeCN)_3)]PF_6$ with $1\text{-}C_9H_6PPh_3$ (**I**), $1\text{-}C_9H_6PPh_2Me$ (I**I**) or $1\text{-}C_9H_6PMe_2Ph$ (**III**), (all of which had been synthesized by a former graduate student) in THF for 15 min afforded the bright red complexes $[CpRu(\textbf{I-III})]PF_6$ (**V**, **VI** and **VII** respectively) in good yields (Figure **55**).[9]

X-ray quality crystals of all three were obtained by the slow evaporation of a dichloromethane solution, but bulk purification of **V**, **VI** and **VII** proved difficult. Recrystallization from a variety of solvent mixtures failed to give pure materials. Washing with benzene removed many of the impurities, but some still remained and this was confirmed by elemental analysis (see Experimental section). Despite these problems, the ruthenium(II) PHIN complexes **V**, **VI** and **VII** were fully characterized by NMR, ESI MS and X-ray crystallography.

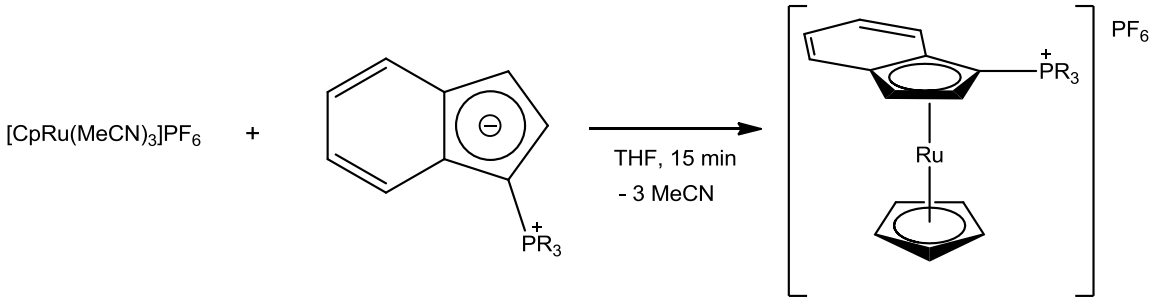

Figure 55. Synthesis of PHIN-Ru(II) complexes $[CpRu(\textbf{I-III})]PF_6$ (**V-VII**)

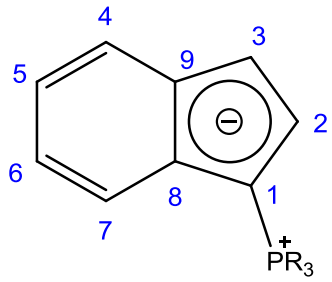

Figure 56. Numbering scheme for PHIN ligands **I-III**

3.2.1 Spectral Analysis of [CpRu(I)]PF_6 (V)

The ^{1}H and ^{13}C NMR assignments for **I** and **V** can be found in Table 3 and the ^{1}H spectrum of **V** is shown in Figure 57. The protons on the Cp ring are readily identified as they appear as a singlet at δ 4.35. Two singlets in the olefinic region at δ 4.66 and 5.86 couple to each other weakly and to nothing else (Figure 58) and are therefore the protons on the C_5 ring. A NOESY (see Appendix A) through space correlation between the signals at δ 5.86 and 7.67 was used to assign these peaks to H(3) and H(4), respectively and the peak at δ 4.66 to H(2). Further correlations in the COSY spectrum allowed resonances at δ 7.14, 7.03 and 6.84 to be assigned to H(5), H(6) and H(7) respectively (Figure 58). ^{13}C assignments were made on the basis of HSQC and HMBC spectra (Appendix A).

Coordination of **I** to Ru results in upfield shifts for protons H(2) and H(3) as well as upfield shifts for all carbons of the C_5 ring. The remaining carbons on the C_6 ring show smaller downfields shifts in the ^{13}C spectrum, while the ^{1}H chemical shifts are relatively unchanged. This is consistent with coordination through the C_5 ring of **I**.

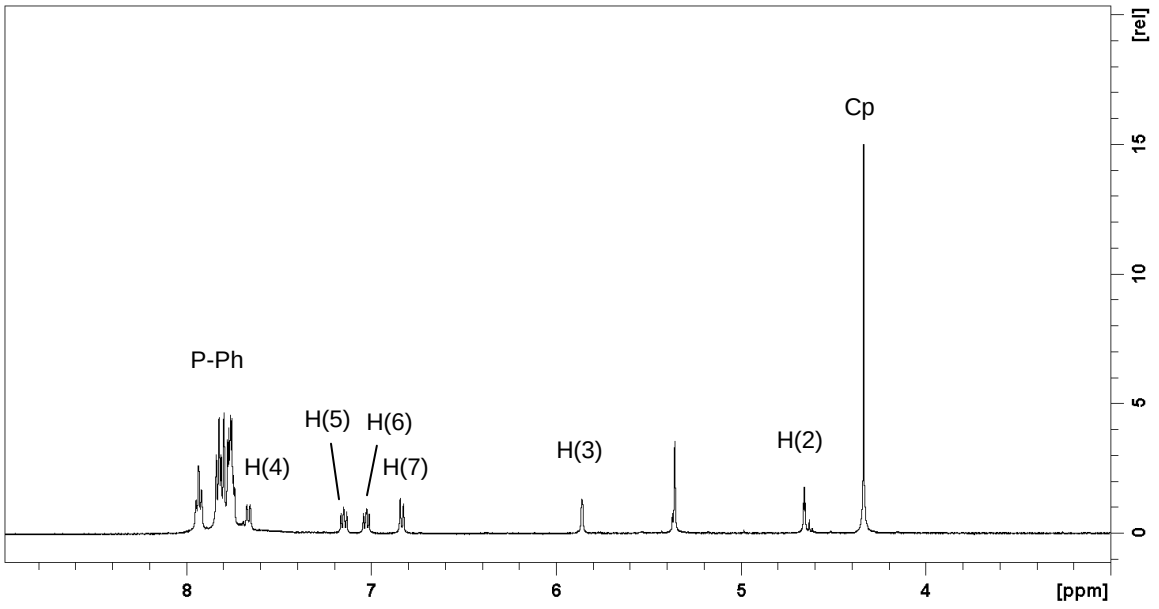

Figure 57. ^{1}H NMR spectrum of $[CpRu(1\text{-}C_9H_6PPh_3)]PF_6$ (**V**) in CD_2Cl_2

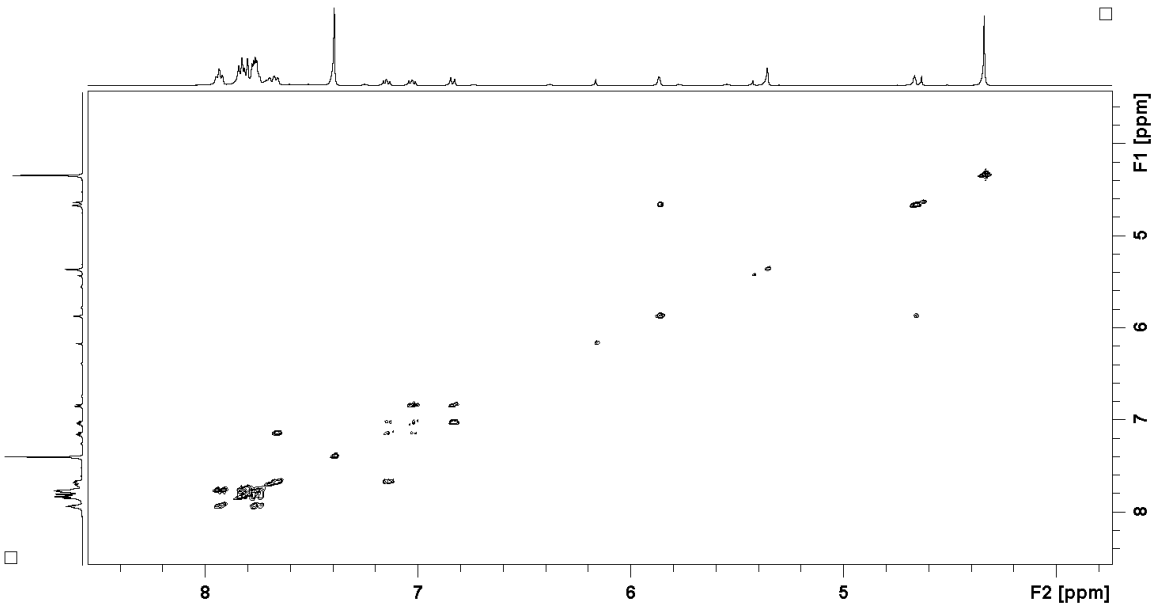

Figure 58. COSY spectrum of $[CpRu(1\text{-}C_9H_6PPh_3)]PF_6$ (**V**)

Coordination of **I** to Ru also results in a downfield shift of the ylidic phosphonium from δ 10.4 to 24.3, a shift of 14 ppm. This is similar to previously reported downfield shifts of around 14 ppm for $Cr(\eta^5\text{-}C_5H_4PMePh_2)(CO)_3$,[12] 10-12 ppm for the compounds $M(\eta^5\text{-}C_5H_4PMePh_2)(CO)_3$ (M = Cr, Mo, W)[12] and 15 ppm for $Cr(CO)_3$(**II**).[10]

Table 3. ^{1}H and ^{13}C NMR data for $C_9H_6PPh_3$ (**I**) and $[CpRu(I)]PF_6$ (**V**)

H, C Position	**I**		**V**	
	δ (^{1}H)[a]	δ (^{13}C)	δ (^{1}H)[a]	δ (^{13}C)
1	-	66.52 (d, $^{1}J_{P-C}$ 123)	-	58.1 (d, $^{1}J_{C-P}$ 104.8)
2	6.61 (t, $^{3}J_{H-H}$ = $^{3}J_{P-H}$ 4.5)	128.2 (d, $^{2}J_{P-C}$ 16.0)	4.66 (s)	78.5 (d, $^{2}J_{C-P}$ 14.5)
3	6.56 (t, $^{3}J_{H-H}$ = $^{4}J_{P-H}$ 4.2)	106.4 (d, $^{3}J_{P-C}$ 16.0)	5.86 (s)	70.9 (d, $^{3}J_{C-P}$ 11.2)
4	7.66 (?, obscured)	117.2 (s)	7.67 (d, $^{3}J_{H-H}$ 8.5)	127.2 (s)
5	6.95 (t, $^{3}J_{H-H}$ 7.2)	120.4 (s)	7.14 (td, $^{3}J_{H-H}$ 7.7)	125.4 (s)
6	6.76 (t, $^{3}J_{H-H}$ 7.2)	117.7 (s)	7.03 (td, $^{3}J_{H-H}$ 7.4)	126.6 (s)
7	6.89 (d, $^{3}J_{H-H}$ 7.9)	118.0 (s)	6.84 (d, $^{3}J_{H-H}$ 8.9)	123.6 (s)
8	-	135.7 (d, $^{3}J_{P-C}$ 13.5)	-	97.7 (d, $^{2}J_{C-P}$ 9.7)
9	-	137.8 (d, $^{2}J_{P-C}$ 14.8)	-	96.2 (d, $^{3}J_{C-P}$ 12.3)
ipso-C	-	125.8 (d, $^{1}J_{P-C}$ 89.8)	-	120.3 (d, $^{1}J_{C-P}$ 92.2)
o-C	7.65-7.68 (m)	133.8 (d, $^{2}J_{P-C}$ 9.84)	7.82 (m)	133.6 (d, $^{2}J_{C-P}$ 10.9)
m-C	7.51 (td, J_{H-H} 3.0, 7.9)	129.1 (d, $^{3}J_{P-C}$ 12.3)	7.76 (m)	130.2 (d, $^{3}J_{C-P}$ 12.4)
p-C	7.62 (t, $^{3}J_{H-H}$ 7.6)	133.6 (d, $^{4}J_{P-C}$ 3.7)	8.00 (m)	130.1 (d, $^{4}J_{C-P}$ 3.8)
C_5H_5	-	-	4.35 (s)	73.8 (s)

Ruthenium has a very distinct isotope distribution which can aid in identifying complexes of the metal in mass spectrometry (^{98}Ru: 1.88%; ^{99}Ru: 12.7%; ^{100}Ru: 12.6%; ^{101}Ru: 17.0%; ^{102}Ru: 31.6%; ^{108}Ru: 18.7%). The ESI MS of **V**, along with that calculated for $[CpRu(\mathbf{I})]^+$ are in excellent agreement and are shown in Figure **59**.

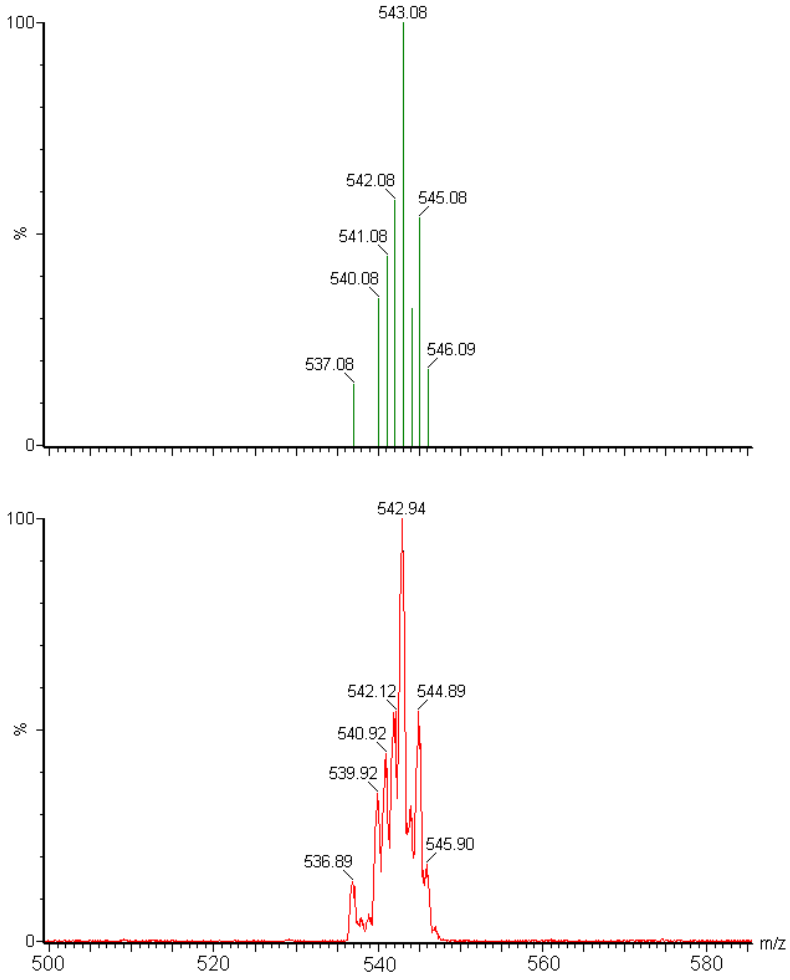

Figure 59. ESI-MS of $[CpRu(1\text{-}C_9H_6PPh_3)]PF_6$ (**V**) (bottom) and the calculated isotope pattern (top)

3.2.2 Spectral Analysis of [CpRu(1-$C_9H_6PMePh_2$)]PF_6 (VI)

^1H and ^{13}C NMR assignments for **II** and **VI** can be found in Table 4 and the ^1H spectrum of **VI** is shown in Figure 60. The Cp resonance is readily identified as a singlet at δ 4.45 along with the P-Me group which appears as a doublet split by phosphorus at δ 2.50. Two singlets at δ 4.64 and 5.82 couple each other and to nothing else in the COSY spectrum (Figure 61) and are therefore the protons on the C_5 ring. The latter has a through space interaction (see NOESY spectrum in Figure 62) with a doublet at δ 7.59. Therefore, the peaks at δ 4.64, 5.82 and 7.59 may be assigned to H(2), H(3) and H(4), respectively. Further correlation in the COSY spectrum (Figure 61) allowed peaks at δ 7.08, 6.93 and 6.98 to be assigned to H(5), H(6) and H(7) respectively.

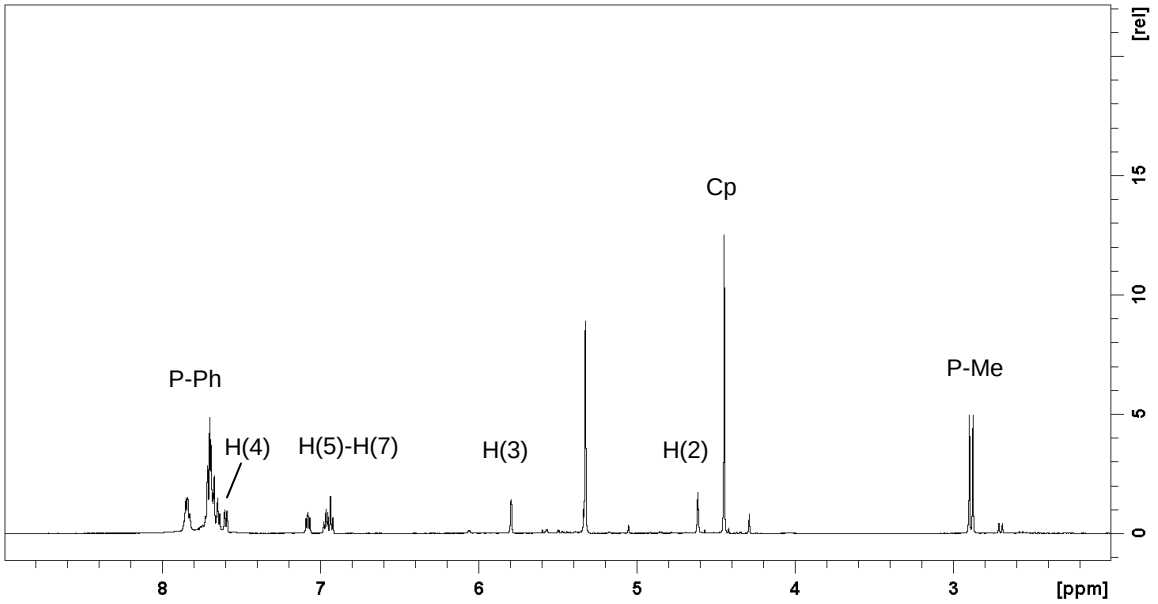

Figure 60. ^1H NMR spectrum of [CpRu(1-$C_9H_6PMePh_2$)]PF_6 (**VI**) in CD_2Cl_2

^{13}C NMR assignments were based on HSQC (Figure 64) and HMBC spectra (see Appendix). Coordination of **II** to Ru again results in upfield shifts for protons H(2) and H(3) as well as upfield shifts for all carbons of the C_5 ring and is consistent with coordination through the

C_5 ring. The protons of the C_6 ring shifted only slightly from the chemical shifts of the uncoordinated ligand **II**.

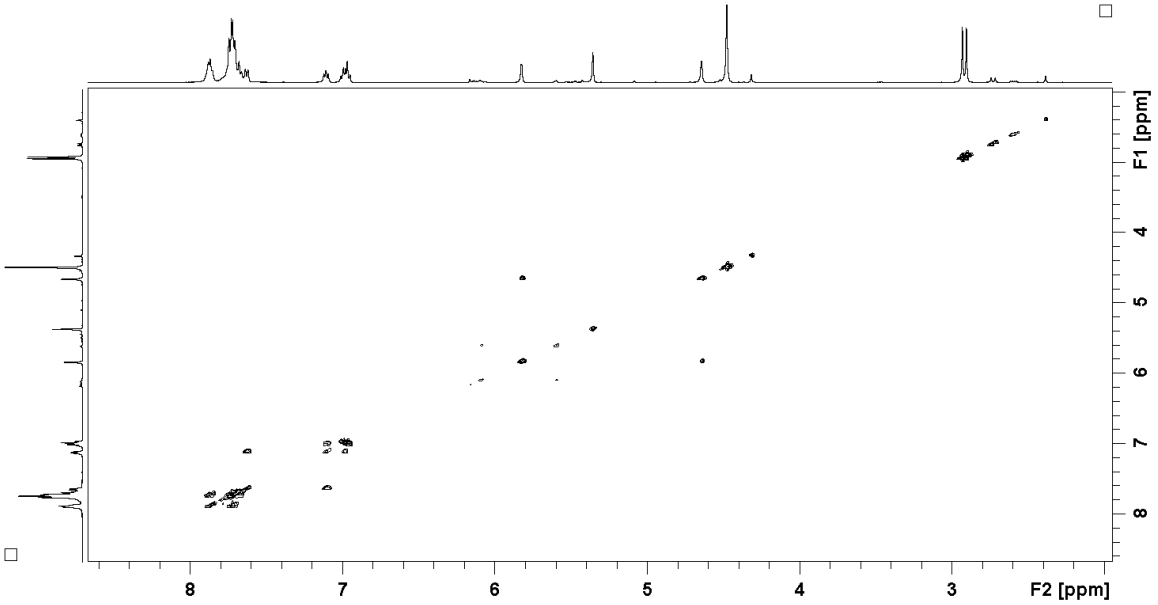

Figure 61. COSY spectrum of [CpRu(1-$C_9H_6PMePh_2$)]PF_6 (**VI**) in CD_2Cl_2

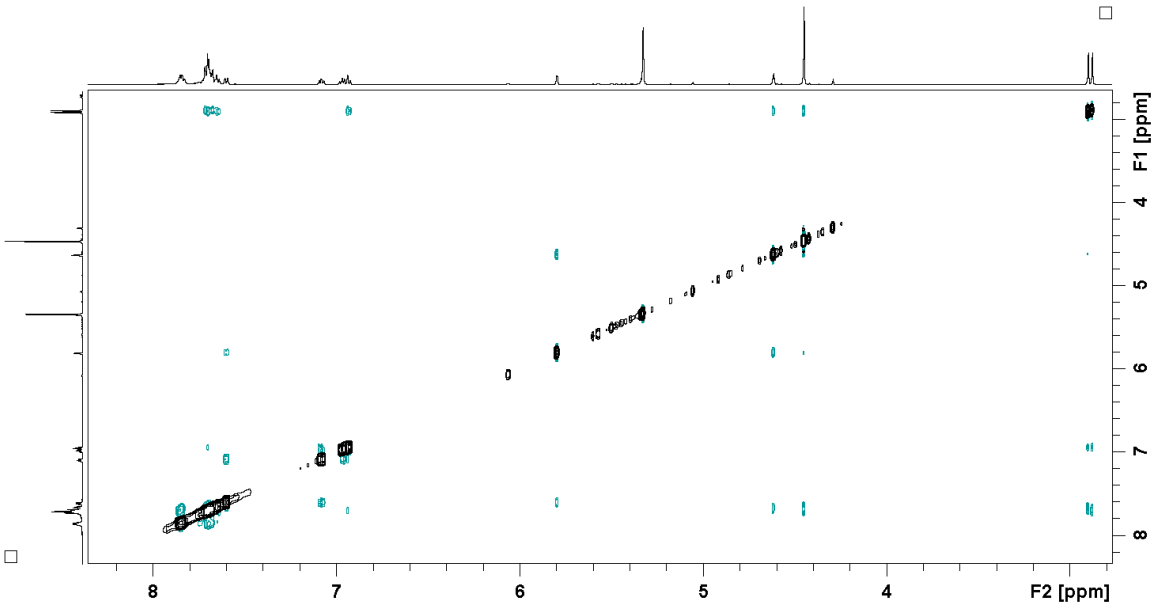

Figure 62. NOESY spectrum of [CpRu(1-$C_9H_6PMePh_2$)]PF_6 (**VI**) in CD_2Cl_2

Because **II** is pro-planar chiral the two phenyl groups of **VI** are diastereotopic and are therefore inequivalent and appear as pairs of closely spaced doublets. While this is impossible to observe in the ^{1}H spectrum due to overlap, it is clear from the ^{13}C spectrum where there are two sets of phenyl resonances. Again, this shows that interfacial exchange of the PHIN ligand is slow on the NMR timescale (Figure **63**).

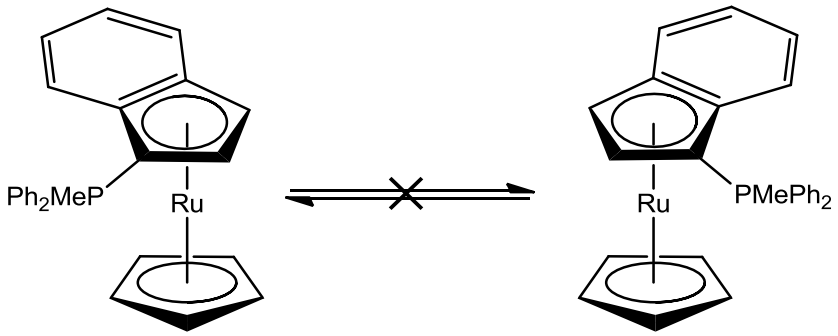

Figure 63. **VI** does not undergo interfacial exchange of the PHIN ligand on the NMR timescale

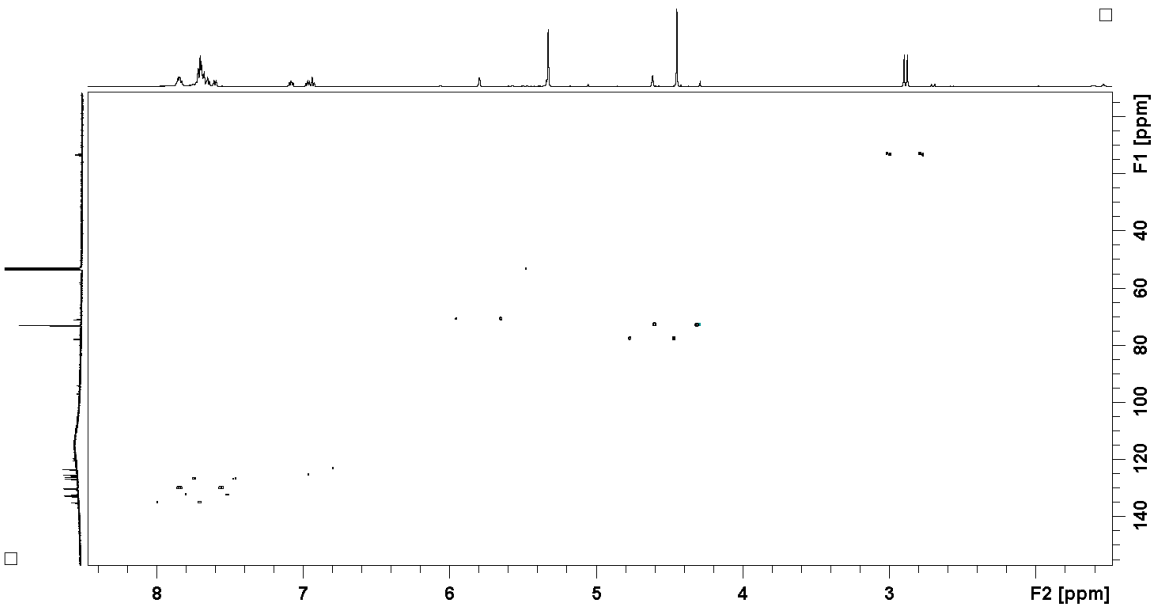

Figure 64. ^{1}H-^{13}C HSQC spectrum of $[CpRu(1\text{-}C_9H_6PMePh_2)]PF_6$ (**VI**) in CD_2Cl_2

Table 4. ^{1}H and ^{13}C NMR data for 1-$C_9H_6PMePh_2$ (**II**) [CpRu(**II**)]PF_6 (**VI**)

H, C Position	**II**		**VI**	
	δ (^{1}H)[a]	δ (^{13}C)	δ (^{1}H)[a]	δ (^{13}C)
1	-	66.14 (d, $^{1}J_{P-C}$ 120.8)	-	57.2 (d, $^{1}J_{C-P}$ 103.4)
2	6.74 (t, $^{3}J_{H-H}$ = $^{3}J_{P-H}$ 4.4)	126.30 (d, $^{2}J_{P-C}$ 17.6)	4.64 (s)	77.8 (d, $^{2}J_{C-P}$ 14.4)
3	6.64 (t, $^{3}J_{H-H}$ = $^{4}J_{P-H}$ 4.2)	105.00 (d, $^{3}J_{P-C}$ 15.4)	5.82 (s)	70.9 (d, $^{3}J_{C-P}$ 9.6)
4	7.68 (m)	117.36 (s)	7.59 (t, $^{3}J_{H-H}$ 8.9 Hz)	126.7 (s)
5	6.97 (t, $^{3}J_{H-H}$ 7.2)	120.82 (s)	6.93 (d, $^{3}J_{H-H}$ 8.0 Hz)	123.1 (s)
6	6.84 (t, $^{3}J_{H-H}$ 6.9)	117.28 (s)	7.08 (d, $^{3}J_{H-H}$ 7.9 Hz)	125.4 (s)
7	7.04 (d, $^{3}J_{H-H}$ 7.9)	117.91 (s)	6.98 (d, $^{3}J_{H-H}$ 6.0 Hz)	126.2 (s)
8	-	135.42 (d, $^{2}J_{P-C}$ 14.3)	-	97.0 (d, $^{2}J_{C-P}$ 8.2)
9	-	137.79 (d, $^{3}J_{P-C}$ 15.4)	-	94.3 (d, $^{3}J_{C-P}$ 13.2)
P-Me	2.50 (d, $^{2}J_{P-H}$ 12.6)	12.97 (d, $^{1}J_{P-C}$ 62.6)	2.91 (d, $^{2}J_{P-H}$ = 13.3 Hz)	13.3 (d, $^{1}J_{C-P}$ 61.9)
ipso-C	-	127.13 (d, $^{1}J_{P-C}$ 87.8)	-	120.1 (d, $^{1}J_{C-P}$ 40.8)
o-C	7.55-7.52	129.45 (d, $^{2}J_{P-C}$ 12.1)	7.71 (m)	132.5 (d, $^{2}J_{C-P}$ 10.9)
m-C	7.67-7.63	132.68 (d, $^{3}J_{P-C}$ 11.0)	7.64 (m)	129.9 (d, $^{3}J_{C-P}$ 12.8)
p-C	7.67-7.53	132.93 (d, $^{4}J_{P-C}$ 3.3)	7.83 (dd, J_{H-H} = 8.9 Hz)	135.0 (d, $^{4}J_{C-P}$ 3.2)
C_5H_5	-	-	4.45 (s)	73.2 (s)

Coordination of **II** to Ru also results in a downfield shift of the ylidic phosphorus from δ 4.83 to 23.3, a similar shift to that seen for coordination of **I** to ruthenium, and again, similar to previously characterized chromium phosphonium indenylide complex $Cr(CO)_3$(**II**).[10] The ESI MS of **VI**, along with that calculated for [CpRu(**II**)]$^+$ are in excellent agreement and are shown in Figure **65**.

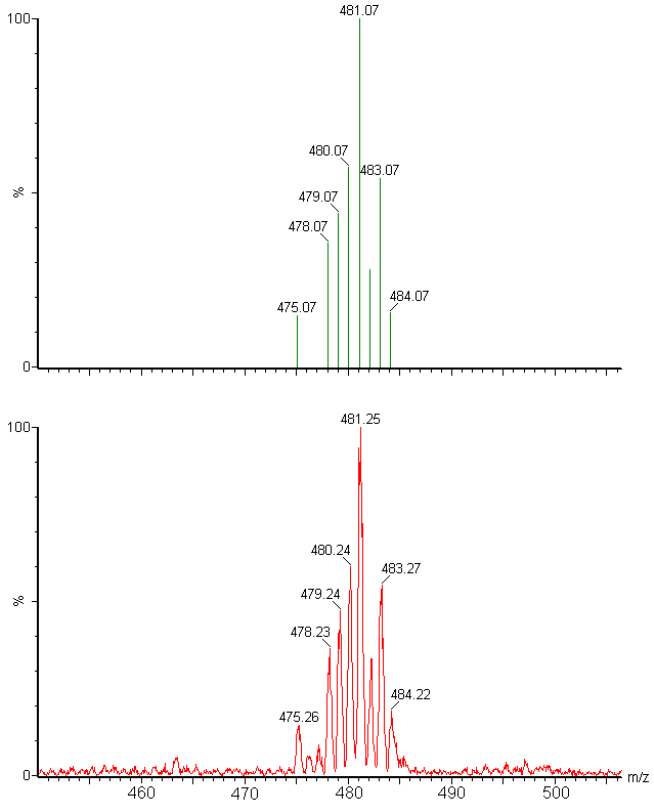

Figure 65. ESI-MS of [CpRu(1-$C_9H_6PMePh_2$)]PF_6 (**VI**) (bottom) and the calculated isotope distribution (top)

3.2.3 Spectral Analysis of [CpRu(1-$C_9H_6PMe_2Ph$)]PF_6 (VII)

^1H and ^{13}C NMR assignments for **III** and **VII** can be found in Table 5 and the ^1H spectrum of **VII** is shown in Figure 66. The protons on the Cp ring are easily identified as they appear as a singlet at δ 4.51. The two P-Me groups appear as two well separated doublets at δ 2.44 and 2.70 and are split only by phosphorus. Two singlets at δ 5.00 and 5.83 couple only to each other (see COSY spectrum Figure 67) and are therefore the protons on the C_5 ring. The latter signal has a through space interaction with a doublet at δ 7.61. Therefore, the peaks at δ 5.00, 5.83 and 7.61 can be assigned to H(2), H(3) and H(4), respectively. Correlations in the COSY spectrum (Figure 67) were used to assign peaks at δ 7.13, 7.10 and 7.21 to H(5), H(6) and H(7), respectively. ^{13}C assignments were made from HSQC (Appendix A) and HMBC (Figure 68) experiments.

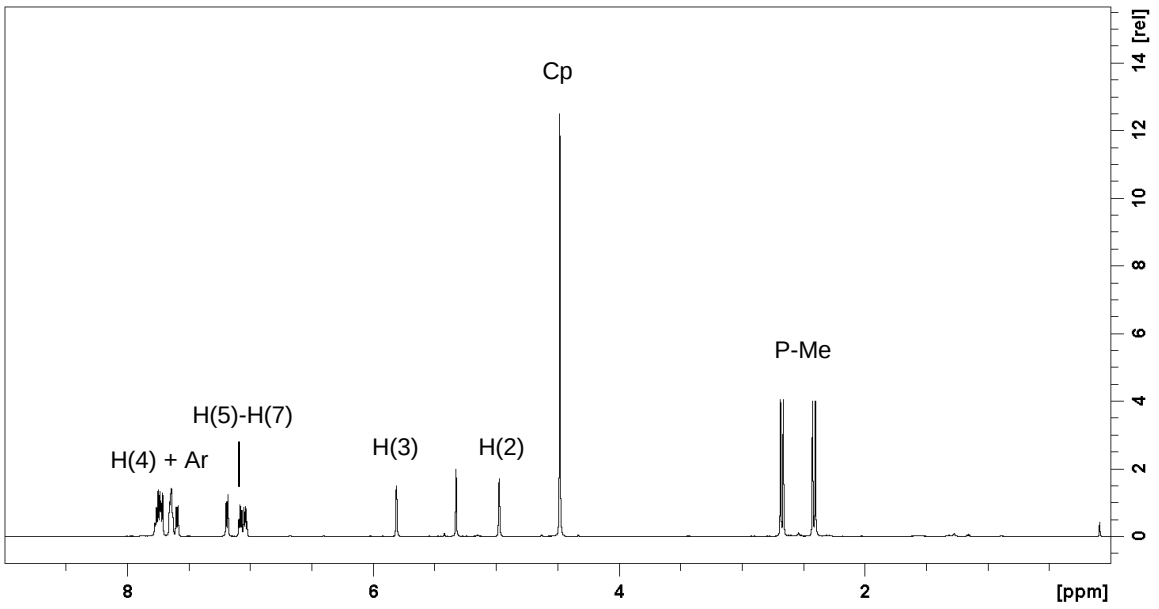

Figure 66. ^1H NMR spectrum of [CpRu(1-$C_9H_6PMe_2Ph$)]PF_6 (**VII**) in CD_2Cl_2

Coordination of **III** to Ru again results in upfield shifts for protons H(2) and H(3) as well as upfield shifts for all carbons of the C_5 ring and is consistent with coordination through the C_5

ring. Due to **III** being pro-planar chiral, the two P-Me groups of **VII** are diastereotopic, as is the case with the phenyl groups in **VI**, and appear as two well separated doublets in the ^{1}H spectrum at δ 2.44 and 2.70. These observations show that inter- and intramolecular interfacial exchange of the coordinated PHIN ligands is slow on the NMR time scale.

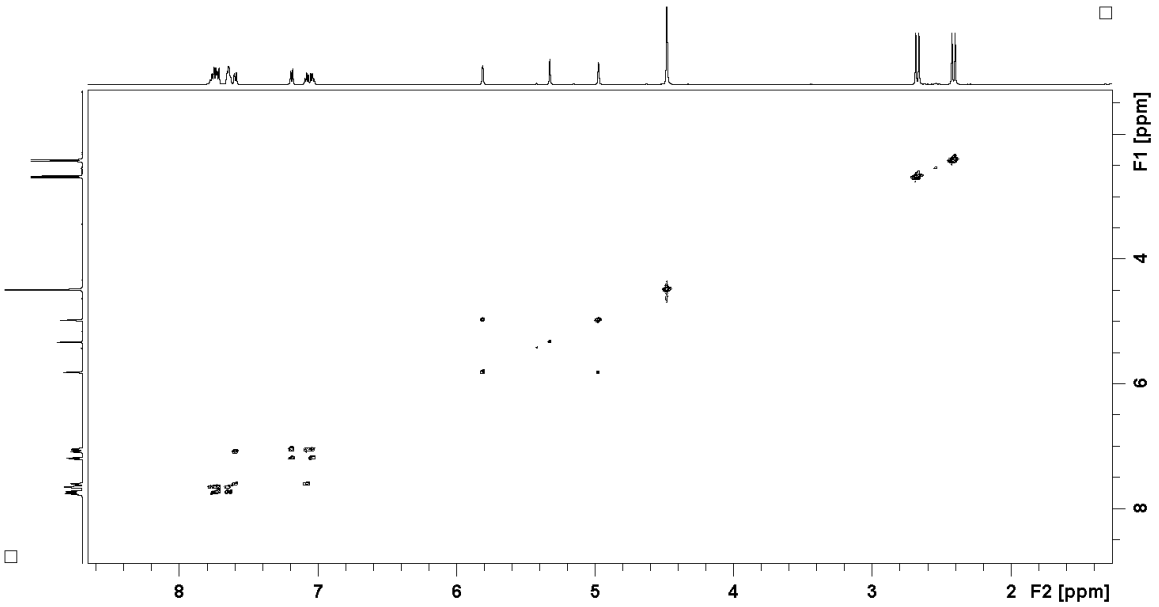

Figure 67. COSY spectrum of[CpRu(1-$C_9H_6PMe_2Ph$)]PF_6 (**VII**) in CD_2Cl_2

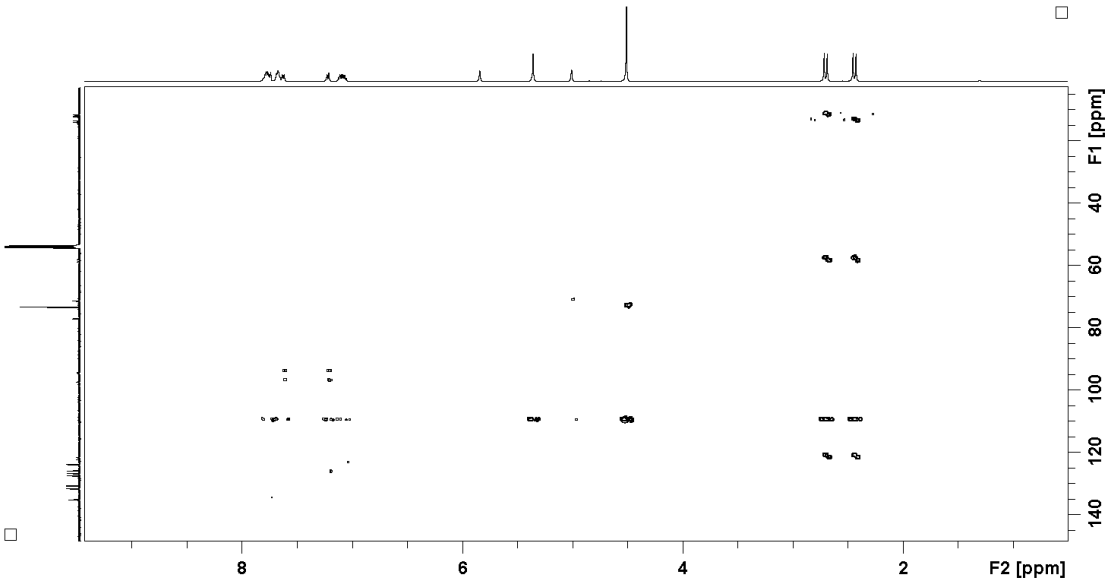

Figure 68. ^{1}H-^{13}C HMBC spectrum of [CpRu(1-$C_9H_6PMe_2Ph$)]PF_6 (**VII**) in CD_2Cl_2

Table 5. ^{1}H and ^{13}C NMR data for 1-$C_9H_6PMe_2Ph$ (**III**) and [CpRu(**III**)]PF_6 (**VII**)

H, C Position	**III**		**VII**	
	δ (^{1}H)[a]	δ (^{13}C)	δ (^{1}H)[a]	δ (^{13}C)
1	-	66.69 (d, $^{1}J_{P-C}$ 121)	-	58.4 (d, $^{1}J_{P-C}$ 102)
2	6.98 (t, $^{3}J_{H-H} = J_{P-H}$ 4.5)	124.2 (d, $^{2}J_{P-C}$ 16.5)	5.00 (s)	77.0 (d, $^{2}J_{P-C}$ 14.5)
3	6.64 (t, $^{3}J_{H-H} = J_{P-H}$ 4.5)	105.8 (d, $^{3}J_{P-C}$ 14.8)	5.83 (s)	71.5 (d, $^{3}J_{P-C}$ 9.6)
4	7.68 (d, $^{3}J_{H-H}$ 8.7)	120.6 (d, $^{4}J_{P-C}$ 1.85)	7.61 (d, $^{3}J_{H-H}$ 8.38)	126.8 (s)
5	6.95 (t, $^{3}J_{H-H}$ 7.6)	116.9 (s)	7.13 (d, $^{3}J_{H-H}$ 7.50)	125.9 (s)
6	6.87 (t, $^{3}J_{H-H}$ 7.6)	117.6 (s)	7.10 (d, $^{3}J_{H-H}$ 7.50)	125.7 (s)
7	7.18 (d, $^{3}J_{H-H}$ 7.9)	116.8 (d, $^{3}J_{P-C}$ 1.85)	7.21 (d, $^{3}J_{H-H}$ 8.52)	123.1 (s)
8	-	134.4 (d, $^{2}J_{P-C}$ 14.8)	-	97.3 (d, $^{2}J_{P-C}$ 8.0)
9	-	137.1 (d, $^{3}J_{P-C}$ 13.0)	-	94.3 (d, $^{3}J_{P-C}$ 14.5)
P-Me	2.21 (d, $^{2}J_{P-H}$ 13.2)	12.92 (d, $^{1}J_{P-C}$ 61.0)	2.70 (d, $^{2}J_{P-H}$ 13.2), 2.44 (d, $^{2}J_{P-H}$ 13.2)	11.8 (d, $^{1}J_{P-C}$ 62.1), 13.7 (d, $^{1}J_{P-C}$ 62.1)
ipso-C	-	128.3 (d, $^{1}J_{P-C}$ 84.2)	-	121.4 (d, $^{1}J_{P-C}$ 86.5)
o-C	7.64 (dd, J_{H-H} 7.3, 13.0)	131.0 (d, $^{2}J_{P-C}$ 11.1)	7.77 (dd, J_{H-H} 5.58, 12.71)	131.5 131.2 (d, $^{2}J_{P-C}$ 10.6)
m-C	7.49 (td, J_{H-H} 2.3, 7.6)	129.3 (d, $^{3}J_{P-C}$ 12.0)	7.67 (td, J_{H-H} 3.25, 7.59)	131.2 (d, $^{3}J_{P-C}$ 12.4)
p-C	7.58 (t, $^{3}J_{H-H}$ 7.9)	132.6 (d, $^{4}J_{P-C}$ 2.77)	7.37 (m)	135.1 (d, $^{4}J_{P-C}$ 3.1)
C_5H_5	-	-	4.51 (s)	73.2 (s)

Coordination of **III** to Ru also results in a downfield shift of the ylidic phosphorus from δ 1.60 to 22.4. The coordination of PHIN ligands to Ru through the C_5 ring results in a downfield shift of the ylidic phosphorus of between 14-21 ppm to a value between δ 22 and 25 and chemical shifts in this range may be anticipated to be from coordinated PHIN-Ru complexes. The ESI MS of **VII**, along with that calculated for $[CpRu(\mathbf{III})]^+$ are in excellent agreement and are shown in Figure **69**.

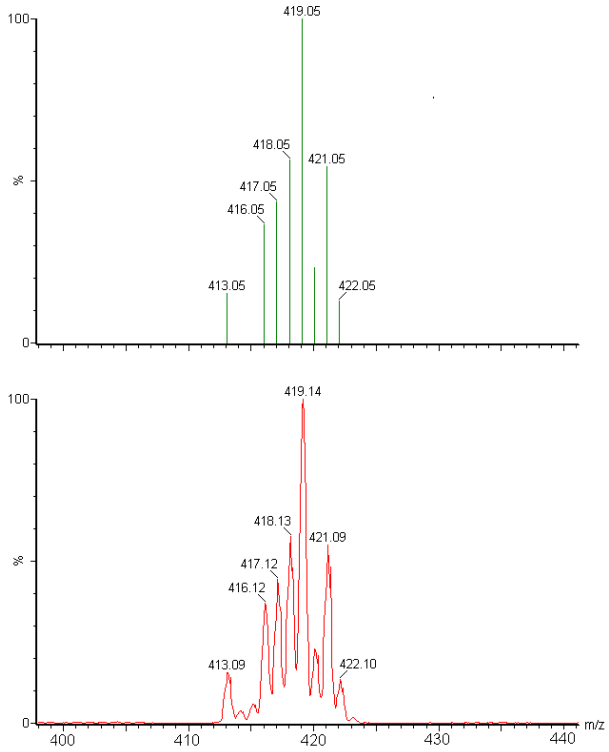

Figure 69. ESI-MS of $[CpRu(1\text{-}C_9H_6PMe_2Ph)]PF_6$ (**VII**) (bottom) and the calculated isotope distribution (top)

3.2.4 X-ray Crystallographic Analysis of V, VI and VII

X-ray quality crystals of **V**, **VI** and **VII** were obtained by the slow evaporation of saturated dichloromethane solutions. The molecular structures of **V**, **VI** and **VII** are shown in Figure **71**, Figure **72** and Figure **73**, respectively and important bond lengths are shown in Table **6**, Table **7** and Table **8**, respectively. Refer to Figure **56** for numbering of the PHIN ligands.

The most important bond length when analyzing coordinated PHIN ligands is the P-C(1) bond length as it is indicative of the relative resonance contributions from the ylene (Figure **70**, left) and ylidic structures (Figure **70**, right). The P-C(1) bond lengths of PHIN ligands are 1.71-1.72 Å; values considerably shorter than the P-Ph bonds which are all over 1.78 Å and are typical for P-C single bonds but are longer that the $P{=}CH_2$ bond length in $Ph_3P{=}CH_2$, 1.66 Å, which is far closer to a P-C double bond. The P-C(1) bond lengths in **V**-**VII** are lengthened by 0.04-0.05 Å compared with the uncoordinated PHIN ligands to a value between 1.768 and 1.761 Å. Thus there appears to be greater contribution from the ylidic resonance structure upon coordination to ruthenium, however, the P-C(1) bond still shows significant double bond character.

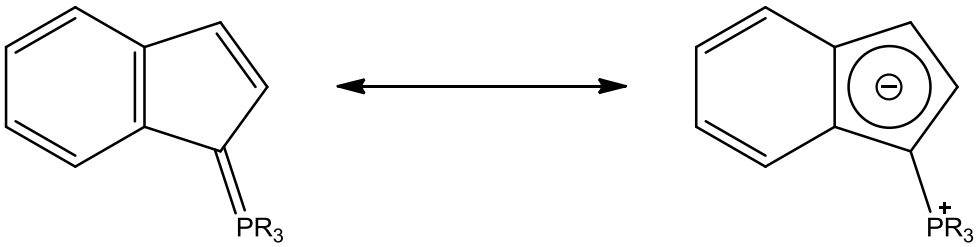

Figure 70. Resonance Structures of the PHINs

The C-C bond lengths in the C_5 ring corroborate this finding. An alternating pattern of 'short' and 'long' C-C bonds indicates there is some degree of localization of π-bond electron density in **I**-**III**. The bonds C(2)-C(3), C(4)-C(5) and C(6)-C(7) for the PHINs **I**-**III** are all

considerably shorter than the bonds C(1)-C(2), C(3)-C(9), C(9)-C(4), C(5)-C(6) and C(7)-C(8). The C(8)-C(9) is 'long' as is observed in the analogous bond of naphthalene (ref 10a from paper).

Upon coordination to form **V**-**VII**, the C(2)-C(3) bond lengthens by around 0.04 Å compared to the PHINs **I**-**III**, and makes all C-C bond lengths in the C_5 ring more similar in length. On the other hand, bond length alternation in the C_6 ring becomes more pronounced with C(4)-C(5) and C(6)-C(7) shortening and C(5)-C(6) and C(7)-C(8) lengthening. This again shows that coordination of the PHIN to Ru(II) results in an increase in contribution from the ylidic resonance structure.

There are large differences in the Ru-C_5 bond lengths in **V**-**VII**, for example, the bonds Ru-C(1), Ru-C(2) and Ru-C(3) of **VI** are all less than 2.183 Å while the bonds Ru-C(8) and Ru-C(9) are over 2.30 Å. This pattern is also seen in the group 6 metal compound Cr(**II**)$(CO)_3$[10]; however, it is not observed for coordinated phosphonium cyclopentadienylides such as $(C_5H_5PMePh_2)M(CO)_3$ (M = Cr, Mo, W).[12]

The Ru-C_5 bond length differences bring to mind indenyl 'slippage' in which the $C_9H_7^-$ ligand can shift from η^5 to η^3 (so-called allyl-ene) mode of coordination.[13,14] The latter is associated with large deviations of the indenyl ligand from planarity. Thus the hinge angle (angle between plane of C(1)-C(2)-C(3) and C(1)-C(3)-C(8)- C(9)) is typically between 20-30° and the fold angle (angle between C(1)-C(2)-C(3) and C(9)-C(4)-C(5)-C(6)-C(7)-C(8)) is typically > 12°.[14] In **V**-**VII** the hinge and fold angles are 2.9-3.7 and 4.3-5.9° respectively and the rings are, therefore, virtually planar.[14]

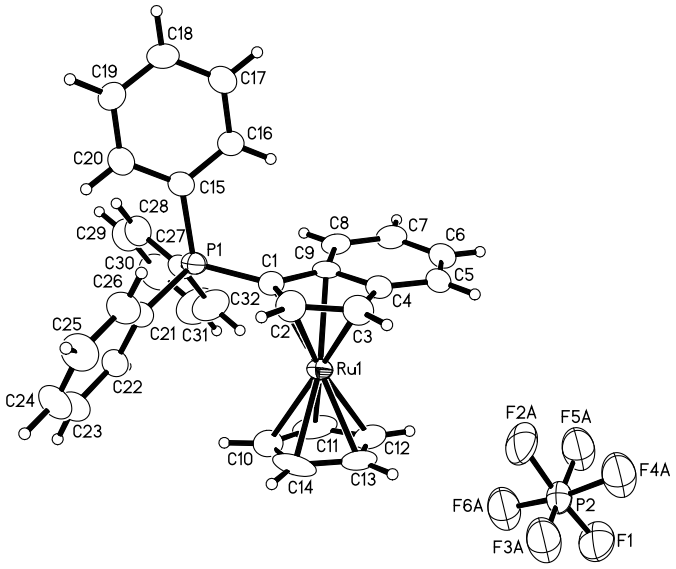

Figure 71. Molecular structure of **V** (Numbering different from that shown in Figure 56)

Table 6. Selected bond lengths for [CpRu(1-$C_9H_6PPh_3$)]PF_6 (**V**)

Bond	Length (Å)	Bond	Length (Å)
C(1)-C(2)	1.444(7)	P(1)-C(1)	1.768(5)
C(2)-C(3)	1.411(8)	P(1)-Ph (avg)	1.794
C(3)-C(9)	1.418(7)	C(1)-Ru	2.163(5)
C(9)-C(4)	1.427(7)	C(2)-Ru	2.176(5)
C(4)-C(5)	1.350(8)	C(3)-Ru	2.176(5)
C(5)-C(6)	1.422(8)	C(9)-Ru	2.20(5)
C(6)-C(7)	1.355(7)	C(8)-Ru	2.24(5)
C(7)-C(8)	1.420(7)	C_5H_5-Ru (avg)	2.16
C(9)-C(8)	1.445(7)		
C(1)-C(8)	1.459(7)		

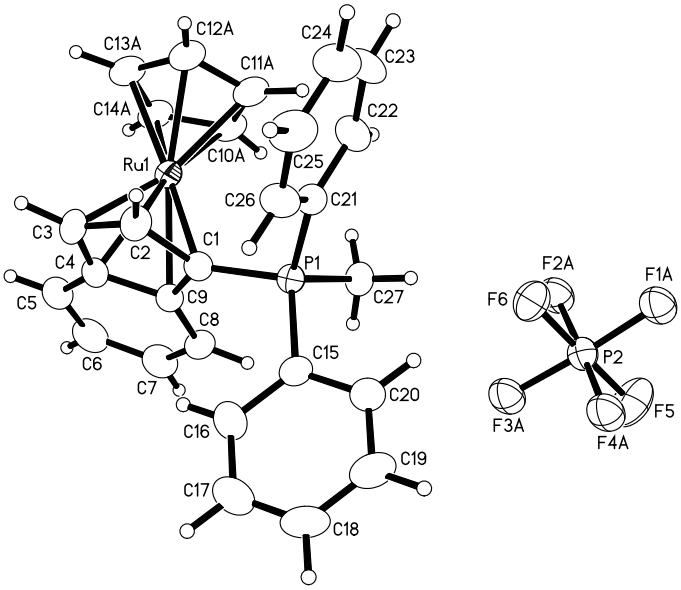

Figure 72. Molecular Structure of **VI** (Numbering different from that shown in Figure 56)

Table 7. Selected bond lengths for [CpRu(1-$C_9H_6PMePh_2$)]PF_6 (**VI**)

Bond	Length (Å)	Bond	Length (Å)
C(1)-C(2)	1.443(5)	P-C(1)	1.763(3)
C(2)-C(3)	1.412(5)	P-Ph (avg)	1.790
C(3)-C(9)	1.427(5)	P - Me	1.787(3)
C(9)-C(4)	1.431(5)	C(1)-Ru	2.170(3)
C(4)-C(5)	1.351(6)	C(2)-Ru	2.172(4)
C(5)-C(6)	1.427(5)	C(3)-Ru	2.183(4)
C(6)-C(7)	1.356(5)	C(9)-Ru	2.230(4)
C(7)-C(8)	1.423(5)	C(8)-Ru	2.242(3)
C(9)-C(8)	1.435(5)	C_5H_5-Ru (avg)	2.17
C(1)-C(8)	1.457(5)		

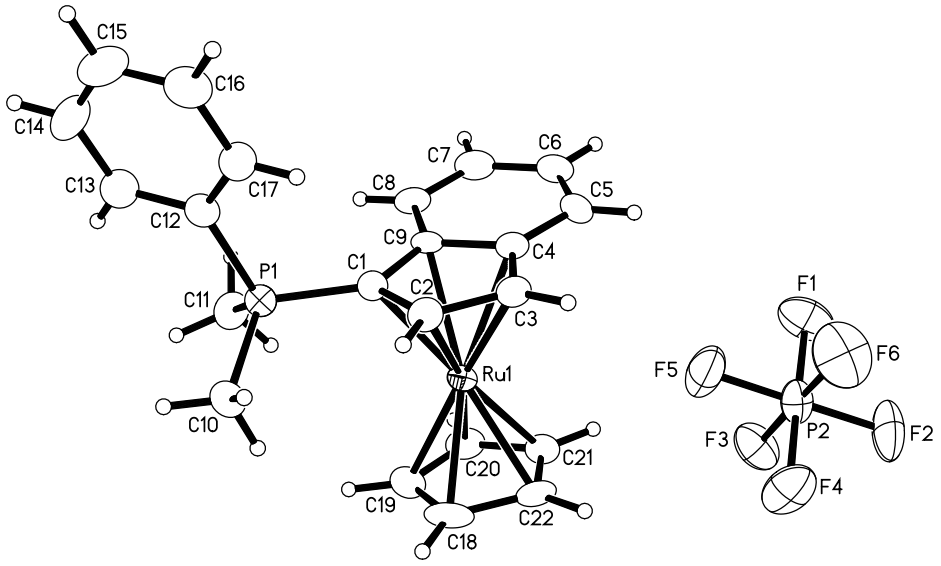

Figure 73. Molecular structure of **VII** (Numbering different from that shown in Figure 56)

Table 8. Selected bond lengths for [CpRu(1-$C_9H_6PMe_2Ph$)]PF_6 (**VII**)

Bond	Length (Å)	Bond	Length (Å)
C(1)-C(2)	1.446(5)	P-C(1)	1.761(4)
C(2)-C(3)	1.414(5)	P-Ph	1.787(4)
C(3)-C(9)	1.435(6)	P-Me (avg)	1.786
C(9)-C(4)	1.423(6)	C(1)-Ru	2.151(4)
C(4)-C(5)	1.365(6)	C(2)-Ru	2.163(4)
C(5)-C(6)	1.415(6)	C(3)-Ru	2.187(4)
C(6)-C(7)	1.367(6)	C(9)-Ru	2.257(4)
C(7)-C(8)	1.423(5)	C(8)-Ru	2.246(4)
C(9)-C(8)	1.439(6)	C_5H_5-Ru (avg)	2.17
C(1)-C(8)	1.449(6)		

3.2.5 Computational Studies of for [CpRu(I-III)]PF_6 (V-VII)

In order to gain more insight into the nature of metal-ligand bonding, the structures of $C_5H_4PMe_3$, $C_5H_4PF_3$, **I-III**, 1-$C_9H_6PMe_3$, 1-$C_9H_6PF_3$ and C_6H_6 as well as their $[Ru(\eta^5\text{-}C_5H_5)]^+$ complexes were calculated were calculated by Peter Budzelaar at the University of Manitoba. The calculated structures of the PHIN ligands were in excellent agreement with the molecular structures obtained from X-ray crystallography. For example, the 'short' C(2)-C(3) bond of **I**, **II** and **III** was calculated to have a length of 1.375 Å, a value very similar to that observed in the X-ray structure. Coordination to Ru(II) results in a calculated lengthening of this bond to 1.417 Å, again, a value similar to that observed and showing that there is an increased contribution for the ylidic resonance structure upon coordination. The ruthenium-aromatic ligand bond dissociation energies of the $[Ru(\eta^6\text{-arene})]^+$ complexes relative to benzene are shown in Table **9**.

Table 9. Calculated bond dissociation energies of the complexes $[CpRu(Ligand)]^+$ relative to C_6H_6 (kcal/mol)

Ligand	ΔG_{273}* (kcal/mol)
$C_5H_4PMe_3$	-32.8
$C_5H_4PF_3$	-6.1
1-$C_6H_9PMe_3$	-19.0
1-$C_9H_6PMe_2Ph$	-20.6
1-$C_9H_6PMePh_2$	-22.6
1-$C_9H_6PPh_3$	-20.4
1-$C_9H_6PF_3$	4.7

The calculated structures of **V-VII** also show the pattern of Ru-C bond lengths found in the X-ray structure. Thus, Ru-C(8) and Ru-C(9) are always found to be 0.1 Å longer than the average of the remaining three Ru-C bonds.

The $C_5H_4PMe_3$ ligand is calculated to bind much more strongly than benzene (by 33 kcal/mol); the PHIN ligands **I-III**, while binding more strongly than benzene (by between 20.4 and 22.6 kcal/mol), bind more weakly than the phosphonium cyclopentadienylide (by 14 kcal/mol).

3.3 Coordination of 1-$C_9H_6PPh_2CH_2PPh_2$ (IV) to [CpRu(MeCN)$_3$)]PF_6

When **IV** was reacted with an equimolar amount of [CpRu(MeCN)$_3$)]PF_6 in CH_2Cl_2 a bright red solution formed which contained two coordinated PHIN species whose relative amounts varied over time. Therefore, the reaction was monitored by NMR spectroscopy in CD_2Cl_2 over a period of approximately two weeks at room temperature. The ^{31}P spectrum contained two pairs of doublets assigned to a kinetic (**VIIIa**) (δ 23.0 and -29.1) and a thermodynamic product (**VIIIb**) (δ 37.7 and 58.1) (Figure **74**). X-ray quality crystals of neither **VIIIa** nor **VIIIb** could be obtained, and therefore, thorough NMR characterization of both isomers was undertaken. Refer to Section 3.3.1 and Section 3.3.2 for a full analysis of the NMR spectra of these two products.

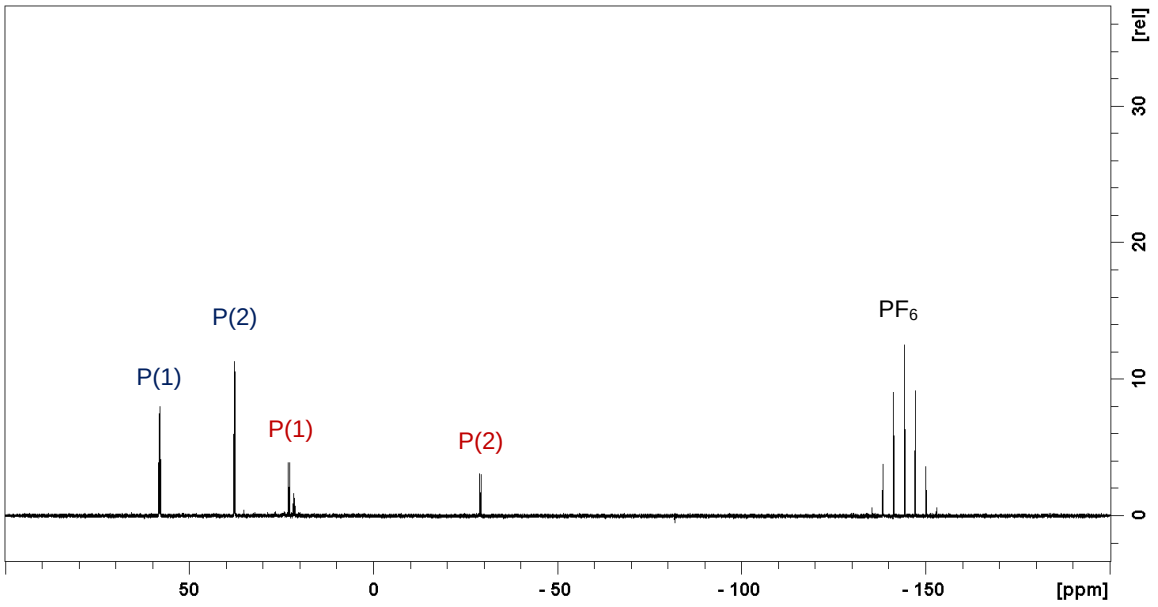

Figure 74. ^{31}P NMR spectrum of a mixture of **VIIIa** and **VIIIb** in CD_2Cl_2

ESI-MS of a freshly prepared reaction mixture showed one series of peaks centered at *m*/*e* 665 with an isotopic pattern in agreement with that calculated for [CpRu(**IV**)]$^+$ and confirming that **VIIIa** and **VIIIb** are isomeric. Over time, another series of peaks centered at *m*/*e* 681 increased in intensity which again appeared to be a monoruthenium species based on the isotope distribution. This was accompanied by a concomitant increase in intensity of an AB quartet in the ^{31}P spectrum at δ 21.63 and 21.24. As the difference in masses between the two species is equal to one oxygen atom, it is possible that the signal at *m*/*e* 681 and the AB quartet in the ^{31}P NMR spectrum are due to oxidation of the phosphine phosphorus by adventitious oxygen to give [CpRu(1-$C_9H_6PPh_2CH_2POPh_2$)]PF_6. The chemical shifts of $Ph_2POCH_2PPh_2$ (δ 27.76)[15] and $PH_2POCH_2POPh_2$ (δ 24.5)[16] are both similar to the AB quartet found around δ 21.5 and the ylidic phosphonium of **VIIIa** (δ 23.0).

3.3.1 NMR Analysis of VIIIa

VIIIa had doublets at δ 23.0 and -29.1 in the ^{31}P spectrum which can be seen in Figure **74**. The former is a value similar to the chemical shift of the ylidic phosphonium in **V-VII** while the latter is similar to the chemical shift of the phosphine in **IV**. Thus it was anticipated that the structure of **VIIIa** involved an η^5 coordination mode similar to that observed for **V-VII** and shown in Figure **75**, with the ^{31}P chemical shift of the ylidic phosphonium being δ 23.0 and the pendant phosphine being δ -29.1.

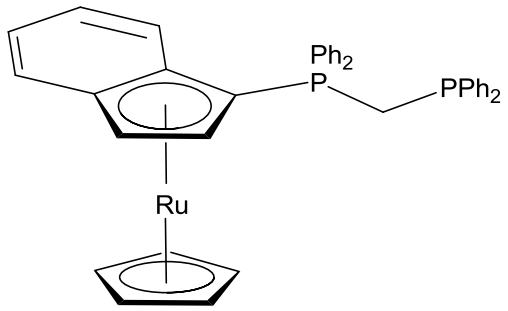

Figure 75. Proposed structure of **VIIIa** based on NMR data

The ^{1}H spectrum of **VIIIa** and **VIIIb**, shown in Figure **76**, is difficult to interpret due to the both isomers containing many inequivalent phenyl groups. Therefore, a series of 1D and 2D NMR experiments were performed to characterize **VIIIa** and assignments of the ^{1}H and ^{13}C NMR spectra can be found in Table **10**. Two sets of peaks are readily identified as they do not have correlations with any other protons in a COSY spectrum (Figure **78**). Thus, the Cp ligand appears as a singlet at δ 4.34; a chemical shift very similar to those of the Cp peaks observed in **V-VII**. The P-CH_2-P protons appear as a multiplet at δ 3.85 which are only split by phosphorus in a ^{31}P NMBC spectrum (Figure **77**). The methylene group simplifies considerably in a $^{1}H\{^{31}P\}$ spectrum where it appears as an AB quartet at δ 3.83 and 3.87. Two triplets with relatively small

coupling constants at δ 4.96 and 5.79 only couple with each other in the COSY spectrum (Figure **78**) and are therefore assigned to the C_5 ring. A NOESY signal between the peak at δ 5.79 and a peak at δ 7.54 (Appendix A) was observed and the peaks at δ 4.96, 5.79 and 7.54 to be assigned to H(2), H(3) and H(4). Correlations in the COSY spectrum allowed peaks at δ 7.03, 6.87 and 6.75 to be assigned to H(5), H(6) and H(7). ^{13}C assignments were made based on HSQC and HMBC spectra (Appendix A).

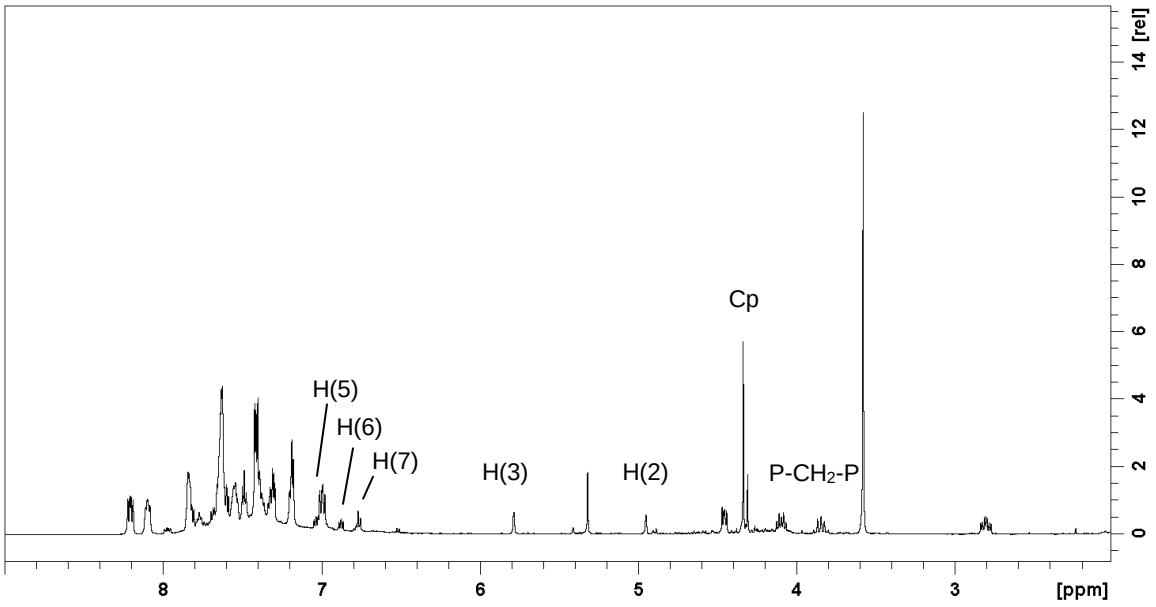

Figure 76. ^{1}H NMR spectrum of a mixture of **VIIIa** and **VIIIb** in CD_2Cl_2 with peaks assigned to **VIIIa** highlighted

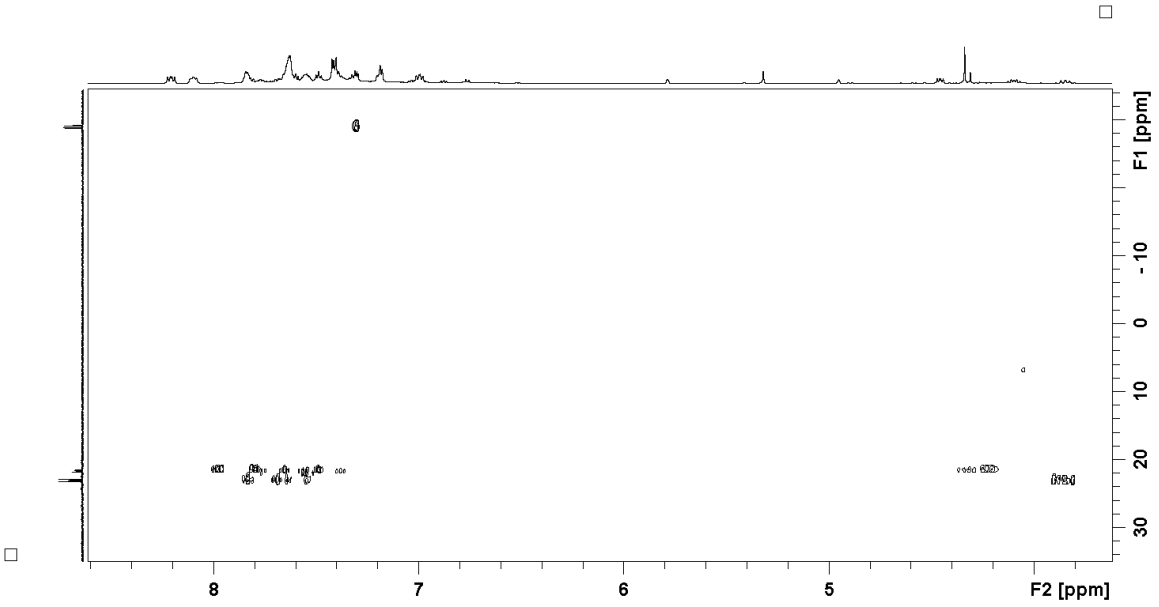

Figure 77. ^{1}H-^{31}P HMBC spectrum of **VIIIa**

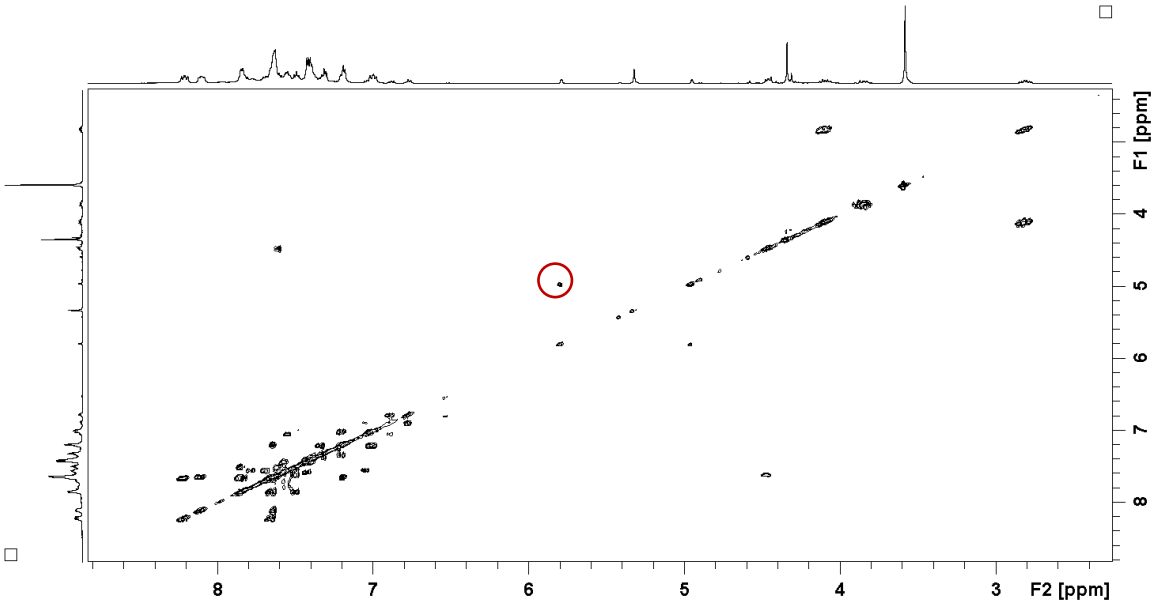

Figure 78. COSY spectrum of a mixture of **VIIIa** and **VIIIb** (H(2)-H(3) correlation is circled).

The ^{1}H chemical shifts of H(2) and H(3) and the ^{13}C chemical shifts of all the C_5 ring carbons undergo significant upfield shifts on coordination, similar to those observed for **V-VII**. The protons on the C_6 ring show little change in chemical shift upon coordination but the ring carbons shift slightly downfield. Thus, the NMR spectra of **VIIIa** are consistent with a sandwich structure analogous to the previously characterized complexes **V-VII** and shown in Figure **75**.

Table 10. ^{1}H and ^{13}C NMR data for **VIIIa**

H, C Position	δ (^{1}H)[a]	δ (^{13}C)
1	-	59.6 (d, $^{1}J_{C-P}$ 102.5)
2	4.96 (t, $^{3}J_{H-H}$ 2.5, $^{3}J_{H-P}$ 2.5)	78.8 (dd, $^{2}J_{C-P}$ 13.7, 6.9)
3	5.79 (t, $^{3}J_{H-H}$ 2.5, $^{4}J_{H-P}$ 2.5)	71.9 (d, $^{3}J_{C-P}$ 9.3)
4	7.54 (m)	126.7 (s)
5	7.03 (ddd, J_{H-H} 8.7, 6.5, 0.8)	126.0 (s)
6	6.87 (ddd, J_{H-H} 8.9, 6.4, 1.2)	125.8 (s)
7	6.75 (dd, J_{H-H} 8.9, 0.6)	124.4 (d, $^{3}J_{C-P}$ 9.4)
8	-	97.4 (d, $^{2}J_{C-P}$ 10.0)
9	-	95.2 (d, $^{3}J_{C-P}$ 12.0)
P-CH_2-P	3.83 (m, $^{2}J_{H-H}$ 15, $^{2}J_{H-P}$ ~ 14), 3.87 (m, $^{2}J_{H-H}$ 15, $^{2}J_{H-P}$ ~ 14)	27.5 (dd, $^{1}J_{C-P}$ 36.9, 27.3)
aromatic	7.30-7.83	128-136
C_5H_5	4.34 (s)	73.8 (s)

Since coordination of the pro-planar chiral ligand **IV** resulted in the P-CH_2-P protons being diastereotopic and appearing as an AB quartet at δ 3.83 and 3.87. Interfacial exchange of the PHIN ligand is slow on the NMR timescale, as with **V-VII**.

3.3.2 NMR Analysis of VIIIb

After standing in CD_2Cl_2 for over 10 days in an NMR tube, **VIIIa** completely isomerized to **VIIIb** and relatively pure samples of the latter could therefore be analyzed by NMR spectroscopy. **VIIIb** had doublets at δ 37.7 and 58.1 in the ^{31}P spectrum (Figure **74**). These chemical shifts are considerably downfield from the typical chemical shifts of PHIN ligands coordinated to ruthenium(II) (δ 21-25) and the dangling $–PPh_2$ group of **IV** (δ -28.3); a phenomenon seen in the coordination of phosphines to a metal centre in which a five-membered ring is formed.[17] The ^{31}P chemical shifts of chelating 1,2-bis(diphenylphosphino) ethane (dppe) metal complexes are typically 20-40 ppm downfield of the chemical shifts of metal complexes of 1,3-bis(diphenylphosphino) propane (dppp) and 1,4-bis(diphenylphosphino) butane (dppb) despite the ^{31}P chemical shifts of the uncoordinated phosphines being similar.[17] It was assumed that an η^3-allylic species had been formed with a coordination site opened up for the pendant phosphine.[18] Two potential η^3-allylic isomers are shown in Figure **79**. In each of these isomers a five-membered ring can be seen which would account for the downfield ^{31}P chemical shifts. As isomers of **VIIIb** are difficult to distinguish spectroscopically, detailed 2D NMR experiments were performed to find evidence for one of them.

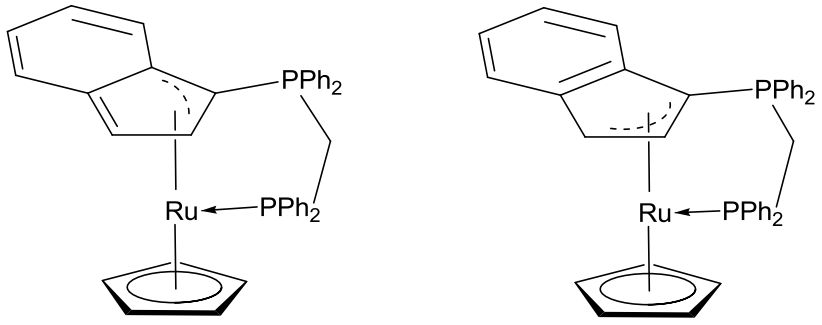

Figure 79. Potential allylic isomers of **VIIIb**

The ^{1}H spectrum of an aged sample containing predominantly **VIIIb** is shown in Figure **80**. The Cp resonance is easily identified as a singlet at δ 3.58 along with the P-CH_2-P methylene group where the protons are again diastereotopic and appear as two well separated doublets of triplets at δ 2.81 and δ 4.10. Interestingly, the P-CH_2-P protons are coupled to both phosphorus atoms, a finding which is of note as only very weak coupling is observed in the corresponding phosphonium salt, uncoordinated ylide **IV** and η^5-coordinated ruthenium(II) complex **VIIIa**.

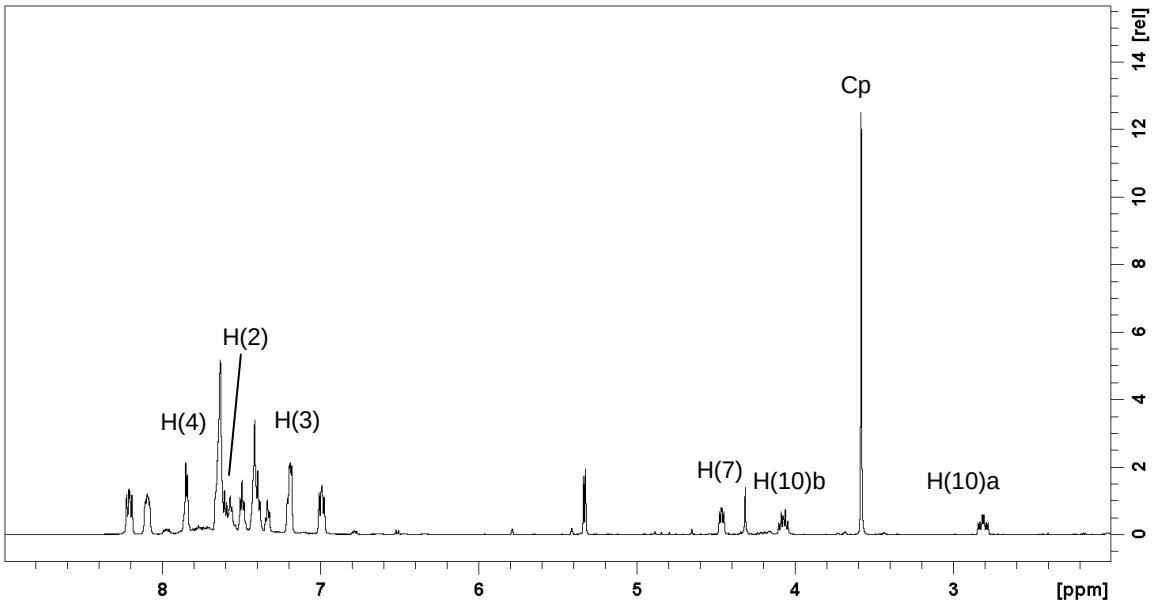

Figure 80. ^{1}H NMR spectrum of an aged sample containing predominantly **VIIIb** in CD_2Cl_2

Unlike typical ruthenium PHIN complexes, two peaks could not be readily identified as the protons on the C_5 ring. A correlation observed in the COSY spectrum (Figure 82) between two protons at δ 7.63 and 7.17 shows the weak coupling which has previously been observed for C_5 ring protons, but not for C_6 ring protons (see Tables 3-5). A NOESY experiment (Figure 81) showed a through space interaction between the resonance at δ 7.17 and that at δ 7.84. Thus the resonance at δ 7.17 was assigned to H(3) the resonance at δ 7.63 to H(2) and the resonance at δ 7.84 to H(4). A ^{31}P HMBC experiment (Figure 83) exhibited a correlation between the proton

resonance at δ 7.17 and the phosphorus resonance at δ 37.8 which was therefore assigned to P(1). A combination of NOESY and COSY data were used to assign resonances at δ 7.49, δ 7.60 and δ 4.45 to H(5), H(6), and H(7), respectively. Full ^{1}H and ^{13}C assignments for **VIIIb** can be found in Table 11. A stronger cross peak in the ^{31}P HBMC experiment between P(1) and H(2) is obscured under the cross-peak for one of the *o*-phenyl protons.

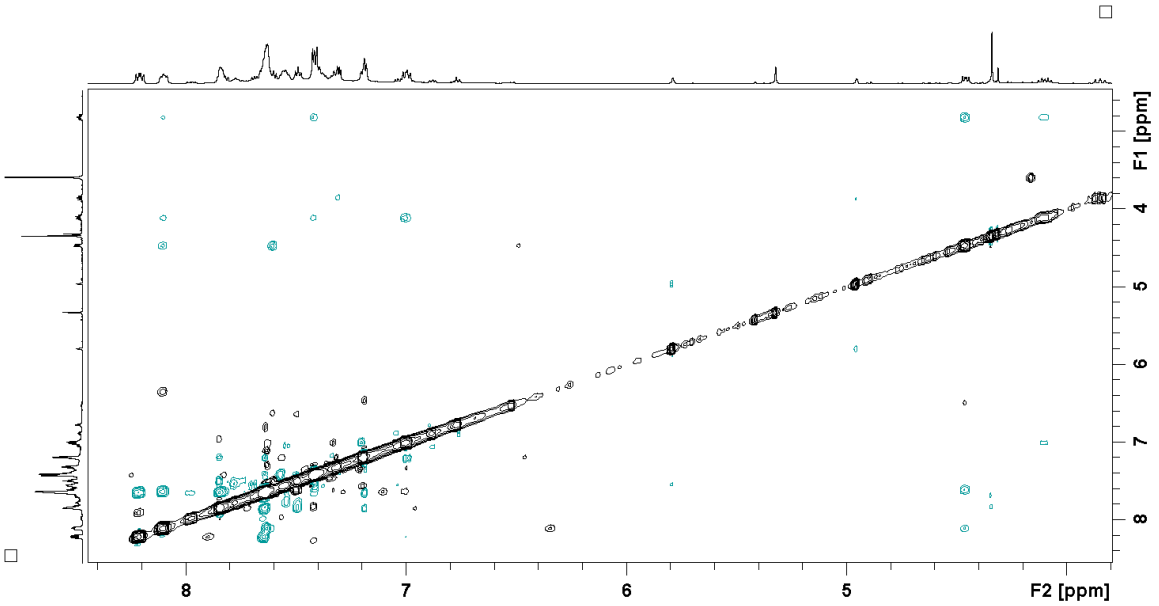

Figure 81. NOESY spectrum of an aged sample containing predominantly **VIIIb** which shows exchange cross peaks from the unknown species **VIIIc** (in teal)

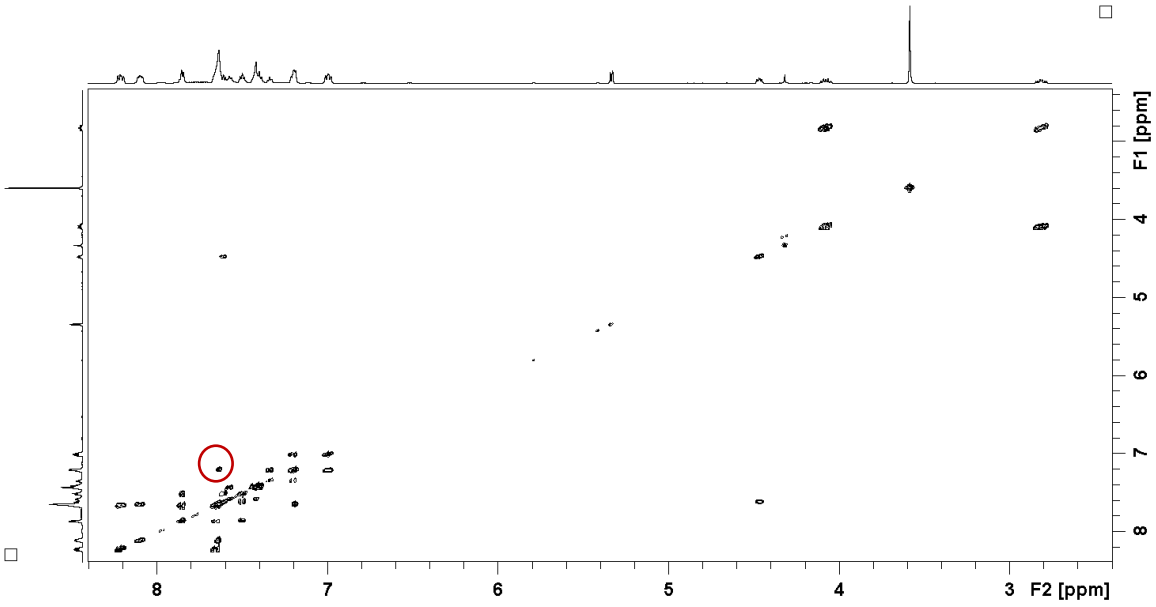

Figure 82. COSY spectrum of an aged sample containing predominantly **VIIIb** (H(2)-H(3) correlation is circled)

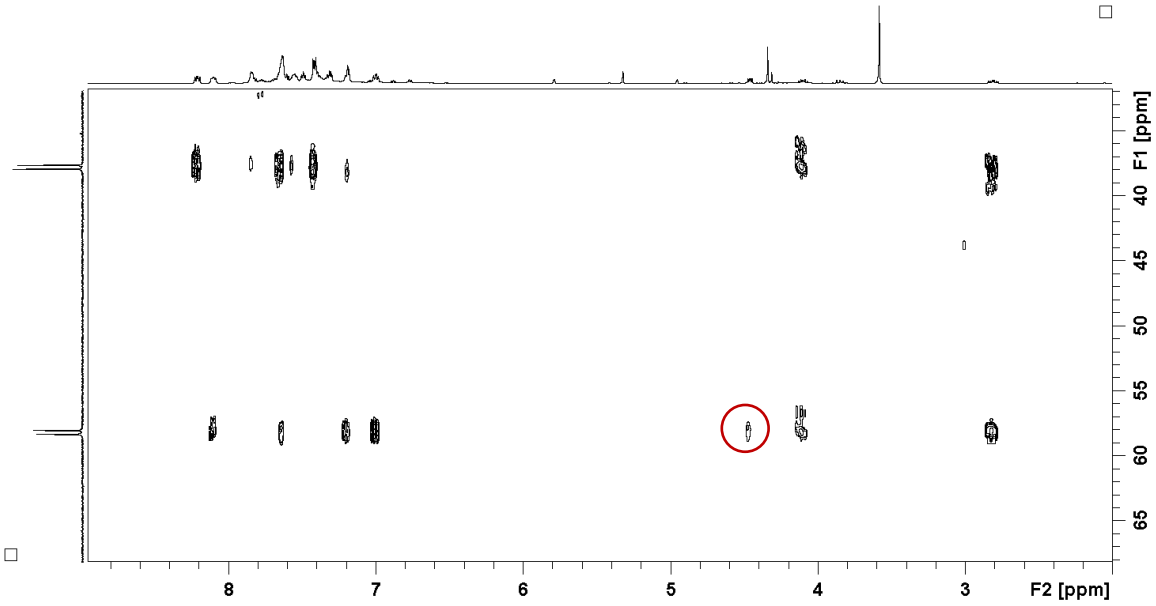

Figure 83. ^{1}H-^{31}P HMBC spectrum of an aged sample containing predominantly **VIIIb** (H(7)-P(2) correlation is circled).

Table 11. ^{1}H and ^{13}C NMR data for chelating complexes **VIIIb** and **VIIIc**

	VIIIb		**VIIIc**
H, C Position	δ (^{1}H)[a]	δ (^{13}C)	δ (^{1}H)[a]
1	-	46.4 (d, $^{1}J_{C-P}$ 81.5)	-
2	7.63 (s)	142.1 (d, $^{2}J_{C-P}$ 8.7)	NA
3	7.17 (s)	123.6 (d, $^{3}J_{C-P}$ 10.7)	6.46
4	7.84 (m)	122.8 (s)	6.96
5	7.49 (m)	125.2 (s)	6.64
6	7.60 (m)	129.0 (s)	6.21
7	4.45(dd, $^{3}J_{H-H}$ 6.4, $^{3}J_{H-P}$ 10.5)	70.4 (s)	6.50
8	-	98.0 (d, $^{2}J_{C-P}$ 6.3)	-
9	-	148.3 (d, $^{3}J_{C-P}$ 6.5)	-
P-CH_2-P	2.81 (dt, $^{2}J_{H-H}$ 16.25, $^{2}J_{H-P}$ 6.9), 4.10 (dt, $^{2}J_{H-H}$ 16.15, $^{2}J_{HP}$ 9.3)	30.6 (dd, $^{1}J_{C-P}$ 70.2, 7.6)	2.81, 4.10
Aromatic	Table 12	125-135	-
C_5H_5	3.58 (s)	80.0(s)	4.16

There are four aromatic resonances that couple strongly with phosphorus at δ 7.41, 8.20, 6.98 and 8.09 which have been assigned to the *ortho* protons of the four inequivalent phenyl groups. The ^{31}P HMBC spectrum (Figure **83**) was used to assign the first two signals to phenyl groups attached to P(1) and the second two to the phenyl groups attached to P(2). A combination of COSY and NOESY (Figure **81**) spectra were used to determine the chemical shifts of the remaining protons on all four phenyl groups and these assignments are shown in Table **12**.

Table 12. ^{1}H NMR data for the four inequivalent phenyl groups of **VIIIb**

	P(1)		P(2)	
H, position	Ph(1) - δ (^{1}H)	Ph(2) - δ (^{1}H)	Ph(1) - δ (^{1}H)	Ph(2) - δ (^{1}H)
o	7.41	8.20	6.98	8.09
m	7.42	7.65	7.19	7.63
p	7.56	7.84	7.33	7.65

The chemical shift of H(7) (δ 4.45) is strange as in previously characterized PHIN-Ru(II) complexes the only resonances observed between δ 4-6.5 are assigned to H(2) and H(3), protons attached to carbons bonded to ruthenium. In addition, the ^{31}P HMBC experiment (Figure **83**) shows that H(7) is coupled to P(2). H(7) is not coupled to any phosphorus resonance in corresponding phosphonium salt, **IV** and **VIIIa**. The only conceivable way in which such a correlation could arise is by three bond coupling through the ruthenium centre and C(7).

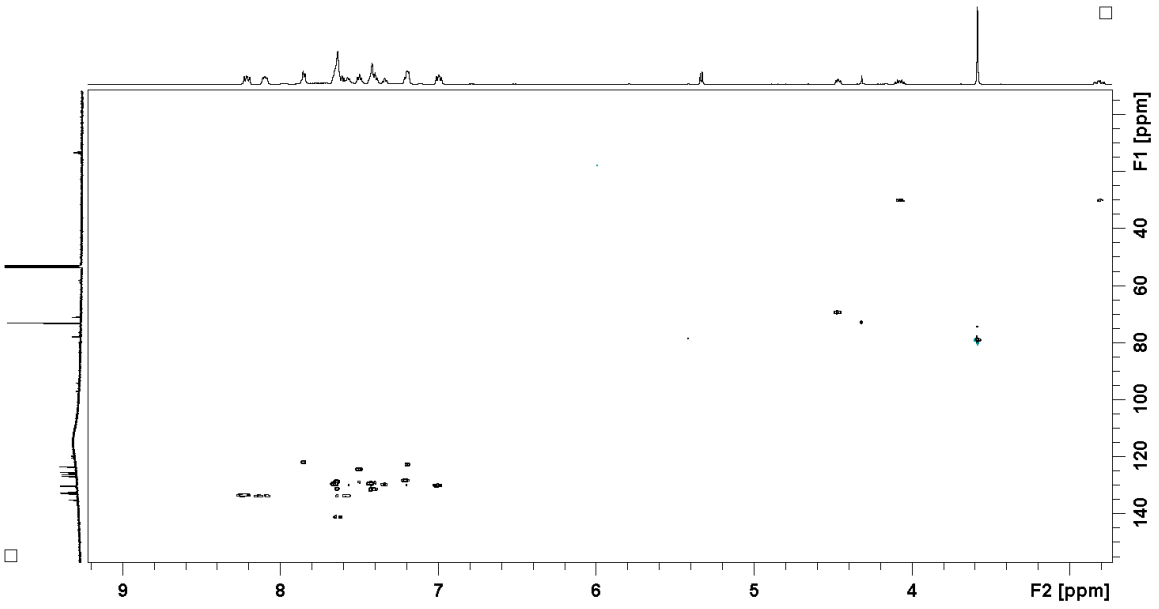

Figure 84. ^{1}H-^{13}C HSQC spectrum of an aged sample containing predominantly **VIIIb** in CD_2Cl_2

Assignment of the ^{13}C spectrum with the aid of HSQC (Figure 84) and HMBC experiments provided further insight into the nature of coordination in **VIIIb** and assignments are shown in Table 11. C(1), C(7) and C(8) are significantly shielded relative to **IV**, while C(2), C(3) and C(4) are significantly deshielded. As discussed for complexes **V-VII**, an upfield shift is observed for carbons bonded to ruthenium, while a downfield shift is observed for those carbons not bonded to ruthenium.

The above observations are consistent with the structure shown in Figure **85** with an unprecedented η^3 mode of coordination through C(1), C(8), and C(7). This structure accounts for the ^{13}C chemical shifts mentioned above and the correlation between H(7) and P(2) from three-bond coupling through the Ru centre. In addition, a five-membered ring is formed with the ruthenium centre, C(1), P(1), C(10) and P(2) which accounts for the otherwise anomalous downfield shifts in the ^{31}P NMR spectrum.

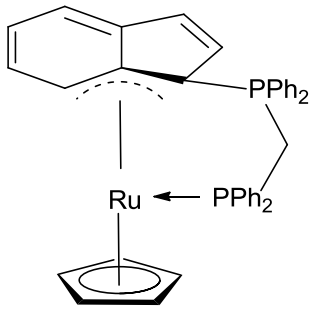

Figure 85. Proposed structure of **VIIIb** based on NMR data

Additional insights into the structure of **VIIIb** may be gained from the NOESY spectrum (Figure **81**). A through space interaction was observed between H(7) and the peak at δ 2.81 (henceforth H(10a)) as well as between the Cp resonance and the peak at δ 4.10 (henceforth H(10b)). Therefore, H(10a) points toward the PHIN C_6 ring, while H(10b) points toward the Cp

ring. That H(10a) points toward the C_6 ring seems to rule out several other possible structures for **VIIIb** where (Figure **79**) η^3 allylic bonding occurs through more than one carbon of the C_5 ring.

Interestingly, the NOESY spectrum of **VIIIb** (Figure **81**) showed a significant number of cross peaks due to exchange in addition to through-space interactions. In fact, every peak assigned to **VIIIb** has an exchange cross peak with an unknown compound **VIIIc**, with the exception of the methylene protons. The peaks in the ^{1}H NMR spectrum corresponding to **VIIIc** are too weak to be analyzed meaningfully, and the equilibrium between these species is strongly in favour of **VIIIb**; however, most of the ^{1}H chemical shifts for **VIIIc** can be assigned and are given in Table 11.

Isomerization of **VIIIb** to **VIIIc** results in shielding of all the protons of the indenylide ring, with the exception of H(7), which is deshielded considerably to a value more typical for a phenyl proton. Coordination of **IV** in **VIIIc** therefore does not involve C(7). Several of the phenyl protons also shift considerably upon isomerization; for example, the ortho proton at δ 8.10 shifts to δ 6.35. The dramatic change in chemical environment may be caused by shifting from the deshielding to the shielding zone of the Cp ring.

3.3.3 Computational Studies on the isomers of VIII

Due to the lack of success obtaining single crystals of **VIIIa** and **VIIIb**, computational studies were carried out by Peter Budzelaar at the University of Manitoba in order to better understand these complexes. A local energy minimum was calculated to have a structure very similar to that of previously characterized PHIN-Ru(II) complexes **V**-**VII** (see Figure **75** and Table **13**). The pattern of Ru-C bond distances was similar to those determined by X-ray crystallography for **V**-**VII**, with three being 'short' (~2.22 Å) and two 'long' (~2.32 Å). In addition, the C-C bonds of the C_6 ring also exhibited a pattern of bond lengths with C(4)-C(5) and C(6)-C(7) being short. Since the NMR data for **VIIIa** are consistent with the η^5 sandwich

structure and computational studies suggest this structure is a local energy minimum, this assignment now seems confirmed.

Table 13. Calculated energies of isomers of [CpRu(**IV**)]PF_6

Compound	G_{rel} (kcal/mol)
VIIIa	0.00
VIIIb	3.24
VIIIc	12.92

Two discrete local minima were found in which coordination of **IV** to Ru(II) was through an η^3-allylic mode, each with a different set of PHIN carbons bonded to ruthenium. Interestingly, the lowest energy isomer was an allylic species which is essentially that determined by NMR data to be **VIIIb** and shown in Figure **86**. The calculated structure has a planar indenyl group with the ylidic phosphorus lying well out of the plane. The Ru-C(1), Ru-C(7) and Ru-C(8) bond distances are calculated to be between 2.27 and 2.55 Å, while the rest of the PHIN carbon-ruthenium distances are calculated to be greater than 3.2 Å and are therefore nonbonding. The C-C bond distances also agree with the structure given, with C(2)-C(3), C(9)-C(4) and C(5)-C(6) all being relatively short as shown in Figure **85**.

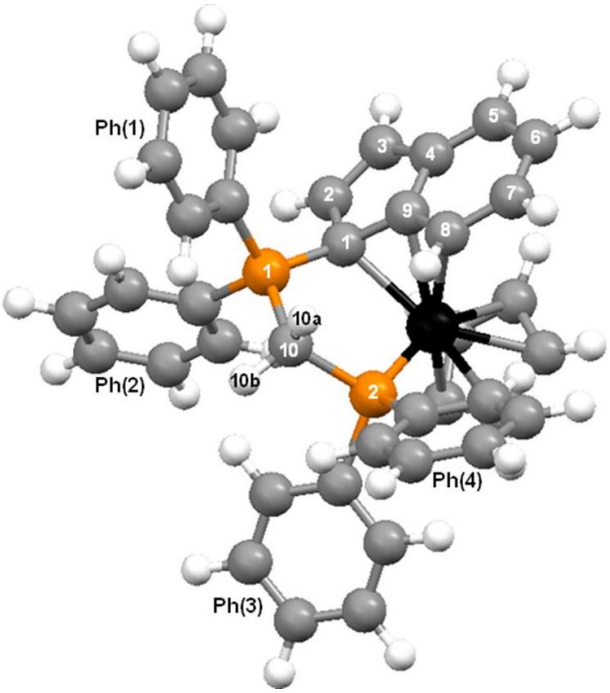

Figure 86. Calculated structure of the η^3-allylic isomer corresponding to **VIIIb**

The calculated energy difference between **VIIIa** and **VIIIb** is small, with a best estimate of 3.2 kcal/mol in favour of **VIIIa**. Therefore, there is disagreement between the calculated energies and the observation that **VIIIb** is the thermodynamically favoured product. However, the calculated energy difference is well within the limits of computational uncertainty and, therefore, all that can be concluded is that the energy difference between the two isomers is small.

Another local energy minimum calculated to be about 13 kcal/mol above that calculated for **VIIIb** was found as well. This again had an η^3-allylic type bonding through C(2), C(3) and C(9) and formed a 6-membered ring through the pendant $-PPh_2$ moiety binding to the Ru(II) centre. Unfortunately, it is impossible to tell if this complex is **VIIIc** as the available NMR data for this species provide few clues as to its structure.

3.4 Attempted Coordination of PHINs to Ruthenium using $RuCl_3 \cdot xH_2O$

Since the vast majority of arene-ruthenium(II) complexes are synthesized by dehydrogenation of cyclohexadienes,[19] it was hoped that a similar approach, involving the deprotonation of a phosphonium salt [1-$C_9H_7PR_3$]X (X = Br, I), would yield PHIN-ruthenium complexes similar to the extensively studied arene complexes, $[RuCl(\mu\text{-}Cl(\eta^6\text{-arene})]_2$. Alternatively, a reducing agent may be used to reduce Ru(III) to Ru(II) in the presence of a PHIN ligand which may then bind the metal centre. Potential problems with reactions of this type are due to the aqua ligands bound to the ruthenium in $RuCl_3 \cdot xH_2O$. The electropositive nature of Ru(III) removes electron density for the oxygen of water and makes the protons very acidic. Therefore, protonation of a PHIN ligand to form the phosphonium salt may be a potential complication.

3.4.1 Reaction of [1-$C_9H_7PMePh_2$]I with $RuCl_3 \cdot xH_2O$

The reaction of a 1:1 ratio of the phosphonium salt [1-$C_9H_7PMePh_2$]I with $RuCl_3 \cdot xH_2O$ in ethanol resulted in the precipitation of a mixture containing a number of phosphorus containing species, none of which appear to contain a PHIN coordinated to ruthenium (see below). In the ^{31}P spectrum, a major species with a resonance at δ 23.9 is observed which is coupled with a P-Me doublet at δ 2.69. These chemical shifts are similar to the previously characterized sandwich complex **VI**. However, the ^{1}H spectrum (Figure **87**) of this species does not have any olefinic peaks for H(2) and H(3). The ^{31}P HMBC spectrum does not help in assigning H(2) and H(3) either. In this spectrum, there are no correlations in the olefinic region; however, there are four in the aliphatic region: a CH_3 group at δ 0.89, two CH_2 groups overlapping at δ 1.55, a CH_2 group at δ 2.92 and the aforementioned P-Me group. The aromatic region contained a set of three partially overlapping peaks between δ 7.5 and 8; however, there was no sign of the aromatic protons of the C_6 ring of the PHIN which are typically slightly upfield of the P-Ph groups.

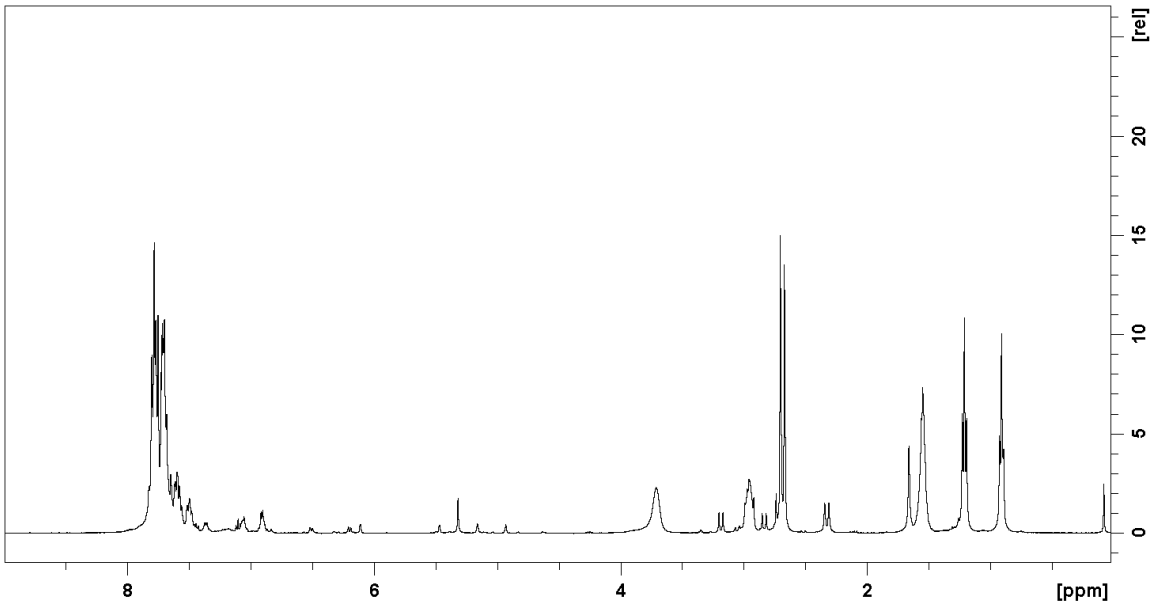

Figure 87. ^{1}H NMR spectrum of the precipitate formed from the reaction of $RuCl_3 \cdot xH_2O$ with [1-$C_9H_7PMePh_2$]I in CD_2Cl_2

Despite the ^{13}P chemical shift of the major product from the reaction of [$C_9H_7PMePh_2$]I with $RuCl_3 \cdot xH_2O$ being similar to that observed for previously characterized ruthenium(II)-PHIN complexes, it appears that this is strictly a coincidence and that the PHIN ligand does not remain intact. The ESI-MS spectrum of this product corroborates this, as signals at 257.4 and 513.3 *m*/*z* are observed, neither of which are from ruthenium containing species. The structure of this phosphorus species has not been deduced; however, it is not a PHIN nor is it the phosphonium salt of a PHIN resulting from protonation.

3.4.2 Attempted Coordination of III to Ruthenium with $RuCl_3 \cdot xH_2O$ and Zn(s)

Reacting **III** with a mixture of $RuCl_3 \cdot xH_2O$ and an excess of Zn powder in MeCN resulted in a dark green solution which contained many phosphorus species. While there were five resonances in the ^{31}P NMR spectrum between δ 20 and 30 (where coordinated PHIN

complexes are likely to be found), no P-Me groups could be identified in the ^{1}H NMR spectrum. There is no evidence that **III** remained intact and the nature of the ^{31}P containing species remains unknown.

It is clear that using $RuCl_3 \cdot xH_2O$ as a ruthenium(II) source is not effective for making ruthenium-PHIN complexes. Under none of the above conditions is there any indication that the PHIN ligand remained intact. The reaction products remain unknown, and another approach to coordinate PHIN ligands to Ru must be investigated.

3.5 Coordination of PHINs to Ruthenium using $[RuCl(\mu\text{-}Cl)(\eta^6\text{-arene})]_2$

After failing to coordinate PHIN ligands to Ru(II) using $RuCl_3 \cdot xH_2O$ as a starting material, arene exchange reactions using complexes of the type $[RuCl(\mu\text{-}Cl)(\eta^6\text{-arene})]_2$ were investigated. Most of the arene exchange reactions reported (see Introduction) have used $[RuCl(\mu\text{-}Cl)(\eta^6\text{-}p\text{-cymene})]_2$ as a starting material and this was investigated in the arene exchange reactions with PHINs. The *p*-cymene ligand binds relatively strongly to the Ru(II) centre while arenes with electron withdrawing substituents are more easily displaced.[20] Therefore, the complex $[RuCl(\mu\text{-}Cl)(\eta^6\text{- ethylbenzoate})]_2$ was also investigated in the arene exchange with PHINs.

3.5.1 Solvent-free Reaction of II with $[RuCl(\mu\text{-}Cl)(\eta^6\text{-}p\text{-cymene})]_2$

The first method to effect arene exchange on ruthenium(II) involved reacting $[RuCl(\mu\text{-}Cl)(\eta^6\text{-arene})]_2$ in a melt of a second arene and was first reported for the synthesis of $[[RuCl(\mu\text{-}Cl)(\eta^6\text{-}C_6Me_6)]_2]$.[21] Therefore, arene exchange of $[RuCl(\mu\text{-}Cl)(\eta^6\text{-}p\text{-cymene})]_2$ with molten **II** was attempted. $[RuCl(\mu\text{-}Cl)(\eta^6\text{-}p\text{-cymene})]_2$ was added to a four-fold excess of **II** in a Schlenk flask and heated to around 250 °C in a sand bath. Although the PHIN did not appear to melt, it was clear that a reaction took place by the formation of a red solid on the sides of the flask. Extraction

of this solid with toluene produced a brown-red solution which was decanted and evaporated to dryness under reduced pressure.

The ^{31}P NMR spectrum of the resulting solid showed two resonances at δ 20.4 and 24.2, both of which are similar to the chemical shifts of **V**-**VII**. However, the ^{1}H NMR spectrum (Figure 88) did not have any of the peaks associated with a PHIN ligand. A P-Me group was found at δ 1.9, a value shielded considerably from that of **II**. From the ^{31}P HMBC spectrum (Figure 90), this P-Me group was coupled to the phosphorus at δ 20.4. These two resonances are identical to the product of cleavage of the chloride bridge of $[RuCl(\mu\text{-}Cl)(\eta^6\text{-}p\text{-cymene})]_2$ with $PMePh_2$, $RuCl_2(p\text{-cymene})(PMePh_2)$.[22] It is therefore proposed that the decomposition of **II** proceeds by homolytic cleavage of the P-C(1) bond resulting in the phosphine, $PMePh_2$, and a carbene (Figure **89**). Although neither the carbene nor its dimerization products were observed, this appears to be the only way to generate $PMePh_2$. All proton resonances reported for $RuCl_2(p\text{-cymene})(PMePh_2)$[22] are also found in the ^{1}H NMR spectrum of this solid (Figure **88**). The ^{31}P resonance at δ -5.8 could not be assigned. It shows no correlations in the ^{31}P HMBC spectrum with protons in the aliphatic region indicating it is likely not a PHIN species.

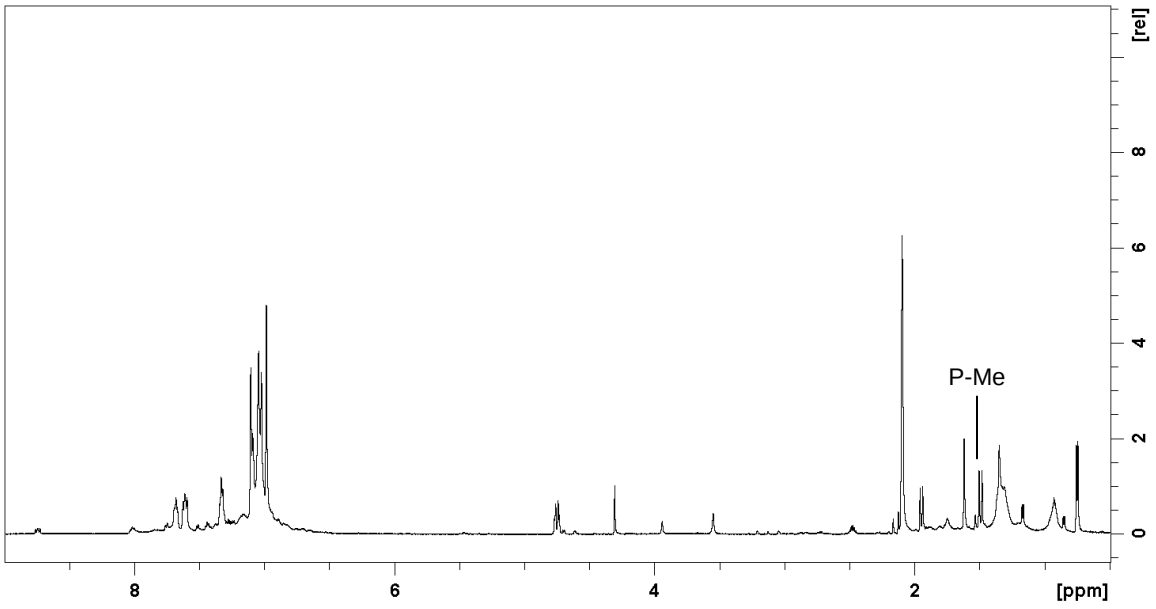

Figure 88. ^{1}H NMR spectrum of the toluene extract from the solvent-free reaction of [RuCl(μ-Cl)(η^{6}-*p*-cymene)]$_2$ with **II** in toluene D_8

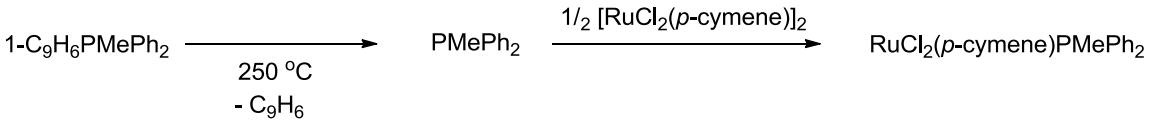

Figure 89. Proposed scheme for the formation of $RuCl_2$(p-cymene)($PMePh_2$) from heating **II** and [RuCl(μ-Cl)(η^{6}-*p*-cymene)]$_2$

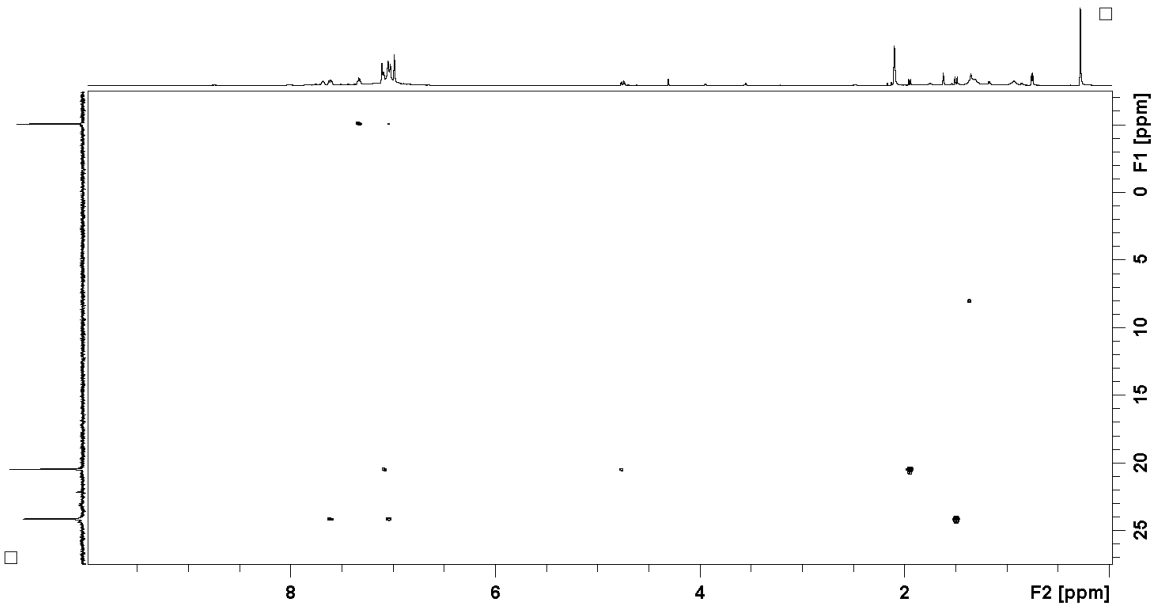

Figure 90. ^{1}H-^{31}P HMBC spectrum of the toluene extract from the solvent-free reaction of [RuCl(μ-Cl)(η^{6}-*p*-cymene)]$_2$ with **II** in toluene D_8

The ^{31}P resonance at δ -5.8 could not be assigned. It shows no correlations in the ^{31}P HMBC spectrum with protons in the aliphatic region.

3.5.2 Synthesis of $RuCl_2(\eta^6$-*p*-cymene)$(\eta^1$-1-$C_9H_6PPh_2CH_2PPh_2)$ (IX)

Many ruthenium(II) arene exchange reactions involve intramolecular attack of a tethered arene (see Introduction). A similar approach may be envisioned with the PHIN **IV** as it has a pendant phosphine which is capable of breaking the chloride bridge of a dimer such as [RuCl(μ-Cl)(η^{6}-*p*-cymene)]$_2$.

Reacting an equimolar amount of 1-$C_9H_6PPh_2CH_2PPh_2$ (**IV**) with [RuCl(μ-Cl)(η^{6}-*p*-cymene)]$_2$ resulted in cleavage of the chloride bridge by the pendant phosphine to form $RuCl_2(\eta^6$-*p*-cymene)$(\eta^1$-1-$C_9H_6PPh_2CH_2PPh_2)$ (**IX**) (Figure **91**), which could be precipitated out by addition of hexanes and evaporation of the dichloromethane solvent under reduced pressure. **IX** is readily

soluble in THF, dichloromethane, acetonitrile and toluene. It is slightly soluble in diethyl ether and not soluble at all in hexanes. Elemental analysis was not performed on **IX** due to solvent contamination which could not be removed even after drying at 0.01 torr overnight.

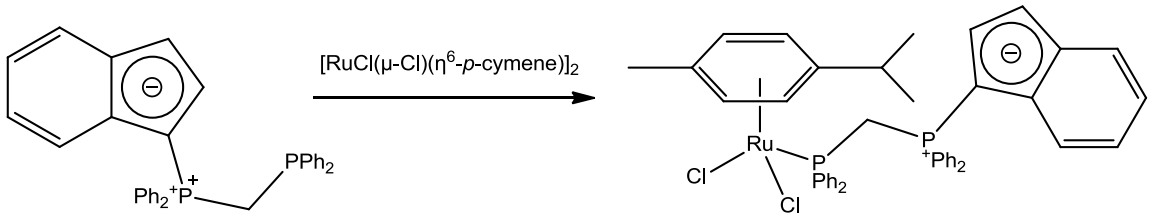

Figure 91. Synthesis of $RuCl_2(\eta^6$-*p*-cymene)(η^1-**IV**) (**IX**)

X-ray quality crystals of **IX** were prepared by slow evaporation of a THF solution and the molecular structure is shown in Figure **92** along with important bond lengths in Table **14**. The P(1)-C(1) bond length in **IX** is 1.720(7) Å, a value very similar to that of **IV**, which is expected given that bonding to ruthenium is through the pendant phosphine. The bonds C(2)-C(3), C(4)-C(5) and C(6)-C(7) are all short relative to the remaining C-C bonds of the PHIN at 1.349(11), 1.344(12) and 1.354(10), respectively, all of which are similar to the bond lengths found in **IV**.

The ^{1}H NMR spectrum of **IX** is show in Figure **93** and ^{1}H and ^{13}C assignments may be found in Table **15**. The P-CH_2-P group is easily identified as a triplet at δ 4.54 that only couples to phosphorus. Two triplets at δ 6.58 and 6.28 are only coupled to a phosphorus resonance at δ 2.5 and each other and are therefore assigned to the C_5 ring protons. A NOESY interaction between the triplet at δ 6.28 and a doublet at δ 7.35 was used to assign the latter to H(4) and the peaks at δ 6.58 and 6.28 to H(2) and H(3) respectively (Figure **94**). Further correlations in a COSY spectrum allowed resonances at δ 6.78, 6.61 and 6.51 to be assigned to H(5), H(6) and H(7), respectively (Figure **95**).

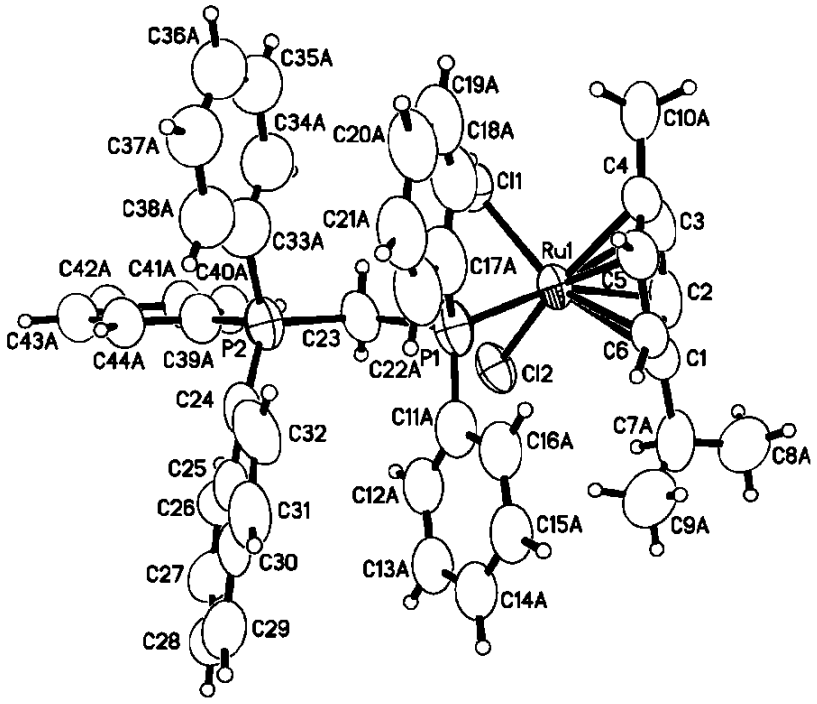

Figure 92. Molecular structure of $RuCl_2(\eta^6$-*p*-cymene)$(\eta^1$-**IV**) (**IX**) (Numbering different from that shown in Figure 46)

Table 14. Selected bond lengths for $RuCl_2(\eta^6$-*p*-cymene)$(\eta^1$-**IV**) (**IX**)

Bond	Length (Å)	Bond	Length (Å)
C(1)-C(2)	1.431(10)	P-C(1)	1.720(7)
C(2)-C(3)	1.349(11)	P(1)-Ph (avg)	1.789
C(3)-C(9)	1.426(11)	P(2)-Ph (avg)	1.831
C(9)-C(4)	1.413(11)	P(1)-C(10)	1.818(6)
C(4)-C(5)	1.344(12)	P(2)-C(10)	1.840(6)
C(5)-C(6)	1.416(12)	P(2)-Ru	2.3421(17)
C(6)-C(7)	1.354(10)		
C(7)-C(8)	1.383(10)		
C(9)-C(8)	1.427(10)		
C(1)-C(8)	1.433(10)		

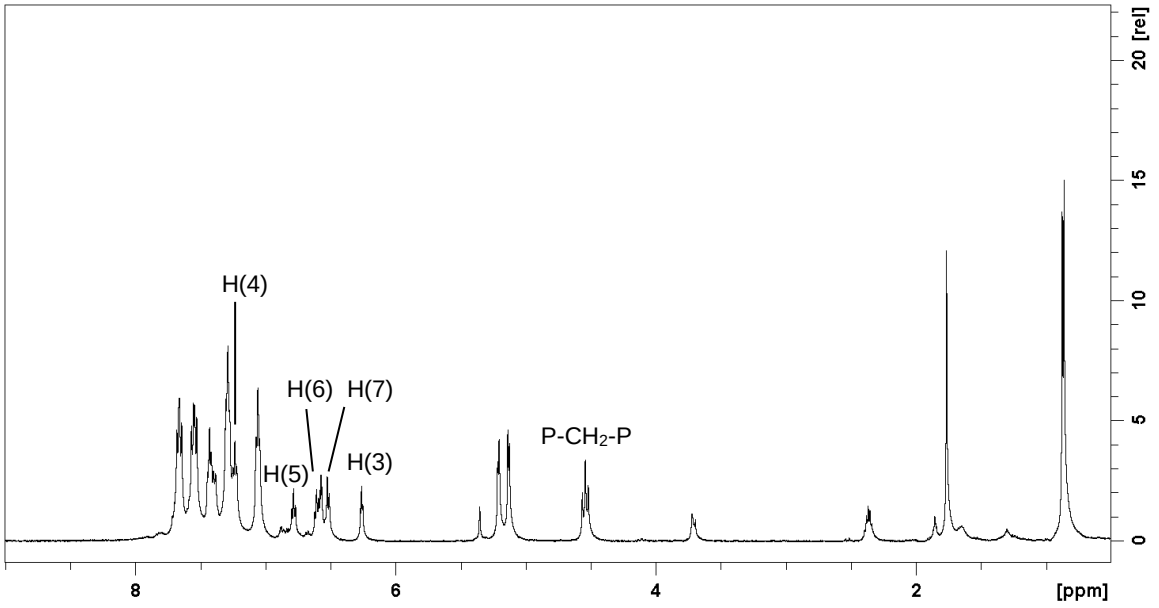

Figure 93. ^{1}H NMR spectrum of $RuCl_2(\eta^6$-*p*-cymene)(η^1-**IV**) (**IX**) in CD_2Cl_2

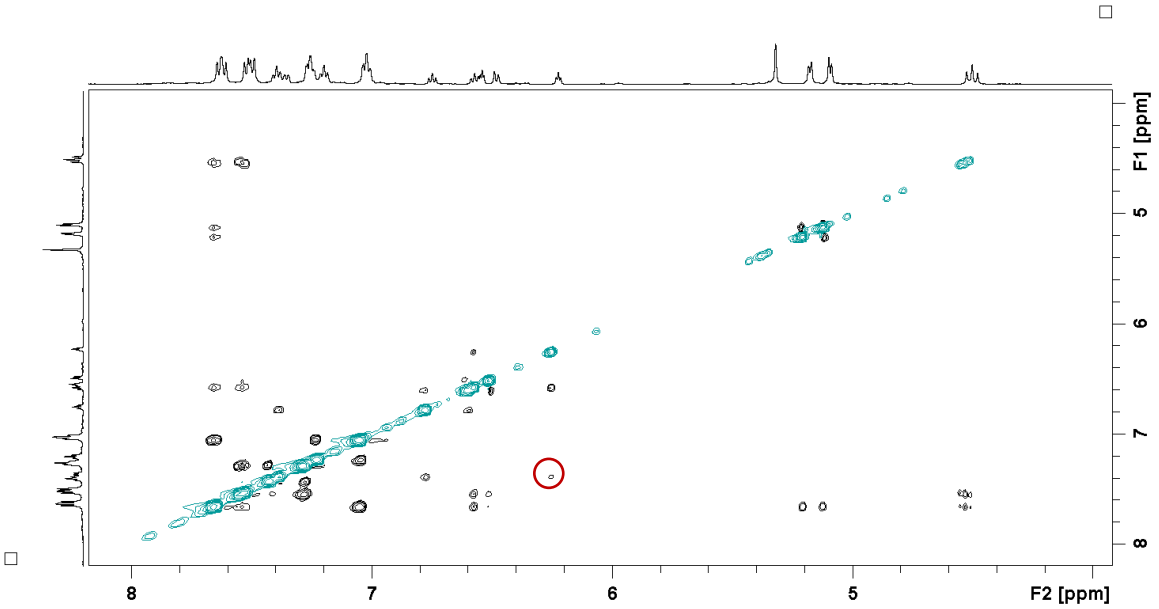

Figure 94. NOESY spectrum of $RuCl_2(\eta^6$-*p*-cymene)(η^1-**IV**) (**IX**) in CD_2Cl_2 (H(3)-H(4) correlation is circled)

The ^{31}P NMR spectrum of **IX** showed two resonances at δ 24.0 and 2.5 belonging to the pendant phosphine and ylidic phosphonium respectively. The latter is coupled with both H(2) and H(3) and can therefore be assigned to P(1). The P-CH_2-P group appears as a triplet at δ 4.54 coupled to both phosphorus nuclei (J_{HP} = 11.5 Hz), a feature not observed in **IV**, in which only the ylidic phosphonium is coupled with the methylene protons. Coordination of the pendant phosphine to the metal centre again increases the *s* character of the P-C bond and thus greatly increases J_{HP}.

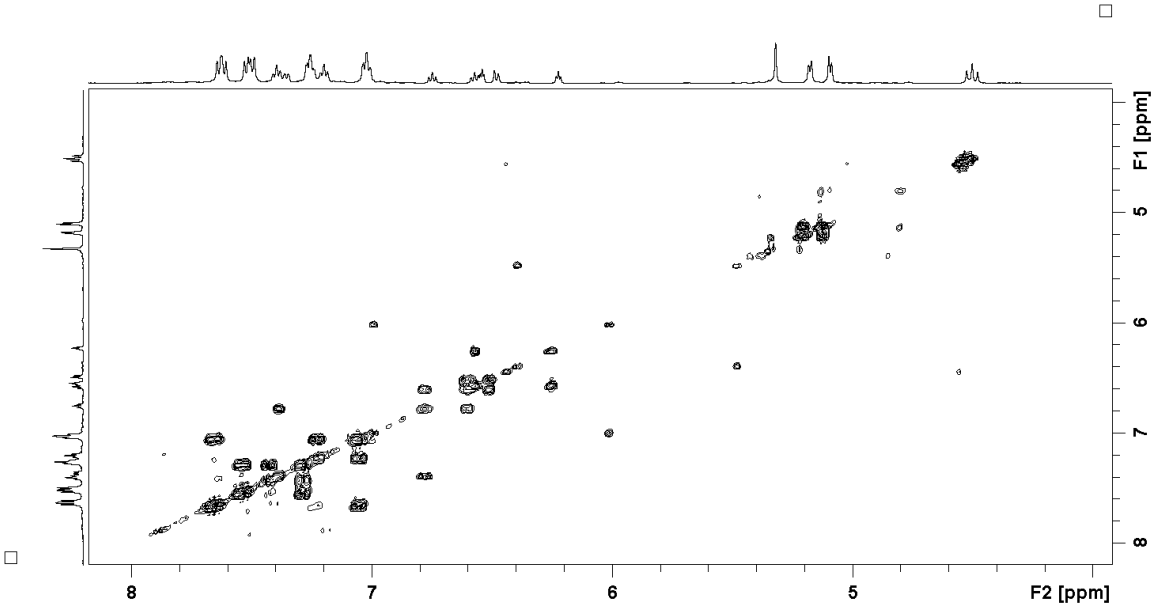

Figure 95. COSY spectrum of $RuCl_2(\eta^6$-*p*-cymene)(η^1-**IV**) (**IX**) in CD_2Cl_2

Two doublets of doublets at δ 7.55 and 7.66 are strongly coupled to phosphorus and are assigned to the *ortho* protons of the two phenyl groups. Correlations in the ^{31}P HMBC spectrum allowed the former to be assigned to the phenyl groups on P(1) and the latter to the phenyl groups on P(2) (Figure **96**). Further correlations in the COSY spectrum allowed assignment of the remaining positions of the phenyl groups.

Table 15. ^{1}H and ^{13}C NMR data for $RuCl_2(\eta^6\text{-}p\text{-cymene})(\eta^1\text{-IV})$ **IX**

H, C Position	δ (^{1}H)[a]	δ (^{13}C)
1	-	62.1 (d, $^{1}J_{C\text{-}P}$ 120.4)
2	6.58 (t, $^{3}J_{H\text{-}H}$ 4.3, $^{3}J_{H\text{-}P}$ 4.0)	127.3 (d, $^{2}J_{C\text{-}P}$ 15.0)
3	6.28 (t, $^{3}J_{H\text{-}H}$ 4.3, $^{4}J_{H\text{-}P}$ 4.0)	106.8 (d, $^{3}J_{C\text{-}P}$ 15.0)
4	7.35 (d, $^{3}J_{H\text{-}H}$ 7.6)	119.7 (s)
5	6.78 (t, $^{3}J_{H\text{-}H}$ 7.6)	116.6 (s)
6	6.61 (t, $^{3}J_{H\text{-}H}$ 7.6)	117.3 (s)
7	6.51 (d, $^{3}J_{H\text{-}H}$ 7.6)	118.0 (s)
P-CH_2-P	4.50 (t, $^{2}J_{H\text{-}P}$ 11.6)	Not Assigned
P(1)-Ph: *ipso*	-	129.5 (d, $^{1}J_{C\text{-}P}$ 45.4)
P(1)-Ph: *o*	7.55 (dd, $^{3}J_{H\text{-}H}$ 7.8, $^{3}J_{H\text{-}P}$ 12.3)	132.0 (d, $^{2}J_{C\text{-}P}$ 10.7)
P(1)-Ph: *m*	7.29 (dd, $^{3}J_{H\text{-}H}$ 7.7, $^{4}J_{H\text{-}P}$ 2.6)	128.8 (d, $^{3}J_{C\text{-}P}$ 12.0)
P(1)-Ph: *p*	7.43 (t, $^{3}J_{H\text{-}H}$ 7.6)	131.8 (s)
P(2)-Ph: *o*	7.66 (dd, $^{3}J_{H\text{-}H}$ 7.7, $^{3}J_{H\text{-}P}$ 10.5)	133.4 (d, $^{2}J_{C\text{-}P}$ 10.3)
P(2)-Ph: *m*	7.06 (dd, $^{3}J_{H\text{-}H}$ 7.6, $^{4}J_{H\text{-}P}$ 1.6)	127.8 (d, $^{3}J_{C\text{-}P}$ 10.0)
P(2)-Ph: *p*	7.23 (t, $^{3}J_{H\text{-}H}$ 7.3)	130.9 (s)

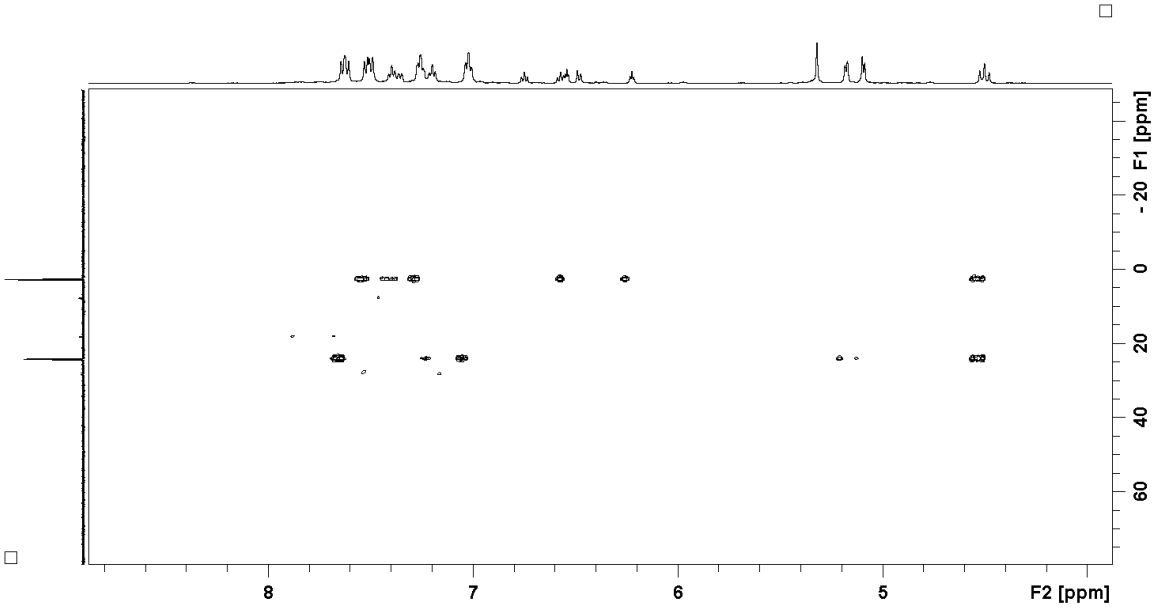

Figure 96. $^{1}H\text{-}^{31}P$ HMBC spectrum of $RuCl_2(\eta^6\text{-}p\text{-cymene})(\eta^1\text{-}$**IV**$)$ (**IX**) in CD_2Cl_2

3.5.3 Reaction of 1-$C_9H_6PPhMe_2$ (III) with $[RuCl(\mu\text{-}Cl)(\eta^6\text{-}p\text{-cymene})]_2$

Reacting **III** with $[RuCl(\mu\text{-}Cl)(\eta^6\text{-}p\text{-cymene})]_2$ resulted in the formation of a kinetic product (**X**) and a thermodynamic product (**XI**). The former was produced as the sole product when the reaction was run in THF at room temperature overnight, while the latter was produced as the sole product in refluxing toluene over two days. A significant amount of $[RuCl(\mu\text{-}Cl)(\eta^6\text{-}p\text{-cymene})]_2$ also precipitated out with the products **X** and **XI**, and was difficult to remove. It should be noted that no matter what conditions were employed (even refluxing for several days in toluene) a large amount of unreacted **III** and $[RuCl(\mu\text{-}Cl)(\eta^6\text{-}p\text{-cymene})]_2$ remained. Interestingly, both **X** and **XI** are soluble in coordinating solvents such as DMSO, acetonitrile and methanol while being poorly soluble in dichloromethane and insoluble in toluene and hexanes.

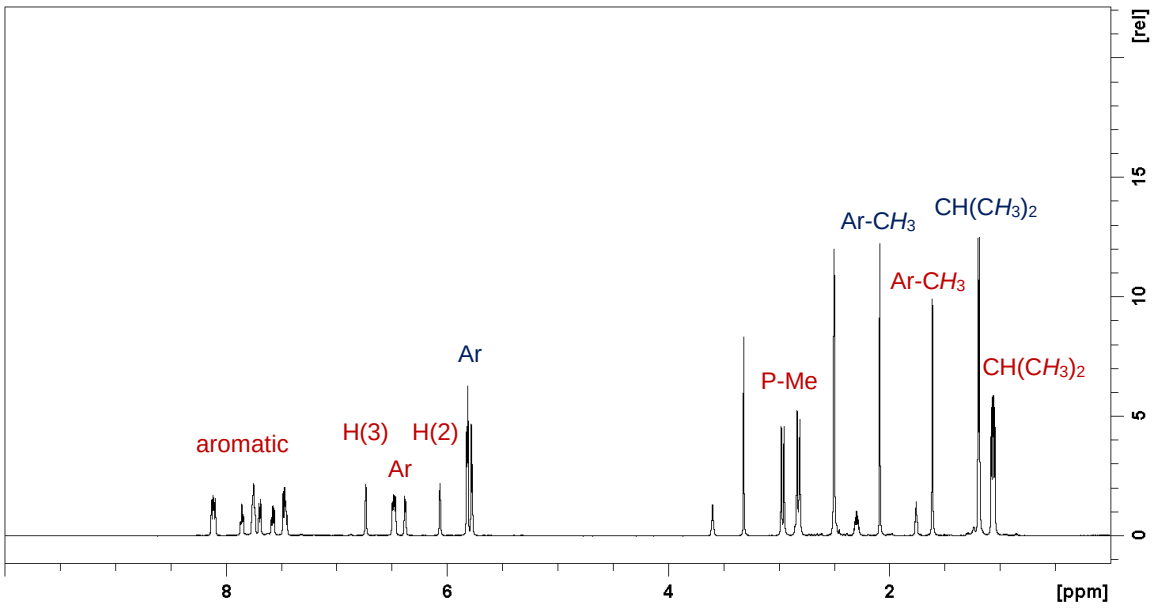

Figure 97. ^1H NMR spectrum of **X** (along with $[RuCl(\mu\text{-}Cl)(\eta^6\text{-}p\text{-cymene})]_2$) in DMSO d_6

The ^1H NMR spectrum of **X** is shown in Figure **97** and ^1H and ^{13}C assignments may be found in Table **16**. The P-Me groups are readily identified as they appear as two well separated doublets at δ 2.82 and 2.90 and are only coupled to phosphorus. Two singlets which only couple to each other at δ 6.06 and 6.74 may be assigned to the C_5 ring (Figure **98**). A NOESY interaction was

observed between the latter and a doublet at δ 7.70 (Figure **99**). Thus peaks at δ 6.06, 6.74 and 7.70 may be assigned to H(2), H(3) and H(4), respectively. Two overlapping peaks at δ 7.49 correlate with H(4) and can be assigned to H(5) and H(6). These overlapping peaks also correlate with a peak at δ 7.58 which is assigned to H(7). The doublet of doublets at δ 8.11 couples strongly to phosphorus and is assigned to the *ortho* protons of the phenyl group. The COSY spectrum allows assignment of triplets at δ 7.75 and 7.85 to the *meta* and *para* protons, respectively (Figure **98**).

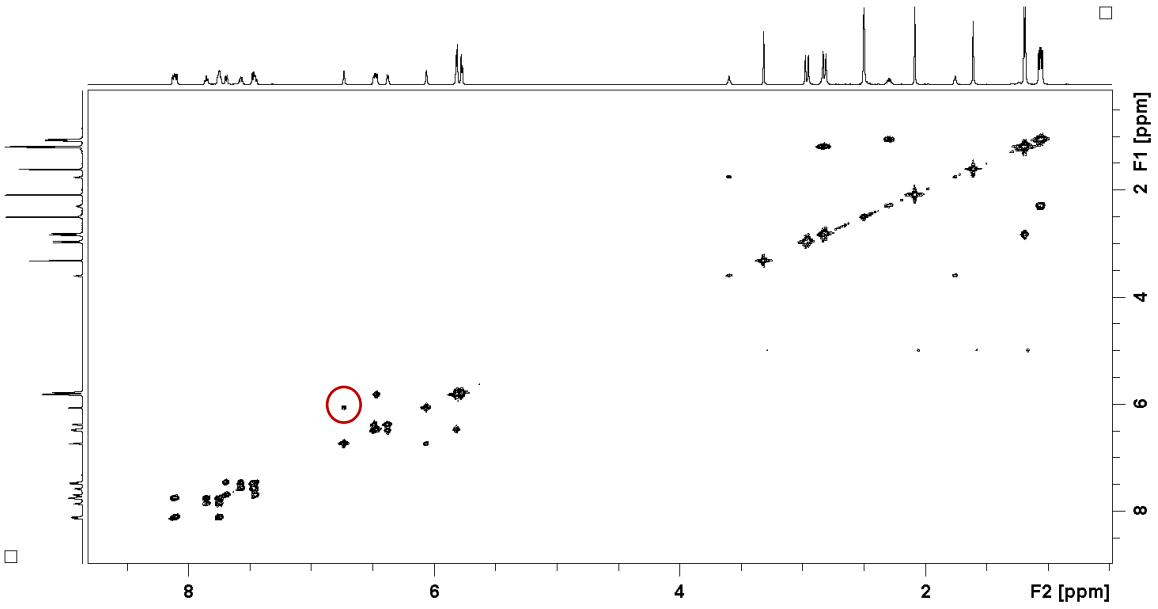

Figure 98. COSY spectrum of a sample containing **X** and $[RuCl(\mu\text{-}Cl)(\eta^6\text{-}p\text{-cymene})]_2$ (H(2)-H(3) correlation is circled)

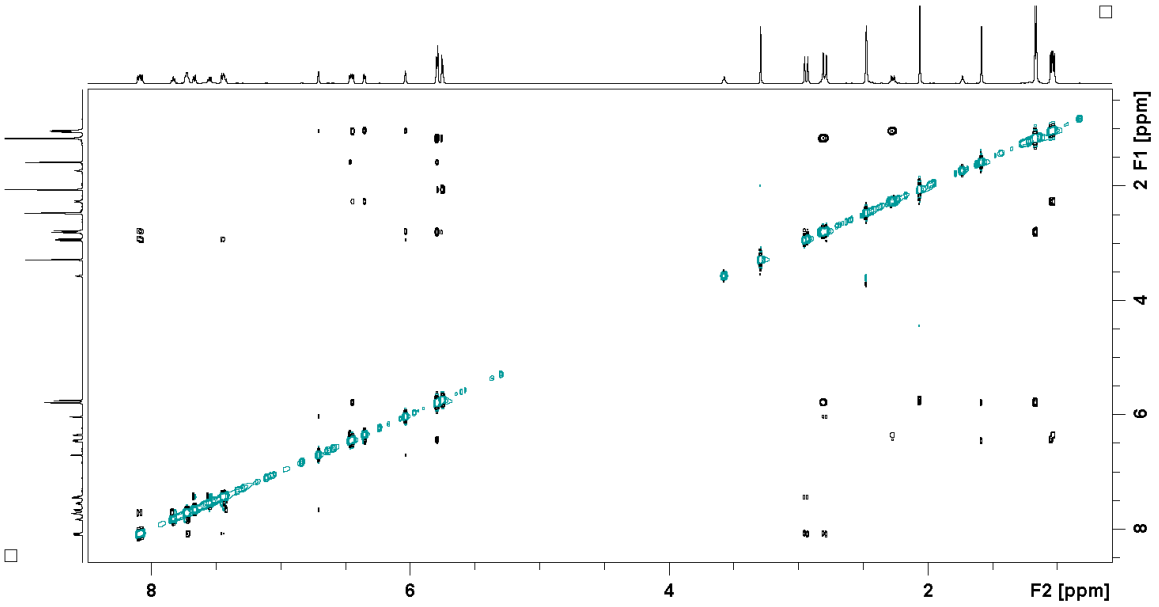

Figure 99. NOESY spectrum of a sample containing **X** and [RuCl(μ-Cl)(η^6-*p*-cymene)]$_2$

The ^{31}P NMR spectrum of **X** in DMSO d_6 contained one peak at δ 23.6 and from the ^{31}P HMBC was correlated with two P-Me doublets at δ 2.87 and 2.97 along with resonances for H(2) and H(3). The chemical shift of H(3) is downfield of that of **III**. Typically, protons attached to carbons that are bonded to ruthenium(II) are shifted upfield from the uncoordinated PHIN ligand. Therefore, there is a possibility that PHIN bonding to ruthenium(II) in **X** is not through an η^5 mode.

In addition to the signals from the PHIN ligand, there were two sets of resonances that could be assigned to *p*-cymene. One of these was from the starting material [RuCl(μ-Cl)(η^6-*p*-cymene)]$_2$; however, the other appears to be coordinated to the same metal centre as the PHIN ligand. A NOESY correlation is observed between both H(2) and H(3) and the two diastereotopic isopropyl CH_3 groups on this *p*-cymene ligand (Figure **99**). That the isopropyl CH_3 groups are inequivalent is a sure indication that the *p*-cymene ligand is attached to the same metal centre as a planar chiral PHIN ligand, making these two methyl groups diasterotopic. Integration of ^{1}H NMR

spectra typically showed an excess of [RuCl(μ-Cl)(η^6-*p*-cymene)]$_2$ relative to **X** of between 2 and 3 to 1. The ratio varied depending on the reaction time, work-up procedure.

As single crystals of **X** could not be obtained, and NMR analysis proved inconclusive, the structure of this complex remains unknown. It is clear, however, that it contains a ruthenium centre coordinated to both a *p*-cymene and a PHIN ligand. As relatively weak nucleophiles are able to cleave the Ru-Cl bridge in [RuCl(μ-Cl)(η^6-*p*-cymene)]$_2$, one possible structure for **X** may be that resulting from nucleophilic attack of the olefin on the PHIN ligand as shown in Figure **100**.

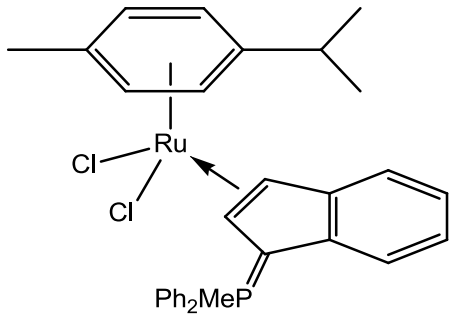

Figure 100. Proposed structure for **X** based on NMR data

Table 16. ^{1}H and ^{13}C NMR data for **X** (^{13}C data from HSQC and HMBC experiments)

H, C Position	δ (^{1}H)[a]	δ (^{13}C)
1	-	71.8
2	6.06 (s)	77.6
3	6.74 (s)	85.1
4	7.70 (d, $^{3}J_{H-H}$ 8.9)	126.1
5	7.45 (m)	129.7
6	7.47 (m)	122.0
7	7.58 (m)	130.8
8	-	100.4
9	-	98.2
P-Me	2.82, 2.97 (d, $^{2}J_{H-P}$ 14.5)	8.8
ipso-C	-	120.6
o-C	8.11 (dd, $^{3}J_{H-P}$ 7.9Hz, $^{3}J_{H-H}$ 13.5Hz)	131.4
m-C	7.75 (td, $^{3}J_{H-H}$ 7.6Hz, $^{4}J_{H-P}$ 3.3)	129.5
p-C	7.86 (t, $^{3}J_{H-H}$ 7.7)	
$CH(CH_3)_2$	1.06 (dd, J_{H-H} 11.5, 6.9)	22.0
$CH(CH_3)_2$	2.29 (h, $^{3}J_{H-H}$ 6.9)	30.0
Ph-CH_3	1.60 (s)	15.8
Aromatic	6.38, 6.48	86.0, 85.2

The ^{1}H NMR spectrum of **XI** is shown in Figure **101** and ^{1}H and ^{13}C assignments may be found in Table **17**. The P-Me groups are readily identified as they appear as two doublets at δ 2.71 and 2.66 which are only coupled to phosphorus. Two singlets which couple only each other at δ 5.58 and 6.20 were assigned to the PHIN C_5 ring (Figure **102**). The latter shows a through space interaction with a doublet at δ 6.86 allowing H(2), H(3) and H(4) to be assigned to resonances at δ 5.58, 6.20 and 6.86, respectively. H(4) couples with two overlapping signals at δ 6.98 which can be assigned to both H(5) and H(6) (Figure **102**). A further correlation in the COSY spectrum between H(6) and a doublet at δ 6.59 allows the latter to be assigned to H(7).

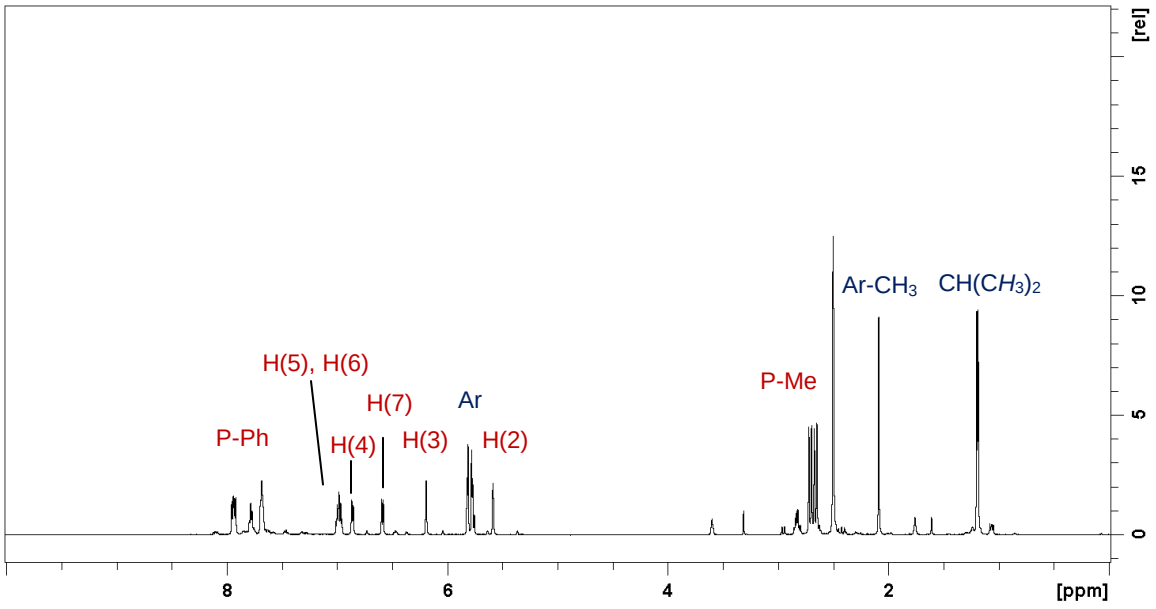

Figure 101. ^{1}H NMR spectrum of **XI** (along with [RuCl(μ-Cl)(η^{6}-*p*-cymene)]$_2$) in DMSO d_6

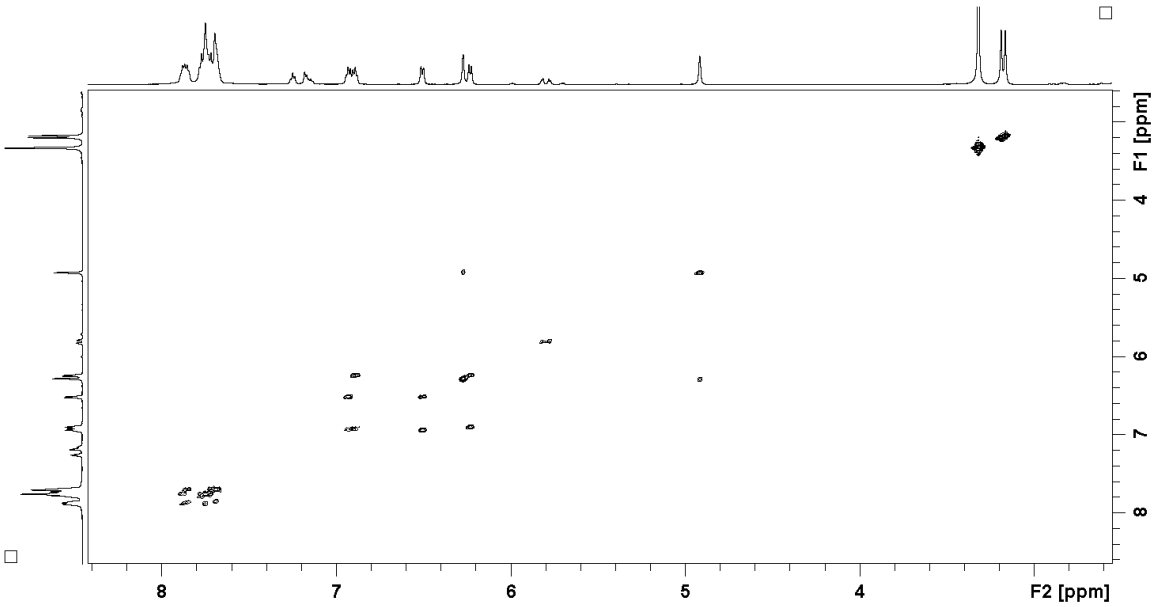

Figure 102. COSY spectrum of **XI** (along with [RuCl(μ-Cl)(η^{6}-*p*-cymene)]$_2$) in DMSO d_6 (H(2)-H(3) correlation is circled)

The ^{31}P NMR spectrum of **XI** in DMSO d_6 contained one resonance at δ 23.2 which was correlated with two diastereotopic P-Me groups with H(2) and H(3). **XI** did not contain a coordinated *p*-cymene ligand.

On reacting **III** with $[RuCl_2(\eta^4\text{-}1,5\text{-cycloctadiene})]_n$ in refluxing toluene, **XI** was obtained as the sole Ru-PHIN product, although, large amounts of starting material were still observed, as was the case using $[RuCl(\mu\text{-}Cl)(\eta^6\text{-}p\text{-cymene})]_2$. Reacting **III** with $[RuCl(\mu\text{-}Cl)(\eta^6\text{-}p\text{-cymene})]_2$ in THF under photolytic conditions produced **XI** along with several side products; however, there remained a substantial amount of both starting materials. Owing to these complications, the structure of **XI** could not be determined. However, the structure of the related complex **XIII** could be determined and will be presented below.

Table 17. ^{1}H and ^{13}C NMR data for **XI**

H, C Position	δ (^{1}H)[a]	δ (^{13}C)
1	-	61.7
2	5.58 (s)	76.6
3	6.20 (s)	71.6
4	6.86 (d, $^{3}J_{H\text{-}H}$ 8.5)	122.8
5	6.98 (m)	124.1
6	6.98 (m)	124.5
7	6.59 (d, $^{3}J_{H\text{-}H}$ 8.6)	120.2
8	-	95.7
9	-	92.4
P-Me	2.71, 2.66 (d, $^{2}J_{H\text{-}P}$ 14.6)	9.1
ipso-C	-	122.0
o-C	7.93(dd, $^{3}J_{H\text{-}H}$ 8.0, $^{3}J_{H\text{-}P}$ 13.3)	131.1
m-C	7.68 (t, $^{3}J_{H\text{-}H}$ 7.9)	129.4
p-C	7.78 (t, $^{3}J_{H\text{-}H}$ 7.9)	133.8

3.5.4 Reaction of 1-$C_9H_6PPh_2Me$ (II) with $[RuCl(\mu\text{-}Cl)(\eta^6\text{-}p\text{-cymene})]_2$

The reaction of **II** with $[RuCl(\mu\text{-}Cl)(\eta^6\text{-}p\text{-cymene})]_2$ resulted in the generation of a kinetic and a thermodynamic product (**XII**). Performing this reaction overnight at room temperature resulted in slow formation of the kinetic product as a major product, with a small amount of **XII**, while running the reaction in refluxing THF or toluene over at least 24 h resulted in **XII** being formed as the major or sole PHIN containing species.

The ^1H spectrum (Figure **103**) of the kinetic product is very difficult to assign as **XII** and $[RuCl(\mu\text{-}Cl)(\eta^6\text{-}p\text{-cymene})]_2$ are also present in significant amounts and all that warrants mention is that the complex evidently contains a Ru(II) centre with both p-cymene and **II** coordinated as the isopropyl methyl groups are diastereotopic and appear as two partially overlapping doublets at δ 0.91. This behavior is similar to that observed for **XI** and since both arene and PHIN ligands appear to be coordinated; this complex was not pursued further.

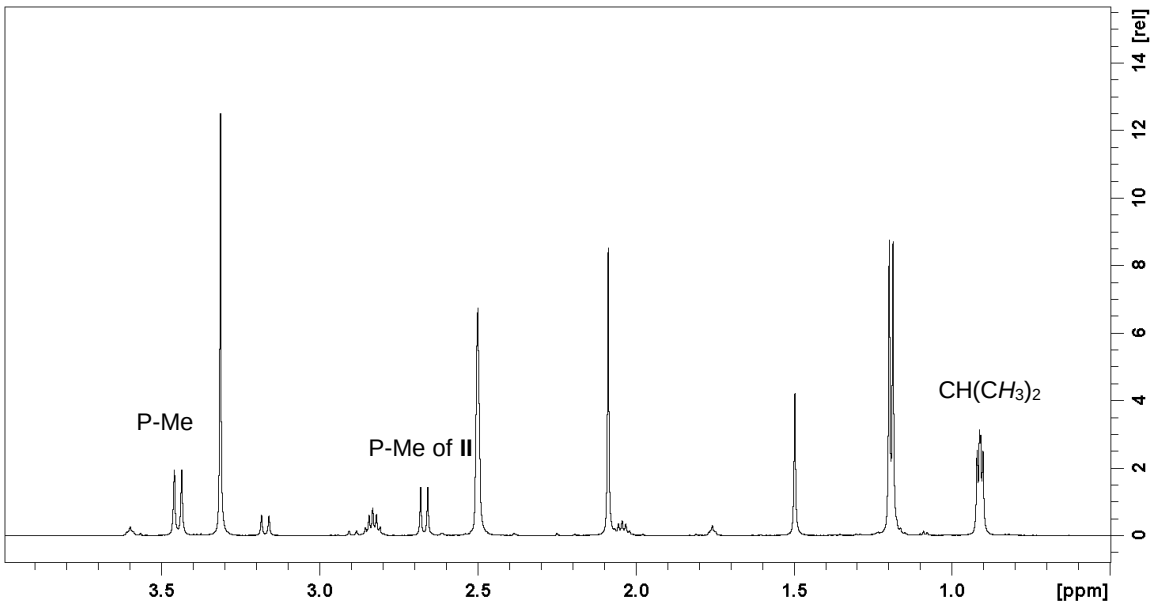

Figure 103. Aliphatic region of the ^1H spectrum of the kinetic product from the reaction of **II** with $[RuCl(\mu\text{-}Cl)(\eta^6\text{-}p\text{-cymene})]_2$ in CD_2Cl_2

The ^{1}H spectrum of **XII** is shown in Figure **104** and ^{1}H and ^{13}C assignments can be found in Table **18**. The P-Me group is readily identified as a doublet split by phosphorus at δ 3.17. Two singlets at δ 4.91 and 6.27 weakly couple each other (Figure **105**) and can be assigned to the protons on the C_5 ring. A through space interaction between the latter and a peak at δ 6.51 allows H(2), H(3) and H(4) to be assigned to δ 4.91, 6.27 and 6.51 respectively. H(4) is coupled with two overlapping peaks at δ 6.91 which can be assigned to H(5) and H(6). The latter shows a further correlation with a peak at δ 6.28 which is assigned to H(7) (Figure **105**). Only one set of *p*-cymene signals was observed and these are identical to those of $[RuCl(\mu\text{-}Cl)(\eta^6\text{-}p\text{-cymene})]_2$.

Table 18. ^{1}H and ^{13}C NMR data for **XII**

H, C Position	δ (^{1}H)[a]	δ (^{13}C)
1	-	60.8 (d, $^{1}J_{C\text{-}P}$ 98.4)
2	4.91 (s)	77.9 (d, $^{2}J_{C\text{-}P}$ 12,3)
3	6.27 (s)	73.4 (d, $^{3}J_{C\text{-}P}$ 9.2)
4	6.51 (d, $^{3}J_{H\text{-}H}$ 8.8)	120.7 (s)
5	6.91 (m)	124.2 (s)
6	6.91 (m)	125.3 (s)
7	6.28 (d, $^{3}J_{H\text{-}H}$ 8.6)	122.1 (s)
8	-	95.4 (d, $^{2}J_{C\text{-}P}$ 9.7)
9	-	91.8 (d, $^{3}J_{C\text{-}P}$ 12.0)
P-Me	3.17 (d, $^{2}J_{H\text{-}P}$ 14.3)	9.7 (d, $^{1}J_{C\text{-}P}$ 57.3)
aromatic	7.6-7.9	129-135

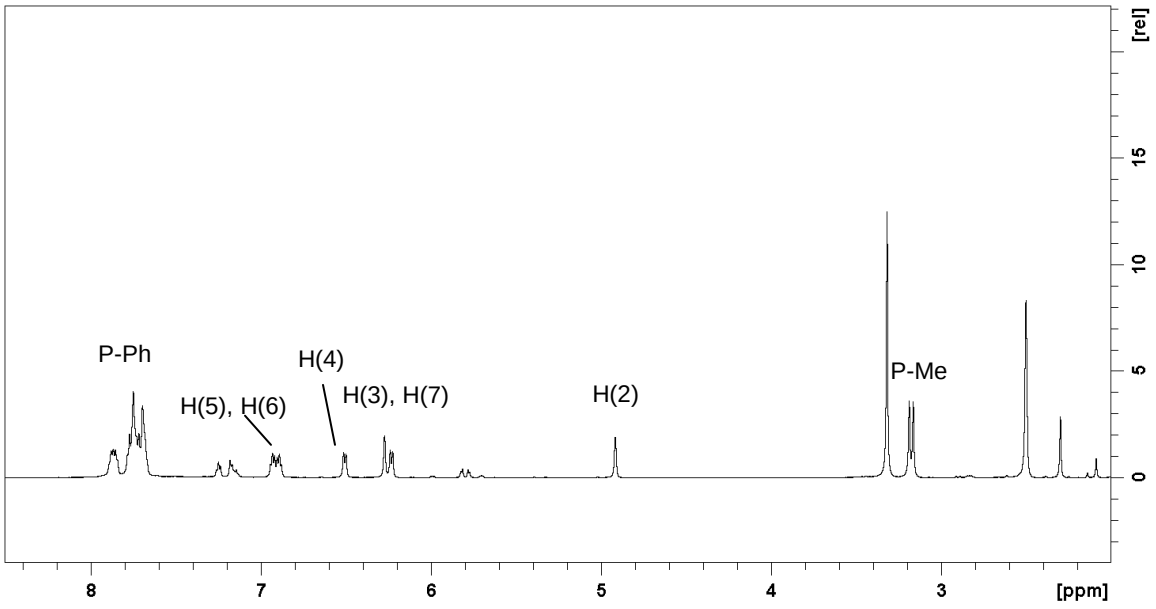

Figure 104. ^{1}H NMR spectrum of **XII** (along with [RuCl(μ-Cl)(η^{6}-*p*-cymene)]$_2$) in DMSO d$_6$

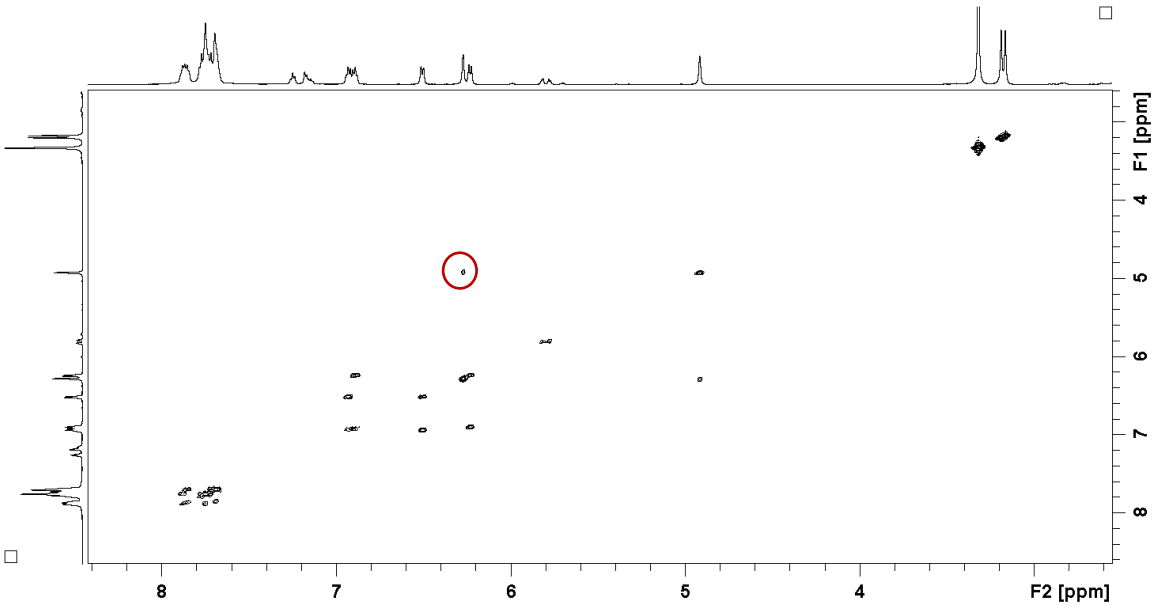

Figure 105. COSY spectrum of **XII** (along with [RuCl(μ-Cl)(η^{6}-*p*-cymene)]$_2$) in DMSO d$_6$ (H(2)-H(3) correlation is circled)

A significant amount of both the ylide and [RuCl(μ-Cl)(η^6-*p*-cymene)]$_2$ was present in all samples of **XII**. This is problematic because the solubility of [RuCl(μ-Cl)(η^6-*p*-cymene)]$_2$ is very similar to that of **XII**, making recrystallization difficult. In order to force this reaction to completion, microwave heating of **II** and [RuCl(μ-Cl)(η^6-*p*-cymene)]$_2$ in THF was attempted, however, decomposition with the formation of a black solid was observed and much [RuCl(μ-Cl)(η^6-*p*-cymene)]$_2$ remained. ESI-MS spectra were difficult to interpret due to the presence of two ruthenium species, and without X-ray crystallographic data, the structure of **XII** could not be elucidated. Sections 1.5.5 and 1.5.6 detail efforts, which were eventually successful, to determine the structure of **XII**.

3.5.5 Reaction of XII with PMe_2Ph

As the NMR spectra indicated that the only non-chloride ligand coordinated to the ruthenium centre in **XII** is a PHIN, it was assumed that the structure of **XII** was similar to that of the starting material with bridging chlorides and an η^5 coordinated PHIN ligand, [RuCl(μ-Cl)(η^5-**II**)]$_2$. Such a structure should react with a suitable nucleophile such as a phosphine to produce the mononuclear complexes $RuCl_2$(η^5-**II**)(PR_3). When using PMe_2Ph as the phosphine, the two P-Me groups would be diastereotopic due to the planar chiral PHIN ligand and would be observed in the ^{1}H NMR as two doublets. Reacting **XII** with PMe_2Ph resulted only in decomposition of the PHIN complex and no set of doublets from the PMe_2Ph group was observed. Thus, it is unlikely that **XII** contains bridging chloride ligands and the structure is therefore not analogous to that of [RuCl(μ-Cl)(η^6-*p*-cymene)]$_2$ with **II** replacing the *p*-cymene group.

3.5.6 Reaction of 1-$C_9H_6PPh_2Me$ (II) with [RuCl(μ-Cl)(η^6-ethylbenzoate)]$_2$

Under all conditions tried, the reaction of **II** or **III** with [RuCl(μ-Cl)(η^6-*p*-cymene)]$_2$ resulted in substantial amounts of unreacted starting material. The more easily displaced ethylbenzoate ligand[20] was therefore used as a reagent for arene exchange with the PHIN ligand **II**. Unexpectedly, the reaction of a 1:1 ratio of **II** to [RuCl(μ-Cl)(η^6-ethylbenzoate)]$_2$ in refluxing THF resulted in consumption of the PHIN and production of **XII**, while a large amount of [RuCl(μ-Cl)(η^6-ethylbenzoate)]$_2$ remained, most of which could be removed by washing with THF. Samples of **XII** which were virtually free of [RuCl(μ-Cl)(η^6-ethylbenzoate)]$_2$ could therefore be analyzed (see Figure **106**). Even after prolonged drying at 0.01 torr, some THF solvent remained. Elemental analysis was therefore not carried out and **XII** was studied by NMR spectroscopy.

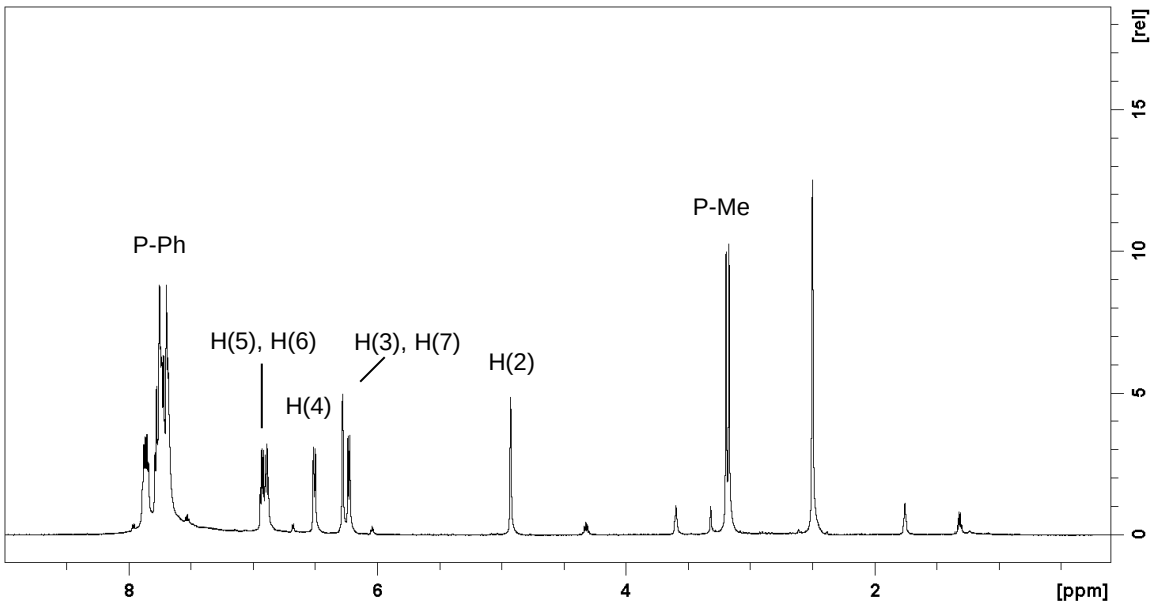

Figure 106. ^{1}H NMR spectrum of **XII** formed by the reaction of **II** with [RuCl(μ-Cl)(η^6-ethylbenzoate)]$_2$

ESI mass spectrometry in the positive ion mode, shown in Figure **107**, gave one set of peaks centered around 365 *m*/*z*. This species is doubly charged and has the isotope distribution expected for a mono-ruthenium(II) species with no chloride ligands.

From this, the formula of **XI** is most likely $[Ru(\eta^5\text{-}\mathbf{II})_2](Cl)_2$ (Figure **108**) which is in excellent agreement with the calculated isotope distribution, both of which are shown in Figure **107**. **XII** therefore has a sandwich structure similar to that of **V**-**VII**, with the Cp ligand being replaced with a neutral PHIN ligand. The NMR data presented above are also consistent with this structure as the only organic ligand is **II** coordinated in an η^5 mode.

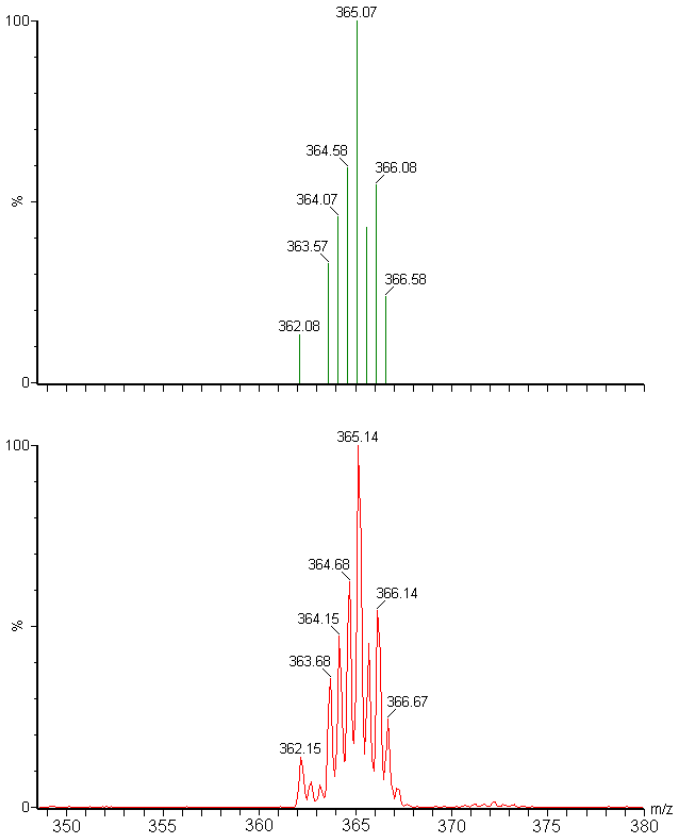

Figure 107. ESI-MS of **XII** (bottom) synthesized from the reaction of **II** and $[RuCl(\mu\text{-}Cl)(\eta^6\text{-}ethylbenzoate)]_2$. The calculated isotope distribution is shown on top

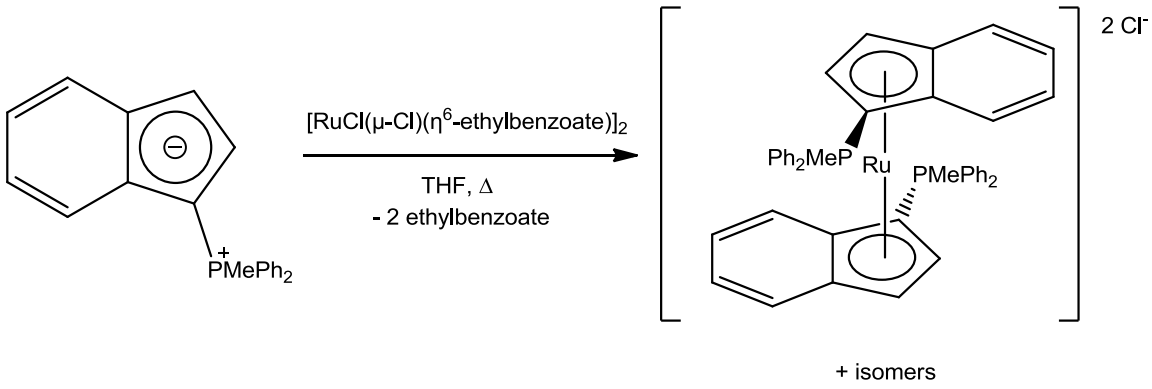

Figure 108. Synthesis of **XII** from $[RuCl(\mu\text{-}Cl)(\eta^6\text{-ethylbenzoate})]_2$

3.5.7 Conclusions from the Reaction of II and III with $[RuCl(\mu\text{-}Cl)(\eta^6\text{-}p\text{-cymene})]_2$

Reacting either **II** or **III** with $[RuCl(\mu\text{-}Cl)(\eta^6\text{-}p\text{-cymene})]_2$ results in two types of compounds: a kinetic product in which the ruthenium(II) centre is coordinated to one PHIN and one *p*-cymene ligand (**X**) and a thermodynamic product in which a ruthenium(II) centre is coordinated to two PHIN ligands (**XI** and **XII**). None of these products have easily removable ligands and are therefore assumed to be useless as catalyst precursors. It seems that arene exchange takes place only after the chloride bridge of $[RuCl(\mu\text{-}Cl)(\eta^6\text{-}p\text{-cymene})]_2$ has been broken by a PHIN ligand acting as a nucleophile. It is possible that once the kinetic product has been formed it may react with a second equivalent of the PHIN ligand to form the thermodynamic product via an arene exchange reaction, a process with only occurs at elevated temperature. A simpler route to ruthenium(II)-PHIN complexes may therefore employ complexes of the type $RuCl_2(\eta^6\text{-arene})(PR_3)$ as a starting material for arene exchange in which the chloride bridge has already been cleaved by a phosphine such as PPh_3.

3.6 Arene Exchange Reactions with $RuCl_2(arene)(PR_3)$

The reaction of a phosphine with complexes of the type $[RuCl(\mu\text{-}Cl)(\eta^6\text{-arene})]_2$ quickly produces the mononuclear complexes $RuCl_2(arene)(PR_3)$ in quantitative yield.[22] Heating $RuCl_2(arene)(PR_3)$ in THF with a PHIN ligand may result in arene exchange of the arene moiety with the PHIN ligand to produce $RuCl_2(PHIN)(PR_3)$. These complexes are useful as the chloride ligands may be removed by abstraction with a silver salt such as $AgPF_6$ thus forming a coordinatively unsaturated species.

3.6.1 Synthesis and Characterization of $RuCl_2(\eta^5\text{-II})(PPh_3)$ (XIII)

The reaction of $[RuCl(\mu\text{-}Cl)(\eta^6\text{-ethylbenzoate})]_2$ with PPh_3 in THF quickly produces $RuCl_2(\eta^6\text{-ethylbenzoate})(PPh_3)$ which is bright red in colour and is readily soluble in THF.[23] Addition of one equivalent of **II** and refluxing this solution overnight results in the formation of $RuCl_2(\eta^5\text{-II})(PPh_3)$ (**XIII**) (Figure **109**). The solution changes colour dramatically finally becoming dark green-brown and virtually opaque, although still homogeneous. **XIII** can be precipitated by cooling a concentrated THF solution to -30 °C. Reacting $RuCl_2(\eta^6\text{-}C_6H_6)(PPh_3)$ (which was prepared by a published method[22]) with a PHIN ligand does not result in arene exchange. This can be attributed to stronger coordination of the benzene ligand than the ethylbenzoate ligand. Unfortunately X-ray quality crystals of **XIII** could not be obtained. All samples of **XIII** contained small amounts of THF, even after drying at 78 °C and 0.01 torr overnight. Therefore, **XIII** was characterized extensively by NMR spectroscopy.

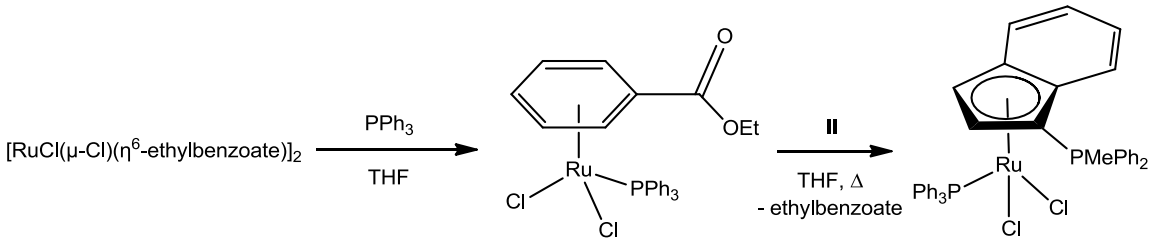

Figure 109. Synthesis of $RuCl_2(\eta^5$-**II**$)(PPh_3)$ (**XIII**)

The ^{31}P NMR spectrum of **XIII** has two doublets at δ 22.6 and 43.1 which couple each other with J_{PP} = 6 Hz. From the ^{31}P HMBC spectrum (Figure **110**), the resonance at δ 22.6 is coupled to a P-Me group at δ 3.45 as may thus be assigned to the ylidic phosphonium. The resonance at δ 43.1 is confirmed to be the PPh_3 group as it is coupled only to three resonances in the aromatic region.

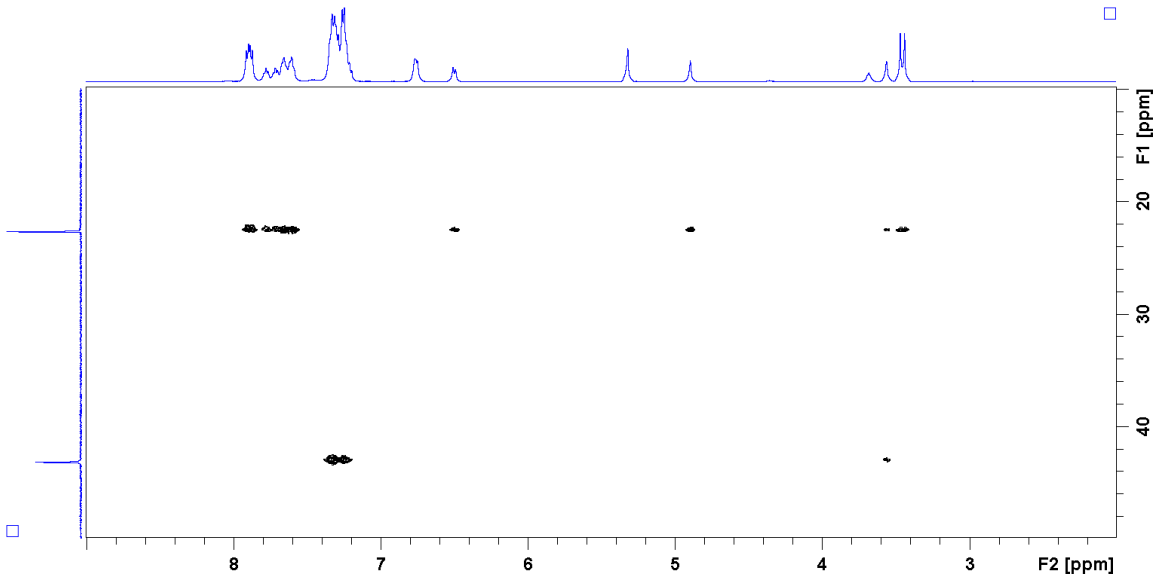

Figure 110. ^1H-^{31}P HMBC spectrum of $RuCl_2(\eta^5$-**II**$)(PPh_3)$ (**XIII**) in CD_2Cl_2

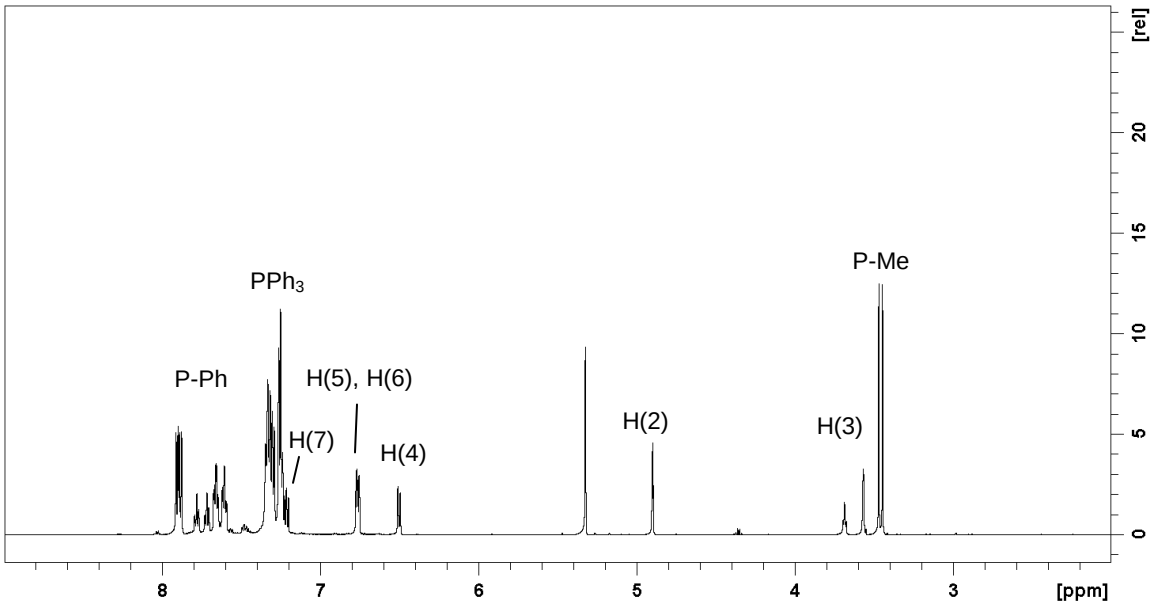

Figure 111. ^{1}H NMR spectrum of $RuCl_2(\eta^5$-**II**$)(PPh_3)$ (**XIII**) in CD_2Cl_2

The ^{1}H spectrum of **XIII** can be found in Figure 111 and ^{1}H and ^{13}C NMR assignments can be found in Table 19. Two singlets are found at δ 4.90 and 3.56 which only weakly couple each other and have no other correlations in the COSY spectrum (Figure 112). These protons are therefore on the C_5 ring. A correlation in the NOESY spectrum (Figure 113) between the peak at δ 3.56 and a resonance at δ 6.50 was used to assign the peaks at δ 4.90, 3.56 and 6.50 to H(2), H(3) and H(4). A correlation was observed between H(4) and a multiplet at δ 6.76 which integrated to 2 protons and can be assigned to the overlapping signals of H(5) and H(6). A correlation between this multiplet and a doublet at δ 7.22 was used to assign the latter to H(7).

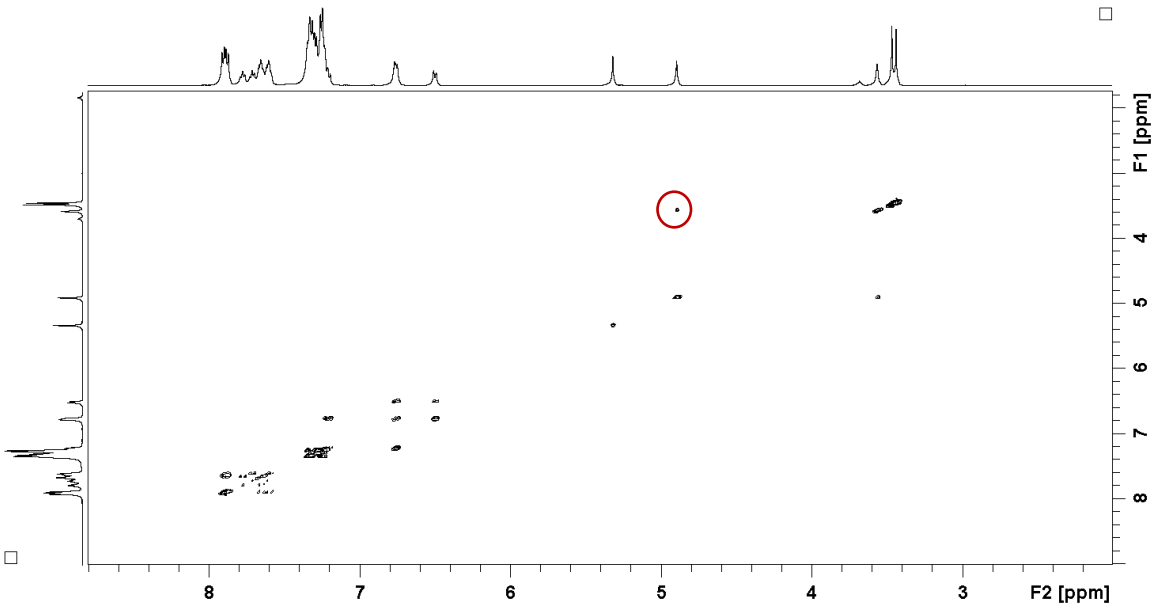

Figure 112. COSY spectrum of $RuCl_2(\eta^5$-**II**$)(PPh_3)$ (**XIII**)in CD_2Cl_2 (H(2)-H(3) correlation is circled)

The protons H(2) and H(3) shift upfield considerably compared to **II** and this has been observed for PHIN complexes coordinating to ruthenium(II) through the C_5 ring as seen in complexes **V**-**VII**. The protons on the C_6 ring are in the range δ 6.5 to 7.22 and do not shift considerably from the chemical shifts of **II**. ^{13}C NMR assignments were made on the basis of HMBC (Figure **114**) and HSQC (Figure **115**) spectra and can be found in Table **19**. All carbons on the C_5 ring show upfield shifts upon coordination, again similar to those observed in **V**-**VII** while the carbon atoms not coordinated to ruthenium shift slightly downfield.

The phenyl group of the PHIN ligand is easily identified as it appears downfield of the PPh_3 group and couples with the ylidic ^{31}P resonance at δ 22.6. The *ortho* resonance at δ 7.89 is easily identified due to its strong coupling with phosphorus. The COSY spectrum (Figure **112**) allows assignment of two sets of *meta* and *para* protons. The two P-Ph groups are expected to be diastereotopic and, surprisingly, are well separated in the ^1H spectrum. Thus, there are two *meta* resonances which are easily distinguishable doublets of triplets at δ 7.61 and 7.66 and two *para*

resonances at δ 7.72 and 7.78. It is unknown why only one doublet of doublets assigned to the *ortho* resonance at δ 7.89 is observed.

Table 19. ^{1}H and ^{13}C NMR data for $RuCl_2(\eta^5\text{-II})(PPh_3)$ (**XIII**)

H, C Position	δ (^{1}H)[a]	δ (^{13}C)
1	-	45.3 (dd, J_{C-P} 106.0, 20.0)
2	4.90 (s)	88.7 (d, $^{2}J_{C-P}$ 15.9)
3	3.56 (s)	64.0 (d, $^{3}J_{C-P}$ 8.9)
4	6.50 (d, $^{3}J_{H-H}$ 8.0)	128.3 (s)
5	6.76 (m)	123.9 (s)
6	6.76 (m)	126.0 (s)
7	7.22 (dd, $^{3}J_{H-H}$ 8.0)	127.6 (s)
8	-	100.1 (d, $^{2}J_{C-P}$ 14.5)
9	-	92.4 (d, $^{3}J_{C-P}$ 9.2)
P-Me	3.45 (d, $^{2}J_{H-P}$ 14.1)	11.3 (d, $^{1}J_{C-P}$ 63.0)
ipso-C	-	123.1 (?)
o-C	7.89 (dd, $^{3}J_{H-H}$ 7.6, $^{3}J_{H-P}$ 13.0)	133.6 (dd, $^{2}J_{C-P}$ 10.6, 7.8)
m-C (a)	7.61 (dt $^{3}J_{H-H}$ 7.9, $^{4}J_{H-P}$ 3.1)	129.8 (d, $^{3}J_{C-P}$ 12.4)
p-C (a)	7.72 (dt $^{3}J_{H-H}$ 7.9, $^{5}J_{H-P}$ 1.6)	134.3 (d, $^{4}J_{C-P}$ 3.0)
m-C (b)	7.66 (dt J_{H-H} 7.9, $^{4}J_{H-P}$ 3.1)	130.3 (d, $^{3}J_{C-P}$ 12.4)
p-C (b)	7.78 (dt $^{3}J_{H-H}$ 7.9, $^{5}J_{H-P}$ 1.5)	134.6 (d, $^{4}J_{C-P}$ 3.0)

The complex **XIII** may be useful as a precatalyst as one or two of the chloride ligands may be removed by a silver salt such as $AgPF_6$ resulting in a coordinatively unsaturated mono- or dicationic complexes, $[RuCl(\eta^5\text{-}\mathbf{II})(PPh_3)]PF_6$ and $[Ru(\eta^5\text{-}\mathbf{II})(PPh_3)](PF_6)_2$, respectively. Such complexes may be employed as catalysts for a variety of organic transformations which have previously been investigated using Ru(II)-arene complexes as catalysts (see Introduction).

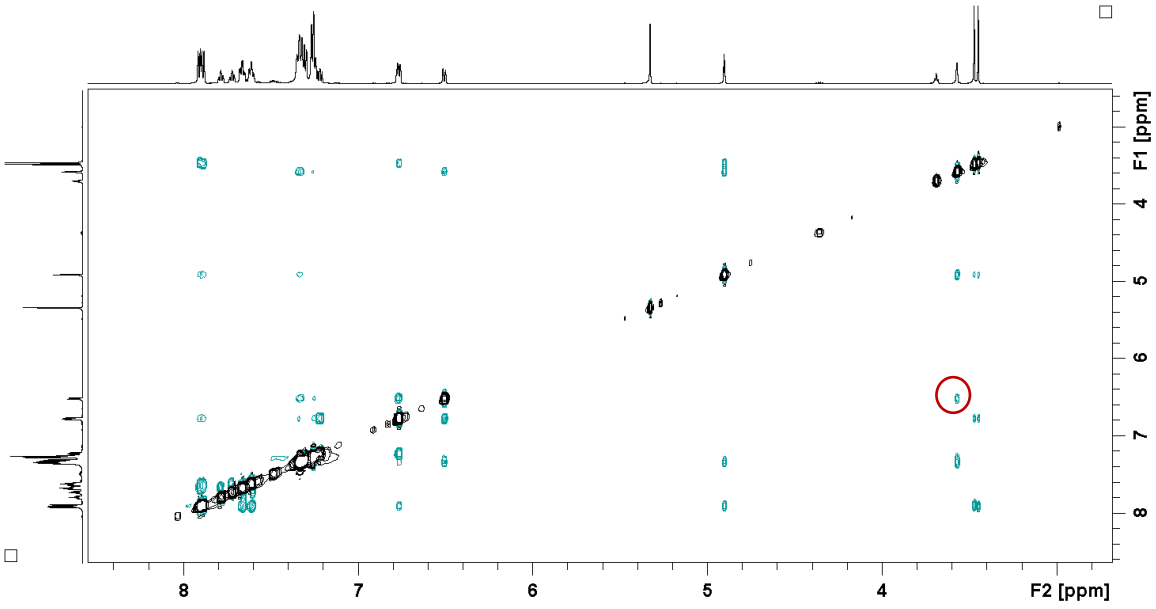

Figure 113. NOESY spectrum of $RuCl_2(\eta^5$-**II**$)(PPh_3)$ (**XIII**) in CD_2Cl_2 (H(3)-H(4) correlation is circled)

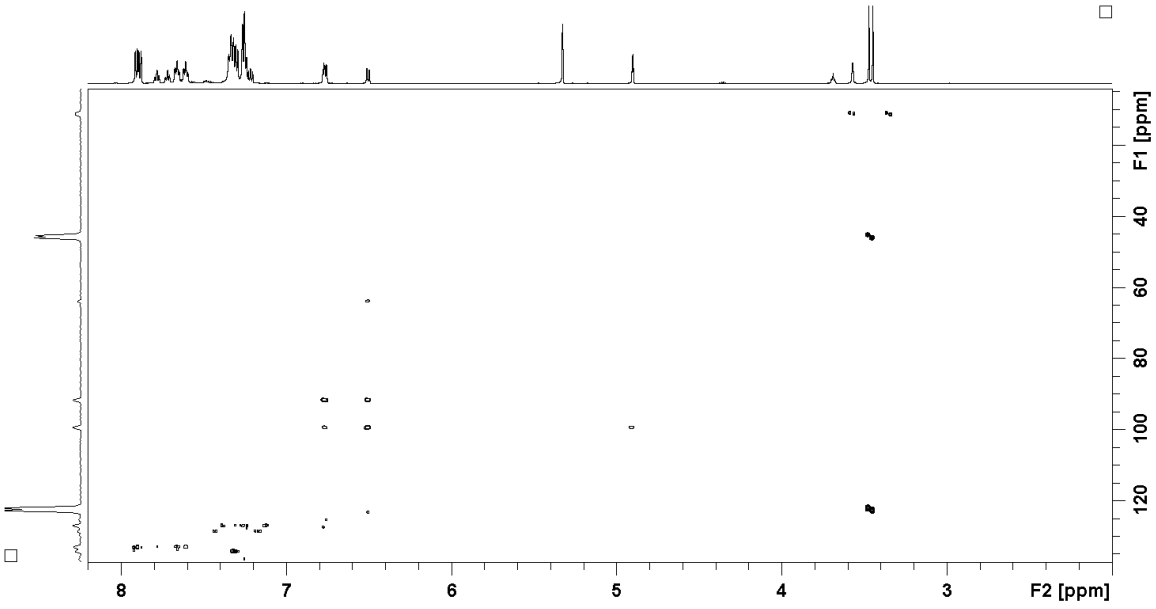

Figure 114. ^{1}H-^{13}C HMBC spectrum of $RuCl_2(\eta^5$-**II**$)(PPh_3)$ (**XIII**) in CD_2Cl_2

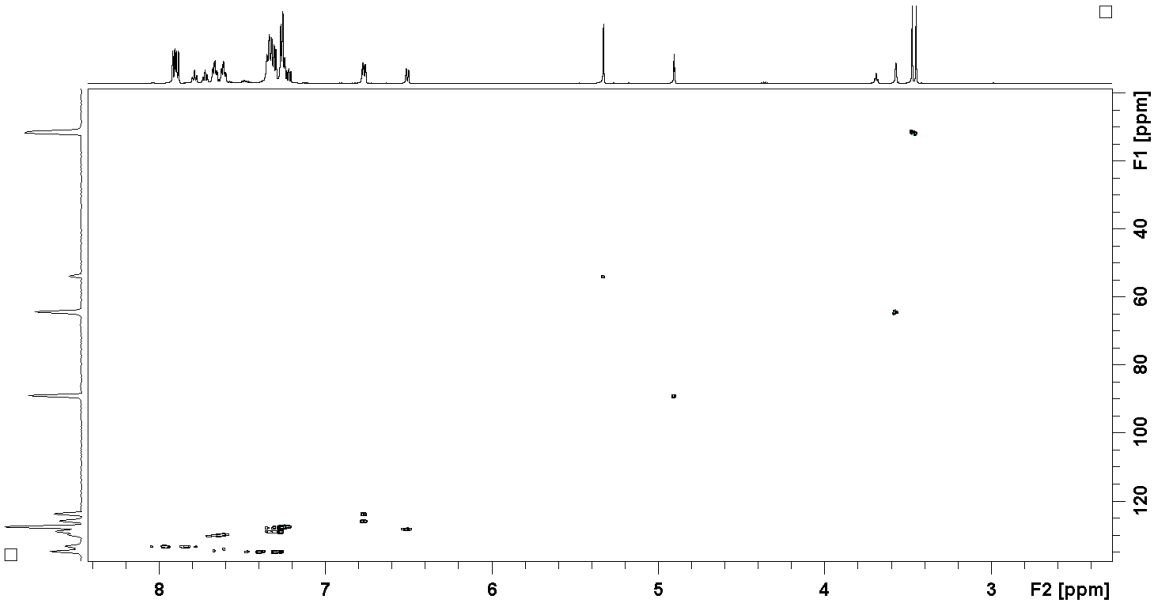

Figure 115. ^{1}H-^{13}C HSQC spectrum of $RuCl_2(\eta^5$-**II**$)(PPh_3)$ (**XIII**) in CD_2Cl_2

3.7 References

(1) Buu-Hoi *Ann.* **1944**, *556*, 1.
(2) Djerassi, C. *Chem. Rev.* **1948**, *43*, 271.
(3) Murphy, J. A.; Patterson, C. W. *J. Chem. Soc., Perkin Trans. 1* **1993**, 405.
(4) Woell, J. B.; Boudjouk, P. *J. Org. Chem.* **1980**, *45*, 5213.
(5) M. Kitching, private communication
(6) Kuhl, O. *Phosphorus-31 NMR Spectroscopy, A Concise Introduction for the Synthetic Organic and Organometallic Chemist*; Springer: Berlin, 2008.
(7) Gorenstein, D. G. In *Phosphorus-31 NMR*; Academic Press: New York, 1984.
(8) Pregosin, P. S.; Kunz, R. W. *31P and 13C NMR of Transition Metal Phosphine Complexes*; Springer-Verlag: New York, 1979.
(9) Fowler, K. G.; Littlefield, S. L.; Baird, M. C.; Budzelaar, P. H. M. *Organometallics* **2011**, *30*, 6098.
(10) Brownie, J. H.; Baird, M. C. *J. Organomet. Chem.* **2008**, *693*, 2812.
(11) Trost, B. M.; Older, C. M. *Organometallics* **2002**, *21*, 2544.
(12) Brownie, J. H.; Baird, M. C.; Schmider, H. *Organometallics* **2007**, *26*, 1433.
(13) Calhorda, M. J.; Romão, C. C.; Veiros, L. F. *Chem. Eur. J.* **2002**, *8*, 868.
(14) Cadiero, V.; Diez, J.; Gamasa, M. P.; Gimeno, J.; Lastra, E. *Coord. Chem. Rev.* **1999**, *193-195*, 147.
(15) Faller, J. W.; Friss, T.; Parr, J. *J. Organomet. Chem.* **2010**, *695*, 2644.
(16) Marchetti, F.; Pettinari, C.; Pizzabiocca, A.; Drozdov, A. A.; Troyanov, S. I.; Zhuravlev, C. O.; Semenov, S. N.; Belousov, Y. A.; Timokhin, I. G. *Inorg. Chim. Acta* **2010**, *363*, 4038.
(17) Garrou, P. E. *Chem. Rev.* **1981**, *81*, 229.
(18) Basolo, F. *Coord. Chem. Rev.* **1982**, *43*, 7.
(19) Gimeno, J.; Cadierno, V.; Crochet, P. *Comprehensive Organometallic Chemistry III*; Elsevier: Oxford, 2007; Vol. 6.
(20) Therrien, B. *Coord. Chem. Rev.* **2009**, *253*, 493.
(21) Bennett, M. A.; Matheson, T. W.; Robertson, G. B.; Smith, A. K.; Tucker, P. A. *Inorg. Chem.* **1980**, *19*, 1014.
(22) Bennett, M. A.; Smith, A. K. *J. Chem. Soc., Dalton Trans.* **1974**, 233.
(23) Akiyama, R.; Kobayashi, S. *Angew. Chem. Int. Ed.* **2002**, *41*, 2602.

Chapter 4: Conclusions and Future Work

4.1 Conclusions

The phosphonium indendylides are potentially interesting ligands due to their tuneable steric and electronic properties as well as their ability to form planar chiral complexes. It has therefore been surprising that the only known examples of PHIN ligands coordinated to transition metals have been the result of work in the Baird lab. In this work, a general synthesis of the PHINs has been described as well as the synthesis of several planar chiral complexes of ruthenium(II).

The synthesis of 1-bromoindene has proven difficult, and to date, the only method that appears to be effective is the cleavage of the C-Si bond of trimethylsilyl indene with dioxane dibromide as brominating agent. A far easier approach has been developed in which indene is lithiated and then quenched with dibromotetrachloroethane. This reaction gives 1-bromoindene in good yield and relatively high purity and should be used henceforth.

The phosphonium indenylides 1-$C_9H_6PPh_3$ (**I**), 1-$C_9H_6PMePh_2$ (**II**) and1-$C_9H_6PMe_2Ph$ (**III**) have been synthesized by the reaction of 1-bromoindene with the appropriate phosphine followed by deprotonation with sodium hydride and have been characterized by NMR spectroscopy, ESI MS and X-ray crystallography. DFT calculations have been performed in order to better understand the electronic structure of the PHINs and these suggest that the HOMO-3 orbital localized on C(1), C(2) and C(3), while the equivalient orbital of phosphonium cyclopentadienylides is distributed throughout the C_5 ring. These PHINs are thought to possess interesting coordination chemistry and thus the preparation of organometallic PHIN complexes of ruthenium was explored, a metal already with a rich metal-arene chemistry.

The reaction of **I-III** with [CpRu$(MeCN)_3$]PF_6 afforded the ruthenium-PHIN complexes [CpRu(**I-III**)]PF_6 (**V-VII** respectively) and these complexes were characterized by NMR

spectroscopy, ESI MS and X-ray crystallography. All three show an η^5 coordination mode with the Ru(II) centre making them ruthenocene derivatives. The P-C(1) bond lengths increased by between 0.04 and 0.05 Å upon coordination to Ru(II), indicating that the contribution from the zwitterionic resonance structure of the PHIN ligands increases upon coordination to the metal centre. This is to be expected, as the C_5 ring of this resonance structure is negatively charged and is isoelectronic with the Cp anion.

The ^{31}P NMR spectra of **V-VII** exhibited downfield shifts of between δ 14-21; a range which is consistent with reported downfield shifts of previously characterized PHIN complexes coordinated to Cr and phosphonium cyclopentadienylides coordinated to group 6 metals. The ^{13}C NMR spectra exhibited upfield shifts for all carbons on the C_5 ring bound to the metal centre, while the remaining carbons of the C_6 ring shifted slightly downfield. Similarly, the protons H(2) and H(3) shifted upfield considerably upon coordination to the metal centre while the protons on the C_6 ring shifted relatively little.

The P-Ph groups of **VI** and the P-Me groups of **VII** are diastereotopic and the resonances associated with these groups appear as doublets. This shows that interfacial exchanges between the two faces of the pro-planar chiral PHIN ligands are slow at least on the NMR timescale.

In an effort to form ruthenium-PHIN complexes with labile or easily displaced ligands, a PHIN or the phosphonium salt of a PHIN were reacted with $RuCl_3 \cdot xH_2O$, but no Ru(II)-PHIN complexes were produced. Arene exchange reactions were therefore attempted. Following previously reported arene exchange reactions for ruthenium(II),[21] the reaction of **II** and **III** with $[RuCl(\mu\text{-}Cl)(\eta^6\text{-}p\text{-cymene})]_2$ was investigated. With each PHIN ligand, this reaction produced a kinetic and thermodynamic product. While the nature of the kinetic product remains unknown, as no pure samples have been prepared, ^{1}H and NOESY spectra were used to determine that the ruthenium(II) centre is coordinated to both the PHIN ligand and a *p*-cymene group. The thermodynamic product produced from the reaction of $[RuCl(\mu\text{-}Cl)(\eta^6\text{-ethylbenzoate})]_2$ and **II**

was relatively pure and was determined to be $[Ru(PHIN)_2](Cl)_2$ from a combination of ESI MS and NMR studies. Unfortunately, neither of the complexes likely contains a ruthenium-PHIN fragment with easily displaced ligands. Fortunately, a new route to potentially catalytically active Ru(II)-PHIN complexes may be envisioned.

Reacting triphenylphosphine as a nucleophile with $[RuCl_2(\eta^6\text{-ethylbenzoate})]_2$ followed by the PHIN ligand **II** in refluxing THF gave the complex $RuCl_2$(**II**)(PPh_3) (**XIII**). This complex has been characterized by NMR spectroscopy. As in complexes **V**-**VII**, the resonances of the ylidic C_5 ring carbons and protons all shift upfield, while the ylidic phosphonium and the P-Me group shifts downfield relative to **II** and thus the mode of coordination of **II** in **XIII** is most likely η^5. The complex **XIII** may be very useful for exploring the chemistry of Ru(II)-PHIN complexes as there are several reactions which may be employed to generate unsaturated complexes. The PPh_3 ligand may be displaced by another ligand, and the Cl^- ligands may be removed with a bulky silver salt such as $AgPF_6$ thus giving rise to complexes which may find applications as catalysts for organic transformations.

4.2 Future Work

The exploration of ruthenium(II)-PHIN complexes has only just begun, with this contribution being the first small steps. Certainly the most interesting research avenue is the investigation of catalytic properties of **XIII** and its derivatives. There is precedent in similar complexes for the displacement of the PPh_3 ligand with a carbene, e.g. C=C-Ph. Removal of a chloride ligand from this complex may then furnish an effective olefin metathesis catalyst. This catalyst system would be even more interesting if the two enantiomers of the complex could be separated as there has been only very limited progress towards effecting asymmetric olefin metathesis reactions. One way to do this is to remove a chloride ligand and replace it with an

enantiopure chiral anion (tartrate salts are probably the most readily available reagents) giving two diastereomers which can then be separated by crystallization.

Another interesting project is arene exchange using complex **IX**. Heating similar complexes with arenes instead of PHINs resulted in exchange of the *p*-cymene group with the arene. As the PHINs are much better electron donors that arenes, arene exchange to form the complex $RuCl_2(\eta^6:\eta^1\text{-}1\text{-}C_9H_6PPh_2CH_2PPh_2)$ should be quite facile. As described in the introduction, tethered phosphine-arene complexes have not been shown to catalyze asymmetric organic reactions effectively. However, none of these complexes have a plane of chirality directly attached to the metal centre. $RuCl_2(\eta^6:\eta^1\text{-}1\text{-}C_9H_6PPh_2CH_2PPh_2)$ may prove to be a much more effective chiral catalyst for a variety of asymmetric organic reactions. Additionally, the ethylene linked PHIN ligand $1\text{-}C_9H_6PPh_2CH_2CH_2PPh_2$ can also be synthesized and may exhibit similar chemistry.

Appendix A: NMR Spectra

4.3 NMR Spectra of the isomers of [1-$C_9H_7PPh_2CH_2PPh_2$]Br and IV

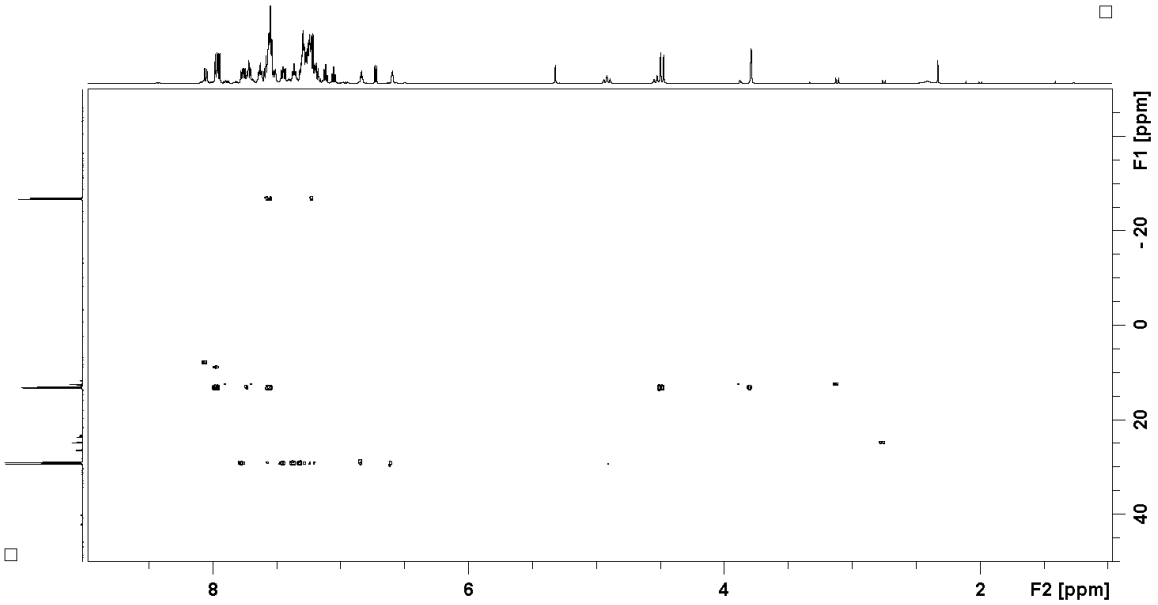

Figure A 1. ^{1}H-^{31}P HMBC Spectrum of the isomers of [1-$C_9H_7PPh_2CH_2PPh_2$]Br

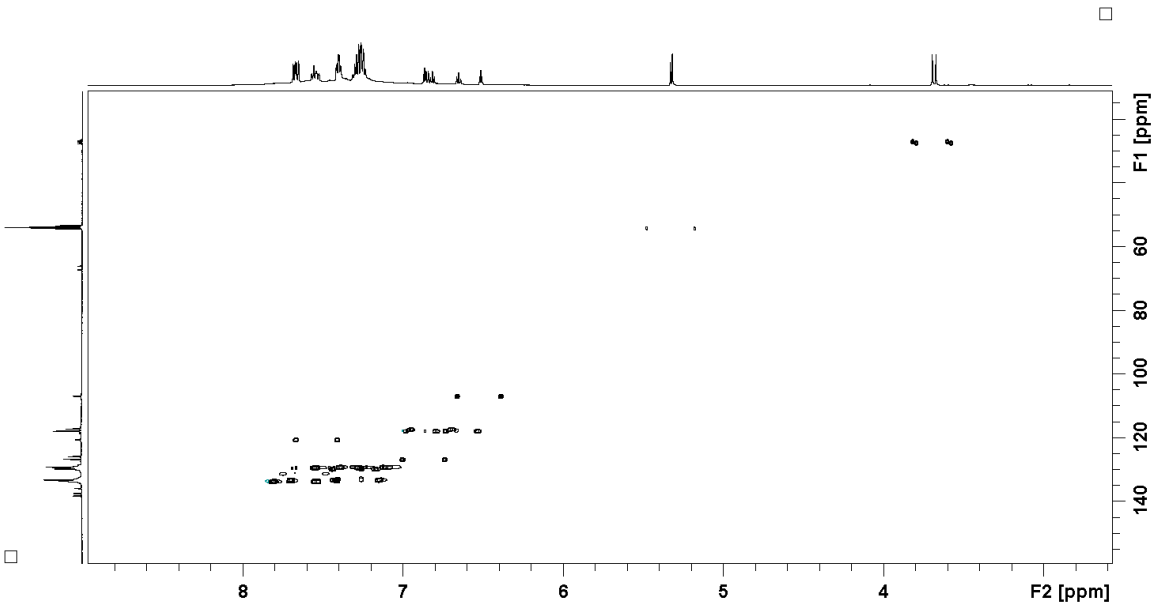

Figure A 2. ^{1}H-^{13}C HSQC Spectrum of IV

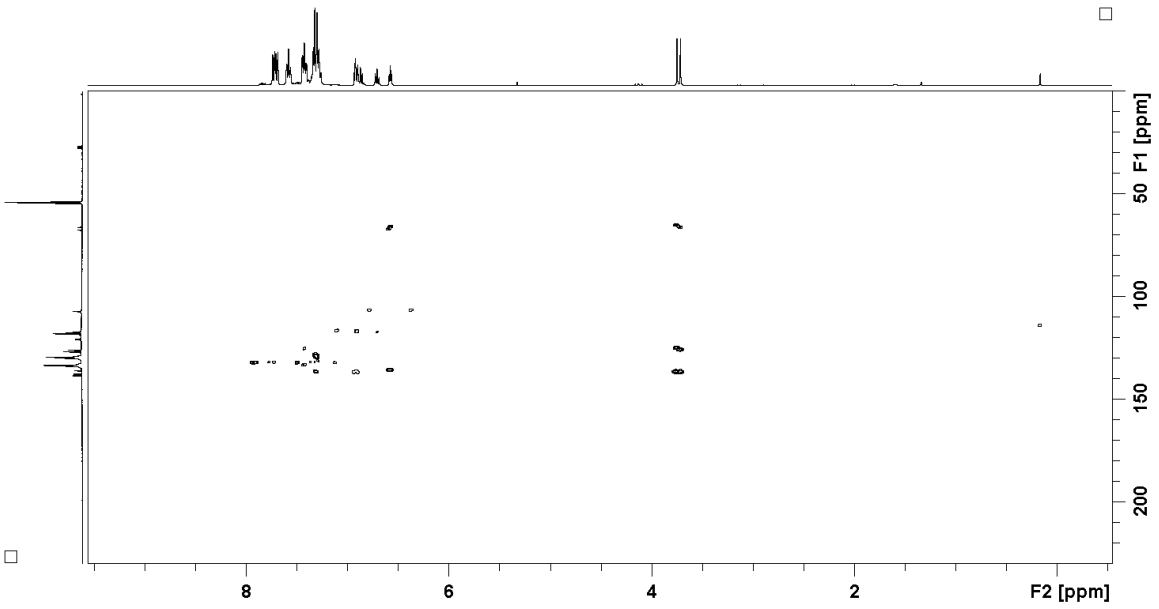

Figure A 3. ^{1}H-^{13}C HMBC spectrum of IV

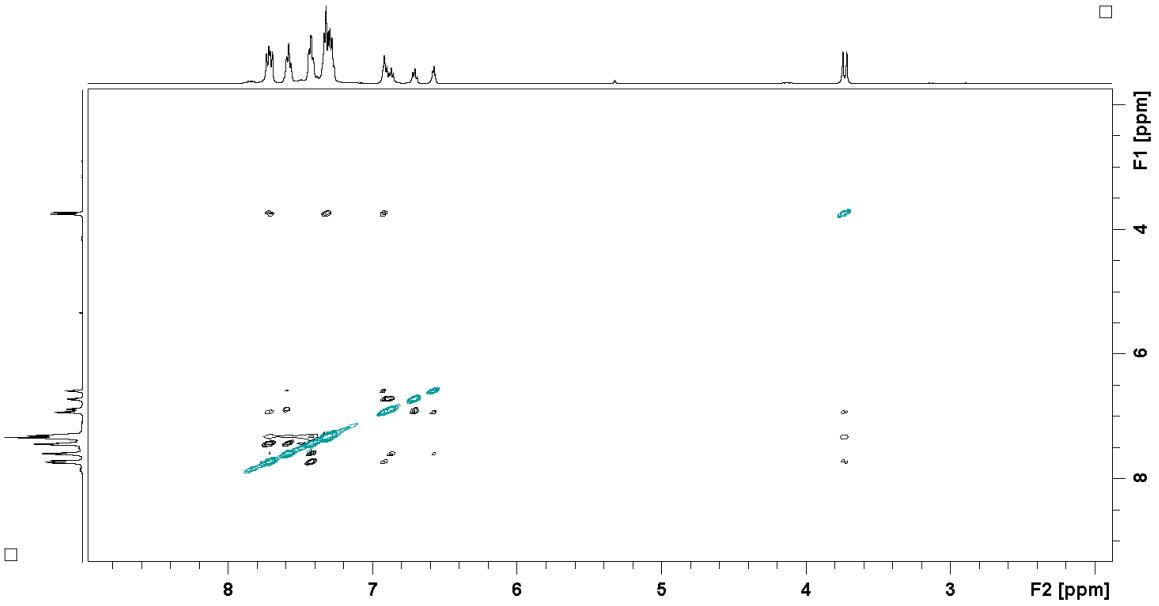

Figure A 4. NOESY spectrum of IV

4.4 NMR spectra of V, VI, and VII

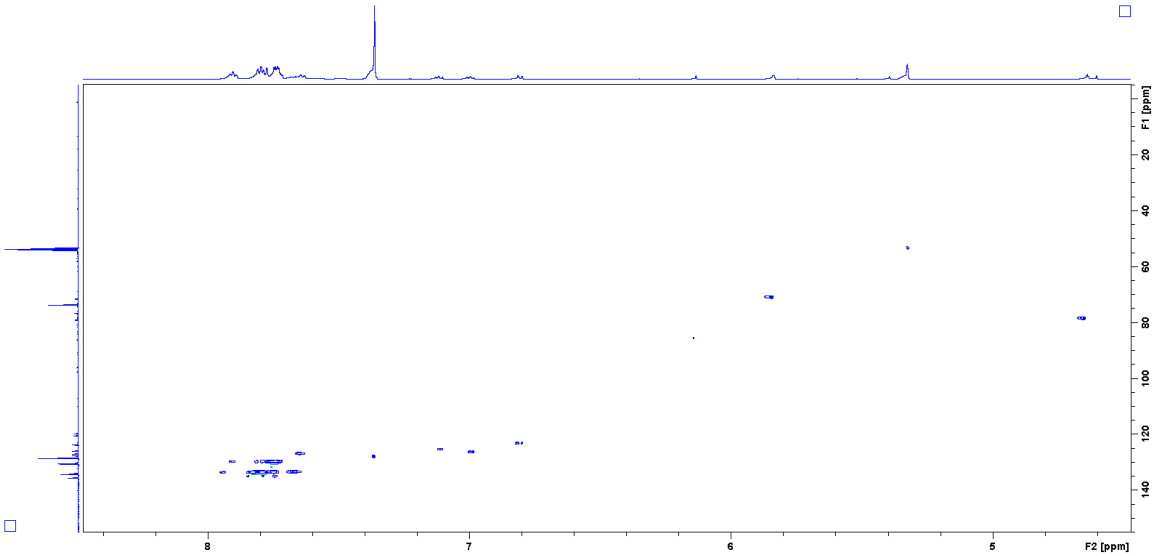

Figure A 5. ^{1}H-^{13}C HSQC spectrum of V

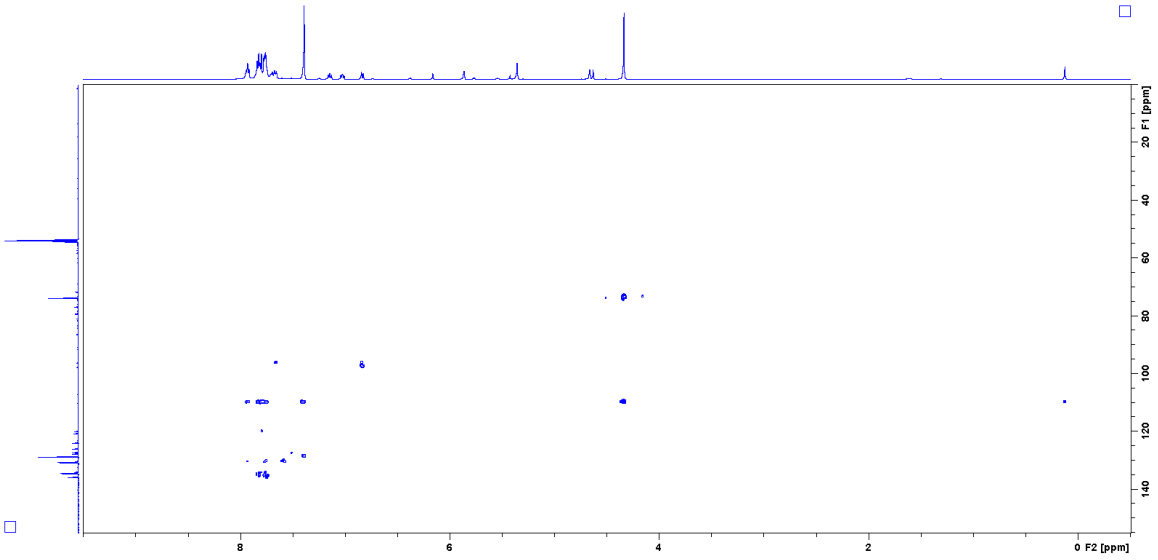

Figure A 6. ^{1}H-^{13}C HMBC spectrum of V

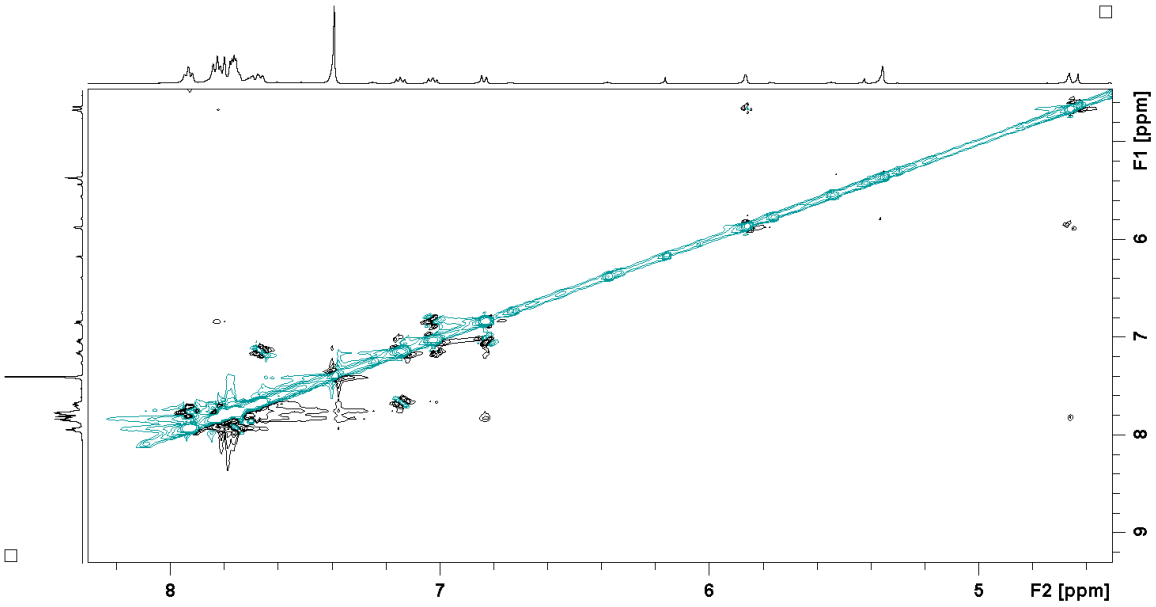

Figure A 7. NOESY spectrum of V

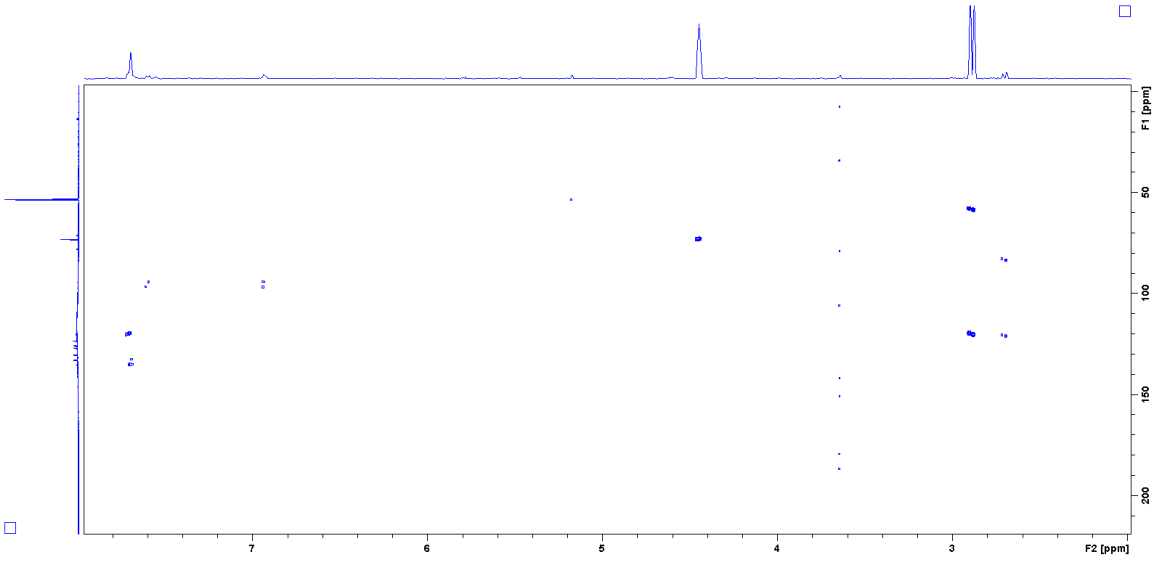

Figure A 8. ^{1}H-^{13}C HMBC spectrum of VI

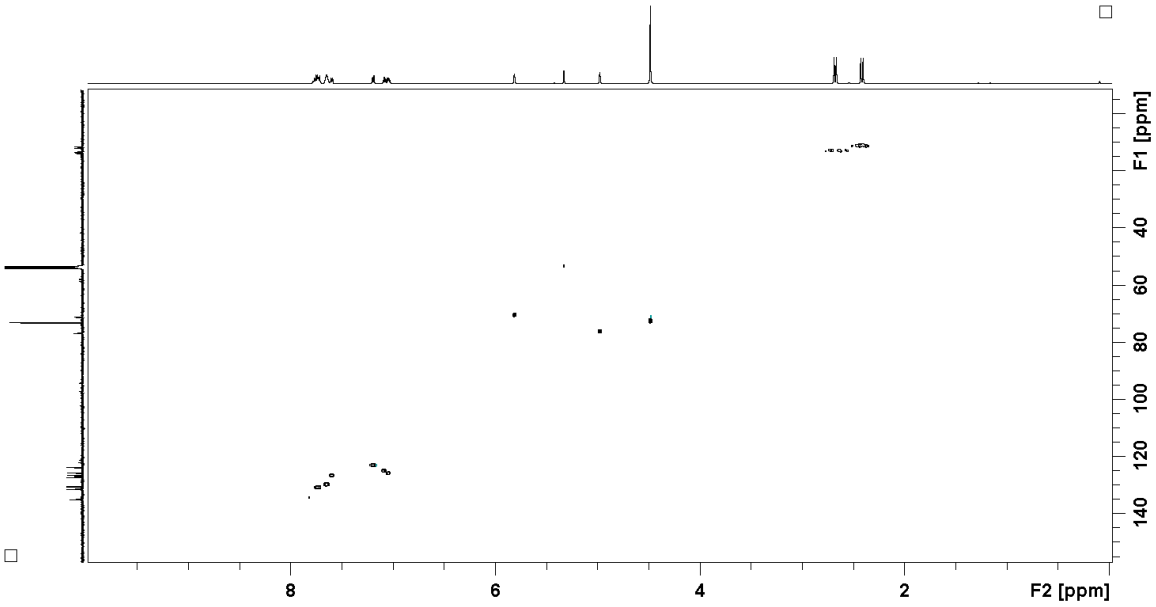

Figure A 9. ^{1}H-^{13}C HSQC spectrum of VII

4.5 NMR spectra of VIIIa and VIIIb

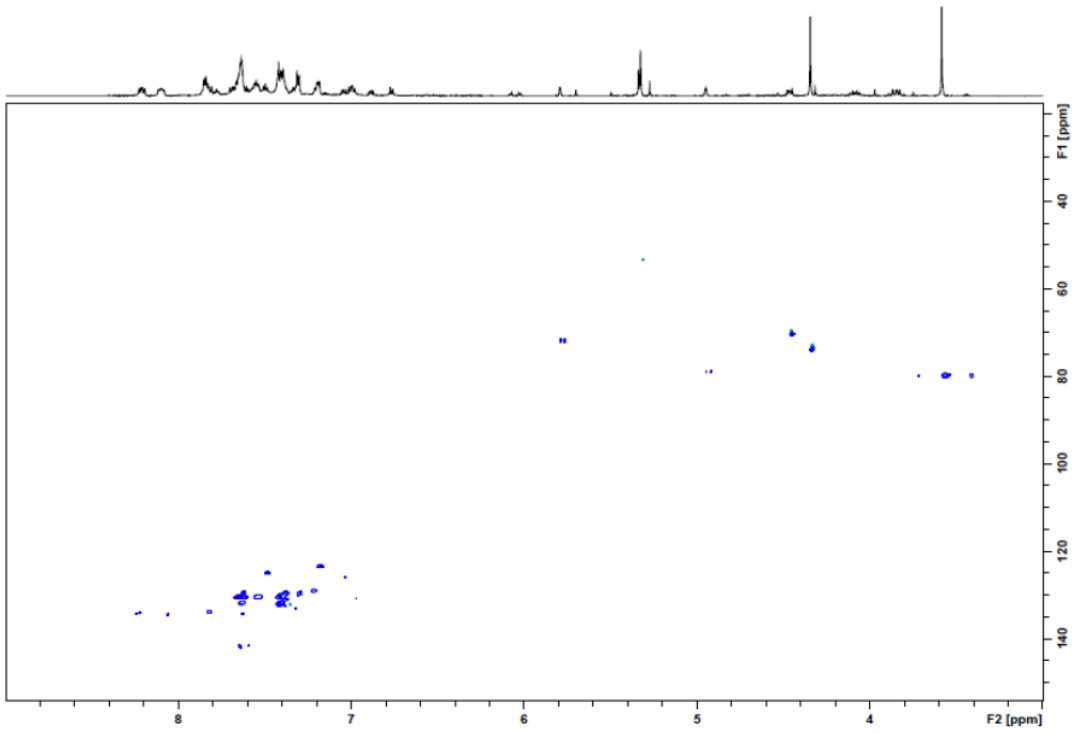

Figure A 10. ^{1}H-^{13}C HSQC spectrum of a mixture of VIIIa and VIIIb

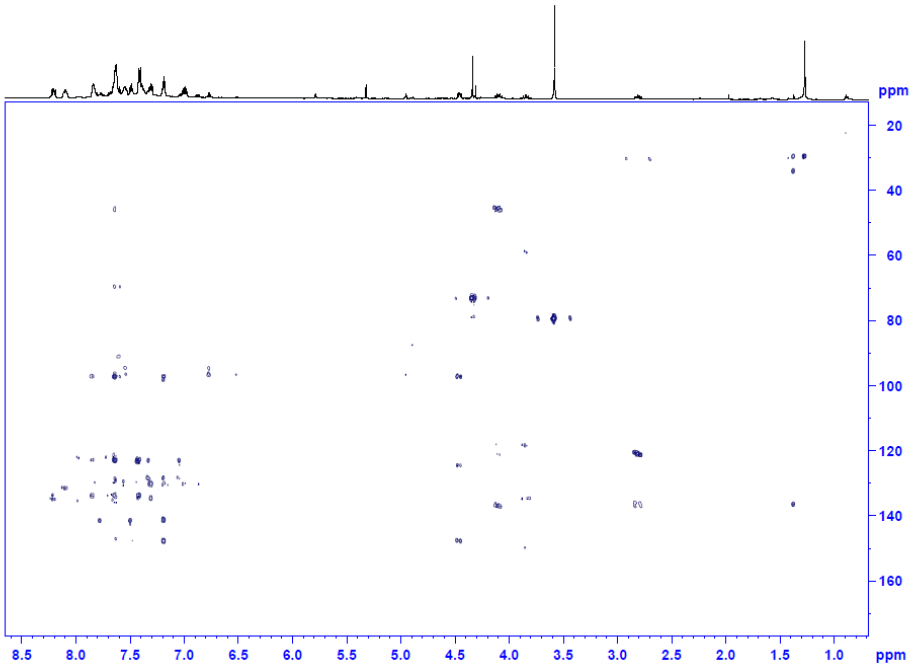

Figure A 11. ^{1}H-^{13}C HMBC spectrum of a mixture of VIIIa and VIIIb

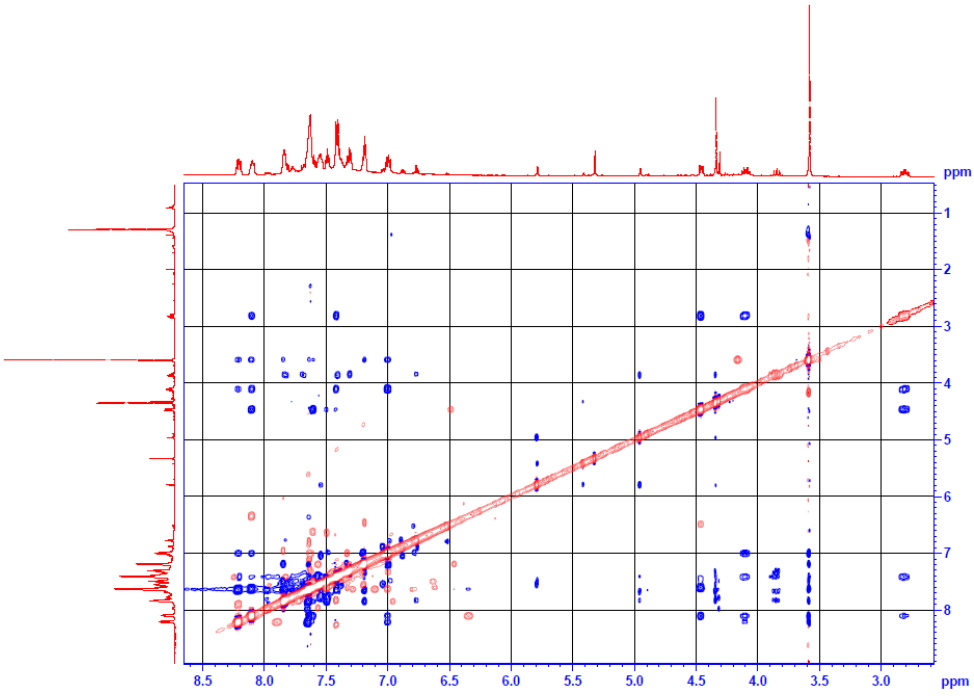

Figure A 12. NOESY spectrum of a mixture of VIIIa and VIIIb

Appendix B: X-ray Crystallographic Data

4.6 Crystal Data for isomer A of [1-$C_9H_6PPh2CH_2PPh_2$]Br

Empirical formula	C35 H31 Br Cl2 P2	
Formula weight	664.35	
Temperature	180(2) K	
Wavelength	0.71073 Å	
Crystal system	Triclinic	
Space group	P-1	
Unit cell dimensions	a = 11.8772(12) Å	α= 99.166(1)°.
	b = 12.1298(12) Å	β= 115.536(1)°.
	c = 12.4458(12) Å	γ = 91.197(1)°.
Volume	1589.1(3) $Å^3$	
Z	2	
Density (calculated)	1.388 Mg/m^3	
Absorption coefficient	1.585 mm^{-1}	
F(000)	680	
Crystal size	0.30 x 0.25 x 0.15 mm^3	
Theta range for data collection	1.85 to 26.00°.	
Index ranges	-14<=h<=14, -14<=k<=14, -15<=l<=15	
Reflections collected	15937	
Independent reflections	6200 [R(int) = 0.0158]	
Completeness to theta = 26.00°	99.4 %	
Absorption correction	Multi-scan	
Max. and min. transmission	0.7969 and 0.6477	
Refinement method	Full-matrix least-squares on F^2	
Data / restraints / parameters	6200 / 0 / 361	
Goodness-of-fit on F^2	1.046	
Final R indices [I>2sigma(I)]	R1 = 0.0269, wR2 = 0.0705	
R indices (all data)	R1 = 0.0310, wR2 = 0.0727	
Largest diff. peak and hole	0.473 and -0.408 e.$Å^{-3}$	

4.7 Crystal Data for 1-$C_9H_6PPh_2CH_2PPh_2$

Empirical formula	C34 H28 P2	
Formula weight	498.50	
Temperature	180(2) K	
Wavelength	0.71073 Å	
Crystal system	Triclinic	
Space group	P-1	
Unit cell dimensions	a = 10.9216(5) Å	α= 94.046(4)°.
	b = 11.6984(5) Å	β= 114.453(3)°.
	c = 12.2897(5) Å	γ = 105.143(3)°.
Volume	1350.89(10) $Å^3$	
Z	2	
Density (calculated)	1.226 Mg/m^3	
Absorption coefficient	0.182 mm^{-1}	
F(000)	524	
Crystal size	0.30 x 0.15 x 0.08 mm^3	
Theta range for data collection	3.63 to 25.99°.	
Index ranges	-12<=h<=13, -14<=k<=14, -15<=l<=14	
Reflections collected	9408	
Independent reflections	5239 [R(int) = 0.0385]	
Completeness to theta = 25.99°	98.6 %	
Absorption correction	Multi-scan	
Max. and min. transmission	0.9856 and 0.9475	
Refinement method	Full-matrix least-squares on F^2	
Data / restraints / parameters	5239 / 0 / 325	
Goodness-of-fit on F^2	1.052	
Final R indices [I>2sigma(I)]	R1 = 0.0495, wR2 = 0.1119	
R indices (all data)	R1 = 0.0758, wR2 = 0.1286	
Largest diff. peak and hole	0.435 and -0.427 $e.Å^{-3}$	

4.8 Crystal Data for $[CpRu(1\text{-}C_9H_6PPh_3)]PF_6$

Empirical formula	C32 H26 F6 P2 Ru	
Formula weight	687.54	
Temperature	180(2) K	
Wavelength	0.71073 Å	
Crystal system	Monoclinic	
Space group	P2(1)/c	
Unit cell dimensions	a = 11.5469(2) Å	α= 90°.
	b = 8.6169(2) Å	β= 91.0110(10)°.
	c = 28.9057(6) Å	γ = 90°.
Volume	2875.63(10) $Å^3$	
Z	4	
Density (calculated)	1.588 Mg/m^3	
Absorption coefficient	0.717 mm^{-1}	
F(000)	1384	
Crystal size	0.20 x 0.15 x 0.06 mm^3	
Theta range for data collection	2.24 to 26.00°.	
Index ranges	-14<=h<=14, -8<=k<=10, -32<=l<=35	
Reflections collected	12543	
Independent reflections	5638 [R(int) = 0.0404]	
Completeness to theta = 26.00°	99.8 %	
Absorption correction	Multi-scan	
Max. and min. transmission	0.9583 and 0.8699	
Refinement method	Full-matrix least-squares on F^2	
Data / restraints / parameters	5638 / 37 / 369	
Goodness-of-fit on F^2	1.047	
Final R indices [I>2sigma(I)]	R1 = 0.0547, wR2 = 0.1312	
R indices (all data)	R1 = 0.0763, wR2 = 0.1446	
Largest diff. peak and hole	1.450 and -1.132 $e.Å^{-3}$	

4.9 Crystal Data for $[CpRu(1\text{-}C_9H_6PPh_2Me)]PF_6$

Empirical formula	C27 H24 F6 P2 Ru	
Formula weight	625.47	
Temperature	180(2) K	
Wavelength	0.71073 Å	
Crystal system	Orthorhombic	
Space group	Pbca	
Unit cell dimensions	a = 12.4585(2) Å	α= 90°.
	b = 16.9795(2) Å	β= 90°.
	c = 24.1574(3) Å	γ = 90°.
Volume	5110.23(12) $Å^3$	
Z	8	
Density (calculated)	1.626 Mg/m^3	
Absorption coefficient	0.798 mm^{-1}	
F(000)	2512	
Crystal size	0.25 x 0.20 x 0.06 mm^3	
Theta range for data collection	2.20 to 26.00°.	
Index ranges	-13<=h<=15, -20<=k<=20, -29<=l<=27	
Reflections collected	35783	
Independent reflections	5023 [R(int) = 0.0631]	
Completeness to theta = 26.00°	100.0 %	
Absorption correction	Multi-scan	
Max. and min. transmission	0.9537 and 0.8255	
Refinement method	Full-matrix least-squares on F^2	
Data / restraints / parameters	5023 / 1 / 329	
Goodness-of-fit on F^2	1.025	
Final R indices [I>2sigma(I)]	R1 = 0.0378, wR2 = 0.0776	
R indices (all data)	R1 = 0.0623, wR2 = 0.0891	
Largest diff. peak and hole	0.784 and -0.441 $e.Å^{-3}$	

4.10 Crystal Data for $[CpRu(1\text{-}C_9H_6PPhMe_2)]PF_6$

Empirical formula	C22 H22 F6 P2 Ru	
Formula weight	563.41	
Temperature	180(2) K	
Wavelength	0.71073 Å	
Crystal system	Orthorhombic	
Space group	Pca2(1)	
Unit cell dimensions	a = 10.82570(10) Å	α= 90°.
	b = 13.0647(2) Å	β= 90°.
	c = 15.7426(3) Å	γ = 90°.
Volume	2226.55(6) $Å^3$	
Z	4	
Density (calculated)	1.681 Mg/m^3	
Absorption coefficient	0.905 mm^{-1}	
F(000)	1128	
Crystal size	0.25 x 0.25 x 0.20 mm^3	
Theta range for data collection	2.44 to 25.99°.	
Index ranges	-13<=h<=12, -12<=k<=16, -19<=l<=15	
Reflections collected	5509	
Independent reflections	3224 [R(int) = 0.0232]	
Completeness to theta = 25.99°	99.3 %	
Absorption correction	Multi-scan	
Max. and min. transmission	0.8398 and 0.8054	
Refinement method	Full-matrix least-squares on F^2	
Data / restraints / parameters	3224 / 1 / 282	
Goodness-of-fit on F^2	1.035	
Final R indices [I>2sigma(I)]	R1 = 0.0258, wR2 = 0.0511	
R indices (all data)	R1 = 0.0300, wR2 = 0.0534	
Absolute structure parameter	0.02(3)	
Largest diff. peak and hole	0.283 and -0.379 $e.Å^{-3}$	

4.11 Crystal Data for $RuCl_2(1\text{-}C_9H_6PPh_2CH_2PPh_2)(\eta^6\text{-}p\text{-cymene})$

Empirical formula	C48 H50 Cl2 O P2 Ru	
Formula weight	876.79	
Temperature	180(2) K	
Wavelength	0.71073 Å	
Crystal system	Trigonal	
Space group	R-3	
Unit cell dimensions	a = 49.7471(16) Å	α= 90°.
	b = 49.7471(16) Å	β= 90°.
	c = 10.4751(4) Å	γ = 120°.
Volume	22450.4(13) $Å^3$	
Z	18	
Density (calculated)	1.167 Mg/m^3	
Absorption coefficient	0.516 mm^{-1}	
F(000)	8172	
Crystal size	0.20 x 0.08 x 0.04 mm^3	
Theta range for data collection	3.57 to 26.00°.	
Index ranges	-43<=h<=61, -57<=k<=47, -12<=l<=12	
Reflections collected	23695	
Independent reflections	9773 [R(int) = 0.0752]	
Completeness to theta = 26.00°	99.6 %	
Absorption correction	Multi-scan	
Max. and min. transmission	0.9797 and 0.9039	
Refinement method	Full-matrix least-squares on F^2	
Data / restraints / parameters	9773 / 12 / 302	
Goodness-of-fit on F^2	0.891	
Final R indices [I>2sigma(I)]	R1 = 0.0692, wR2 = 0.1737	
R indices (all data)	R1 = 0.1454, wR2 = 0.2030	
Largest diff. peak and hole	0.888 and -0.587 $e.Å^{-3}$	